

**Petrographic Analysis of Bonanza Epithermal Vein Textures at Buckskin
National and Fire Creek Deposits, Northern Nevada**

Tadsuda Taksavas

A Thesis Submitted to the Graduate Faculty of
Auburn University
in Partial Fulfillment of the
requirements for the Degree of
Master of Science

Auburn, Alabama
May 6, 2017

Keywords: Epithermal, Silica textures, Colloform, Buckskin National,
Fire Creek, Northern Nevada

Copyright 2017 by Tadsuda Taksavas

Approved by

James A. Saunders, Chair, Professor Emeritus of Geosciences
Willis E. Hames, Professor of Geosciences
Haibo Zou, Associate Professor of Geosciences

Abstract

The Buckskin National and Fire Creek epithermal deposits, which are located in the Northern Great Basin in northern Nevada, exhibit a variety of gangue-mineral vein textures. Gangue minerals, which are valueless minerals, commonly include quartz, chalcedony, adularia, and calcite, and occur with ore-minerals in the veins. In this study, petrographic analysis was conducted of gangue textures and associated ore minerals in two deposits in both transmitted and reflected light. The petrographic details were then compared to Sleeper and Midas deposits, which are well-known epithermal ores in northern Nevada. In addition, X-ray powder diffraction (XRD) and hot-cathode CL data augmented petrographic interpretations. Silica vein textures found in the Buckskin National and Fire Creek deposits generally exhibit jigsaw quartz textures in colloform-bands, replace calcite, and also define enigmatic fibrous-acicular structures. This fibrous-acicular texture appear to be composed of pseudomorphs after unknown mineral. Other vein textures that also found in two deposits include comb, flamboyant, plumose, and groups of pseudomorphs after bladed calcite such as lattice-bladed, parallel-bladed, and pseudoacicular. XRD analysis indicates that the Buckskin National veins commonly contain quartz, kaolinite, and minor amount of adularia, whereas the Fire Creek samples consist of quartz, later calcite, and adularia. The CL microscope provides important

additional information on original silica textures and as silica phases emit distinct CL colors that indicate hydrothermal origins of quartz in the veins of this study. The CL technique also sheds light on textures of colloidal precursors that have already (re)crystallized to quartz and chalcedony in some colloform bands. The Buckskin National deposit and the Fire Creek deposit in northern Nevada contain similar silica textures to other epithermal deposits and can exhibit specific characteristics that are controlled by the complexity of hydrothermal events, ore-fluid evolution, and water-rock chemical reactions with wall rocks of varying composition. However, results from this study have implications for interpreting vein textures in other epithermal deposits around the world including the Sleeper, Midas, and Mule Canyon deposits in the US, Koryu and Hishikari deposits in Japan, and the epithermal deposits in Queensland, Australia.

ACKNOWLEDGEMENTS

This research is supported by the grants from (1) the Geological Society of Nevada; Elko chapter, (2) Geosciences Advisory Board and Waters/Folse research grants for Auburn University, and (3) the Graduate Student Fellowship of the Society of Economic Geologists Foundation. These funds provided the cost of field trip, sample preparation and analysis of this research. Importantly, I would like to thank Dr. James Saunders for the support of my master study and related research, for his patience to guide and help me all the time of research and writing this thesis, and thank for his strong motivation and immense knowledge. This research would never been complete without his helps in all parts. My sincere thanks also go to my committee members, Dr. Willis Hames and Dr. Haibo Zou, for their suggestions and corrections in this thesis. I thank Dr. Thomas Monecke, a faculty of Colorado Schools of Mines, who offered the hot-cathode CL microscope in this study. I would also like to thank Dr. Zeki Billor for his help in XRD analysis at Auburn University. I am very thankful to my friend, Khomchan Promneewat, for his supports in graphic data. Also, his positive thinking always convince me to focus and concentrate on this thesis. Thanks for the scholarship from the Thai government and thank for all encouragement from family and friends. Thank you for the faculty stuffs and students at the Department of Geosciences to give me relaxation and very warm feeling during my education here at Auburn University.

Style manual or journal used: Economic Geology

Computer software used: Microsoft Word, Microsoft Excel, Microsoft PowerPoint,
Adobe Photoshop CS, Paint, and DIFFRAC.EVA.

TABLE OF CONTENTS

ABSTRACT.....	ii
ACKNOWLEDGEMENTS.....	iv
TABLE OF CONTENTS.....	vi
LIST OF FIGURES.....	viii
1. INTRODUCTION.....	1
1.1 Objectives.....	2
1.2 Significance.....	3
2. BACKGROUND.....	4
2.1 Epithermal Ores and Their Genesis.....	4
2.2 Epithermal Ores in Nevada.....	7
2.3 Mid-Miocene Clan of Epithermal Ores in Northern Great Basin.....	10
2.4 Previous Works on Buckskin National and Fire Creek Deposits.....	16
2.4.1 Buckskin National Deposit.....	18
2.4.2 Fire Creek Deposit.....	22
2.5 Gangue-Mineral Textures of Epithermal Veins.....	25
2.6 Textural Terminology for this study.....	34
3. METHODOLOGY.....	38
3.1 Field Work.....	38

3.2 Petrographic Methods.....	40
3.3 X-ray Powder Diffraction.....	41
3.4 Hot-Cathode Cathodoluminescence Microscope.....	41
4. RESULTS.....	44
4.1 Vein Textures of the Buckskin National Deposit.....	44
4.2 Vein Textures of the Fire Creek Deposit.....	72
4.3 Precious-Metal Minerals.....	93
4.4 Cathodoluminescence (CL) images.....	101
4.5 X-Ray Powder Diffraction Data.....	114
5. DISCUSSIONS.....	119
5.1 Gangue-Mineral Textures.....	119
5.2 Comparisons of Silica Textures to Sleeper, Midas, and Mule Canyon Deposits.....	127
5.3 Relationships of Silica Textures and Precious Metal Minerals.....	131
6. CONCLUSIONS.....	137
REFERENCES.....	142
APPENDIX 1: Silica Textural Counts of the Buckskin National (BN) and Fire Creek (FC) samples.....	152
APPENDIX 2: XRD Samples from the Buckskin National and Fire Creek Deposits in Nevada, and additionally Hishikari Deposit, Japan.....	154

List of Figures

FIG 1. Schematic model showing relations between low- and high-sulfidation epithermal deposits and porphyry deposit (from Hedenquist and Lowenstern, 1994).....	7
FIG 2. Map of the Great Basin in western United States showing middle Miocene igneous and tectonic features. Darker shaded area represents the Great Basin and lighter shaded exhibits the western andesite assemblage forming the Western Cascades at around 21 Ma. Heavy line in the north-central Great Basin indicates the continental northern Nevada rift. Other lines represent feeder dikes within the Columbia River Basalt Group (CRB). NNR = northern Nevada rift, M= McDermitt caldera, SM = Steens Mountain (from John, 2001)	9
FIG 3. Map showing low-sulfidation deposits in the North Great Basin (black border) that are associated with a bimodal basalt-rhyolite assemblage indicated by grey shades (John, 2001). [SL=Sleeper, M=Midas, FC=Fire Creek, N=National/Buckskin National, MC=Mule Canyon, DE=DeLamar (e.g. Silver City district), GM=Grassy Mountain, QM=Quartz Mountain, HG=High Grade, HR=Hog Ranch, MV=Mountain View, WM=Wind Mountain, R=Rosebud, SU=Sulphur, ST=Seven Troughs, FL=Florida Canyon, GB=].....	11
FIG 4. Schematic model (from John, 2001) showing magmatic and tectonic events of the bimodal basalt-rhyolite assemblage in the northern Great Basin. These processes are relating to continental extension and mantle plumes underneath the area.....	11
FIG 5. Diagrammatic model showing magmatic and hydrothermal processes forming the low-sulfidation epithermal ore deposits in the North Great Basin in Nevada. The bimodal basalt-rhyolite assemblage in northern Nevada and granitic intrusion in southwestern Idaho host bonanza ore deposits (from Saunders et al., 2008).....	13
FIG 6. Schematic NE-SW cross section showing the emplacement of bonanza veins along main oblique-normal faults during 15.6-15.4 Ma at the Midas low-sulfidation epithermal system (from Leavitt et al., 2004). [Au=Bonanza ores, Ts=accumulation of sinter, Tts=opalized sediment, ES=Eastern Star, Trf=rhyolite flows, CG=Colorado Grande structure].....	15
FIG 7. Map showing general geology of a portion of the NGB that contains Buckskin National and Fire Creek deposits (indicated by red and yellow dot, respectively). The bimodal basalt-rhyolite assemblage and the northern Nevada rift are the major geologic features of the region (modified from Leavitt et al., 2004).....	17

FIG 8. Map showing the northern part of the northern Great Basin that includes Elko, Lander, and Humboldt counties, Nevada. Locations of the principal deposits studied here (Buckskin National and Fire Creek deposits) are shown, as are two other deposits (Sleeper and Midas) that are used for comparison in this study. (Google Map, 2017).....	18
FIG 9. A: Topographic map showing the Buckskin National deposit with mine entrance shown by the red circle. B: Satellite map of the Buckskin Peak area with the red dot showing the location of the Buckskin National adit. (Google map, My Topo, 2017).....	20
FIG 10. <i>Top</i> : Index map of Vikre (2007) showing the location of Bell vein, which refers to Buckskin National deposit in National district. <i>Bottom</i> : Schematic model showing rhyolitic-volcanic sequence of the Buckskin Mountain that host veins. Dash line indicates a recent surface (Vikre, 2007).....	21
FIG 11. Map showing the locations of Fire Creek deposit, which is mined at the northeast of Bald Mountain as an underground mine owned by Klondex Mines Limited, shown as a yellow dot and the Mule Canyon deposit shown as a red dot. (Google map, 2017).....	23
FIG 12. <i>Left</i> : Map (left) showing underground workings vein traces projected to surface, and the NNW of vein structures at Fire Creek deposit (from O’Neill, 2016). <i>Right</i> : Stratigraphic column of volcanic sequences host ore veins formed in the Fire Creek deposit (from Kassos et al., 2015).....	24
FIG 13. Sketches of primary growth textures including crustiform, cockade, colloform, moss, comb, and zonal quartz veins are referred from other previous studies. Grain sizes, form, morphology, and internal structure are provided (from Dong et al., 1995).....	28
FIG 14. Sketches of recrystallization/crystallization textures including mosaic (jigsaw), feathery, flamboyant, and ghost-sphere quartz that are found in this study (from Dong et al., 1995).....	30
FIG 15. Diagrammatic illustrations of proposed origins of recrystallization/crystallization textures of amorphous or/and cryptocrystalline silica (from Dong et al., 1995).....	30
FIG 16. Sketches of replacement textures including pseudo-lattice bladed, ghost-bladed, parallel-bladed, pseudo-acicular, and saccharoidal (from Dong et al., 1995).....	32
FIG 17. Sketches of interpreted evolution of replacement textures of silica-carbonate veins in epithermal deposits (from Dong et al., 1995).....	32
FIG 18. Photograph of Fire Creek underground mine taken from the top of basalt flows as paleosurface on the Bald Mountain. The Fire Creek deposit is located on the Crescent Valley and the Tenabo Mountain is on the other side, where is the location of giant Cortex mine operated by the Barrick Gold Corporation.....	39
FIG 19. Photographs taken underground showing carbonate-silica veins from the Fire Creek deposit. A: Photograph of a calcite-silica vein (yellowish white color) cutting the country rock (dark color). The approximately width of the vein is about 30 cm. B: Feathery dendrites of electrum occurring within calcite-silica replacement texture.....	39

FIG 20. Photographs of Buckskin National mine. A: Location of Buckskin National underground mine that is at the southeast of the Buckskin Mountain. B: The mine dumps of the underground mine, where samples were collected.....40

FIG 21. Photographs of X-ray powder Diffraction equipment and sample preparation made at the X-ray lab at Auburn University. [Retrieved from <http://www.auburn.edu/cosam/departments/geosciences/Equipment/XRD-XRF/index.htm>: 02/10/2017]42

FIG 22. Photograph of hot-cathode CL microscope in the Fluid Inclusion/Cathodoluminescence laboratory of Colorado School of Mines, Golden, CO. This system is operated at 14 kV with a current density of about $10 \mu\text{A}/\text{mm}^2$. [Retrieved from <http://geology.mines.edu/FI-CL-Laboratory>: 02/01/2017].....43

FIG 23. Photomicrographs of asymmetrically- and symmetrically-banded crustiform textures from the Buckskin National deposit. A: Multiple layers showing typical crustiform silica texture. The layers exhibit different colors (black, white, yellow, and grey). Colorless and white-colored bands are composed of several layers that were formerly formed by silica colloids and some of them contain fine-grained black opaque minerals. B: Symmetrical crustiform-colloform textures include varieties of colloform bands consisting of microcrystalline quartz-adularia layers (white, milky and grey) and cryptocrystalline chalcedony layers formed near the open spaces (black).....46

FIG 24. Photographs of colloform textures from the Buckskin National deposit. A: Colorless and milky colloform bands that exhibit mammillary or botryoidal structures. Each mound is around 0.5 cm of diameter. The sample's surface consists of altered materials including clay minerals. B: Cockade texture that is produced by numerous of colloform bands, one of which contains precious-metal minerals (grey).....47

FIG 25. Photographs of colloform structures in parallel- and perpendicular-oriented directions of the vein wall. A: (oriented parallel to vein wall), Colorless spheroids are surrounded by milky background, whereas, in opposite direction, mammillary-formed bands occur within the same sample. B: Moss texture characterized by disseminated colorless sphere in a white milky groundmass. These spheres range from 0.1-0.5 cm.....48

FIG 26. Photograph of prismatic euhedral quartz in a hand specimen from the Buckskin National deposit. The scale in this photograph is in centimeters.....49

FIG 27. Photograph of lattice-bladed calcite pseudomorphs that are formed above bands of black Ag-minerals. All the precursor calcite has been replaced by silica.....49

FIG 28. Photomicrographs taken under cross-polarized light of the mosaic or jigsaw texture. A: Jigsaw quartz in various crystal sizes. B: Coarse-grained jigsaw quartz and moss quartz. C: Jigsaw texture associated with sericite as an alteration product of adularia. D: Very fine-grained quartz showing jigsaw texture. [qtz = Quartz].....52

FIG 29. Photomicrographs of varieties of comb quartz textures. A: Comb quartz growth direction from opposite sides of the vein and intersecting in the center, which was infilled with fine-grained quartz. B: Teeth-like structures of comb quartz are caused by rounded-sutured contacts and they

are intergrown with colloform features. C: Photomicrograph (plane-polarized light) of comb and colloform textures in open space. Comb texture contains euhedral clear crystals of quartz. D: Same field of view as C taken under crossed polars, photomicrograph showing interface zone and late mineralization in open space.....53

FIG 30. Photomicrograph (cross-polarized light) of comb quartz at lower part of image, and multiple-layers of mosaic textures in the upper part of image. Inclusions and impurities were trapped along the wedges of euhedral comb quartz crystals, as well as within recrystallized textures. Fine to medium grained quartz exhibit local fibrous structures, which formed perpendicular to the vein walls.....54

FIG 31. Photomicrographs of colloform textures. A: Photomicrograph (plane-polarized light) exhibiting multiple colloform layers. Lower sides of mounds are formed near the open space of veins. B: Photomicrograph (crossed polars) showing fibrous chalcedony in the colloform layers occurred with recrystallized jigsaw textures.....55

FIG 32. Photomicrograph (cross-polarized light) of (re)crystallized textures in colloform bands. Various crystal sizes are observed in these layers. Fibrous chalcedony are also found [qtz=Quartz].....56

FIG 33. Photomicrograph (plane-polarized light) showing concentric bands encrust spherical quartz grains and euhedral quartz crystals. These concentric group (or cockade) range from 0.1 to 0.3 mm in diameter.....56

FIG 34. Photomicrographs of moss quartz from the Buckskin National deposit. A: Photomicrograph (plane-polarized light) showing spherical individual grains occurred with cryptocrystalline quartz (Qcpt). B: Photomicrograph (cross-polarized light) of moss quartz in a jigsaw quartz groundmass. Some of the moss quartz exhibits flamboyant extinction.....58

FIG 35. Photomicrographs of moss-colloform textures. A: Photomicrograph (plane-polarized light) of spheres with inclusion zones showing concentric rounded grains. No inclusion zone at the middle of the photomicrograph indicates the open space in this system. B: Photomicrograph (crossed polars) of A showing completely recrystallized textures in moss structures, containing spherical inclusion zones.....59

FIG 36. Photomicrographs of plumose or feathery textures under cross-polarized light. A: Photomicrograph of plumose quartz in a background of typical quartz. B: Photomicrograph of microplumose textures associated with silica replacement and jigsaw quartz.....61

FIG 37. Photomicrographs of flamboyant textures under cross-polarized light. A: Photomicrograph of spherical quartz with fan-like extinction. B: Photomicrograph of fibrous extinction in colloform layers encrusting prismatic euhedral crystals.....62

FIG 38. Photomicrographs of relic-acicular features in replacement texture under cross-polarized light. Yellow lines probably illustrate rims or cleavages of blades that are replaced by silica. The gaps between yellow lines range from 0.2 – 0.5 mm.....64

FIG 39. Photomicrographs (cross-polarized light) showing semi-parallel bladed textures. A: Jigsaw quartz vary in sizes and replace in former bladed minerals or mineral cleavages. Sericite are found as alteration products of adularia. B: Spherical-shaped quartz grains contained fibrous-radial zones of inclusions occur between acicular grains. Yellow lines indicate acicular grained boundaries.....65

FIG 40. Photomicrographs showing reticular-patterned zones that are indicated by red and yellow lines. The angles between these lines are approximately 90°. A: Net-like patterns seen in plane-polarized light are indicated by the cutting of parallel inclusion zones in the central portion of the image. B: (crossed polars) Quartz and adularia grains ranging from 0.025 to 0.05 mm. replace in the former blades. Rectangular fibrous are found along with alteration minerals such as clays and sericite.....66

FIG 41. Photomicrograph (cross-polarized light) of intersected lines showing an X-pattern. Acicular shapes or blades of former minerals are indicated by yellow lines. Orange lines indicate single quartz crystal boundaries.....67

FIG 42. Photomicrograph (cross-polarized light) of needle-mosaic structures showing a combination of three main silica textures including crustiform (macro-texture), mosaic, and replacement textures. (Kl=Kaolinite, Qtz=Quartz, Ad=Adularia).....68

FIG 43. Photomicrographs showing needle-jigsaw replacement textures. A: Photomicrograph (plane-polarized light) of needle or fibrous-acicular shapes (red lines). These acicular shapes formed perpendicular to the vein wall. B: Photomicrograph (crossed polars) showing jigsaw quartz in colloform bands and quartz filling elongate cavities that were probably former dissolved crystals.....69

FIG 44. Photomicrograph (cross-polarized light) of zoned euhedral quartz crystals. Zones of fluid inclusions appear as bands of black tiny spots. Red line illustrates the interface boundary of crystals growth lines.....71

FIG 45. Photograph of fibrous-acicular texture in colloform bands found in the Fire Creek deposit. Colloform bands contain black tiny metallic minerals such as electrum and Ag-S-Se phases located along fibrous acicular structures (dashed lines).....73

FIG 46. Photograph of lattice bladed texture occurring with colloform bands from the Fire Creek deposit. The bladed calcite cross-cut other blades, forming an “x-shaped” structures. Late stage calcite (not bladed) is also present along pseudomorphs.....73

FIG 47. Photomicrographs of calcite found in the Fire Creek deposit. A: Calcite staining with Alizarin red S represents calcite that are indicated by red colors. This photomicrograph was taken under plane-polarized light. Colorless minerals including small grains of quartz and adularia replace carbonates. B: Photomicrograph taken under cross-polarized light showing blades and platy calcite partially replaced by silica. Later calcite likely occur perpendicular to these bladed structures exhibiting crystal growth-zoned patterns.....75

FIG 48. Photomicrographs showing adularia encrusting silica replacement texture from the Fire Creek deposit. A: Photomicrograph (plane polar) exhibits adularia, which are indicated by yellow colors, during cobalt-nitrite staining. No color zone is exhibited on quartz grains. B: Photomicrograph (crossed polars) exhibits parallel bladed texture that consists of quartz and adularia that are replacing bladed minerals (e.g. calcite).....76

FIG 49. Photomicrograph of jigsaw texture that are found in the Fire Creek samples. This photomicrograph was taken under cross-polarized light. Pseudo-rhombic adularia and quartz grains are present. The crystal boundaries exhibit sharp and straight patterns more than irregular and interpenetrated boundaries.....77

FIG 50. Photomicrographs of jigsaw texture that occurs with other textures in the Fire Creek deposit. Fibrous-acicular structures that likely formed in colloform layers occur with jigsaw textures. A: Photomicrograph (plane-polarized light) represents yellow staining colors of adularia, which is a major mineral in this texture. B: Photomicrograph (crossed polars) of A represents jigsaw features in colloform layers exhibiting various grain sizes.....78

FIG 51. Photomicrograph (cross-polarized light) of fibrous-acicular structures and jigsaw texture from the Fire Creek deposit. Adularia is present as a pseudo-rhombic crystal associated with quartz grains. The crystals vary in sizes and shapes. Needle-like shapes containing aligned inclusions and impurities are found through the crystals.....79

FIG 52. Photomicrographs of precursor amorphous silica and quartz replacement of calcite found in the Fire Creek deposit. A: Photomicrograph (plane-polarized light) exhibits calcite (high-relief) and quartz (low-relief). B: Photomicrograph (crossed polars) represents some perfectly euhedral crystals and elongated quartz surrounded by crystallized and recrystallized silica that are found in platy calcite. [Qtz = Quartz, Cb = Carbonates such as calcite].....81

FIG 53. Photomicrographs (crossed polars) of lattice-bladed textures. A: Photomicrograph represents calcite plates that are partially replaced by euhedral quartz. Quartz crystals contain inclusions and impurities along growth zones. B: Photomicrograph exhibits intersected blades separated by quartz grains. Amorphous silica are also found in some platy calcite as replacement materials. [Cb = calcite blades, Qtz = Quartz].....82

FIG 54. Photomicrograph (crossed polars) showing parallel-bladed texture found in the Fire Creek deposit. Quartz and adularia rang from less than 0.1 to 0.2 mm that are found along grain boundaries of calcite. Quartz also form in multiple textures such as jigsaw and plumose. Adularia are probably found.....83

FIG 55. Photomicrograph (plane-polarized light) of amorphous silica layers formed as spherical and colloform structures. The layers are separated by inclusions and subtextures exhibiting black, dark brown, or pale yellow color zones.....84

FIG 56. Photomicrographs showing flower-like structures and colloform-recrystallized bands from the Fire Creek deposit. A: Photomicrograph (plane-polarized light) shows radially euhedral quartz covered by very thin colloform layers. B: Photomicrograph (crossed polars) of A exhibits

inclusion trapping zones between the rims of comb quartz and colloform layers. Flamboyant extinction and (re)crystallized textures are present along colloform structures.....85

FIG 57. Photomicrographs of same area showing colloform textures found in the Fire Creek deposit. A: plane-polarized light; multiple concentric bands have encrusted larger crystals of mostly quartz and adularia along the vein walls. The open space is present at the middle between the vein walls. B: crossed polars; concentric layers individually exhibit (re)crystallized textures as elongate jigsaw quartz.....87

FIG 58. Photomicrographs (crossed polars) of fibrous chalcedony found in the Fire Creek deposit. A: Three colloform bands exhibit fibrous features that have encrusted other colloform layers and a crystal of adularia, which is approximately 0.5 mm of diameter. B: Fibrous chalcedony exhibiting flamboyant extinction occurs with a single quartz crystal and microcrystalline quartz.....88

FIG 59. Photomicrographs (crossed polars) showing flamboyant textures in colloform bands. A: Fan-shaped structure perfectly exhibits flamboyant extinction, also visible is another fan-like shape that likely recrystallized to jigsaw quartz, yet still occurs with flamboyant extinction. B: Zonal euhedral quartz is encrusted by colloform textures showing flamboyant extinction. [Qtz = Quartz].....89

FIG 60. Photomicrographs of moss quartz or ghost-sphere texture found in the Fire Creek deposit. A: plane-polarized light; perfectly spherical forms in 2D slice with nucleuses that are accumulated by colloform bands. B: crossed polars; moss quartz in 0.1 – 0.2 mm of diameter. These moss quartz have radial structures typical of (re)crystallized textures, which occur with jigsaw quartz.....91

FIG 61. Photomicrograph (crossed polars) showing rare plumose textures in the Fire Creek deposit. Large crystals of euhedral clear quartz occur with group of smaller elongate quartz, which are subdivided by different extinction angles, has formed by encrusting the large euhedral crystals. Flamboyant and jigsaw quartz also occur.....92

FIG 62. Photographs of precious-metal minerals found in Buckskin National samples. A: Ore minerals are indicated by dark fibrous-needle structure at the lower part of bands occurred with banded milky quartz. B: Ore minerals form along colloform bands. C: Polished-section of Buckskin National deposit shows dendritic and disseminated metal minerals. D: Polished-section exhibiting dendritic textures, disseminate minerals and banded ore minerals associated with colloform bands and milky glassy quartz.....95

FIG 63. Photomicrographs of dendritic-banding structures of precious metals (electrum and silver-minerals) found at the Fire Creek deposit. A: Photomicrograph taken under plane-polarized (transmitted) light showing a dendritic band of silica and opaque ore minerals in colloform bands. B: Photomicrograph taken under reflected light of the same view as that of A. These opaque ore minerals exhibit bright yellow reflecting colors. C: Photomicrograph under reflected light exhibits bright yellow individual grains and bright pale grey minerals that indicate as electrum and Ag-S-Se phases. D: Photomicrograph under the combination of reflected and transmitted lights of the

same view as that C showing colloform bands and microcrystalline textures occurred with these precious metal minerals.....96

FIG 64. Photomicrograph (reflected light) of grains of silver-selenides (grey) electrum (yellow) associated with gangue minerals from the Fire Creek deposit.....97

FIG 65. Images of ore minerals from the Fire Creek deposit and associated gangue minerals (silica and calcite). A: Photomicrograph (reflected light) showing precious metals form together with quartz and adularia that represent transformed textures. B: Photomicrograph (reflected light and crossed polars of transmitted light) showing precious metals are encrusted by calcite.....98

FIG 66. Photomicrograph (reflected light) of metal-sulfides found in the Buckskin National mine. Pseudocubic crystals indicate acanthite (Ag_2S) and associate with other sulfides in silica veins. Gangue minerals as quartz exhibit jigsaw-microcrystalline quartz in colloform banding.....99

FIG 67. Photomicrographs (reflected light) showing pyrargyrite or ruby silver minerals found in the Buckskin National deposit. A: Ore mineral band consisting of pyrargyrite (red color) and Ag-S-Se phases (black and silvery reflected colors) occurs with colloform bands of gangue minerals such as milky quartz. B: Individual grains of pyrargyrite exhibit sub-hexagonal structure and red to black colors with adamantine to submetallic lusters. These grains are surrounded by jigsaw quartz in colloform bands.....100

FIG 68. Photomicrographs of the CL emissions showing various colors that were emitted by silica phases in same view. A: Photomicrograph (plane-polarized light) showing a replaced blade associated with clear quartz crystals and zones of inclusions that are the darker zones. B: Photomicrograph (crossed polars) of jigsaw and replacement quartz textures. C: CL photomicrograph taken at 11:58:14:734 (hr:min:sec:millisec), this is a beginning period after the electron bombardment started. There are blue, yellow and dark purple bands in this texture. D: CL photomicrograph taken for 9.469 seconds later showing the disappearance of blue band. (11:58:24:203) E: After the bombardment had been started for 18.922 seconds, the brightness of yellow band was decreased and dark band became brighter (11:58:33:656). F: Dark bands completely changed to be reddish brown for a minute later (11:59:20:953)102

FIG 69. Images showing jigsaw-acicular texture from the Buckskin National deposit in same view. A: Photomicrograph (plane-polarized light) showing a needle-like structure. B: Photomicrograph (crossed polars) contains various sizes of microcrystalline-jigsaw quartz. C: Photomicrograph after the bombardment was started at 09:39:27:468, two CL colors were shown including blue and yellow. D: Photomicrograph taken on 7.657 seconds later, blue CL color is mostly disappeared and yellow band remains visible with lower brightness (at 09:39:35:125)104

FIG 70. Images showing (re)crystallized texture including jigsaw and plumose quartz from the Buckskin National deposit in same view. A: Photomicrograph (plane-polarized light) showing clear quartz crystals and small particles of impurities. B: Photomicrograph (crossed polars) showing coarse- to fine-crystal sizes occurred with euhedral to subhedral crystal forms. C: Photomicrograph taken after the bombardment started (11:34:57:734), blue band is emitted showing a homogenous texture. D: Photomicrograph taken 9.437 seconds later (11:35:07:171),

blue band is partly gone. Spots of bright reddish orange and blue colors represent calcite and pores, respectively.....105

FIG 71. Images showing euhedral comb-plumose quartz crystals from the Buckskin National deposit. A: Photomicrograph (plane-polarized light) exhibits euhedral quartz containing inclusions and impurities. B: After electron bombardment started, short-lived blue CL emission occurs with long-lived yellow CL color, which is found in zones of inclusions and impurities.....106

FIG 72. Images of colloform bands and jigsaw texture found in the Buckskin National deposit in same view. A: Photomicrograph (plane-polarized light) showing zones of inclusions and a needle structure cut across clear quartz crystals. B: Photomicrograph (crossed polars) of replacement and jigsaw textures. C: CL photomicrograph after the bombardment started (11:55:09:125), non-luminescence is occurred together with yellow and blue CL colors. D: CL Photomicrograph at 1 minute and 15 seconds after the process (11:56:24:750), multiple shades of reddish brown CL colors exhibit colloform bands.....108

FIG 73. Images of colloform textures from the Fire Creek deposit in same view. A: Photomicrograph (plane-polarized light) showing numerous colloform layers that encrust euhedral quartz crystals. B: Photomicrograph (crossed polars) represents jigsaw, flamboyant, and zonal quartz. C: CL image taken at 14:09:46:296 exhibits yellow CL colors that mostly emit from colloform layers and these layers are separated by non-luminescence boundaries. Euhedral individual crystals contain blue CL color at the cores and yellow at rims. D: CL image taken at 18.922 seconds later (14:10:05:218), yellow CL colors decrease in brightness to cream as well as blue. Black zones become brown to reddish-brown colors.....109

FIG 74. Images showing crystal growth zones in quartz and colloform textures in same view. A: Photomicrograph (plane-polarized light) exhibits a single quartz encrusted by colloform bands. Zones of inclusions and impurities are occurred. B: Photomicrograph (crossed polars) exhibits similar features found in A. Colloform bands (re)crystallized to jigsaw quartz. C: Photomicrograph (CL) at the beginning of bombardment (14:23:06:593), crystal growth zones are indicated by short-lived blue emitted colors. Note that: colloform bands do not emit any CL colors. D: Photomicrograph (CL) taken 18.969 seconds later (at 14:23:25:562), dark zones in colloform texture and in a single crystal show brown bands. Yellow and blue colors are completely disappeared.....111

FIG 75. Images showing many crystal growth zonal textures from the Fire Creek deposit. A: Photomicrograph (crossed polars) contains likely large grains and various sizes of jigsaw quartz. B: Photomicrograph (CL) of same sample as A and CL brings out a new texture not observed under crossed polars. Yellow, blue, and dark CL colors are present. C: Photomicrograph (crossed polars) showing euhedral crystals associated with jigsaw quartz. D: Photomicrograph (CL) of C exhibits zonal quartz crystals and colloform features.....112

FIG 76. Images of fibrous-acicular textures from the Fire Creek deposit. A: Photomicrograph taken under plane-polarized light exhibiting acicular structures that contain opaque minerals, likely including precious-metal minerals. B: Photomicrograph (CL) of A represents reddish pink

background associated with scatters of short-lived blue emitted colors that are caused by different quartz formations.....113

FIG 77. X-ray diffraction patterns of the epithermal veins at the Buckskin National, Fire Creek deposits, Nevada, and one sample from the Hishikari deposit in Japan. Quartz peaks occur in all samples indicated by red lines. Kaolinite peaks exhibit smaller numbers than quartz and are found only in the Buckskin National samples. Calcite indicated by blue peaks only show in the Fire Creek and Hishikari samples.....115

FIG 78. X-ray diffraction patterns of the Buckskin National samples showing almost similar patterns. (Top): XRD pattern of sample BN1 exhibits distinct quartz peaks (Q). The sample exhibits chalcedony and recrystallized-jigsaw textures in colloform layers observed by the microscope. (Bottom): XRD pattern of sample BN5 represents quartz peaks and very small kaolinite peak (K). This sample exhibits fibrous-acicular textures on hand specimen and under microscope.....116

FIG 79. X-ray diffraction patterns of the samples from Fire Creek (top) and Hishikari (bottom) deposits. (Top): XRD pattern exhibits quartz and calcite peaks found in the Fire Creek sample. The sample also exhibits lattice-pseudobladed silica texture occurred with late platy calcite. (Bottom): XRD pattern showing peaks of truscottite sample from the Hishikari deposit in Japan. This pattern exhibits broad peaks occur at 21-24 °2θ, which indicate truscottite minerals (in red rectangular). These peaks do not occur in Fire Creek.....118

FIG 80. Diagrammatic sketches of interpreted agate-forming processes from top to bottom. Spherical layers are accumulated by surface tensional forces of colloidal particles. When these spheres are connected, the fibrous-acicular structures appear to have filled tension cracks (red lines) and cross-cut colloform bands (adapted from Landmesser, 1984).....123

FIG 81. Photomicrograph (CL) of the Fire Creek sample showing hypothetical fibrous-acicular structures highlighted by red lines that are perpendicular to the colloform bandings. Colloform layers emit yellow CL color, whereas blue and dark CL colors exhibit alpha-quartz crystals.....124

FIG 82. Photomicrograph (Fire Creek sample) of interlayers of alpha-quartz and recrystallized silica colloid showing progressive growth directions of vein-forming hydrothermal fluids. Alpha-quartz (blue colors) represent trigonal structures perpendicular to wall rocks and vein direction. Silica colloids (yellow colors) repeatedly precipitated to form colloform layers.....125

FIG 83. Photograph and photomicrographs of samples from the Midas deposit showing adularia (A), and bladed calcite (B and C) found in the hydrothermal veins (from Unger, 2008).....131

FIG 84. Photographs of precious-metal minerals are associated within spherical colloform bands
A: Photograph showing silver-mineral band found in the Fire Creek deposit occurs with colloform bands. B: Photograph showing mammillary-colloform layers contain clearly comb euhedral quartz and milky quartz found in the Buckskin National deposit. Silver minerals also occur along colloform textures.....133

FIG 85. Sketch showing coarse-grained aggregates of precious-metal minerals (light grey) occur with quartz crystals (dark grey) found in the Fire Creek deposit. These features are surrounded by microcrystalline jigsaw quartz.....134

FIG 86. Sketch of precious-metal minerals (grey) in late platy calcite (indicated by blue color) from the Fire Creek deposit. Yellow particles indicate electrum. These features are surrounded by microcrystalline jigsaw quartz.....134

FIG 87. Sketch showing precious-metal minerals and multiple colloform bands in a high-grade sample from the Fire Creek deposit. Each number indicates specific feature including; 1 = Large quartz crystal, 2 = Cryptocrystalline quartz bands with disseminated electrum, 3 = Microcrystalline quartz band slightly contains coarse-grained silver minerals, 4 = Dendritic precious-metal minerals associated with euhedral and elongated crystals, and 5 = Jigsaw quartz disseminated by electrum (yellow particles).....135

FIG 88. Photomicrographs (crossed polars) of (re)crystallized-colloform bands A: Photomicrograph of Buckskin National sample showing an ore-mineral-rich band is formed between microcrystalline bands. B: Photomicrograph of Fire Creek sample exhibits opal bands interlayered with cryptocrystalline and microcrystalline colloform layers that occur below ore-rich bands (black).....136

1. INTRODUCTION

The northern Great Basin (NGB) is a large geologic province that hosts numerous high-grade gold-silver epithermal deposits, and is located in northern Nevada. Epithermal ores are of great interest to economic geologists because they are a significant source of 16% for silver and 7% for gold from epithermal historic worldwide production (Simmons et al., 2005), and because their high-grade “bonanza” nature makes them very valuable. The NGB bonanza epithermal ores commonly have striking gangue-mineral vein textures that are likely formed as a byproduct of the precious-metal ore-formation processes. Gangue minerals are economically valueless minerals, typically including quartz, adularia, and carbonates, which can be closely associated with more valuable ore minerals. However, gangue-minerals are useful for geologists to better understand the overall ore-forming processes (Rimstidt, 1997). For example, some quartz vein textures formed during gold-silver precipitation formed by crystallization of an amorphous silica precursor (Saunders, 1990; Saunders, 1994; Saunders, 1995; Dong et al., 1995). The deposition of amorphous silica requires much higher concentrations of dissolved silica than does quartz; thus this fact adds chemical constraints on one aspect of the ore-forming solution. In bonanza epithermal system, silica, electrum, and perhaps other precious-metal minerals can form colloids that can be transported upward by the rising ore-forming fluids, and they all can be co-deposited to form a colloform texture (Saunders, 1990 and 1994). Thus, these gangue-minerals textures warrant a detailed

study to better understand the overall ore-forming processes. Further, they are useful in identifying the relationship between Au-Ag precipitation and co-deposited silica-mineral textures. Standard petrographic study, augmented by cathodoluminescence investigations of vein textures, can reveal geologic evidence of mineral depositional processes and chemical composition of ore-forming fluids.

1.1 Objectives

This research is focused on two epithermal gold-silver deposits including the Buckskin National deposit, a historic gold-silver producer in Humboldt County, and the Fire Creek deposit, which is a modern underground Au-Ag mine in Lander County. To date, the Buckskin National and Fire Creek deposits have a lack of published detailed petrographic information, despite exhibiting many interesting vein textures such as colloform banding, fibrous-acicular intergrowths, and silica replacing bladed calcite. Moreover, silica textures from these deposits are similar to those observed in other well-known epithermal deposits, suggesting that these textures perhaps are universal in bonanza epithermal ores found worldwide. Therefore, the objectives of this study are to focus on the petrographic details of epithermal vein textures at the Buckskin National and Fire Creek deposits and to compare these textures to previously studied epithermal deposits, particularly the Sleeper and Midas deposits that were studied by Dr. James Saunders and former graduate students. The Mule Canyon deposit, which is located around 15 km north of Fire Creek deposit, is also compared

Additionally, in order to help constrain the hydrothermal conditions of ore-forming fluid, it is important to understand the relationship between silica phases and other gangue-minerals, and their association with Au-Ag minerals. Recognition and

understanding of the processes that led to the formation of gangue-mineral textures that are closely associated with deposition of ore minerals at the Buckskin National and Fire Creek deposits, aids in understanding of the overall ore-formation process. If the bonanza vein textures at Buckskin National and Fire Creek deposits are similar to other epithermal deposits, then petrographic interpretations based on these two deposits have implications for epithermal ore-forming processes elsewhere in the world.

1.2 Significance

This research documents and provides details of bonanza epithermal vein textures primarily through petrographic interpretations. These interpretations build on previous research on epithermal gangue-vein textures. Petrographic analysis of bonanza vein textures of the two deposits studied here, and comparisons to two other deposits in the northern Nevada, will likely lead to a better understanding of the processes that produced ore- and gangue-mineral textures.

Moreover, the use of cathodoluminescence to augment standard petrography greatly enhances textural interpretations. In particular, CL can show original quartz or silica depositional textures prior to (re)crystallization. If the gangue-mineral textures are generally similar in the northern Great Basin epithermal ores, then interpretations of the significance of relationships between gangue-mineral textures and precious-metal mineral occurrences made here perhaps can apply to epithermal deposits elsewhere.

2. BACKGROUND

2.1 Epithermal Ores and Their Genesis

Epithermal ore deposits form in certain hydrothermal systems that are related to shallow subvolcanic magmas generally formed at subduction zones. They range in age from Holocene to at least as old as the Cambrian (Simmons et al., 2005; Foley and Ayuso, 2012). However, deposits studied here formed in a narrow time range in the middle Miocene. The Northern Great Basin is an exception, having formed in association with bimodal volcanism related to the initial emergence of the Yellowstone mantle plume (Saunders et al., 2008). Epithermal deposits are typically formed by hydrothermal solutions composed of meteoric water that has mixed with magmatic fluids in various ratios. These deposits occur at shallow depth below the paleosurface, at temperatures ranging from 100 to 350 °C (Hedenquist and Lowenstern, 1994). Even though the temperature of ore-forming fluid is low by hydrothermal ore standards, ore-forming solutions episodically boiled, which was controlled by fluctuations in the ambient hydrostatic pressure. According to Lindgren (1933), epithermal ore deposits form less than 2 km below the paleosurface in veins, irregular fissures, stockworks, or pipes (as cited by White and Hedenquist, 1995). Epithermal deposits are commonly classified into two types: 1) high-sulfidation (HS) or acid-sulfate deposits, and 2) the more common low-sulfidation (LS) or adularia-sericite epithermal deposits that are distinguished by the distribution of alteration zones and geochemical compositions of ores and gangue minerals as well as ores

structures (Heald et al., 1987; Hedenquist and Lowenstern, 1994; White and Hedenquist, 1995) (Fig. 1).

High-sulfidation epithermal ore deposits are formed from acidic and oxidized solutions with pH of 0-2, and occur near magmatic source with only a small amount of groundwater mixing with metal-bearing magmatic fluids. High-sulfidation systems typically contain gold with associated copper minerals, including tennantite, tetrahedrite, covellite, and chalcopyrite. Gangue-minerals in high-sulfidation ores include kaolinite, alunite, pyrophyllite, and diaspore, and extreme acid-leaching of host rocks forms “vuggy silica” that often characterize high-sulfidation ores. High-sulfidation ore deposits usually form as disseminated and replacement ores typically controlled by local geologic structures including faults, breccia pipes, etc. The common characteristics of these deposits are the vuggy quartz bodies that locally are cross-cut by massive sulfides zones. High-sulfidation ores generally lack silica sinters at the paleosurface (e.g. Ransome, 1907; Barton and Skinner, 1979; Stoffregen, 1987; Rye, 1993; Hedenquist et al., 1994; White et al., 1995). Advanced argillic alteration is induced by high-temperature acidic fluids, which results in the characteristic mineral assemblages (e.g. alunite etc.), which are formed at the core of the mineralization and grade outward to argillic alteration in surrounding area (Steven and Ratte, 1960).

In contrast, according to Hedenquist and Lowenstern (1994), low-sulfidation ore deposits are dominated by meteoric water and with only minor amounts of magmatic fluid mixed in. Yet that “minor” magmatic contributions appears to be the source of gold and silver, associated epithermal elements (As, Sb, Se, etc.), and sulfur needed to form a bonanza epithermal ore (Saunders, et al., 2008). These systems are geothermal systems (Henley and Ellis, 1983), but geothermal systems rarely evolve to make economic epithermal ores (Saunders et al., 2008). Low-sulfidation ore-forming

fluids are near neutral-pH, typically are reduced, and thus typically form sulfide minerals associated with Au-Ag. These fluids are principally composed of NaCl, CO₂ and H₂S. CO₂ and H₂S in fluids are generally removed to vapor phase during boiling of the solutions. This results in an increase of pH, calcite precipitation, and importantly gold precipitation from gold-bisulfide aqueous complex (Au(HS)₂⁻) that enhance dissolved gold concentration in the ore-forming solutions (Shettel, 1974; Barton and Skinner, 1979; Drummond and Ohmoto, 1985; Giggenbach, 1992). Ore deposits formed in low-sulfidation system usually exhibit open-space or cavity-filling veins and stockworks as well as breccias. The common ore minerals in low-sulfidation systems consist of electrum, native gold, Ag-sulfides and sulfosalts, Au-Ag tellurides and selenides, and sphalerite, galena, and arsenopyrite also occur (White et al., 1995). Quartz, adularia, and calcite are the most common gangue-minerals. Silica and adularia show a variety of textures such as banded crustiform, chalcedonic layers, and hydrothermal vein breccias. Calcite most commonly is bladed in these deposits and formed by boiling. Boiling causes silica to concentrate in the remaining aqueous solution. Thus, boiling, along with water-wall rock reactions can lead to extreme quartz supersaturation. Boiling also leads to cooling of the aqueous solution, and this causes silica phases to precipitate and replace bladed calcite when the previously formed (Shettel, 1974; Fournier, 1985; Simmons and Christenson, 1994).

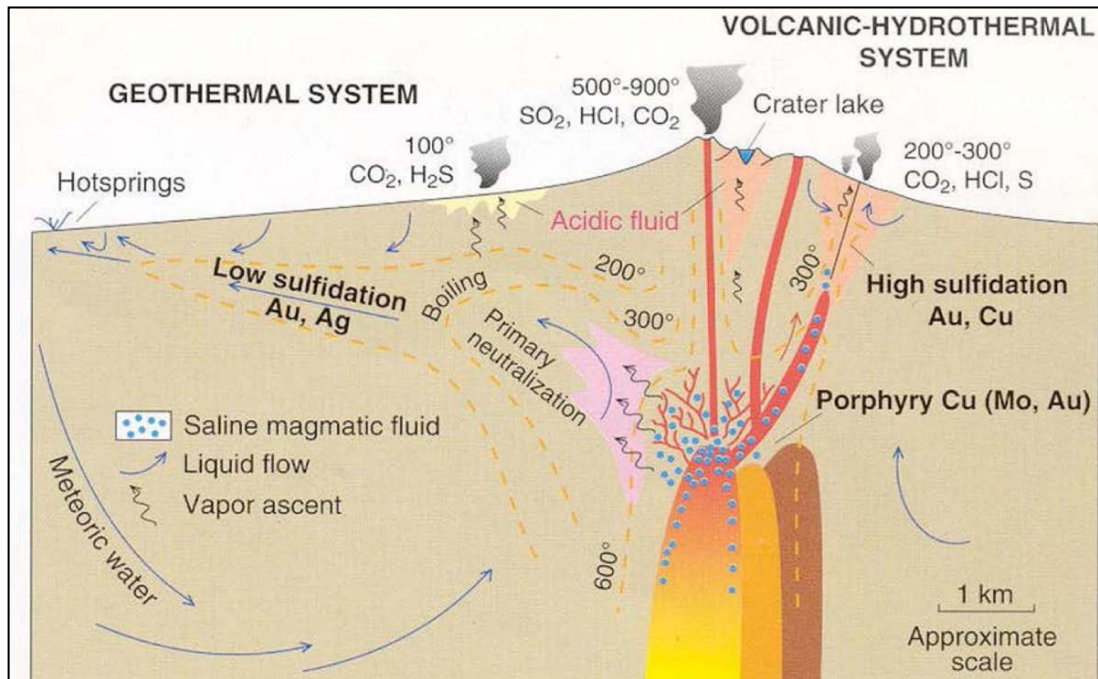


FIG 1. Schematic model showing the relations between low- and high-sulfidation epithermal deposits and porphyry deposit (from Hedenquist and Lowenstern, 1994).

2.2 Epithermal Ores in Nevada

The Great Basin hosts numerous gold-silver epithermal deposits and it includes parts of Nevada, eastern California, western Utah, and southern Oregon and Idaho. Epithermal deposits in the northern Great Basin are typically hosted by three distinct volcanic assemblages formed in the Tertiary period including the interior andesite-rhyolite, the western andesite, and the bimodal basalt-rhyolite (Best et al., 1989). Interior andesite-rhyolite assemblage is dominated by magmatism related to crustal extension and occurred as widespread andesite-rhyolite volcanic eruptions in northeast Nevada during Eocene to early Miocene epoch ranging from 43 to 24 Ma, and formed more than 50 calderas in central Nevada and western Utah (Best et al., 1989; Morris et al., 2001; John 2001). The epithermal gold-silver deposits hosted by these caldera complexes are typically smaller than other epithermal deposits in the northern Great Basin (McKee and Moring, 1996; as cited by John, 2001). Early

Miocene western andesite and middle Miocene bimodal basalt-rhyolite assemblages provide variations of tectonic settings, distinct magmatic and volcanic activities that induce specific characteristics of hydrothermal activities in the Great Basin. However, most of epithermal ores in the Great Basin have spatial and temporal relationships with the early Miocene western andesite and middle Miocene bimodal basalt-rhyolite assemblages (John et al., 1999; John, 2001).

The western andesite assemblage occurs in western Nevada and eastern California and it formed in a continental-arc environment related to a subduction zone at western continental margin of the North America plate from early Miocene to early Pliocene or at about 22 to 4 Ma. Igneous rocks in this assemblage formed by partial melting of the mantle wedge above subduction zone and are composed of volatiles and water-rich magmas related to a high potassium, calc-alkaline series (John, 2001). This western andesite assemblage hosts both low- and high-sulfidation epithermal deposits located in the west of the Great Basin (John, 2001).

In contrast, the bimodal basalt-rhyolite assemblage, has been interpreted to have formed by continental rifting along the northern Nevada rift (NNR) (Fig. 2). This rifting is interpreted to be related to back-arc extension that began at middle Miocene or around 16.5 Ma in the northern Great Basin, and help form the recent topography of the Great Basin. Hydrothermal activities appear to be directly related to magmatic activities, which occurred around 16-14 Ma (Noble, 1972; Zoback et al., 1981; Zoback et al., 1994; Christiansen and Yeats, 1992; John, 2001). The bimodal assemblage is a potassium-rich tholeiitic series consisting of mafic components of basalt to andesite forming lava flows, feeder dikes, and cinder cones, and felsic components such as flows, domes, and ash-flow tuffs of peralkaline composition. The 16-14 Ma bimodal igneous rock assemblage hosts only low-sulfidation epithermal ore

deposits including with magmatic mixing and non-magmatic fluid. Sulfur and oxygen fugacities in the bimodal assemblage are lower than the western andesite assemblage, as same as the base metal contents and silver/gold ratios, whereas the selenides mineral content from the bimodal assemblage is significantly greater than the western andesite assemblage (John et al., 1999; Hedenquist et al., 2000).

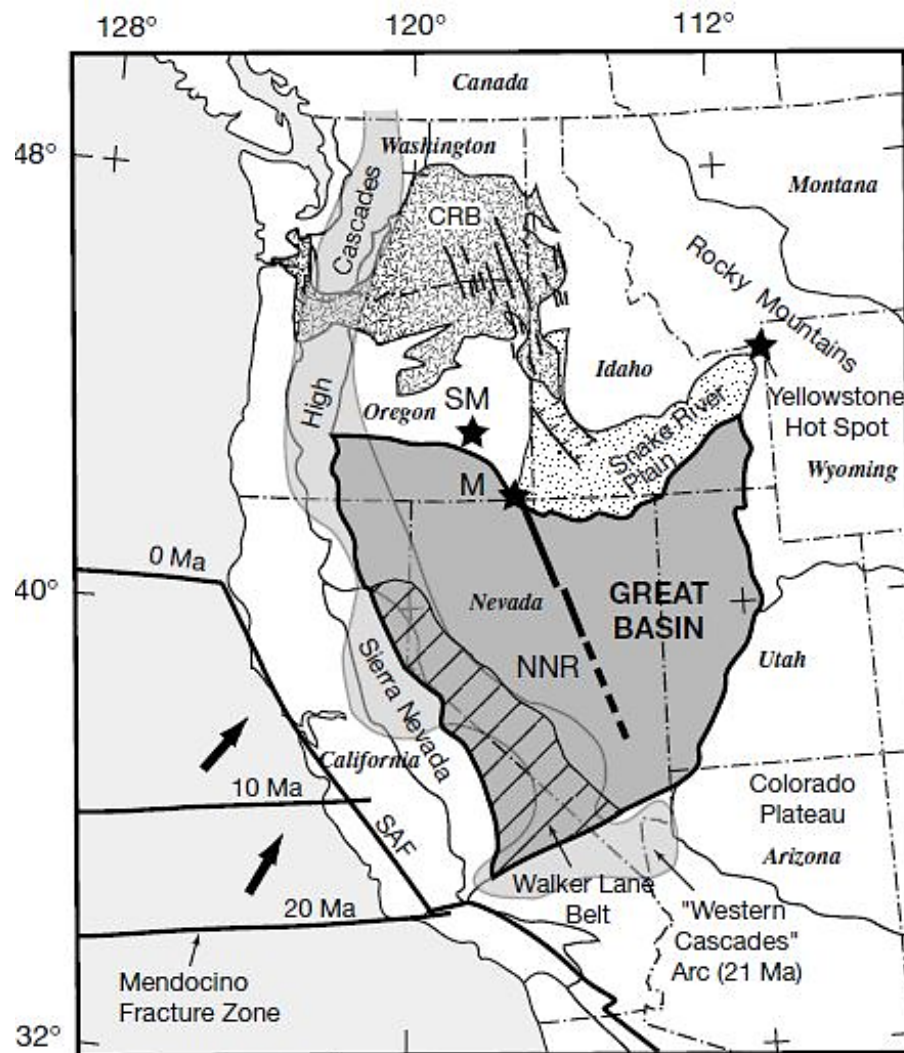


FIG 2. Map of the Great Basin in western United States showing middle Miocene igneous and tectonic features. Darker shaded area represents the Great Basin and lighter shaded exhibits the western andesite assemblage forming the Western Cascades at around 21 Ma. Heavy line in the north-central Great Basin indicates the continental northern Nevada rift. Other lines represent feeder dikes within the Columbia River Basalt Group (CRB). NNR = northern Nevada rift, M= McDermitt caldera, SM = Steens Mountain (from John, 2001).

2.3 Middle Miocene Clan of Epithermal ores in Northern Great Basin

Noble et al. (1988) noted that most of epithermal gold-silver deposits in northern Great Basin are associated with magmatic and hydrothermal activities occurring from 16 to 14 Ma (middle Miocene). Importantly, significant high-grade epithermal ore deposits, many of which contain more than 1 million ounces of gold, occurred at this time (Vikre, 1985; Wood, 1988). Many authors relate the formation of both the bimodal magmatism and epithermal ores to the development of the northern Nevada rift (Noble et al., 1988; McKee and Moring, 1996; Long et al., 1998; John et al., 1999; John, 2001).

Saunders et al. (1996) first proposed that the middle Miocene epithermal ores and the associated bimodal volcanism were driven by the initial emergence of the Yellowstone in the northern Great Basin. In contrast, John et al. (1999) and John (2001) concluded the magmatic and tectonic processes related to the middle Miocene epithermal ores in the northern Great Basin were must closely related to the northern Nevada rift. The bimodal assemblage occurs widespread in mostly northern Nevada, Owyhee Plateau in southeastern Oregon, and southwestern Idaho (Fig. 3). During the early stages of extension in the Great Basin, the basin and range topography formed, and rift grabens, basaltic dike swarms, rhyolitic domes, and shield volcanoes occurred (Fig. 4). Kamenov et al. (2007) studied the Pb-isotopic ratios in precious-metal- and gangue-minerals in the epithermal ore deposits of the NGB. They concluded that precious metals were derived from mafic magmas of the bimodal magmatic assemblage, which formed as a result of the northern Nevada rift, which they proposed was caused by crustal extension related to the initial appearance of the Yellowstone hot spot in middle Miocene.

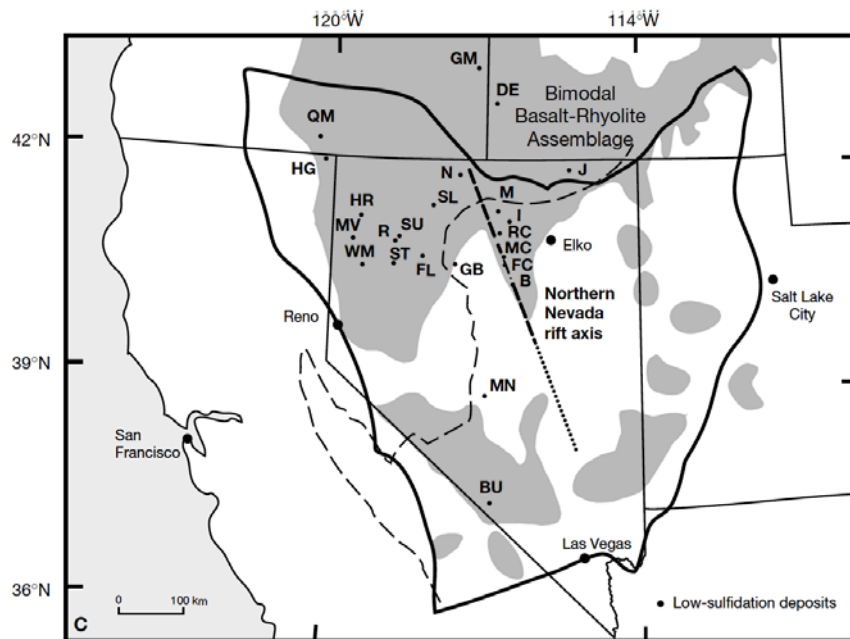


FIG 3. Map showing low-sulfidation deposits in the North Great Basin (black border) that are associated with a bimodal basalt-rhyolite assemblage indicated by grey shades (from John, 2001). [SL=Sleeper, M=Midias, FC=Fire Creek, N=National/Buckskin National, MC=Mule Canyon, DE=DeLamar (e.g. Silver City district), GM=Grassy Mountain, QM=Quartz Mountain, HG=High Grade, HR=Hog Ranch, MV=Mountain View, WM=Wind Mountain, R=Rosebud, SU=Sulphur, ST=Seven Troughs, FL=Florida Canyon, GB=Goldbanks, RC=Rock Creek, B=Buckhorn, J=Jarbidge, MN=Manhattan, BU=Bullfrog].

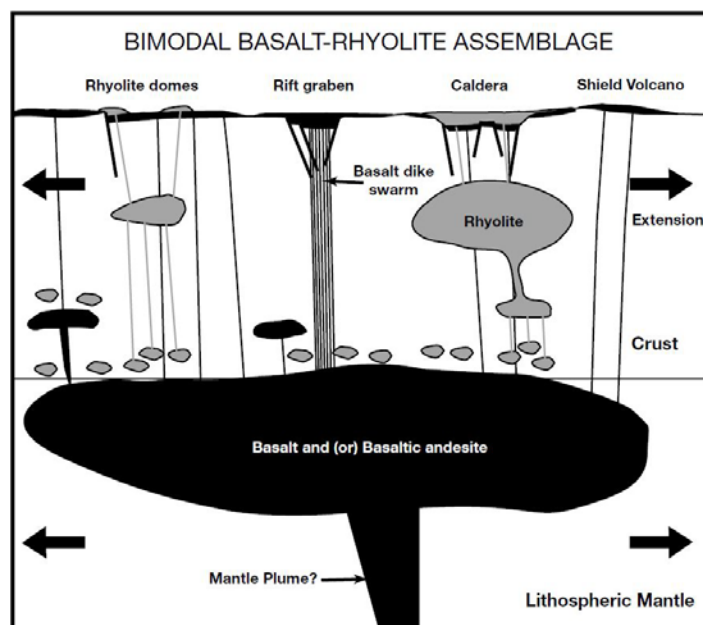


FIG 4. Schematic model (from John, 2001) showing magmatic and tectonic events of the bimodal basalt-rhyolite assemblage in the northern Great Basin. These processes are relating to continental extension and mantle plumes underneath the area.

Saunders et al. (2008) and Hames et al. (2009) proposed that the mafic magmas of the bimodal assemblage are the source of metals, metalloids, and sulfur required to produce these middle Miocene low-sulfidation epithermal deposits in northern Great Basin. They suggested that precious metals were initially derived from partial melting of “fertile” mantle to produce basalts enriched in Au and then released from mafic magmas as magmatic fluids that eventually reached the epithermal setting. The magmatic fluids were transported upward and mixed and absorbed by the heated meteoric water that was generated by rhyolitic magmas at shallower depths. These mixed fluid formed the bonanza veins in open fractures and faults, and locally discharged to the surface to form metal-bearing silica sinter (Fig. 5) (e.g. Vikre, 1985; Nash et al., 1989, Conrad et al., 1993; Saunders et al., 2008). The NGB paleosurface sinter deposits are best preserved in the National district (Vikre, 1985, 1987, and 2007), Silver City district, Idaho (Mason et al., 2015), Holister gold deposit in Ivanhoe district (Bartlett et al., 1991; Wallace and John, 1998; Wallace, 2003), and also Fire Creek deposit (Blakely and Jachens, 1991; Wallace and John, 1998; J.P. Whitemore, pers. commun., 2016).

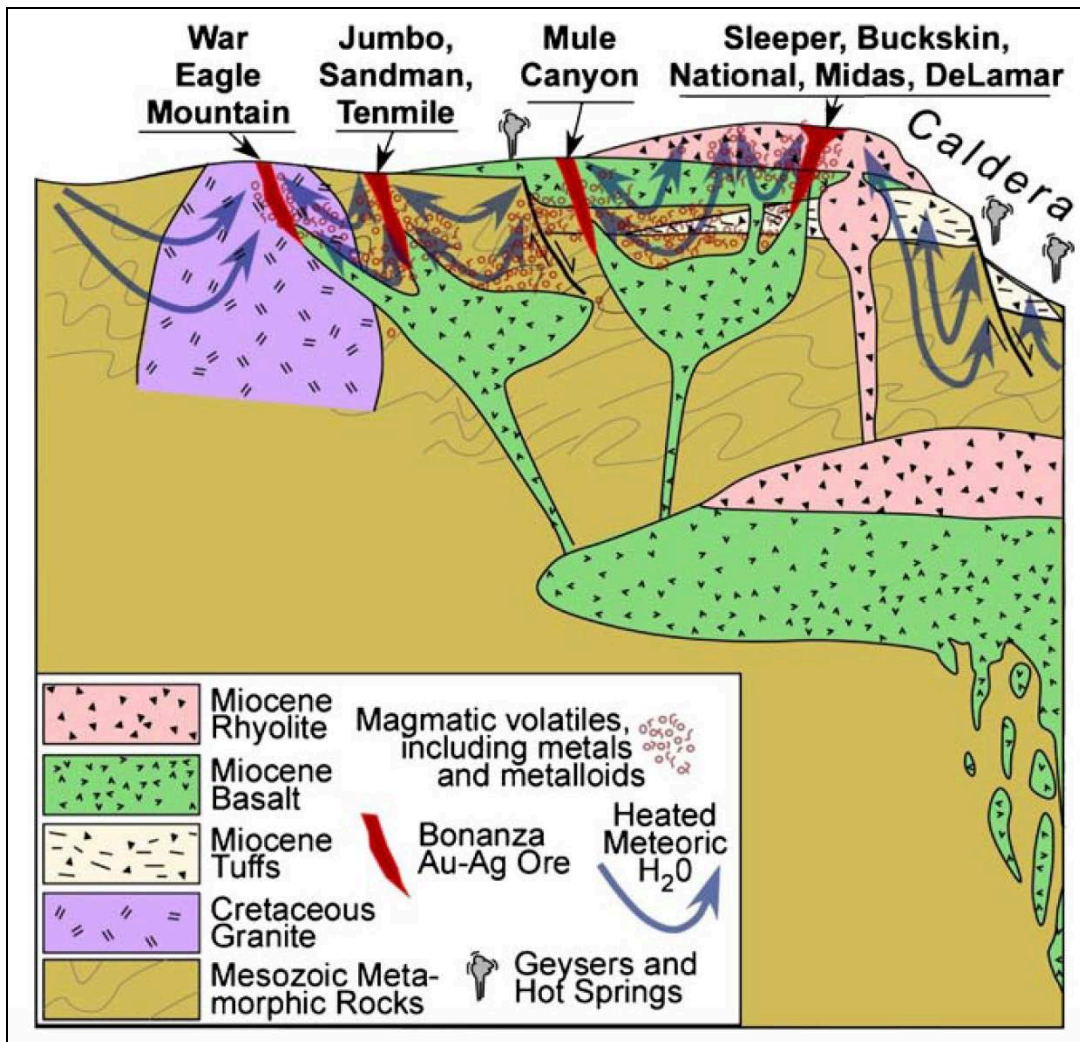


FIG 5. Diagrammatic model showing magmatic and hydrothermal processes forming the low-sulfidation epithermal ore deposits in the North Great Basin in Nevada. The bimodal basalt-rhyolite assemblage in northern Nevada and granitic intrusion in southwestern Idaho host bonanza ore deposits (from Saunders et al., 2008).

Super-high-grade ores where electrum is the main ore minerals are found in the Sleeper, National, and Fire Creek deposits. Lindgren (1915) proposed that, in the National mining district, ores are hosted by rhyolites, which come from the same epoch of eruption with basalts in the northern Nevada. Gold and quartz precipitated together from the same solution. Lindgren (1933) also showed a photomicrograph of ore from the National deposit and stated that both electrum and silica formed as colloids. Saunders (1990 and 1994) documented that the multiple gold depositing

events at the Sleeper deposit were recorded in the banded veins there, and the ore bands typically consisted of aggregated electrum and silica colloids. Conrad et al. (1993) also studied on the geochronology of the Sleeper using the ^{40}Ar - ^{39}Ar age dates and suggested that hydrothermal alteration and ore mineralization occurred at about 16.2-14 Ma. The origin of Sleeper deposit are related to bimodal volcanism in the northern Nevada. Saunders et al. (1996) stated that colloidal electrum in nanoparticles can be transported upward in the ore-forming solutions and simultaneously deposited with silica colloids caused the high-grade ores at the Sleeper and National deposits in northern Nevada. These processes were important to form bonanza epithermal ores in the North Great Basin and western United States.

One of the most detailed studies of low-sulfidation deposits in the NGB is the Mule Canyon (John et al., 2003). It is a basalt-andesite hosted, middle Miocene epithermal deposit that formed at around 15.6 Ma. Basaltic-andesitic dikes formed between 16.4-15.8 Ma, which host ores in the Mule Canyon deposit have been interpreted to be part of the bimodal rhyolite-basalt assemblage that occurs throughout the northern Great Basin. The hydrothermal ore-forming solutions consisted of meteoric water that perhaps flowed through the deep Paleozoic sedimentary basement rocks and mixed with some magmatic fluids derived from Miocene volcanism. The ores mostly formed at temperatures below 200°C at near hydrostatic pressures, causing episodic boiling. Ore types include 1) disseminated base-metal sulfide minerals in altered and weakly silicified rocks, and 2) open-space filling ores including electrum, Ag-sulfides, Ag-selenides, and minor ores such as pyrite, marcasite, and arsenopyrite. These ores occur with gangue minerals consisting of quartz, opal, chalcedony, adularia, calcite, and dolomite (John et al., 2003).

The Midas deposit is hosted by Miocene rhyolitic-volcanic rocks (Goldstrand and Schmidt, 2000). Leavitt et al. (2004) documented that high-grade epithermal gold-silver veins in the Midas low-sulfidation epithermal deposit formed in faults at around 15.4 Ma and were induced by the northern Nevada rift in northern Nevada (Fig. 6). Leavitt et al. (2004) proposed that middle Miocene bimodal basaltic-rhyolitic magmas served primarily as a heat source, which caused circulation of meteoric water and ore formation. The authors also concluded that the ages of rhyolitic host-rocks and ore mineralization are linked together and the felsic volcanism of bimodal assemblage and tectonic events (e.g. faults and tilting) induced the deposition of the high-grade ores in the Midas deposit. More recent study of the Midas deposit by Chitwood (2012) suggested that the temperatures that induced precious-metal precipitation are around less than 250°C. Precious-metal minerals precipitation was also induced by boiling events, which caused bladed calcite in epithermal ores such as at the Midas deposit (Simmons and Christenson, 1994).

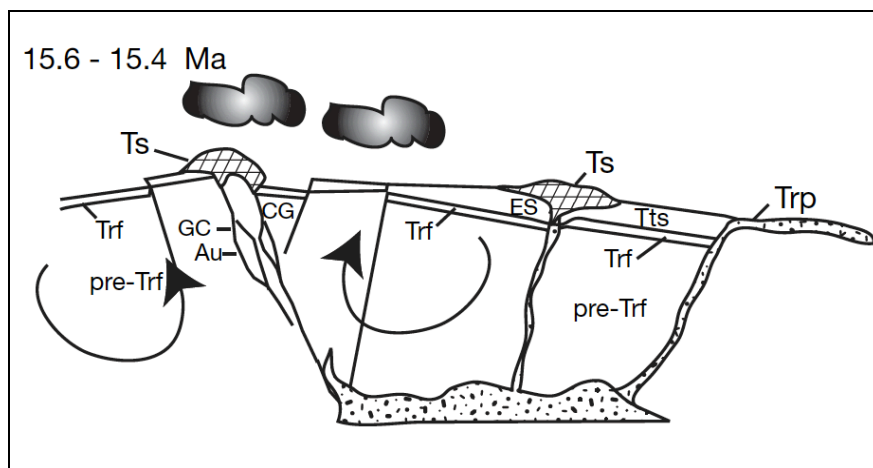


FIG 6. Schematic NE-SW cross section showing the emplacement of bonanza veins along main oblique-normal faults during 15.6-15.4 Ma at the Midas low-sulfidation epithermal system (from Leavitt et al., 2004). [Au=Bonanza ores, Ts=accumulation of sinter, Tts=opalized sediment, ES=Eastern Star, Trf=rhyolite flows, CG=Colorado Grande structure]

Mason et al. (2015) studied epithermal veins in Silver City district, Idaho, which are the northernmost middle Miocene epithermal ores associated with the bimodal magmatic assemblage in the northern Great Basin. However, the Silver City district does not appear to be related to northern Nevada rift as it is well north of it (see Fig. 3). The authors also documented that the epithermal veins formed slightly later than the middle Miocene basalt and rhyolite wall rocks in deposits on War Eagle and Florida Mountains in the Silver City district. The main ore minerals observed are naumannite, aguilarite, Se-rich acanthite, electrum, and ruby-silvers, along with minor base-metal sulfides such as galena, sphalerite, chalcopyrite, and pyrite. Silica sinter deposits formed at the paleosurface in the Silver City district have been preserved by down-faulting, and are similar to sinters at the crest of Buckskin Peak in the National district.

2.4 Previous Works on Buckskin National and Fire Creek Deposits

Epithermal deposits in this study include the Buckskin National and Fire Creek deposits, which are located in the northern Great Basin and hosted by middle Miocene volcanic and intrusive rocks, which are part of the regional bimodal basalt-rhyolite magmatism (Fig. 7). Vein textures in these deposits also briefly compared to those at the Sleeper deposit, which is located 80 km southwest of the Buckskin National deposit, and the Midas deposit, which is located 100 km north of the Fire Creek deposit (Fig. 8). According to Vikre (1985, 1987 and 2007), John (2001), and Klondex Mines Ltd. (2015), the Buckskin National and Fire Creek deposits, which are located 240 km far from each other in northwest-southeast, have different host-rock compositions, although similar in age. General details of their geologic formations and settings are described based on previous works.

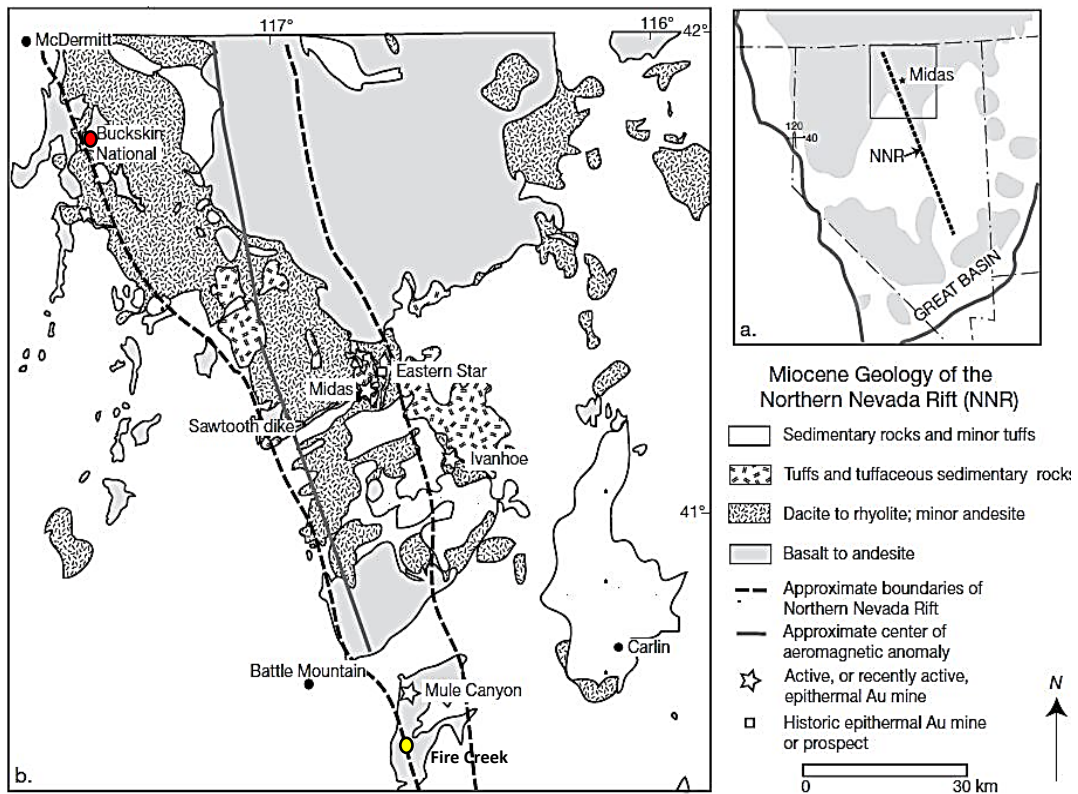


FIG 7. Map showing general geology of a portion of the NGB that contains Buckskin National and Fire Creek deposits (indicated by red and yellow dot, respectively). The bimodal basalt-rhyolite assemblage and the northern Nevada rift are the major geologic features of the region (modified from Leavitt et al., 2004).

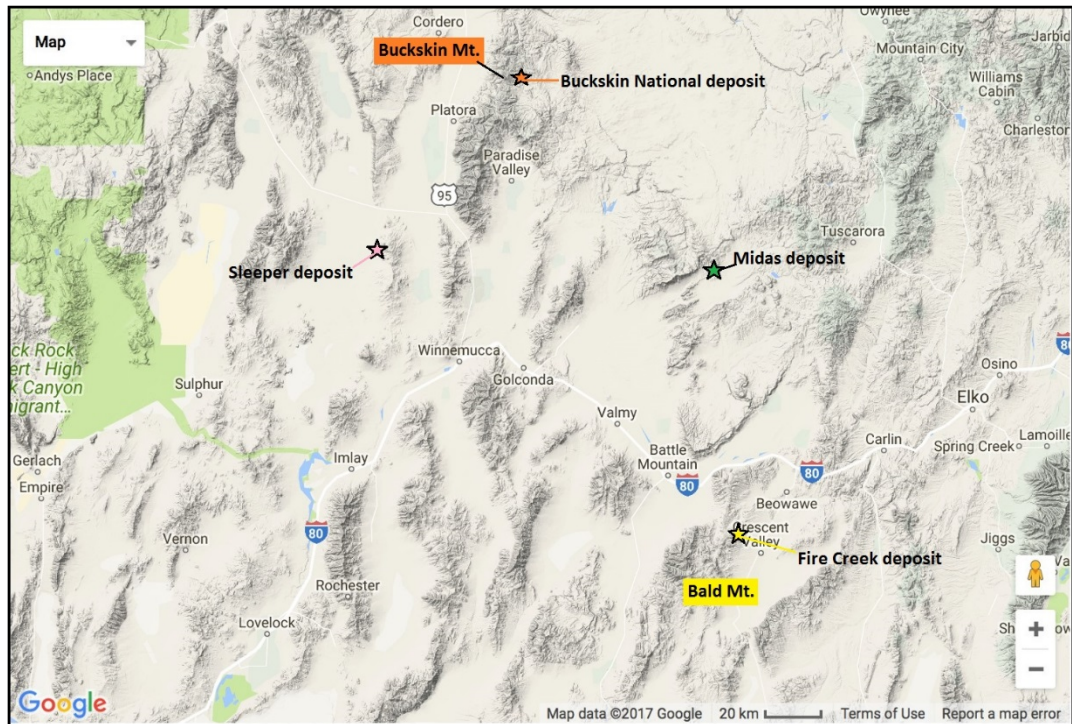


FIG 8. Map showing the northern part of the northern Great Basin that includes Elko, Lander, and Humboldt counties, Nevada. Locations of the principal deposits studied here (Buckskin National and Fire Creek deposits) are shown, as are two other deposits (Sleeper and Midas) that are used for comparison in this study. (Google Map, 2017)

2.4.1 Buckskin National Deposit

The Buckskin National deposit, which is located 120 km north-northeast of Winnemucca, Nevada, was a minor underground Au-Ag producer in the 1930s. It is located along the east slope of the Buckskin Mountain in Humboldt County at N 41.79239 °, W 117.54069 ° with an elevation of 7729 ft. mean sea level (Diggings™, 2017) (Fig. 9).

Lindgren (1915) proposed that the Buckskin Mountain in the National district in Nevada was formed by rhyolitic dikes that were probably a similar age as associated basaltic flows. Silica sinter at the top of the Buckskin peak, which is evidence of former hot springs, defines the middle Miocene paleosurface in this area. Later studies by Vanderburg (1938), Willden (1964), and Vikre (1985) also suggested

that this deposit is hosted by early to middle Miocene volcanic-clastic rocks, including rhyolitic pyroclastic rocks, andesite, rhyolite, and basalt. Ore minerals such as silver, electrum, naumannite (Ag_2Se), and base metal sulfides are associated with gangue minerals such as quartz, adularia, and chalcedony. Mercury also occurs on the sinter of the Buckskin Mountain. Vikre (1985) studied precious-metal veins in the National district and described the Bell vein at the Buckskin Mountain. The terms Bell vein and Buckskin National deposit are essentially synonymous in the economic geology literature for the area. The Bell vein was mined approximately 270 to 440 meters beneath the paleosurface and produced around 24,000 ounces of gold and 300,000 ounces of silver from 34,000 tons of ores during 1906 to 1941. The author described that veins formed around 15.6 Ma, and are hosted by approximately 18-15 Ma rhyolites (Fig. 10). Vein minerals include cinnabar, stibnite, electrum, silver sulfosalts, silver selenides, and base-metal sulfides occurred with silicate minerals such as quartz and kaolinite. The ore minerals precipitated in open-space veins at about 250°C and 40 bars of pressure from boiling solutions. The temperatures then dropped to 200°C, which caused continued silica deposition. At the paleosurface, the temperatures decreased to approximately 100°C in the hot springs. Vikre (1987) described the paleohydrology of epithermal veins that cross-cut in altered Miocene volcanic rocks at the Buckskin Mountain in the National district, Nevada. The author also suggested that the geomorphology of Yellowstone National Park in Wyoming today and of the Buckskin Mountain in Miocene would have been very similar. Vikre (2007) interpreted four stages of time-space variations of the Bell vein on Buckskin Mountain. Each stage was observed at different elevations and consists of specific vein and mineral assemblage. Stage 1 represents the oldest hydrothermal quartz veining, whereas stage 2 exhibits banded quartz and precious-metal minerals

including silver selenides, silver sulfides, and electrum. Stage 3 veins contain predominantly base-metal sulfides and chalcedony. The last event (stage 4) includes quartz and chalcedony with cinnabar forming the sinter at the paleosurface. Vikre (2007) also found several narrow bands (beds) in the sinter that had a similar enrichment of Au-Ag-Se as the deeper epithermal vein.

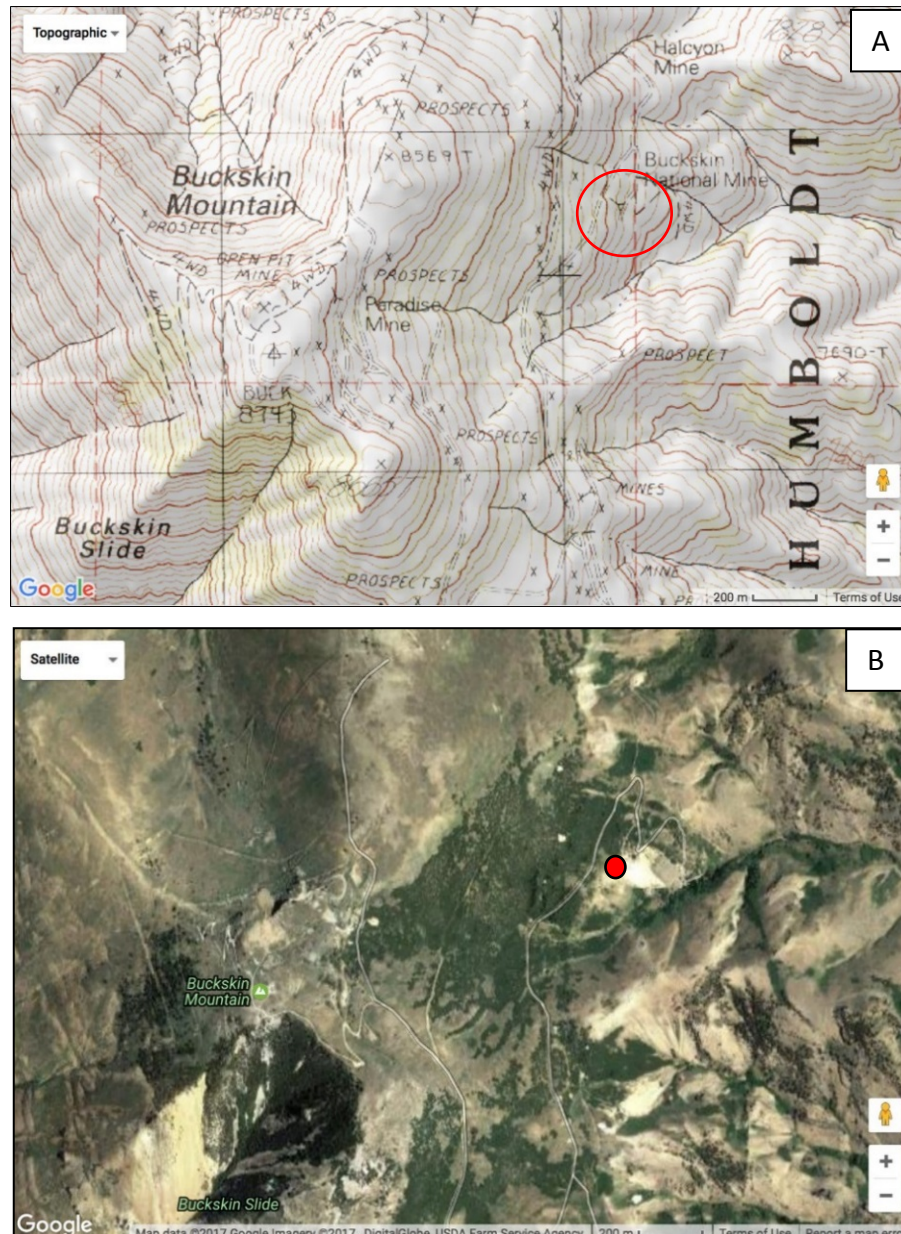


FIG 9. A: Topographic map showing the Buckskin National deposit with mine entrance shown by the red circle. B: Satellite map of the Buckskin Peak area with the red dot showing the location of the Buckskin National adit. (Google map, My Topo, 2017)

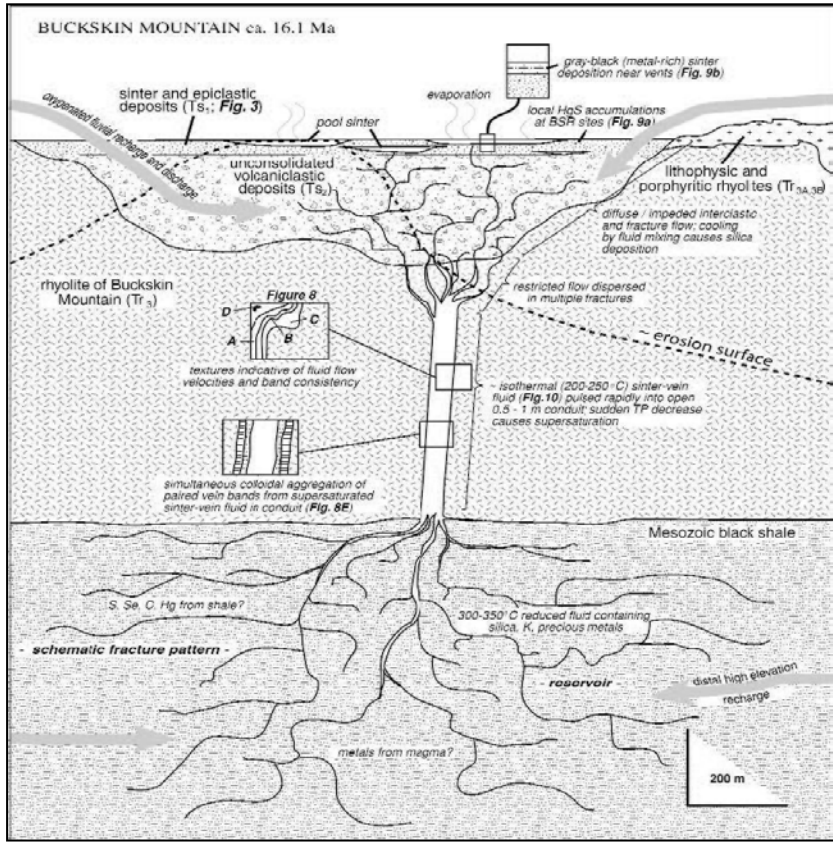
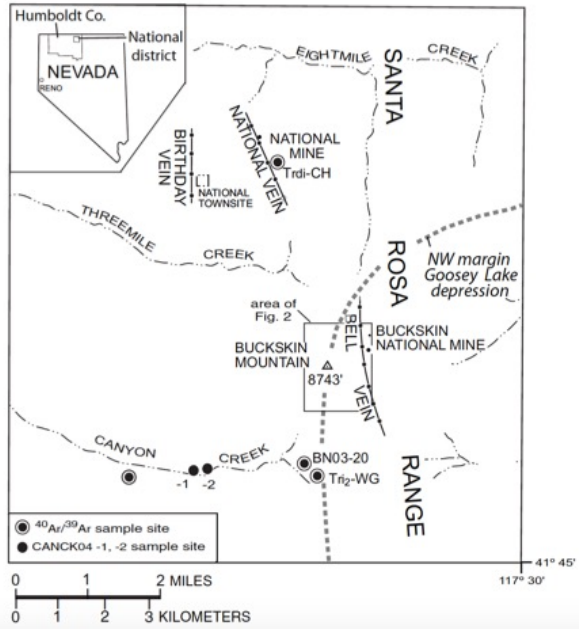


FIG 10. *Top*: Index map of Vikre (2007) showing the location of Bell vein, which refers to Buckskin National deposit in National district. *Bottom*: Schematic model showing rhyolitic-volcanic sequence of the Buckskin Mountain that host veins. Dash line indicates a recent surface (Vikre, 2007).

2.4.2 Fire Creek Deposit

The Fire Creek deposit is a currently producing underground mine located approximately 240 km southeast of the Buckskin National mine at N 40.467068°, W 116.656967°. It is located in Lander County, approximately 40 km south-southeast of Carlin, NV. Additionally, the Fire Creek mine is approximately 15 km south of the Mule Canyon deposit that was associated with the same bimodal magmatism assemblage as the Buckskin National, Sleeper, Midas, Mule Canyon, and National deposits (John, 2001) (Fig. 11).

Klondex Mines Limited, which operates this deposit, described the general geology of the Fire Creek deposit (Klondex Mine Ltd., 2015). There, epithermal quartz-calcite veins are hosted by Miocene basalts and basaltic andesites and these veins formed along the regional north-northwest trending structures. They are underlain by early Paleozoic clastic rocks (Fig. 12). Veins at the Fire Creek deposit formed at 15.81-15.99 Ma with approximately growth rate of one band per 27,000 years (Kassos et al., 2015; W. Hames, pers. commun., 2017).

Reported recoveries include 94% for gold and 92% for silver. The total ore reserves are currently around 240,000 tons averaging 41.59 g/t of Au and 32.2 g/t of Ag. The total resources are 931,000 tons with 18.43 g/t of Au and 16.4 g/t of Ag. Gold mineralization are found two types, including (1) shallow structure-controlled gold in altered Tertiary basaltic host rocks, and (2) a native gold occurring with quartz and calcite in discrete banding veins, which are investigated in this study. The vein textures, gangue mineral assemblages, and alteration indicate that Fire Creek is a low-sulfidation epithermal system (Klondex Mines Ltd., 2015). The Fire Creek deposit is arguably the highest grade operating large gold mine in the world.

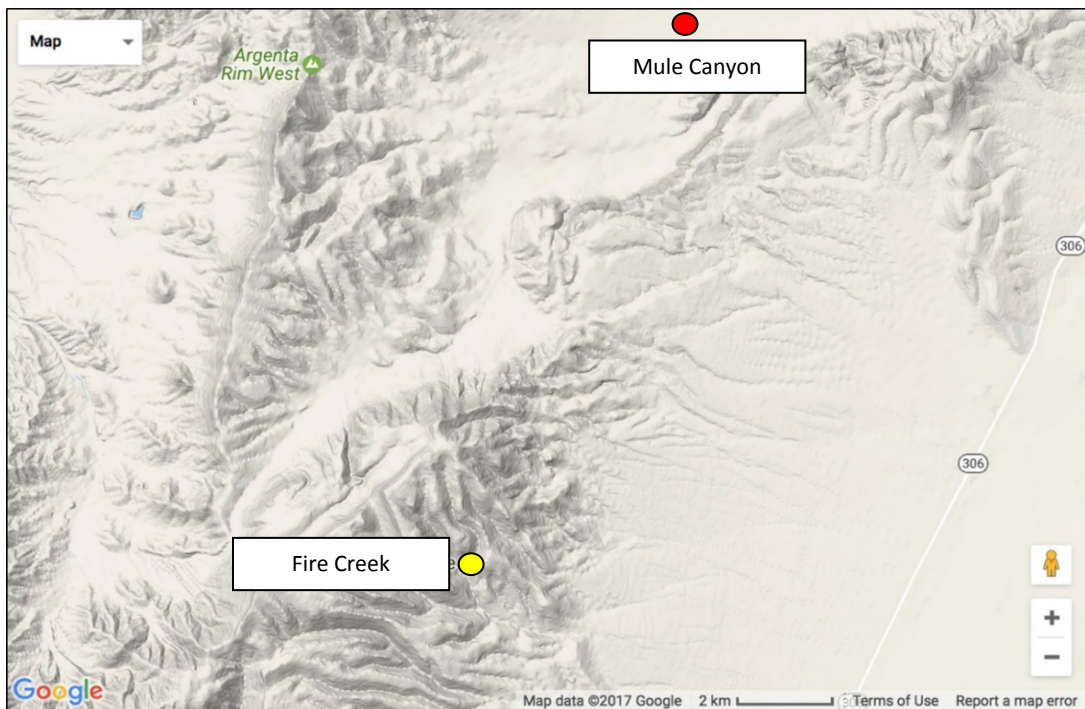


FIG 11. Map showing the locations of Fire Creek deposit, which is mined at the northeast of Bald Mountain as an underground mine owned by Klondex Mines Limited, shown as a yellow dot and the Mule Canyon deposit shown as a red dot. (Google map, 2017)

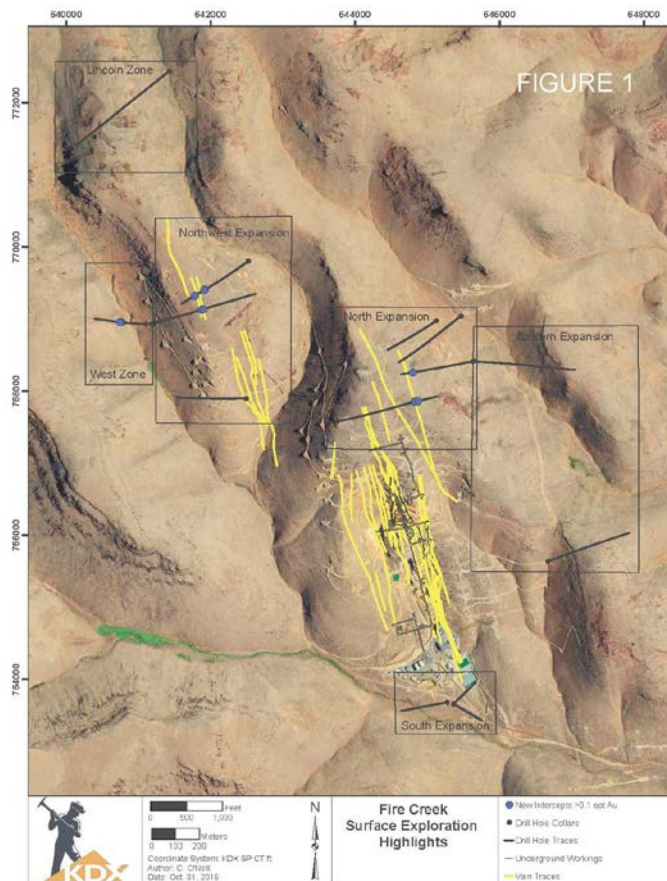
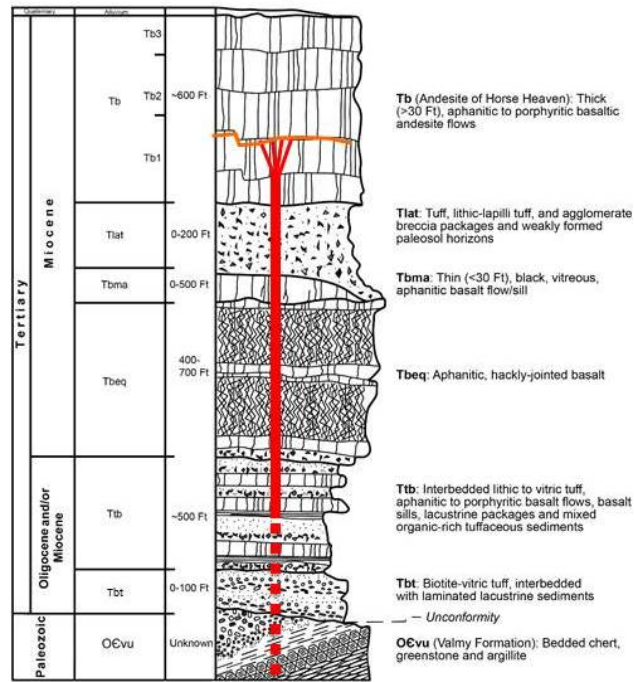


FIG 12. *Left:* Map (left) showing underground workings vein traces projected to surface, and the NNW of vein structures at Fire Creek deposit (from O’Neill, 2016). *Right:* Stratigraphic column of volcanic sequences host ore veins formed in the Fire Creek deposit (from Kassos et al., 2015).

2.5 Gangue Mineral Textures of Epithermal Veins

According to previous studies, epithermal-hydrothermal ore deposits commonly consist of quartz, adularia, and calcite, which are gangue minerals that occur with precious-metal minerals in the veins (Hedenquist and Lowenstern, 1994). These gangue minerals, which exhibit variable vein textures, are common in the low-sulfidation epithermal systems in the North Great Basin. Their textures have been interpreted and described in many previous studies.

Lindgren (1915) described pseudomorphic replacement of bladed calcite found in hydrothermal veins in the National mining district, northern Nevada. Quartz and adularia are formed together in these veins. Precious-metal minerals including electrum, ruby silver, cerargyrite, and other Ag-minerals are found in these veins. Lindgren (1933) described dendritic gold in very fine-grained quartz, which he interpreted formed from colloids, and often formed after coarse-grained (comb) quartz. Fine-grained electrum is also accompanied by small portions of other ore minerals such as pyrite, chalcopyrite, naumannite, and argentite.

Adams (1920) studied silica veins of hydrothermal origin in epithermal ore deposits in the United States, Japan, Canada, Mexico, New Zealand, and Australia. The author investigated the variety of silica textures that occur in epithermal-hydrothermal vein deposits, silica crystallization, quartz structures in free space, recrystallized silica and replacement textures. Adams (1920) proposed several names for textures found in the hydrothermal vein systems including crustiform, cockade, colloform, micro-botryoidal gel structure, comb quartz, ghost-sphere, lamellar quartz, pseudoacicular, and retiform structure. The classification of silica textures of Adams (1920) was essentially adopted and modified by Dong et al. (1995).

Sander and Black (1988) suggested that it is common for opal and chalcedony to crystallize and recrystallize to form quartz in epithermal environment. The authors proposed the term plumose quartz to describe anomalous extinction that occurs at the rims of quartz crystals. Then quartz grains also commonly exhibit discoloration and variable refractive indices due to the presence of former silica phases.

Silica veins in the Sleeper deposit exhibit a variety of silica textures including colloform, fine-grained, and microcrystalline highly banded quartz often containing gold and silver particles. The extensive banding in the veins at Sleeper represent discrete ore- and gangue-mineral depositional events during vein formation (Saunders, 1994). Moreover, the author noted that silica textures typically formed by crystallization of amorphous silica in the bands, which formed by coagulation and aggregation of colloidal silica particles along the vein wall. Thus, each band represents a coating of the vein wall at a particular time. Although former amorphous silica is very common and formed numerous silica bands in the veins, many such bands contain no electrum.

Dong et al. (1995) classified and reviewed silica mineral textures in epithermal deposits from northern Queensland, and from previous works elsewhere. Their classification includes three main groups, which follows crystal behaviors and structures. Many silica vein textures found in northern Great Basin in the United States are apparently similar to these found by Dong et al. (1995) in Queensland. The authors also proposed that there is a positive correlation between gold precipitation and amorphous silica that were observed as colloform bandings. The three groups defined by Dong et al. (1995) for hydrothermal vein textures including primary, recrystallization, and replacement textures are described below.

1. Primary quartz textures are directly formed by cooling, boiling, repeatedly mixing, or chemical reactions of hydrothermal fluids. These textures include crustiform, cockade, colloform, moss, comb, zonal, and flamboyant quartz textures (Fig. 13). Crustiform texture consists of multiple discrete bands of ores and gangue minerals and it exhibits different colors, mineral compositions, and micro-textures. This texture is often best observed in hand specimens (Adams, 1920). A texture showing concentric crustiform bands that include layers and pieces of previous veins and/or wall-rocks, is called a cockade texture. Importantly, a crustiform band that typically consists of colloidal silica that recrystallized to form a colloform texture. According to Wherry (1914), the term of colloform is applied to unstable colloidal particles. Rogers (1917) then proposed the term colloform for rounded spherical forms of silica/silicate colloids deposited in open space. These layers occur as spherical and mammillary forms probably caused by surface tension and very slow rate of impurity diffusion compared with rate of crystal growth (as cited by Marinova et al., 2014). Even though amorphous silicate layers commonly crystallized to quartz, chalcedony, and adularia, the colloidal precursor layers are commonly still visible. This texture sometimes represents rounded spheres, which are probably caused by other orientations. Because of a moss-like shape, Dong et al. (1995) proposed that this sphere like textures is called “moss quartz”, whereas Adams (1920) called as micro-botryoidal gel structure. The most distinct primary texture in epithermal veins is comb quartz. This texture consists of a layer of euhedral quartz crystals that have one side connected to vein walls and another side pointed out to open space representing euhedral to subhedral crystal forms.


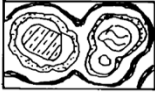

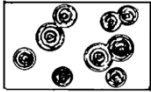
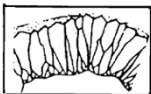

Texture Type	Sketch of Texture	Grain Size	Grain Form	Internal Feature of Individual Crystal	Morphology of Crystal Aggregate	References
Primary Growth Textures						
Crustiform		variable	variable	not applicable	successive banding	Adams (1920) Shaub (1934) Lindgren (1933) Buchanan (1981)
Cockade		variable	variable	not applicable	concentric banding	Adams (1920) Spurr (1926)
Colloform		fine	fibrous anhedral	not applicable	semi-spherical, reniform, mammillary	Rogers (1917) Adams (1920)
Moss		fine	variable	not applicable	spherical	Adams (1920)
Comb		variable	prismatic	not applicable	parallel-orientated	Adams (1920) Schieferdecker (1959) Boyle (1979)
Zonal		variable	prismatic zonal		not applicable	Smirnov (1962)

FIG 13. Sketches of primary growth textures including crustiform, cockade, colloform, moss, comb, and zonal quartz veins are referred from other previous studies. Grain sizes, form, morphology, and internal structure are provided (from Dong et al., 1995).

2. Recrystallized textures are textures that are induced by crystallization or recrystallization process. These textures exhibit the changing of amorphous silica microcrystalline quartz to crystalline quartz, or chalcedony to quartz. Jigsaw, plumose, and ghost-sphere quartz indicate recrystallization processes occurred in microstructures of vein textures (Fig. 14 and 15). Jigsaw or mosaic quartz was described by Lovering (1972) from silica jasperoids in Nevada, and is a common texture of silica veins in epithermal deposits (Saunders, 1990). It is a group of crystalline to microcrystalline anhedral quartz crystals that have irregular or sutured boundaries between crystals. Thus, these irregular boundaries look like a jigsaw puzzle. Plumose texture is a feathery or plumose extinction within a euhedral quartz crystal. This extinction radiates out from a core of crystal crossing the crystal growth

zones. When small crystals form within a large euhedral crystal, they then synchronously develop and recrystallize, but these small quartz crystal aggregates provide slightly different extinction. There are two appearances of plumose texture controlled by behavior of fine-grained quartz crystals and one coarse-grained quartz. If these quartz crystals continually grew together, plumose texture is defined as fine-grained elongated quartz crystals formed along growth zones of the euhedral host quartz with different extinction angle. On the other hand, if only a single large host quartz continually grew, these fine-grained quartz eventually encapsulated within the host grain with different extinction. Moreover, Adams (1920) focused on flamboyant as a fibrous structural habit in quartz veins (as cited by Sander and Black, 1988). Flamboyant texture is a recrystallized texture that chalcedony is transformed to quartz (Williams et al., 1985). Flamboyant texture in Dong et al. (1995) is defined as fibrous extinctions with rounded surfaces that typically encrust euhedral crystals. The last texture is a ghost-sphere. After moss quartz grains are formed, the surrounding unstable amorphous silica, microcrystalline quartz, and moss itself start to transform to quartz, which is the most stable silica phase thermodynamically. This texture is not obviously recrystallization because it sometimes represents crystallization of amorphous silica to chalcedony or quartz. It clearly indicates a secondary texture that composes of crystallized or/and recrystallized textures.

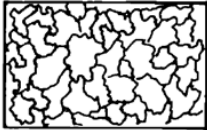

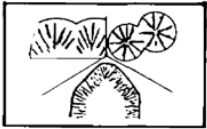

Texture Type	Sketch of Texture	Grain Size	Grain Form	Internal Feature of Individual Crystal	Feature Morphology of Crystal Aggregate	References
Recrystallization Textures						
Mosaic		fine	anhedral	not applicable	interpenetrating	Lovering (1972) Saunders (1990)
Feathery		variable	prismatic	plumose	not applicable	Adams (1920) Sander and Black (1988)
Flamboyant		variable	round	radial	not applicable	Adams (1920) Sander and Black (1988)
Ghost-sphere		fine	anhedral	spherical	not applicable	Adams (1920)

FIG 14. Sketches of recrystallization/crystallization textures including mosaic (jigsaw), feathery, flamboyant, and ghost-sphere quartz that are found in this study (from Dong et al., 1995).

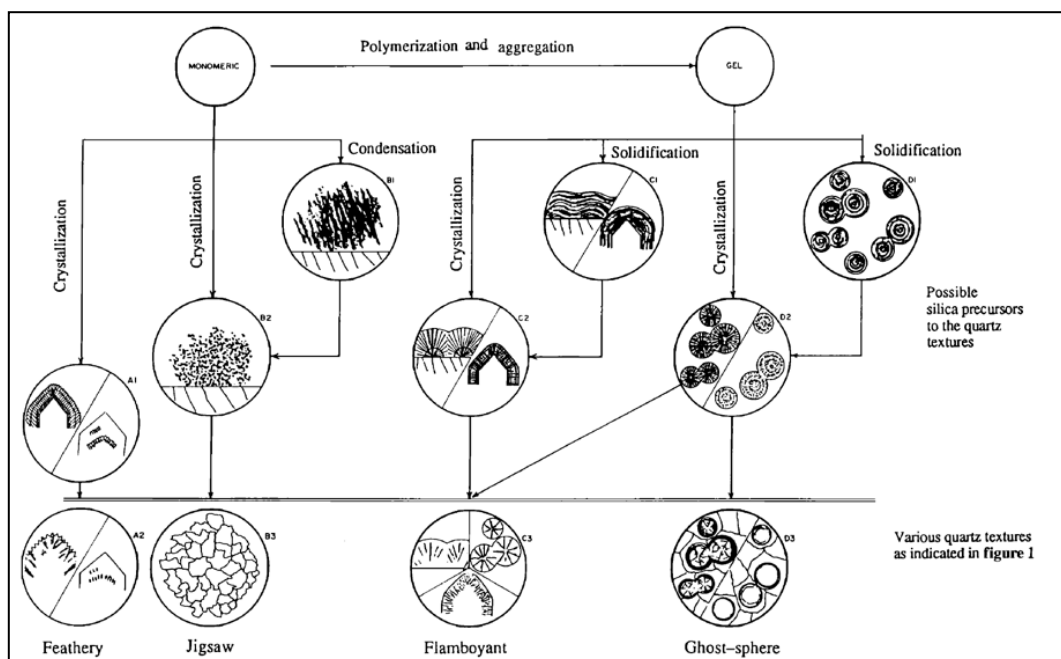


FIG 15. Diagrammatic illustrations of proposed origins of recrystallization/crystallization textures of amorphous or/and cryptocrystalline silica (from Dong et al., 1995).

3. Replacement textures involve preservation of the shape of the original mineral that has been replaced by another mineral. Replacement is caused principally by changing ore-forming composition due to chemical mixing of other hydrothermal fluids or boiling. Replacement processes possibly occur multiple times during vein formation. Shettel (1974) suggested that quartz or silica is dissolved in the volatile-poor solutions, whereas calcite commonly precipitates in the same conditions during boiling. Fournier (1985) noted that the remaining silica-supersaturated solutions, which provide acidic components, can react with calcite and induce neutralization at shallow depth. Calcite is then dissolved and replaced by silica when the temperature drops. Silica replacement of bladed calcite is very common in low-sulfidation systems (Simmons and Christenson, 1994). Because calcite has a retrograde solubility, it is dissolved during a temperature drop at the constant pressure and can be replaced by silica precipitation (Holland and Malinin, 1979). After silica replacement of calcite occurs, bladed forms still exist as silica pseudomorphs including pseudobladed, pseudoacicular, and saccharoidal textures (Fig. 16 and 17). A pseudobladed texture is a calcite blade replaced by silica and occurs with three distinct patterns including lattice bladed, impurities-concentrated bladed, and parallel bladed. A pseudoacicular texture is a radial bladed texture related to the growth of carbonate crystals within silica gels. These crystals then were dissolved by hydrothermal fluids and left the original shapes as voids for later silica replacement. A saccharoidal texture is caused by randomly silica diffusion within a granular carbonate crystal. Quartz commonly forms as interlocking anhedral crystal shape. Occasionally, calcite blades are only partly dissolved and exists along with the replacing silica. Rarely, bladed calcite can be completely preserved from replacement, which is common at the Midas deposit (Leavitt et al., 2004; Unger, 2008), and locally at Fire Creek deposit.



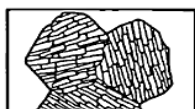

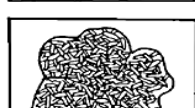
Texture Type	Sketch of Texture	Grain Size	Grain Form	Internal Feature of Individual Crystal	Morphology of Crystal Aggregate	References
Replacement Textures						
<u>Pseudo-bladed</u> <u>Lattice-bladed</u>		fine	anhedral	not applicable to prismatic	intersecting bladed	Lindgren (1899) Schrader (1912) Morgan (1925)
<u>Ghost-bladed</u>		fine	anhedral	not applicable	intersecting bladed	
<u>Parallel-bladed</u>		fine	anhedral to rectangular	not applicable	parallel bladed	Adams (1920)
Pseudo-acicular		fine	anhedral to rectangular	not applicable	acicular	Lindgren and Bancroft (1914) Adams (1920) Schrader (1923)
Saccharoidal		fine	anhedral to prismatic	not applicable	interlocking	Lindgren (1901) Adams (1920) Lovering (1972)

FIG 16. Sketches of replacement textures including pseudo-lattice bladed, ghost-bladed, parallel-bladed, pseudo-acicular, and saccharoidal (from Dong et al., 1995).

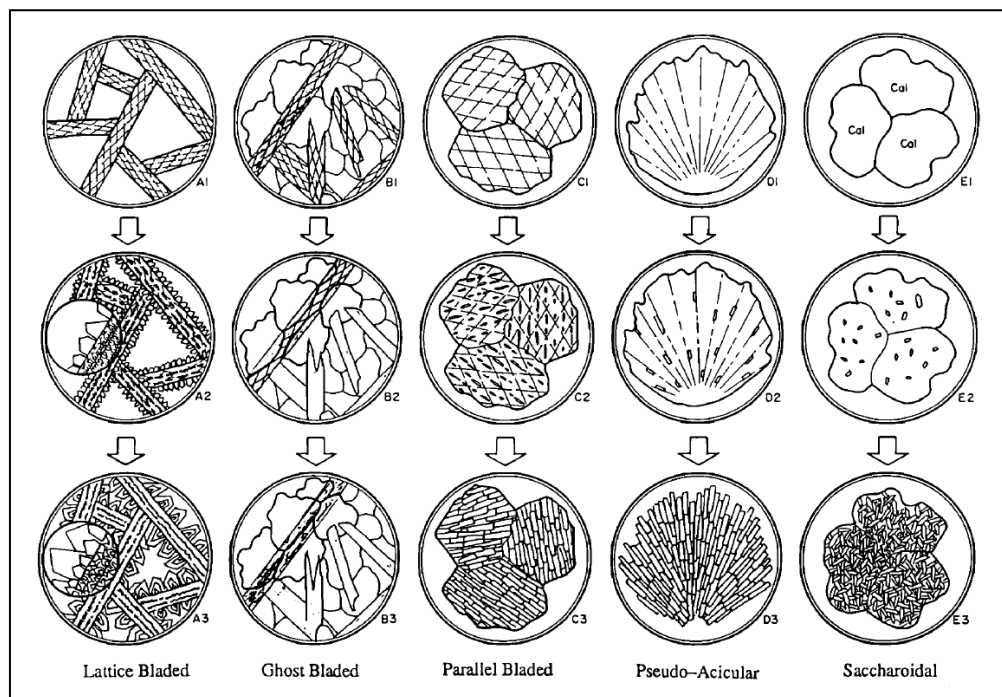


FIG 17. Sketches of interpreted evolution of replacement textures of silica-carbonate veins in epithermal deposits (from Dong et al., 1995).

Although the work of Dong et al. (1995) is still the most comprehensive description and interpretation of silica textures in epithermal ores, more recent studies have also described them in individual deposits. Shimizu et al. (1998) described a variety of quartz textures that were found in the Koryu epithermal Au-Ag deposit, Hokkaido, Japan. They described textures that include such terms as comb, feathery, microcrystalline, fibrous, dendritic, flamboyant, ghost-sphere, colloform, and pseudoacicular textures. Many of the textures described by Shimizu et al. (1998) are similar to the textures exhibited by Buckskin National and Fire Creek deposits in Nevada. A more recent study at Koryu by Shimizu (2014), documented multiple quartz textures (including crustiform, comb, microcrystalline, colloform, cockade, and platy) that occur with bonanza-grade ores. Fluid inclusions in the variable quartz textures were used to determine the temperature and presence or absence of boiling condition in the fluids. Comb quartz formed early in the veins at deeper levels and is overgrown by varieties textures of later quartz. At Koryu, boiling apparently caused bonanza precious-metal precipitation concurrent with silica colloids deposition, resulting in a colloform textures that formed at less than 500 meters depth.

Vikre (2007) described the detailed hydrothermal events that formed vein-sinter textures at Buckskin Mountain. He documented symmetrical to asymmetrical bands, plumose dendrites, delaminated bands, fibrous bands, and pseudomorphs after carbonates from the banded quartz veins exposed in underground mine workings. These vein textures were derived from silica gels caused by supersaturated fluids and transported as colloids to deposit at the shallow paleosurface. The author also described amorphous silica crystallization and the relationship between precious metal transportation and specific silica textures found in veins and sinter at the Buckskin Mountain.

Moncada et al. (2012) interpreted conditions for each silica texture observed at an epithermal silver-gold deposits along the Veta Madre deposit at Guanajuato, Mexico. They interpreted fluid inclusion characteristics that were found in silica textures to identify conditions of vein-forming fluids. These fluid inclusions can be separated into three types, including non-boiling, boiling, and flashing conditions of hydrothermal fluids. Non-boiling state, which is indicated by only liquid-rich inclusion assemblages and no vapor-rich inclusion, induced rhombic and massive calcite, zonal, cockade, and comb quartz textures, whereas jigsaw, plumose, colloform banding, bladed calcite, crustiform, ghost-sphere, and moss textures indicated boiling-supersaturated solutions. Fluid-inclusion assemblages in the boiling state consisted of liquid-rich and vapor-rich inclusions. This “flashing” stage induce amorphous silica precipitation from silica gels that occurs in response to rapid pressure and temperature decreases. These amorphous silica then (re)crystallized to quartz and chalcedony. Boiling conditions appear to have led to precipitation of precious-metal minerals at the Veta Madre deposit in Guanajuato.

2.6 Textural Terminology for This Study

The silica texture classification scheme proposed by Dong et al. (1995) is essentially adopted for this study to classify and identify silica vein textures in the Buckskin National and Fire Creek deposits. In these two deposits, veins are composed of quartz, adularia, and alteration products of adularia including sericite and kaolinite. Variations in quartz grain sizes or crystal structure, are likely affected by hydrothermal and crystallization and recrystallization processes. Three main types of silica textures including primary, (re)crystallized, and replacement occur in the two

deposits. Thus, the proposed textural terms that are used to describe bonanza vein textures observed in this study are summarized below.

Crustiform is defined as a group of symmetrical layers formed in open spaces in fractures and faults. The layers exhibit variable colors, morphologies, and mineral composition. This texture is commonly best observed in hand specimens. If the layers exhibit a concentric pattern that was deposited on individual grains or fragments during earlier vein formation, this is called a cockade texture.

Colloform is a term used to define colloids or nanoparticles. Nanoparticles, which are less than 100 nm in diameter, do not have requirement to be in an aqueous state, whereas colloids are mixed substances with properties between solution and fine suspension (“Colloid”, 2006). This texture refers to a mammillary spherical banding exhibited on the external surface (e.g., points toward vein center). It consists of, chalcedony, recrystallized quartz, and fibrous-acicular structures that are generally perpendicular to vein walls (Dong et al., 1995). Colloform texture is produced by aggregation of colloidal silica (or nanoparticles) that may also include dendritic electrum features formed by precipitation and transportation of Au-Ag colloids (Saunders, 1990; Saunders, 1994). Colloform silica textures are 3-dimensional coating on vein walls; a 2-dimensional silica (as in a thin-section) through this can result in circular features in microcrystalline-quartz groundmass. Moss quartz is also a name for this feature (Dong et al., 1995). If microcrystalline quartz is the groundmass for the (re)crystallized spheres, then it is called as a ghost-sphere texture (Adams, 1920).

Comb quartz is a term for a euhedral quartz crystals that formed perpendicular to vein walls occurred with adjacent quartz crystals. It sometimes exhibits teeth-like

form. Zonal texture also forms in euhedral quartz that contains zones of fluid inclusions and impurities along the crystal growth zones.

Jigsaw quartz, the most common feature that occurs in the Buckskin National and Fire Creek deposits, exhibits aggregates of microcrystalline or cryptocrystalline quartz with irregular and jigsaw-like boundaries (Lovering, 1972; Saunders, 1990). In Dong et al. (1995), mosaic texture for this jigsaw texture, was interpreted as the result of a recrystallization process in the veins.

Flamboyant texture exhibits radial-fibrous extinction on outer edges of quartz crystals. This texture usually occurs when colloform silica layers have recrystallized. It may also have formed by recrystallization of a fibrous chalcedony (Sander and Black, 1988). Plumose texture in this study is classified in slightly different way from Sander and Black (1988). Plumose quartz is used for a texture that exhibits feathery-extinction only along the rim of coarse-grained quartz crystals. This texture was called a feathery by Adams (1920).

Silica replacing texture can be found in the Buckskin National and Fire Creek deposits. These replacement textures mostly exhibit silica pseudomorphs after bladed calcite. Lattice-bladed texture is a platy form that contains quartz and adularia, also chalcedony in some cases. This texture is indicated by intersected blades that distinctly exhibit sets of elongate silicates, which are pseudomorphs after bladed calcite, and occur with comb, jigsaw, and flamboyant textures (Dong et al., 1995). Parallel-bladed texture refers to parallel traces surrounded by rectangular-elongate quartz in space in the pseudomorphs (Dong et al., 1995). This texture was also called lamellar quartz by Adams (1920). Pseudoacicular texture is a silica replacement of calcite blades that exhibit radial patterns occurred with silica textures (Adams, 1920; Dong et al., 1995).

For this study, a texture called fibrous-acicular commonly forms in colloform layers. This texture is slightly different from other replacement textures that the replaced minerals are unknown and formed fibrous-acicular patterns along colloform-crustiform bands. Fibrous-acicular texture sometimes occurs with opaque ore minerals in colloform bands.

Textures of precious-metal minerals in this study are described using the terminology based on Saunders (1994) and Saunders and Schoenly (1995). Fractal dendritic texture is a texture showing tree-like or dendrite-like structure of electrum, which was formed by aggregation of electrum colloids. The dendrites are typically associated with microcrystalline silica phases and even doubly terminated quartz crystals. Banded structures of metallic minerals also occur with gangue mineral bands. Additionally, disseminated texture is found as individual grains widespread in some layers.

3. METHODOLOGY

3.1 Field work

Prior to this study, an extensive suite of ore samples had been collected by Saunders, Hames, and Auburn University students from the Buckskin National deposit over the last 10 years, along with a few samples of Fire Creek deposit collected in 2015. To augment these for the present study, a field trip was conducted in late July, 2016 to northern Nevada from the Fire Creek and Buckskin National deposits to collect additional samples. At the Fire Creek deposit, samples were collected in the underground mine directly from out-cropping veins (Fig. 18). During the visit, numerous carbonate-silica veins were observed cross-cutting the basaltic host-rocks, and coarsely crystalline electrum was observed in-place in the mine working (Fig. 19). Thirteen samples were collected for further study in the lab. Additionally, samples were collected on dumps from the Buckskin National mine, and the adit and dumps are located on eastern flank of the Buckskin peak at an elevation of around 8,000 feet (Fig. 20). A number of new samples were collected that exhibit variety of vein textures were collected to prepare for thin-sections and polished-sections at Auburn University and a commercial lab (Precimat, which is a division of Precilab, L.L.C.)

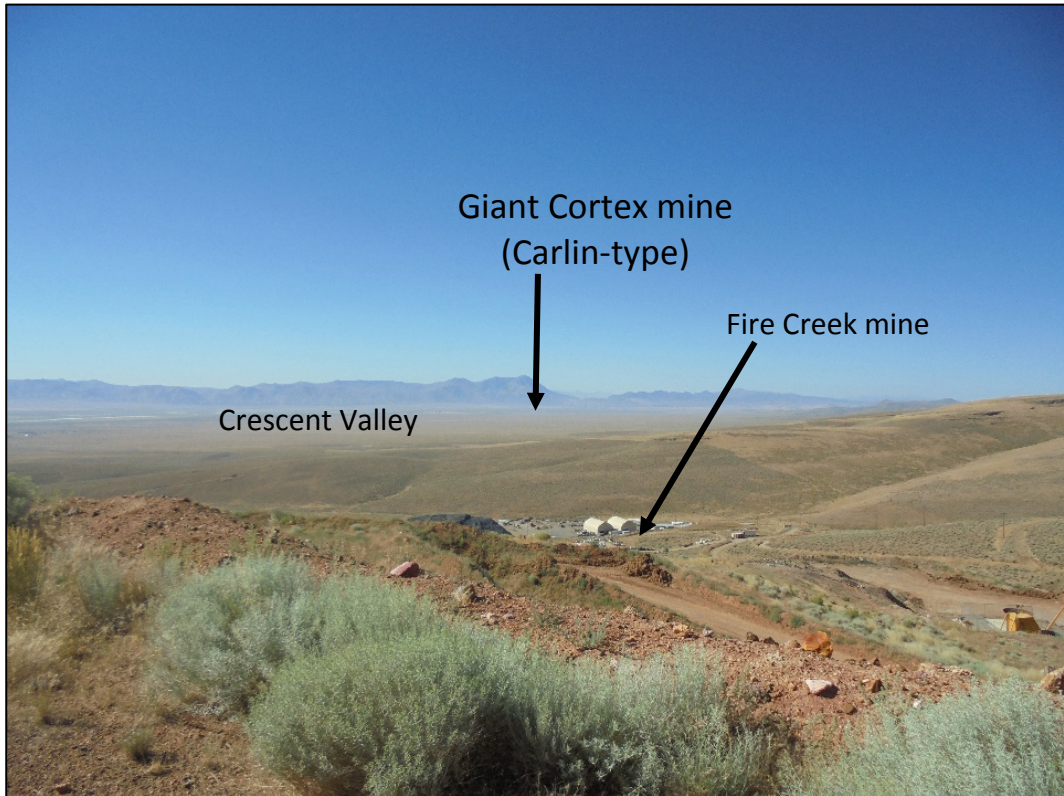


FIG 18. Photograph of Fire Creek underground mine taken from the top of basalt flows as paleosurface on the Bald Mountain. The Fire Creek deposit is located on the Crescent Valley and the Tenabo Mountain is on the other side, where is the location of giant Cortex mine operated by the Barrick Gold Corporation.

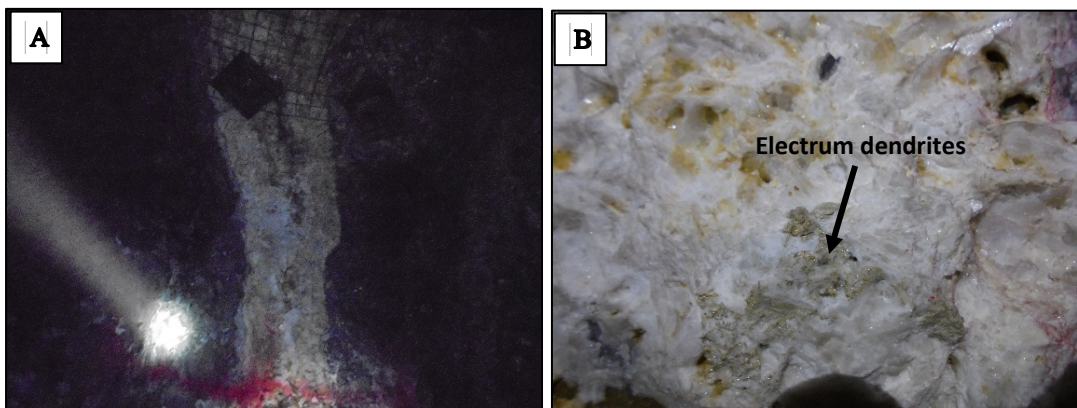


FIG 19. Photographs taken underground showing carbonate-silica veins from the Fire Creek deposit. **A:** Photograph of a calcite-silica vein (yellowish white color) cutting the country rock (dark color). The approximately width of the vein is about 30 cm. **B:** Feathery dendrites of electrum occurring within calcite-silica replacement texture.

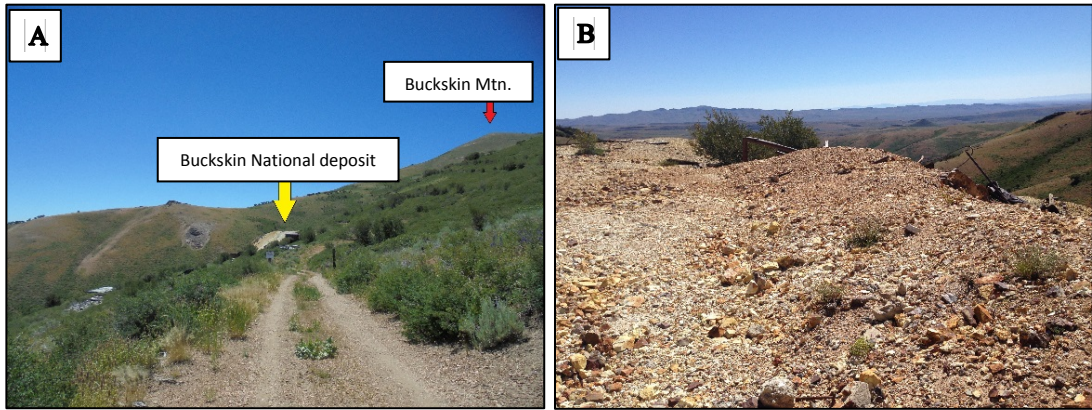


FIG 20. Photographs of Buckskin National mine. A: Location of Buckskin National underground mine that is at the southeast of the Buckskin Mountain. B: The mine dumps of the underground mine, where samples were collected.

3.2 Petrographic Methods

Petrographic analysis of silica veins of the Buckskin National and Fire Creek deposits was done using a conventional petrographic optical microscope at Auburn University. Fifty-nine thin sections of Buckskin National and Fire Creek deposits, along with nine polished-sections, were made for petrographic study.

Microscopically, silica textures and mineral components were observed under plane- and cross-polarized light and the interpretations and descriptions of these textures were classified based primarily on the previous work of Dong et al. (1995) as discussed above. The silica textures that were found in the samples were enumerated and the most common and least common textures of each deposit were determined. Reflected light was also used to observe precious-metal minerals associated with silica/gangue minerals and to identify silica textures that are associated with these phases.

3.3 X-Ray Powder Diffraction

Selected gangue minerals exhibiting interesting textures were interpreted for mineral composition by using X-ray powder diffraction method (XRD) of the Bruker model. The rock slabs were grounded to powder. These powders then were interpreted in the D2 PHASER XRD analyzer of the Bruker model using Cu K-alpha radiation with 1.54184 Å (Bragg Brentano geometry) at 30 kV of voltage and 10 mA of current. The coupled two theta/theta of scan type and the continuous PSD fast of scan mode were used with effective total time of 3365 seconds or about 56 minutes per sample. The 2-theta angle was started at 7.001611515° and stopped at 70.001611° with 0.02021° of increment. After the running processes, the XRD data were acquired and analyzed by using PC-based Datascan software DIFFRAC.EVA. The data represented as a graph of counts versus 2-theta and their peaks were recorded for each sample. Comparison of these peaks on the graphs revealed specific mineral components associated with those textures. This method was done at the X-ray Diffraction laboratory of the Department of Geosciences, Auburn University (Fig. 21). Five samples from the Buckskin National deposit and three samples from the Fire Creek deposit were analyzed. Additionally, a sample from the epithermal Hishikari deposit in Japan was X-rayed for a comparison.

3.4 Hot-Cathode Cathodoluminescence (CL) Microscope

The hot-cathode CL microscope is a modified optical microscope with a vacuum system that encapsulates the sample in the stage (Fig. 22). CL serves as an additional tool to study mineral textures and augments standard petrographic techniques. Quartz commonly exhibit optical properties using the CL microscope that are not observable using a standard petrographic microscope. Thus, this CL method is

a technique that is very useful and effective for studying textural features of quartz and silica precursor phases. Different internal structures caused by different mineral growth features can be observed by various visible light wavelengths emitted by the transition of anions or elements in the minerals in high-energy states to low-energy states (Marfunin, 1979). For sample preparation, the polished-sections were coated with carbon, placed in the vacuum chamber, and then bombarded with a defocused electron beam. As a result, minerals show their luminescence behaviors as different visible-light colors under a video camera that captures every 7-9 seconds. These CL images were taken during CL operations by a high-sensitivity, double-stage Peltier cooled Kappa DX40C CCD camera (Götze et al, 2001). This work was done under the supervision of Dr. Thomas Monecke from the Department of Geology and Geological Engineering at Colorado School of Mines.



FIG 21. Photographs of X-ray powder Diffraction equipment and sample preparation made at the X-ray lab at Auburn University. [Retrieved from <http://www.auburn.edu/cosam/departments/geosciences/Equipment/XRD-XRF/index.htm>: 02/10/2017]

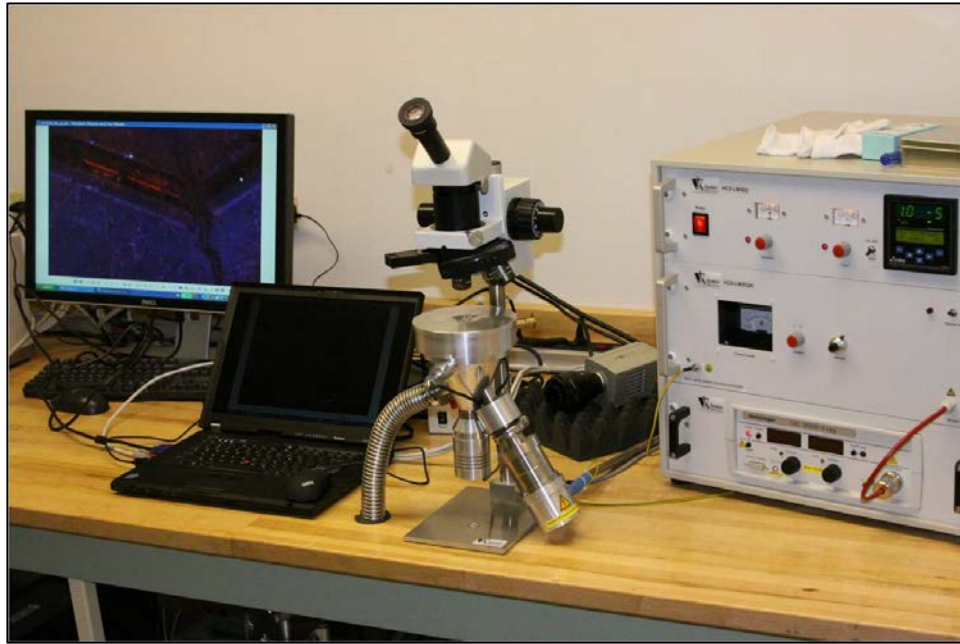


FIG 22. Photograph of hot-cathode CL microscope in the Fluid Inclusion/Cathodoluminescence laboratory of Colorado School of Mines, Golden, CO. This system is operated at 14 kV with a current density of about $10 \mu\text{A}/\text{mm}^2$. [Retrieved from <http://geology.mines.edu/FI-CL-Laboratory>: 02/01/2017]

4. RESULTS

Detailed descriptions of gangue-mineral textures and their association to co-deposited precious-metal minerals in the Buckskin National and Fire Creek deposits are included in this chapter. In addition, X-ray diffraction (XRD) and cathodoluminescence (CL) data from the deposits are also included.

4.1 Vein Textures of the Buckskin National deposit

Samples collected from the Buckskin National deposit typically exhibit symmetric to asymmetric bandings at the macroscale. These bands are defined by differences of colors, textures, grain sizes, and thickness. Colors observed include colorless, white, yellow, black, and grey that likely are primarily the result of variations in mineralogy and physical properties of materials forming the layers. Some bands have a fibrous texture, whereas others contain massive granular quartz as well as spherical and botryoidal forms (Fig. 23). In addition, crustiform bands that consist of mammillary- or spherical-formed layers are commonly observed in samples from Buckskin National. For this study, these mammillary features are basically called colloform texture following the terminology of Dong et al. (1995). Colloform bands from the Buckskin National deposit exhibit colorless, milky, yellowish-cream, and greyish-black-colored bands ranging from 1 to 5 mm of thickness, and never exceed 1 cm in thickness. The colloform bands exhibit

asymmetrical forms. Upper surfaces of the bands are characterized by spherical shapes and formed in open-spaces of the veins. Colloform bands commonly encrust earlier-formed irregular bands to generate a cockade texture, which is a subtype of colloform structures (Fig. 24). In another case, colloform textures not only exhibit mammillary or botryoidal layers but also contain white and colorless round shapes (or circles) that are likely two-dimensional features of spheres. These spheres are formed by aggregation of colloidal particles and related to botryoidal layers of colloform textures in the veins. Some vein samples from Buckskin National exhibit dispersion of round quartz surrounded by milky microcrystalline quartz, which are called moss textures (Adams, 1920; Dong et al., 1995) (Fig. 25). In some hand specimens, quartz crystals occur as a group of coarse-grained euhedral clear crystals that are approximately 5 mm in length radiating out from the vein wall (Fig. 26).

Another vein texture consists of intersected blades that are typically white, yellowish-white and cream-colored, and form a lattice of blades. This feature is the pseudomorphic replacement of calcite by silica, where no calcite remains (Fig. 27). Hand-specimens also contain white and cream-colored clay minerals, which generally occur as powders covering sample surfaces. Moreover, some colorless colloform layers contain black metallic-luster grains that likely formed in shadow of paleocurrent (Saunders et al., 2010).

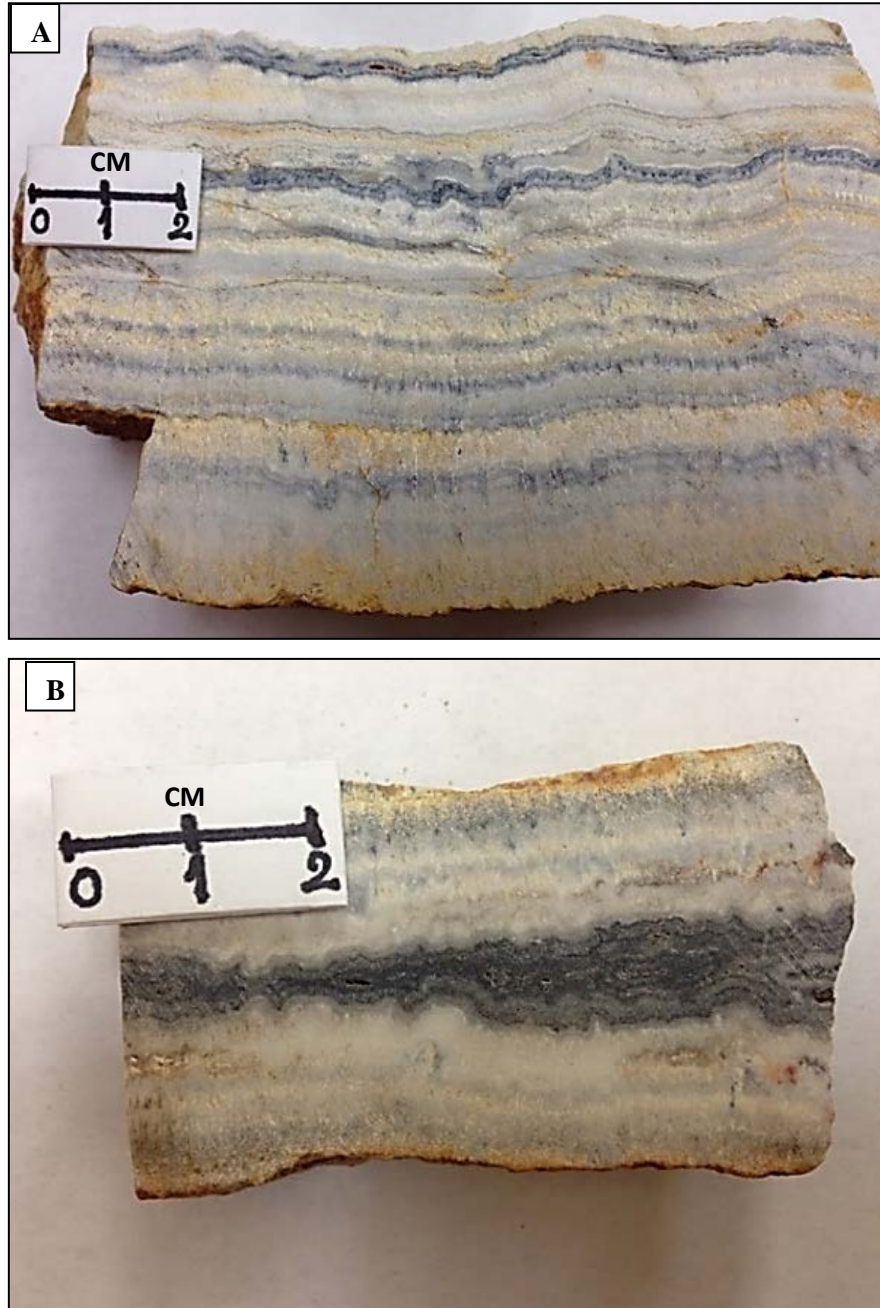


FIG 23. Photomicrographs of asymmetrically- and symmetrically-banded crustiform textures from the Buckskin National deposit. A: Multiple layers showing typical crustiform silica texture. The layers exhibit different colors (black, white, yellow, and grey). Colorless and white-colored bands are composed of several layers that were formerly formed by silica colloids and some of them contain fine-grained black opaque minerals. B: Symmetrical crustiform-colloform textures include varieties of colloform bands consisting of microcrystalline quartz-adularia layers (white, milky and grey) and cryptocrystalline chalcedony layers formed near the open spaces (black).

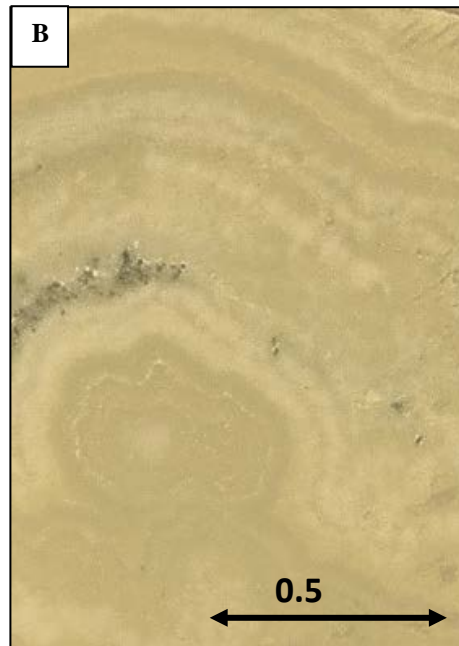
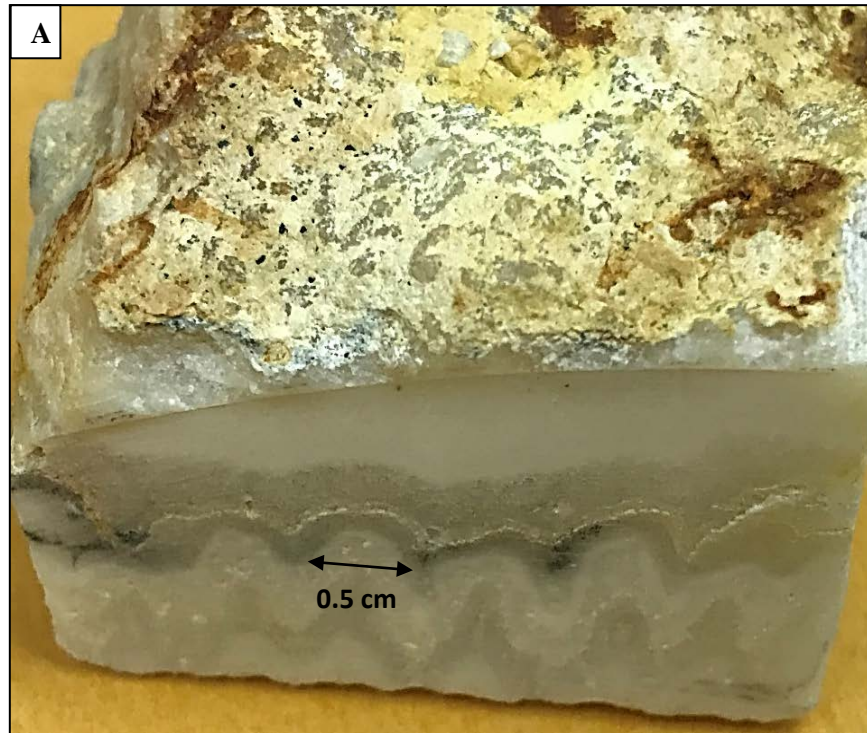


FIG 24. Photographs of colloform textures from the Buckskin National deposit. A: Colorless and milky colloform bands that exhibit mammillary or botryoidal structures. Each mound is around 0.5 cm of diameter. The sample's surface consists of altered materials including clay minerals. B: Cockade texture that is produced by numerous of colloform bands, one of which contains precious-metal minerals (grey).

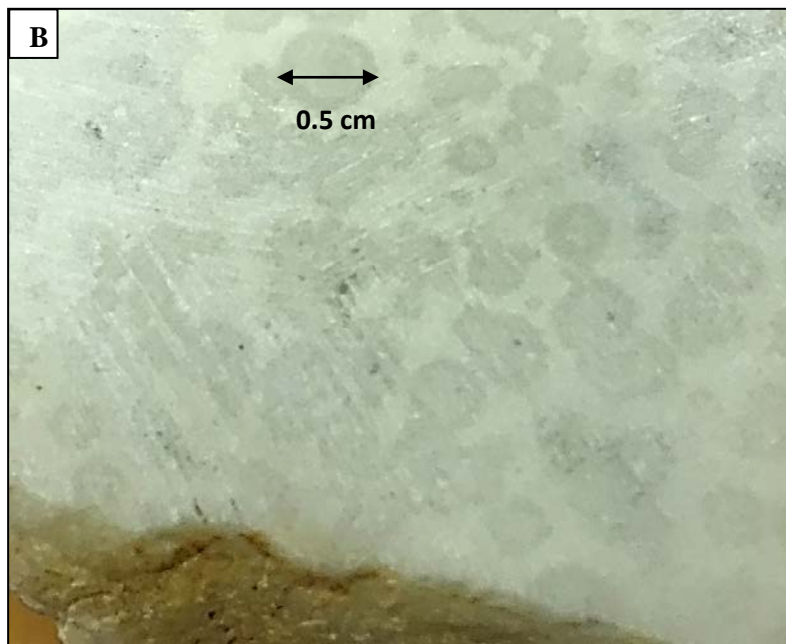
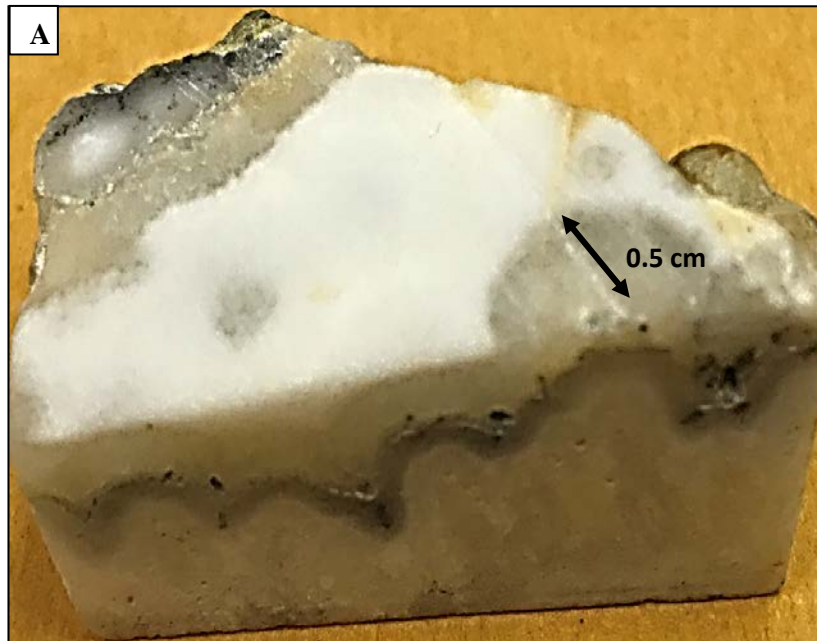


FIG 25. Photographs of colloform structures in parallel- and perpendicular-oriented directions of the vein wall. A: (oriented parallel to vein wall), Colorless spheroids are surrounded by milky background, whereas, in opposite direction, mammillary-formed bands occur within the same sample. B: Moss texture characterized by disseminated colorless sphere in a white milky groundmass. These spheres range from 0.1-0.5 cm.



FIG 26. Photograph of prismatic euhedral quartz in a hand specimen from the Buckskin National deposit. The scale in this photograph is in centimeters.

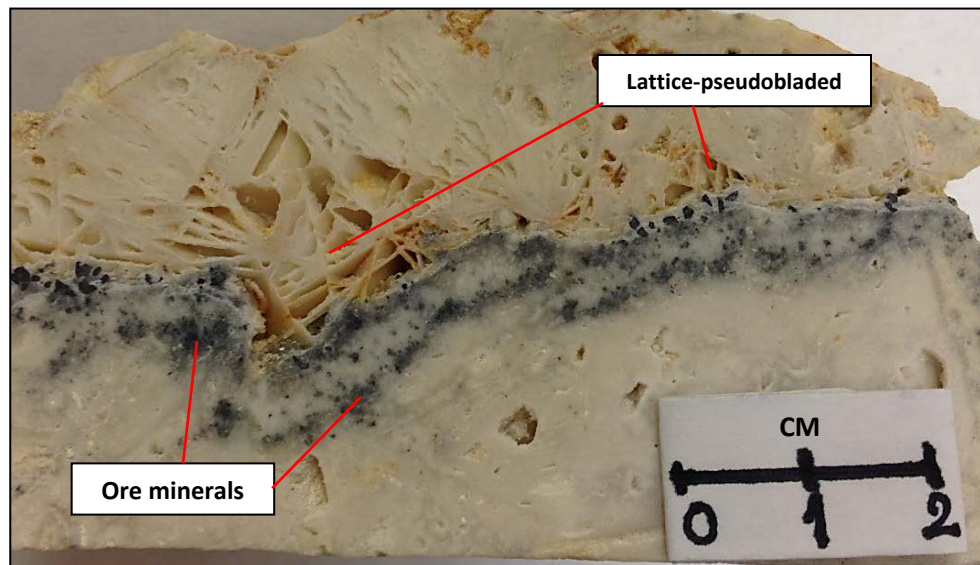


FIG 27. Photograph of lattice-bladed calcite pseudomorphs that are formed above bands of black Ag-minerals. All the precursor calcite has been replaced by silica.

Thirty-nine samples examined for this study from the Buckskin National deposit commonly contain microcrystalline quartz in various grained-sizes. Optical properties observed under crossed polars indicate that quartz grains exhibit anhedral shapes divided by irregular, sutured, and jigsaw boundaries and vary in sizes ranging from 0.01 to 0.1 mm in diameter. Sericite and kaolinite occur rarely around quartz boundaries. Jigsaw textures mostly occur as intergrowth with other features such as moss, feathery, and in colloform bands (Fig. 28). Moreover, jigsaw quartz and adularia also occur in replacement textures that are widely observed in the samples.

Under the microscope, some vein samples exhibit perfectly euhedral clear quartz crystals (0.5-1 mm in length) that project into open space in the veins and are called comb quartz for this study. Quartz crystals, which are elongated parallel to the c-axes, occur mostly as parallel and/or subparallel clusters that can also exhibit radial patterns (Fig. 29A). Near the center of the open spaces in the vein, sutured boundaries occur, which indicate the intersection of the growing quartz crystals. Comb-quartz bands also are intergrown with colloform layers that were subsequently deposited on comb-quartz bands. Further, spherical-banded structures are commonly coating these comb textures. These sub-spherical quartz features sometimes exhibit “teeth-like” shapes (Fig. 29B). Distinguishing layers in this texture is sometimes difficult because of the embedded boundaries. Encrusting a former vein wall by colloform bands is a process that is repeated over the time and produce sub-symmetrical complex silica textures that filled in open spaces. Moreover, under cross-polarized light, at the zone of comb quartz, blocky euhedral texture are evident that were probably caused by different orientations of the crystals (Fig. 29C and 29D). Comb quartz also is associated with other silica textures

such as flamboyant and jigsaw quartz. Another variation of comb-quartz texture involves quartz crystals with 0.25-0.5 mm of sizes that are candle-shaped euhedral clusters and coexist with jigsaw texture at the upper part (Fig. 30). Comb-texture is the second-most common vein feature at the Buckskin National deposit, which occurs in 23 of 39 samples examined, and is common in many epithermal veins (Lindgren, 1933; Simmons et al., 2005).

Another texture, which is also found in 23 of 39 samples, exhibits botryoidal and mammillary layers consisting of chalcedony, (re)crystallized quartz, and amorphous silica. These colloform layers are likely formerly produced by aggregation of colloidal particles to precipitate as amorphous silica in the veins. Although, amorphous silica has commonly crystallized to quartz and chalcedony in the Buckskin National deposit, the layers of former colloidal silica still can be distinguished. Chalcedonic layers, which are about 0.05 mm of thickness, occur with fibrous extinction and some of them contain lots of inclusions and impurities. Spherical-shaped (re)crystallized quartz aggregates are also observed (Fig. 31). Distinct colloform layers can be easily observed under plane-polarized light. However, under cross-polarized light, these colloform layers exhibit (re)crystallized textures, which are mostly changed to form chalcedony and/or microcrystalline jigsaw quartz. These (re)crystallized colloform layers also vary in crystal sizes and grained shapes (Fig. 32). Some colloform layers contain spherical-shaped quartz and these layers locally encrust fragments of wall rocks. This feature is commonly called a cockade texture (Adams, 1920; Spurr, 1926) (Fig. 33).

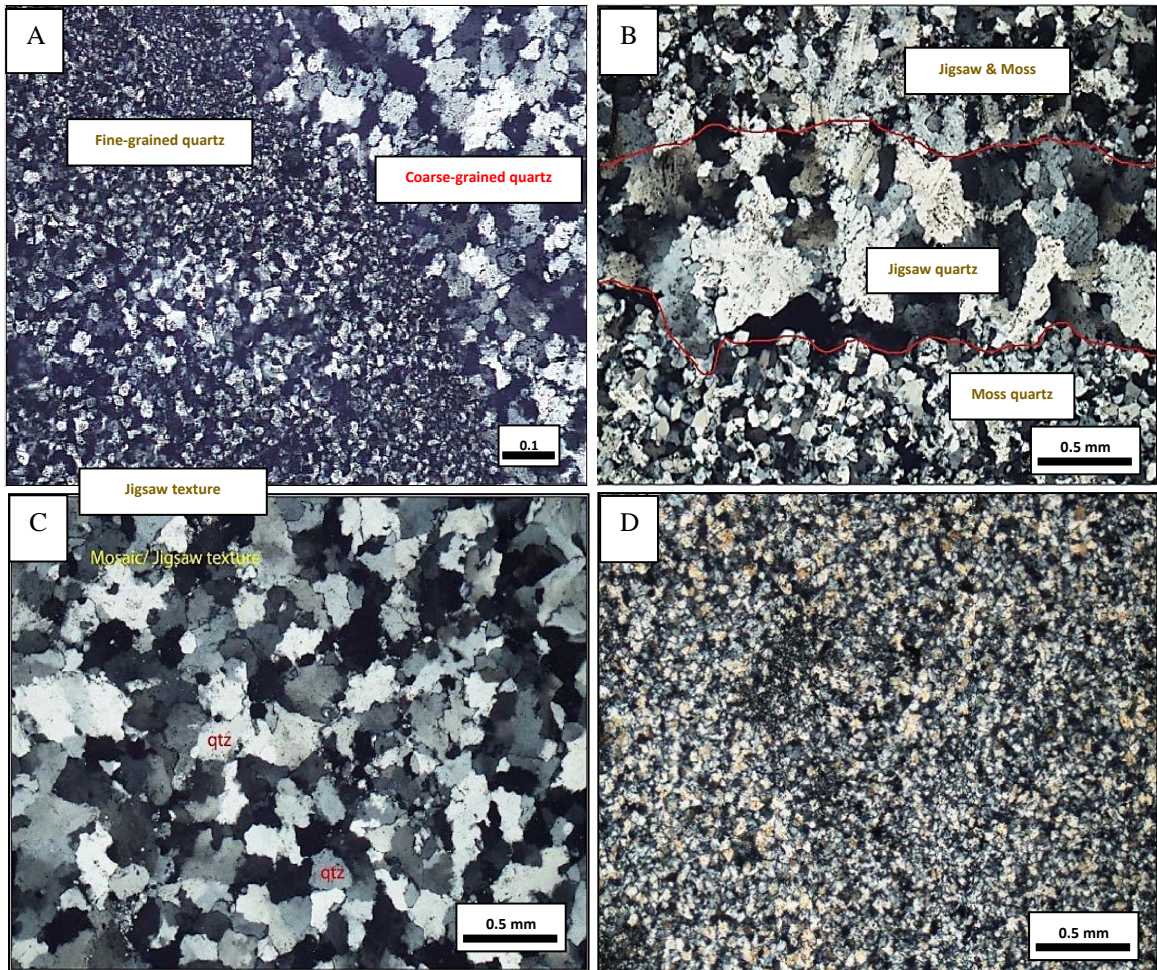


FIG 28. Photomicrographs taken under cross-polarized light of the mosaic or jigsaw texture. **A:** Jigsaw quartz in various crystal sizes. **B:** Coarse-grained jigsaw quartz and moss quartz. **C:** Jigsaw texture associated with sericite as an alteration product of adularia. **D:** Very fine-grained quartz showing jigsaw texture. [qtz = Quartz]

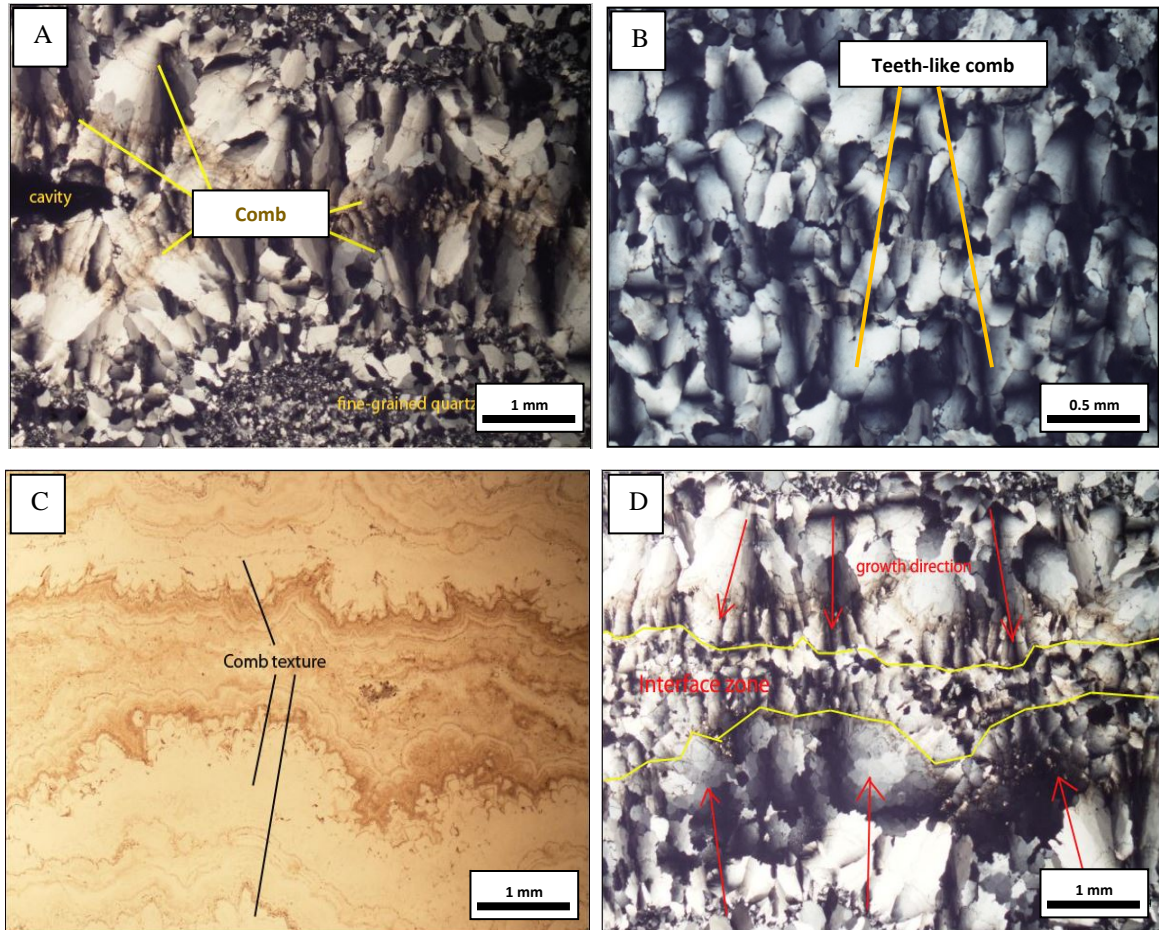


FIG 29. Photomicrographs of varieties of comb quartz textures. A: Comb quartz growth direction from opposite sides of the vein and intersecting in the center, which was infilled with fine-grained quartz. B: Teeth-like structures of comb quartz are caused by rounded-sutured contacts and they are intergrown with colloform features. C: Photomicrograph (plane-polarized light) of comb and colloform textures in open space. Comb texture contains euhedral clear crystals of quartz. D: Same field of view as C taken under crossed polars, photomicrograph showing interface zone and late mineralization in open space.

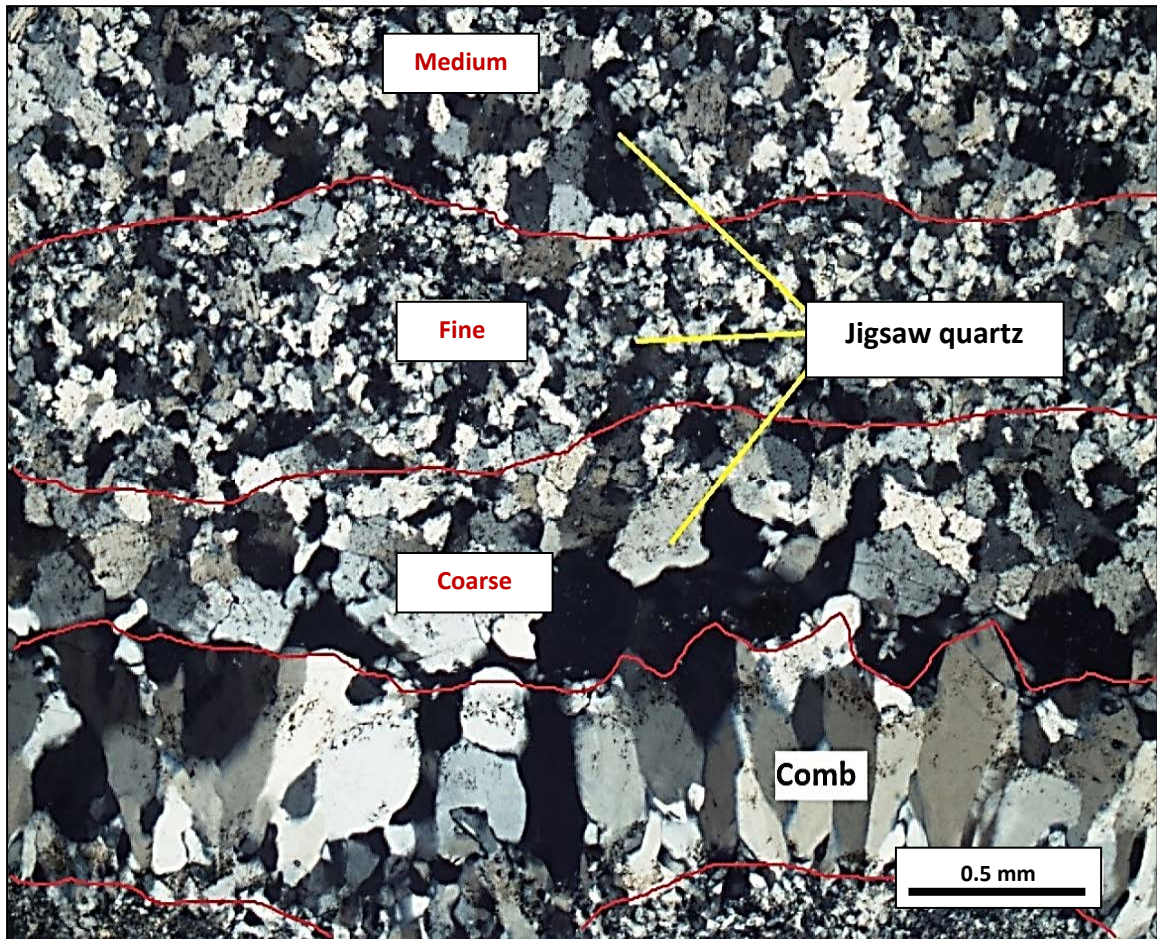


FIG 30. Photomicrograph (cross-polarized light) of comb quartz at lower part of image, and multiple-layers of mosaic textures in the upper part of image. Inclusions and impurities were trapped along the wedges of euhedral comb quartz crystals, as well as within recrystallized textures. Fine to medium grained quartz exhibit local fibrous structures, which formed perpendicular to the vein walls.

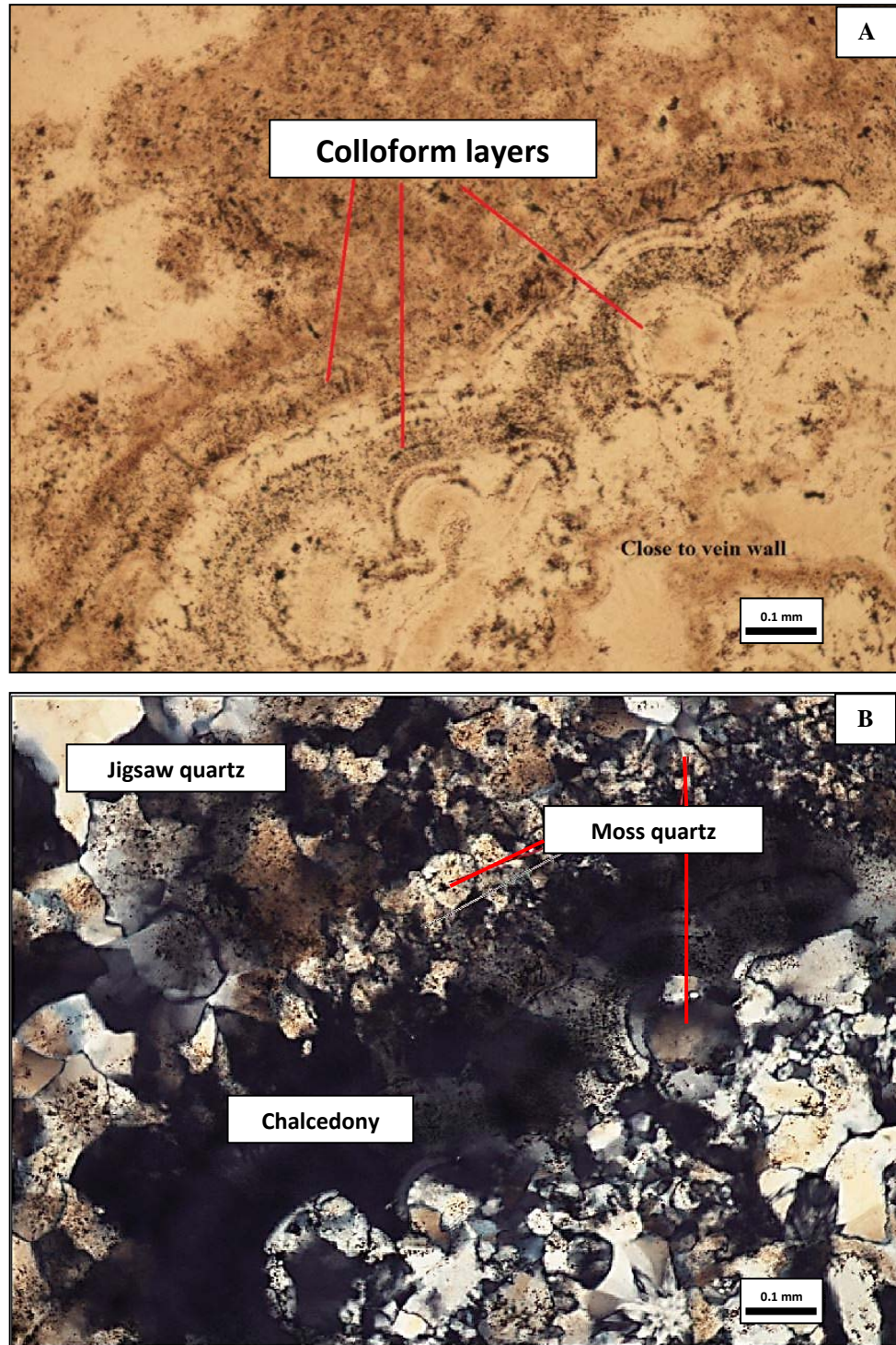


FIG 31. Photomicrographs of colloform textures. A: Photomicrograph (plane-polarized light) exhibiting multiple colloform layers. Lower sides of mounds are formed near the open space of veins. B: Photomicrograph (crossed polars) showing fibrous chalcedony in the colloform layers occurred with recrystallized jigsaw textures.

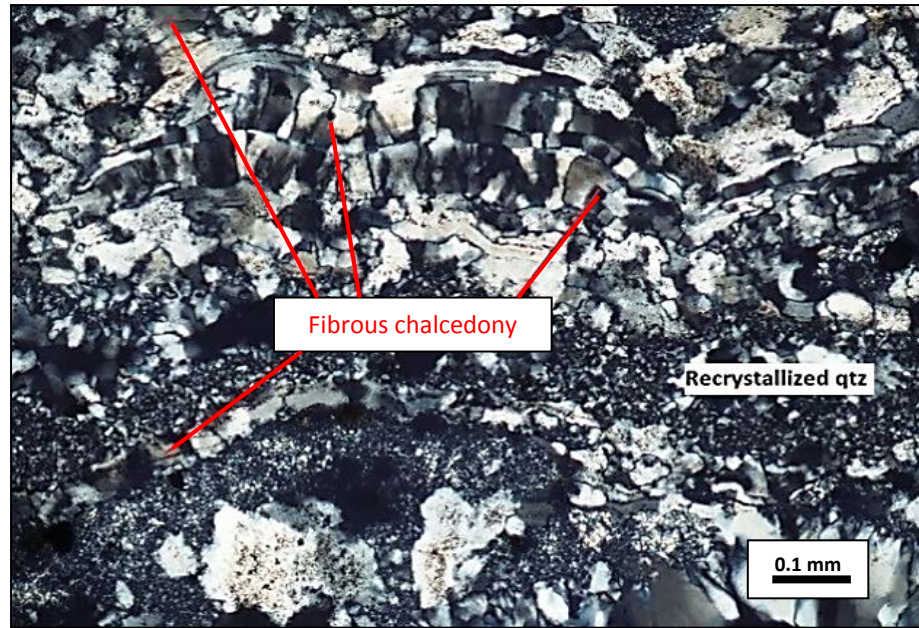


FIG 32. Photomicrograph (cross-polarized light) of (re)crystallized textures in colloform bands. Various crystal sizes are observed in these layers. Fibrous chalcedony are also found. [qtz=Quartz]

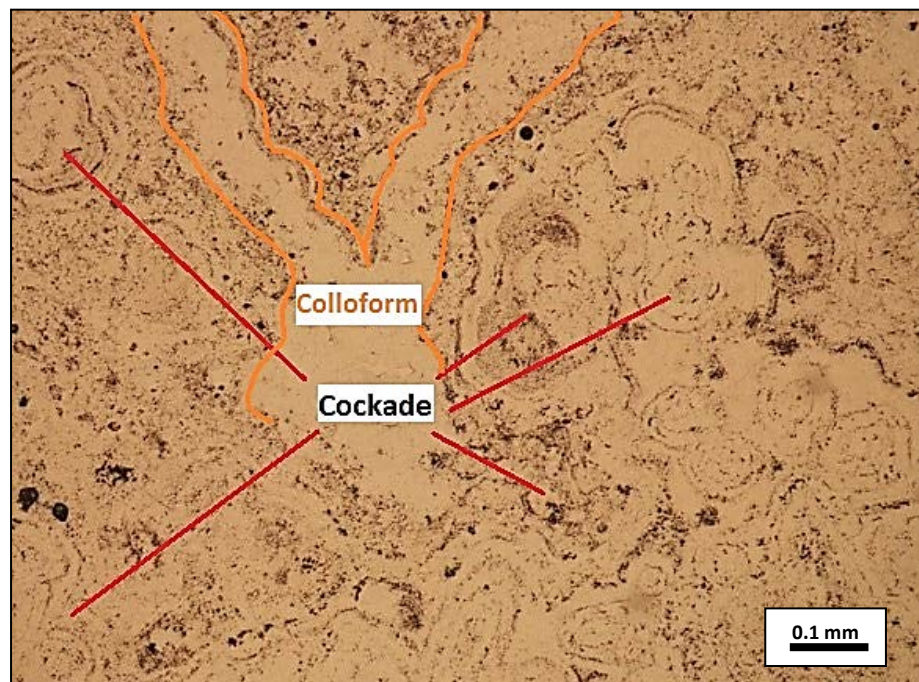


FIG 33. Photomicrograph (plane-polarized light) showing concentric bands encrust spherical quartz grains and euhedral quartz crystals. These concentric group (or cockade) range from 0.1 to 0.3 mm in diameter.

Eighteen of 39 samples contain many perfectly individual round quartz grains. As mentioned previously, these rounded shapes appear in two-dimensional spheroidal shapes within colloform bands. These spherical features also illustrate concentric and partly radiating patterns that are indicated by fluid inclusions zones and grain boundaries. These spherical forms range from 0.1 to 0.2 mm of diameter. Spherical quartz grains are surrounded by jigsaw quartz. It also occurs with other features including chalcedony, flamboyant extinction, and plumose quartz (Fig. 34). In this study, this texture is called moss texture, which is named by Adams (1920) and spherical quartz. Moreover, these spherical features are different to colloform banding structures. Spheres are commonly found in horizontal dimension or 2D-slice through a circular “mound” of amorphous silica-forming colloform bands. The spheres sometimes formed along vein walls, which provided a substrate to allow later colloform bands to encrust. Fluid- and solid inclusions are also trapped along spherical surfaces (Fig 35).

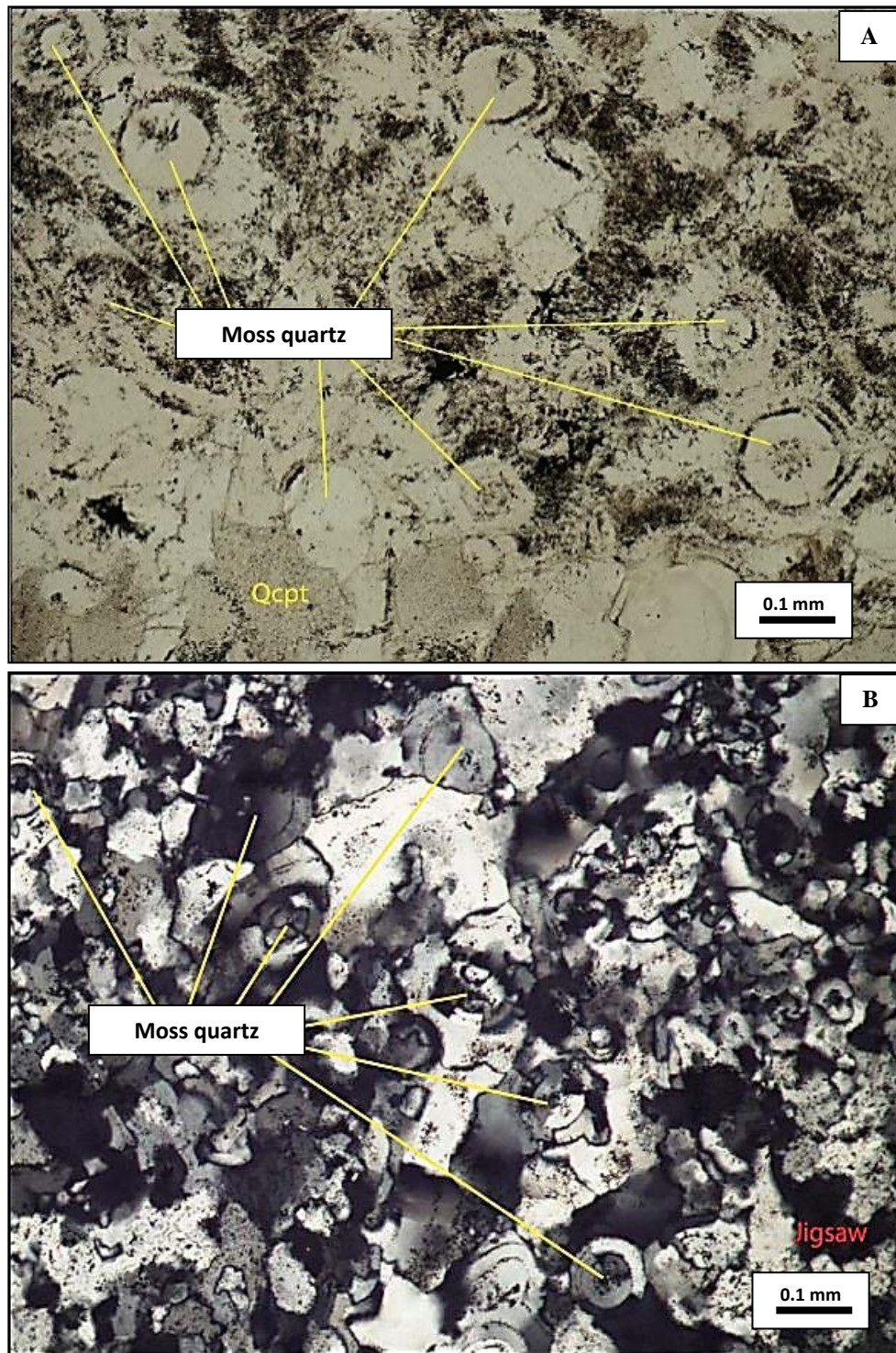


FIG 34. Photomicrographs of moss quartz from the Buckskin National deposit. A: Photomicrograph (plane-polarized light) showing spherical individual grains occurred with cryptocrystalline quartz (Qcpt). B: Photomicrograph (cross-polarized light) of moss quartz in a jigsaw quartz groundmass. Some of the moss quartz exhibits flamboyant extinction.

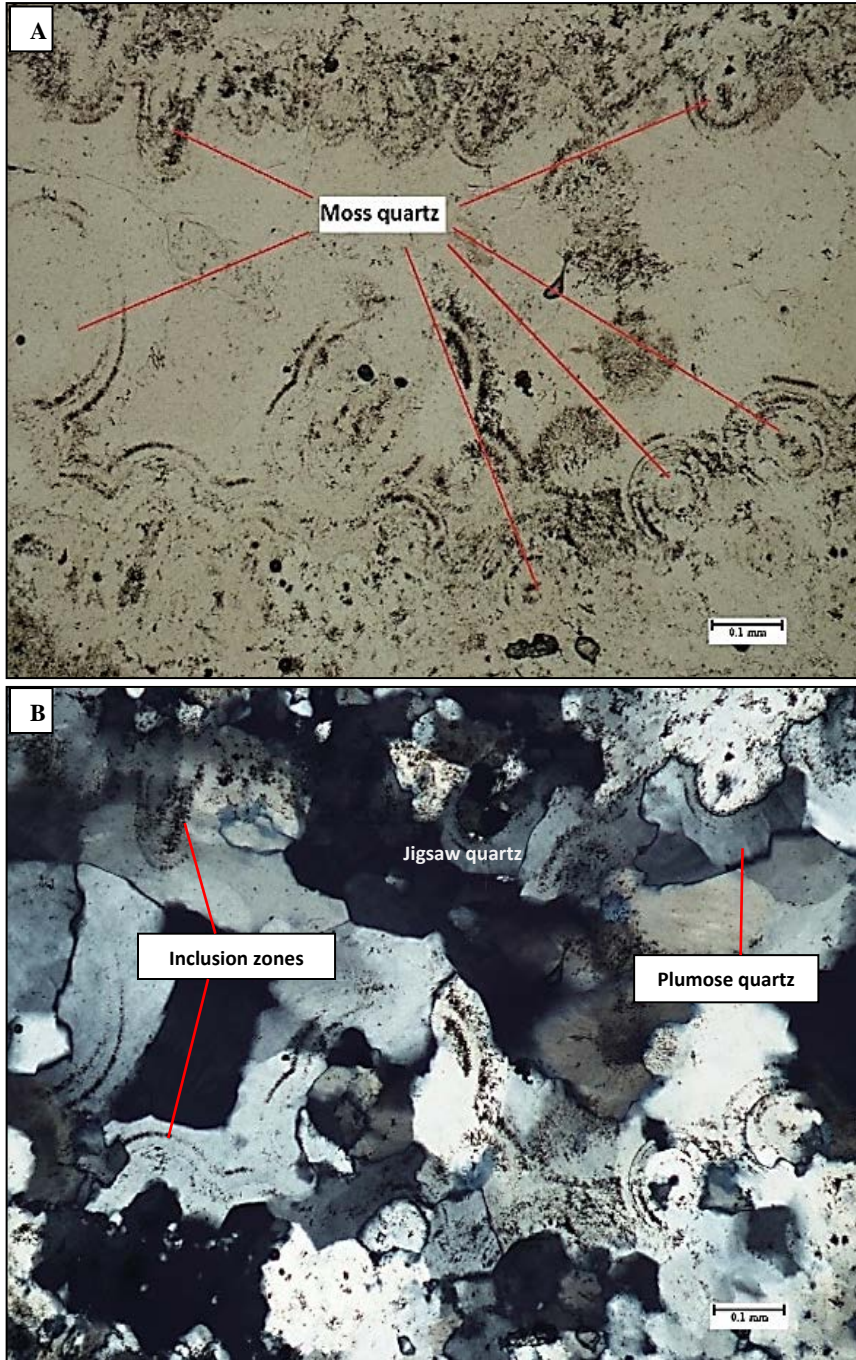


FIG 35. Photomicrographs of moss-colloform textures. A: Photomicrograph (plane-polarized light) of spheres with inclusion zones showing concentric rounded grains. No inclusion zone at the middle of the photomicrograph indicates the open space in this system. B: Photomicrograph (crossed polars) of A showing completely recrystallized textures in moss structures, containing spherical inclusion zones.

At the Buckskin National deposit, quartz grains typically exhibit undulose extinction. Seventeen vein samples exhibit plumose features that are caused by different extinction angles of two-sized quartz that are intergrown. The features typically include small quartz, which are aggregate grains, and one large quartz. The previously formed quartz exhibits individual euhedral to subhedral crystal similar to a comb quartz structure. The group of fibrous chalcedony crystals that were later deposited on this host quartz exhibit different extinction angles compared to the host crystal. These fibrous shapes of chalcedony have formed at rims of the host quartz and point out of the center of the crystal core. Thus, this feature has a similar appearance as a bird feather (Fig. 36A) and it is called a feathery by Adams (1920). However, this texture has been named by Sander and Black (1988) as a plumose texture, which is the term used in this study. Microscale plumose quartz exhibits small plumose zones in host grains that commonly form at the grain margins. Microplumose also occurs with other silica textures such as jigsaw and replacement textures (Fig. 36B). Additionally, 11 samples from the Buckskin National deposit exhibit flamboyant extinction, which is a fibrous radial extinction in rounded grains and colloform layers of recrystallized quartz. This texture was called a flamboyant texture by Adam (1920) and Sander and Black (1988). Under plane-polarized light, multiple colloform layers are visible and contain inclusions and impurities (less than 0.1 mm in thickness) that come after euhedral prismatic grains formed. However, under cross-polarized light, fan-like extinction of fibrous prismatic grains can be seen. Another common textural feature includes rounded spherical quartz aggregates ranging from 0.1-0.2 mm diameter. This texture is found with mostly comb quartz, colloform, moss, ghost-sphere, jigsaw, and former chalcedonic textures (Fig. 29A and 37).

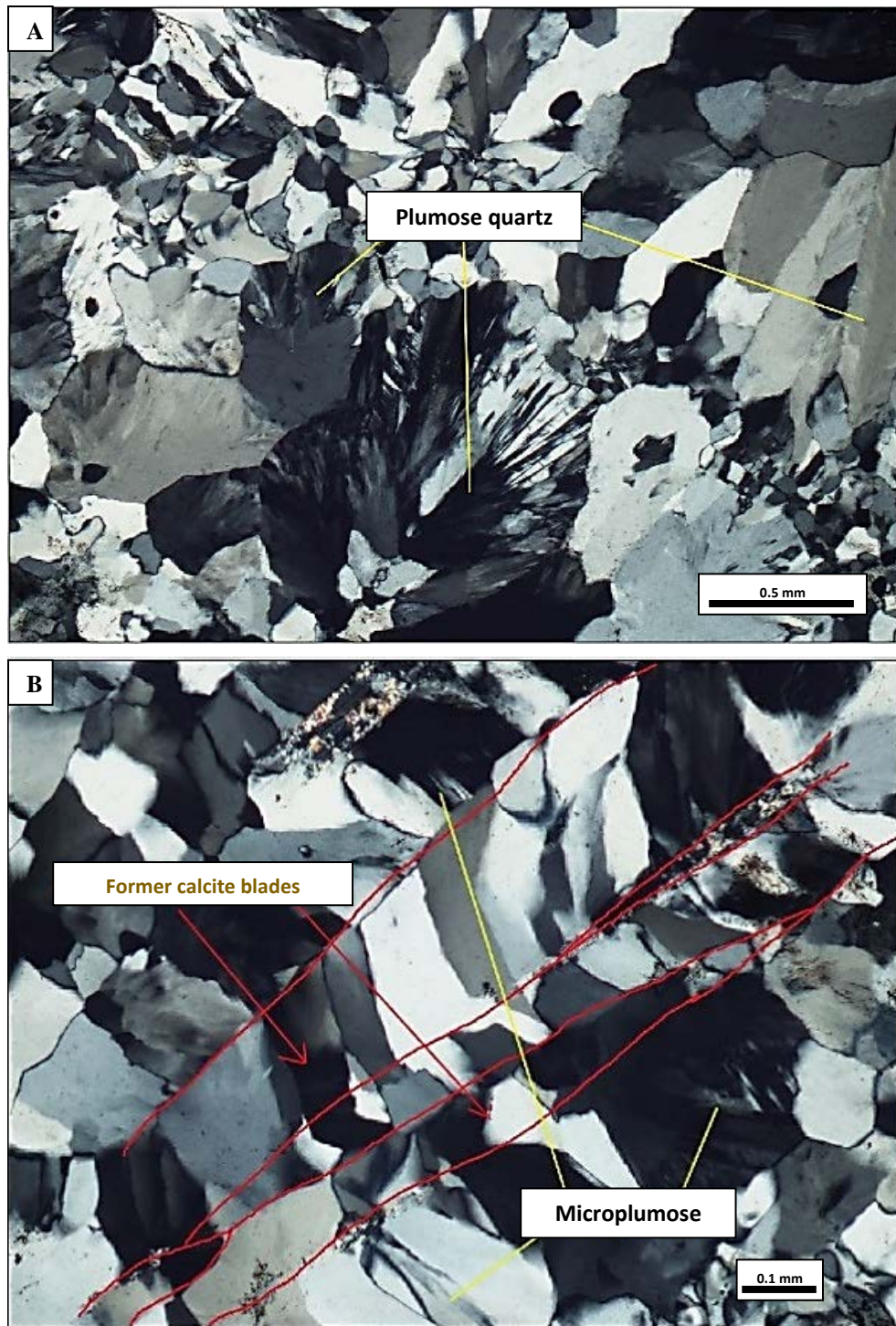


FIG 36. Photomicrographs of plumose or feathery textures under cross-polarized light. A: Photomicrograph of plumose quartz in a background of typical quartz. B: Photomicrograph of microplumose textures associated with silica replacement and jigsaw quartz.

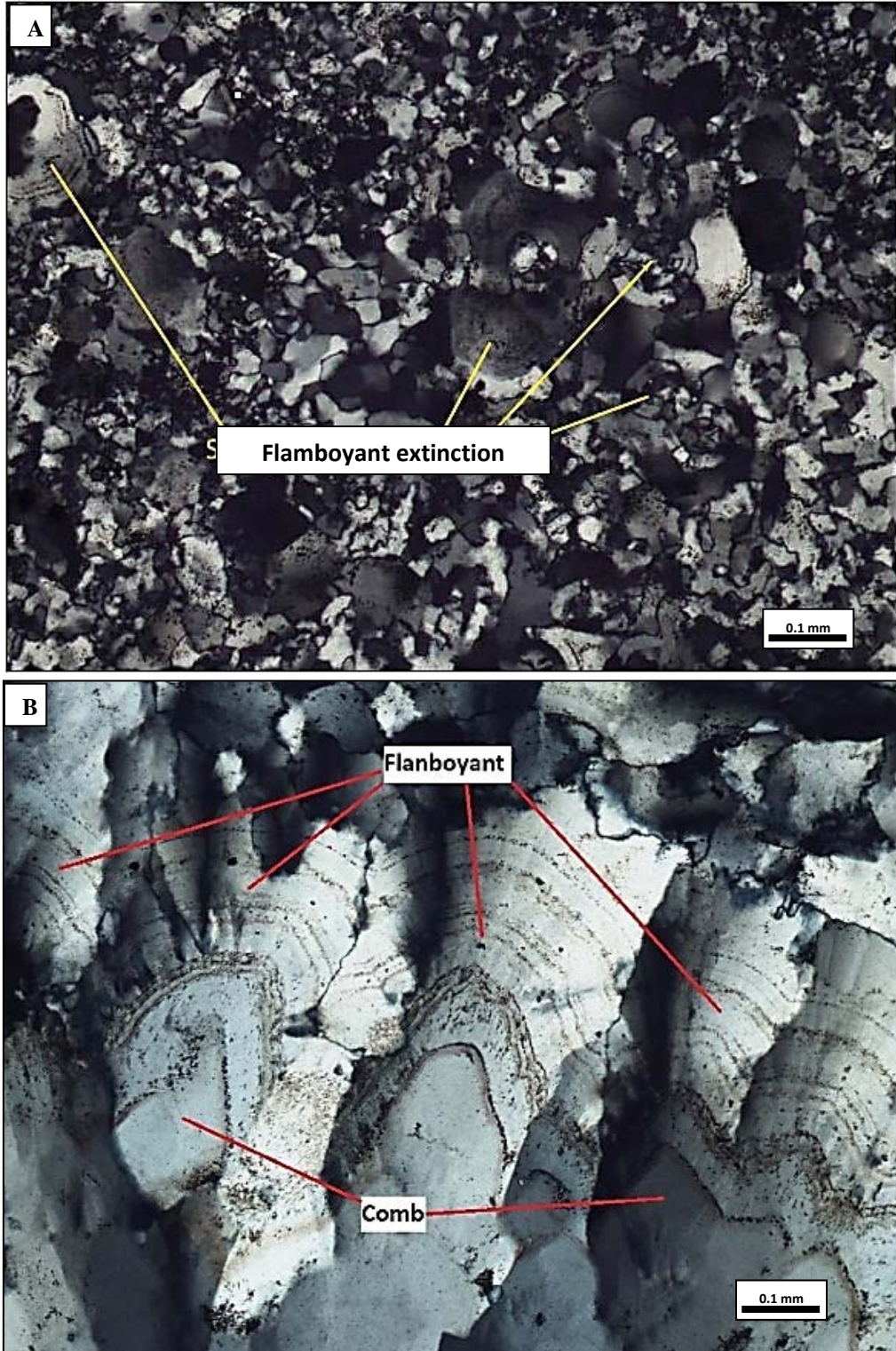


FIG 37. Photomicrographs of flamboyant textures under cross-polarized light. A: Photomicrograph of spherical quartz with fan-like extinction. B: Photomicrograph of fibrous extinction in colloform layers encrusting prismatic euhedral crystals.

Vein textures from the Buckskin National deposit exhibit several silica replacement textures that are divided into two types, including the pseudomorphs of silica after platy/bladed calcite and fibrous acicular structures of unknown minerals that are replaced by silica. Quartz, adularia, and chalcedony are the most common replacement minerals.

The pseudomorphic replacement of calcite by silica in the Buckskin National deposit can be subdivided into three textures using the classification of Dong et al. (1995). These include parallel-pseudobladed, lattice-pseudobladed, and pseudo-acicular silica textures. Calcite replacement textures also commonly occur with other recrystallized textures such as jigsaw, microplumose, and flamboyant. Sericite and kaolinite locally are found along bladed forms (Fig. 38). Parallel relic-bladed texture exhibits parallel structures of former calcite blades that are completely replaced by silica minerals such as quartz and chalcedony. The parallel-pseudobladed features mostly occur with jigsaw quartz and round quartz grains exhibiting radial patterns of inclusion zones (Fig. 39). The parallel calcite blades sometimes perpendicularly cut across another parallel-bladed texture, and then exhibit intersected zones showing reticular or net-like patterns (Fig. 40). Moreover, some silica vein textures exhibit decussate pseudomorphs of silica after bladed calcite, which are randomly cross-cut by other blades. This intersected acicular-bladed feature is also called lattice-pseudobladed texture (Dong et al, 1995). Anhedral to subhedral quartz perpendicularly forms along the acicular-pseudobladed structures and occurs with other crystallized and recrystallized textures including moss, jigsaw, and euhedral clear quartz (Fig. 41).

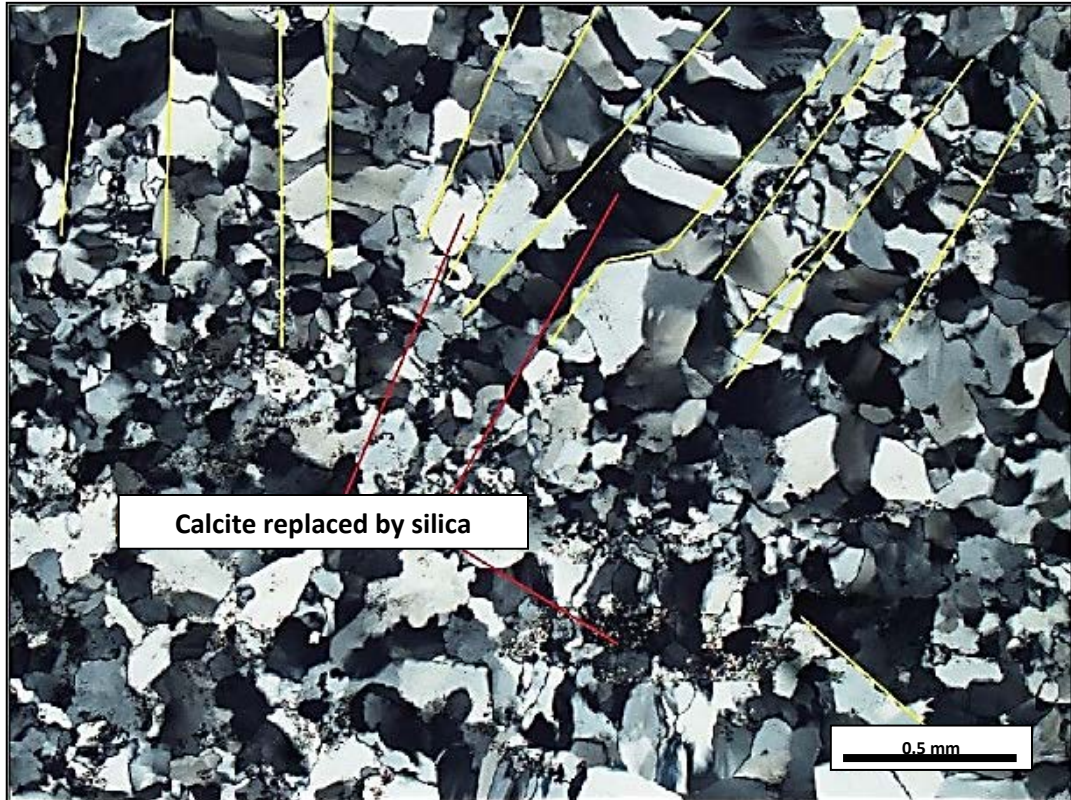


FIG 38. Photomicrographs of relic-acicular features in replacement texture under cross-polarized light. Yellow lines probably illustrate rims or cleavages of blades that are replaced by silica. The gaps between yellow lines range from 0.2 – 0.5 mm.

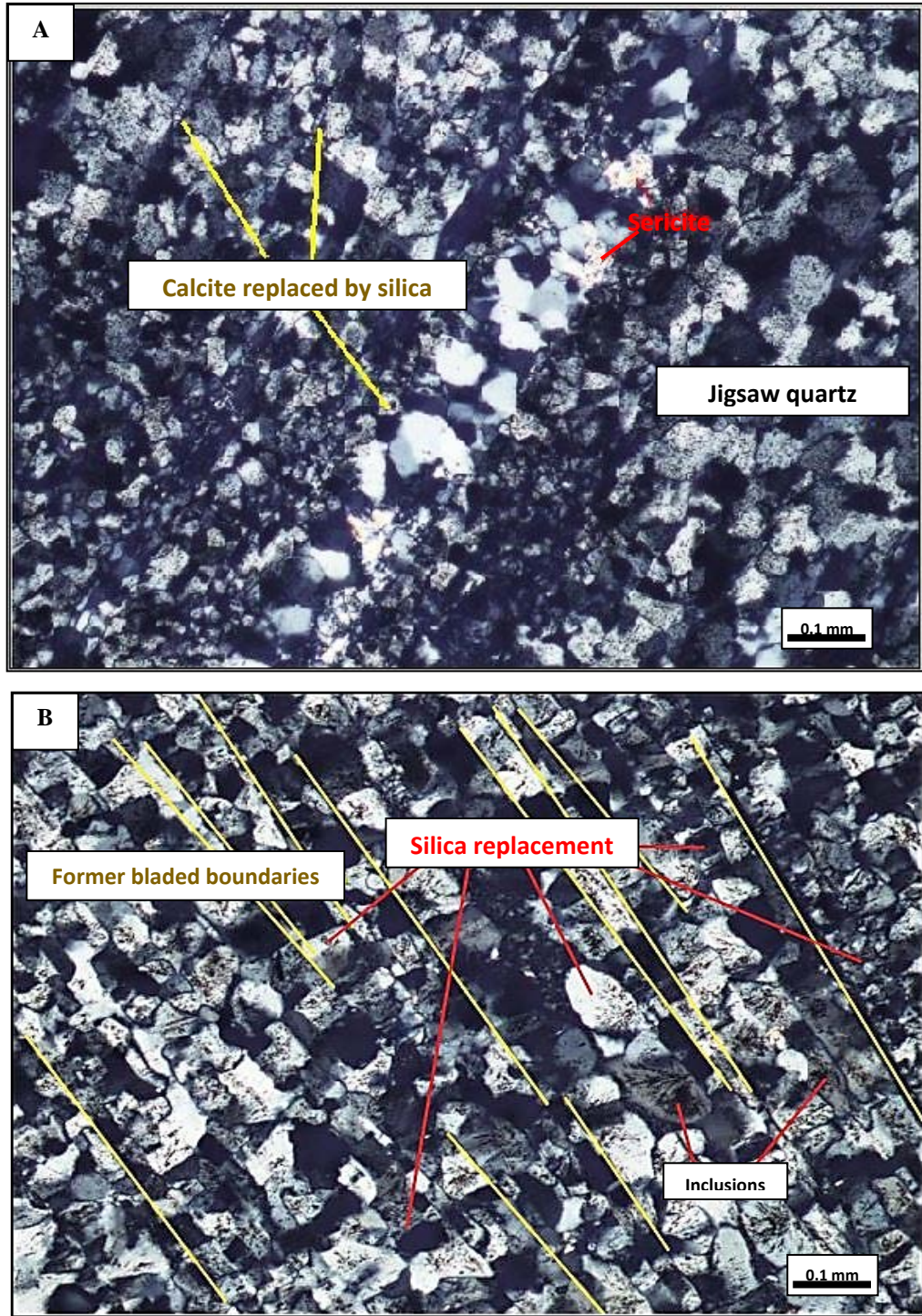


FIG 39. Photomicrographs (cross-polarized light) showing semi-parallel bladed textures. A: Jigsaw quartz vary in sizes and replace in former bladed minerals or mineral cleavages. Sericite are found as alteration products of adularia. B: Spherical-shaped quartz grains contained fibrous-radial zones of inclusions occur between acicular grains. Yellow lines indicate acicular grained boundaries.

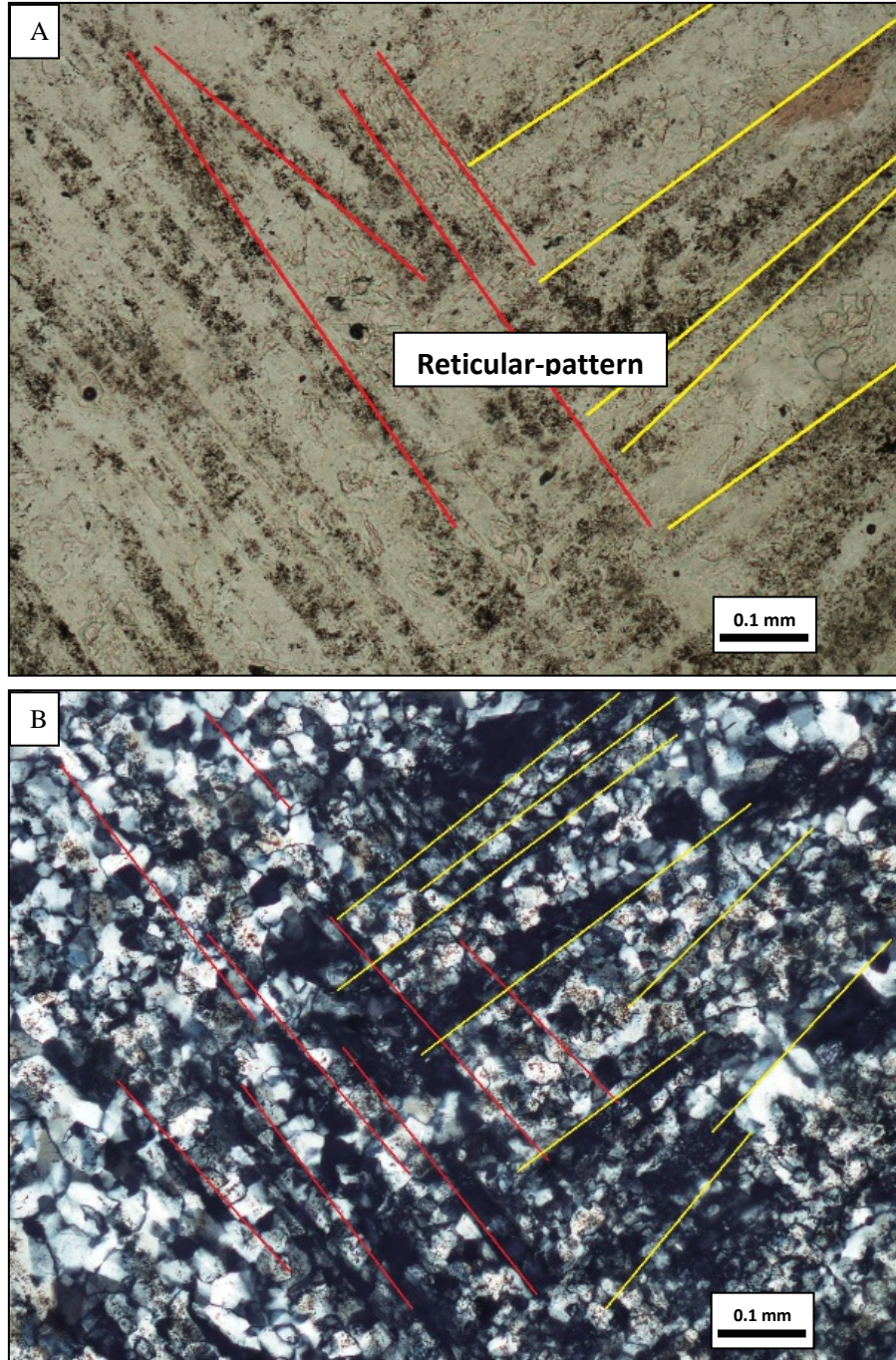


FIG 40. Photomicrographs showing reticular-patterned zones that are indicated by red and yellow lines. The angles between these lines are approximately 90°. **A:** Net-like patterns seen in plane-polarized light are indicated by the cutting of parallel inclusion zones in the central portion of the image. **B:** (crossed polars) Quartz and adularia grains ranging from 0.025 to 0.05 mm. replace in the former blades. Rectangular fibrous are found along with alteration minerals such as clays and sericite.

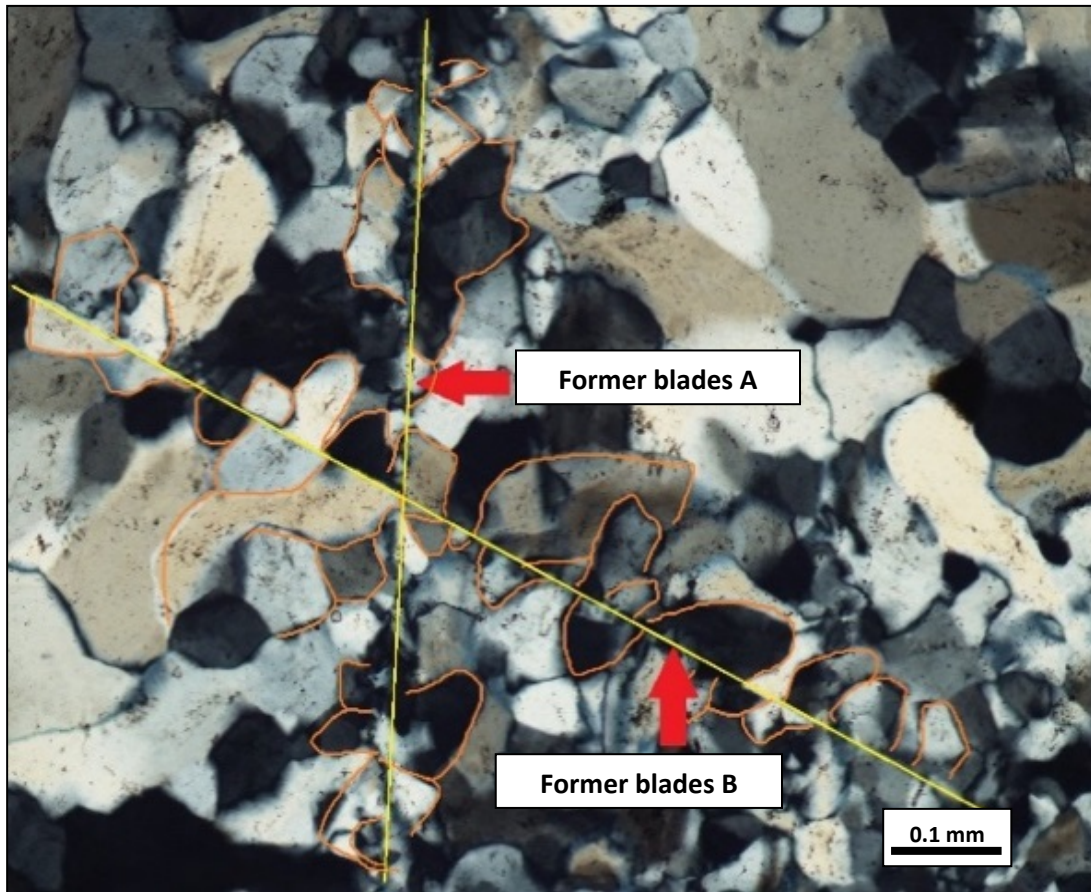


FIG 41. Photomicrograph (cross-polarized light) of intersected lines showing an X-pattern. Acicular shapes or blades of former minerals are indicated by yellow lines. Orange lines indicate single quartz crystal boundaries.

The second group of silica replacement texture found in the Buckskin National deposit exhibits needle-mosaic or fibrous-acicular features. These fibrous-acicular structures widely occur in crustiform-colloform bands and extend to several bands. The fibrous-acicular features are subparallel and sometimes contain elongate cavities that are probably filled by kaolinite. Surrounded jigsaw quartz grains vary in grain sizes and they probably concurrently formed with the fibrous-acicular features occurred in the bands (Fig. 42). These structures are easily seen in both plane- and cross-polarized light.

Moreover, fibrous-acicular bands importantly contain disseminate opaque ore minerals. In some situations, the former fibrous minerals are removed and then replaced by jigsaw quartz (Fig. 43). This texture is also difficult to decipher because it commonly forms within the bands that exhibit crustiform, recrystallized textures as jigsaw textures, and silica replacement features. Thus, the fibrous-acicular texture is not grouped with the silica replacement of calcite but unknown minerals found in colloform bands.



FIG 42. Photomicrograph (cross-polarized light) of needle-mosaic structures showing a combination of three main silica textures including crustiform (macro-texture), mosaic, and replacement textures. (Kl=Kaolinite, Qtz=Quartz, Ad=Adularia)

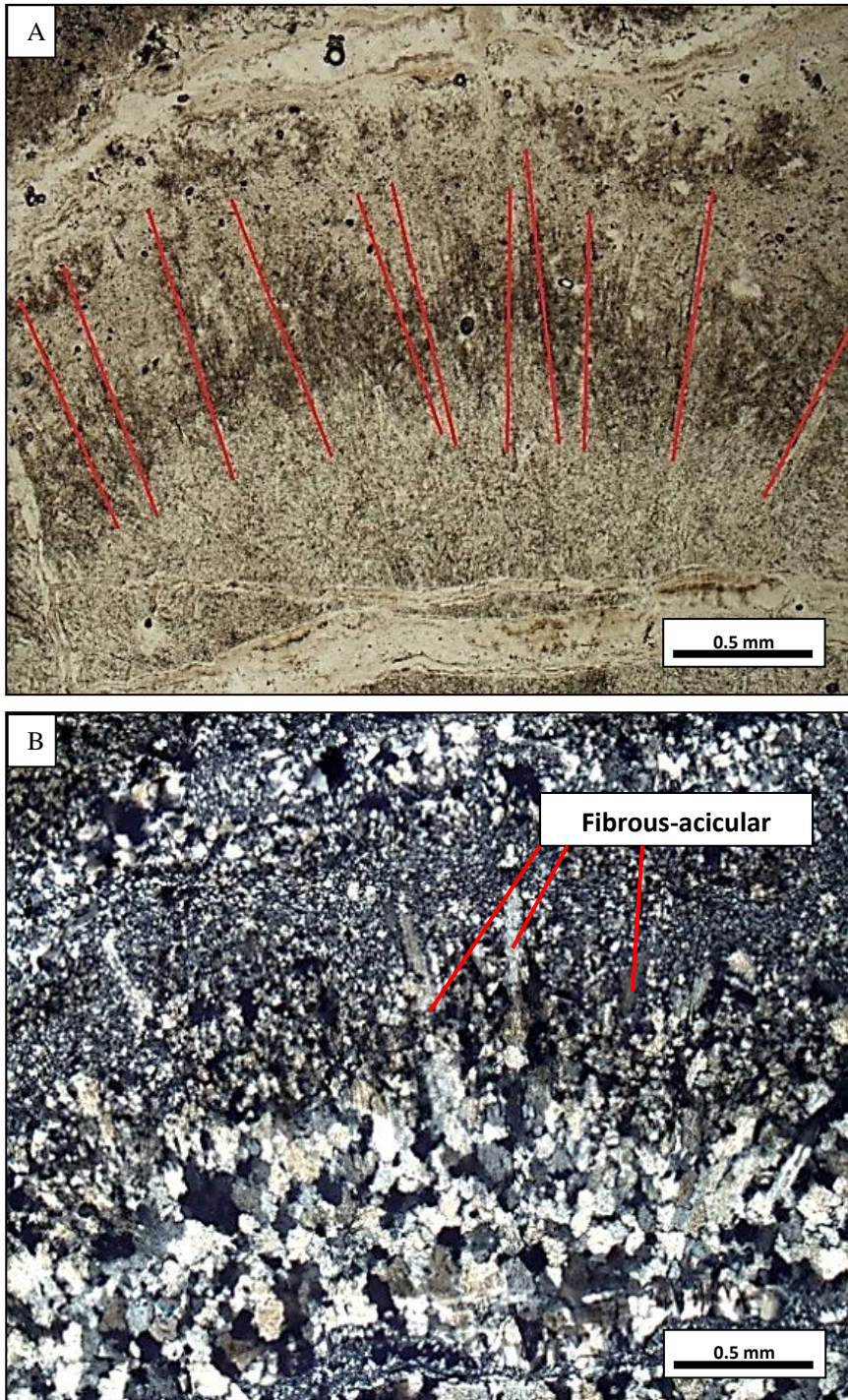


FIG 43. Photomicrographs showing needle-jigsaw replacement textures. A: Photomicrograph (plane-polarized light) of needle or fibrous-acicular shapes (red lines). These acicular shapes formed perpendicular to the vein wall. B: Photomicrograph (crossed polars) showing jigsaw quartz in colloform bands and quartz filling elongate cavities that were probably former dissolved crystals.

Finally, a quartz texture reflecting its growth history common in many epithermal ores also occurs at the Buckskin National deposit. Euhedral quartz crystal commonly contains fluid inclusions and impurities parallel to its growth zones (Fig. 44). This texture can be observed on hand specimens and thin-sections with various sizes ranging from 0.1 mm to 1 mm. The approximately width of zones range from less than 0.01 to 0.1 mm and the distances between inclusion zones are various and less than 0.1 mm. These zoned quartz grains are certainly found with other textures such as flamboyant quartz and spherical quartz. Moreover, fluid inclusions and impurities zones are represented in colloform layers showing spherical lines, even though, the spherical host materials already crystallized or recrystallized. Importantly, the fluid inclusions assemblages found in epithermal veins commonly provide details of hydrothermal conditions that formed various vein textures. For examples, fluid-rich inclusion assemblages that found in many textures such as zonal and comb quartz indicate non-boiling stage of hydrothermal event, whereas vapor-rich and fluid-rich inclusion assemblages indicate boiling stage and only occur with colloform, moss, and plumose textures (Moncada et al., 2012).



FIG 44. Photomicrograph (cross-polarized light) of zoned euhedral quartz crystals. Zones of fluid inclusions appear as bands of black tiny spots. Red line illustrates the interface boundary of crystals growth lines.

4.2 Vein Textures of Fire Creek deposit

Vein textures from the Fire Creek deposit are interpreted using the same criteria as detailed in the descriptions of the Buckskin National textures. Gangue minerals of Bonanza veins of the Fire Creek deposit predominantly exhibit multiple replacement textures where quartz and adularia replaced after calcite, and later platy/bladed calcite also occur.

Hand specimens from the Fire Creek deposit, exhibit multiple colloform bands that consist of fibrous-acicular structures within the bands. These acicular features radially formed perpendicular to vein walls and cross-cut some bands. Some layers contain metallic minerals such as electrum along these acicular structures showing disseminated pattern. Some fibrous-acicular structures contain clay, which is probably the alteration product of adularia. The colloform layers also exhibit various distinct colors including milky, grey, and glassy white (Fig. 45). Another texture showing in hand specimens is lattice-bladed texture that occurs in colloform layers. This texture represents intersected blades of replacing minerals such as quartz and adularia. These blades exhibit white and milky colors that cross-cut other blades showing an “x-shaped” features. Moreover, the groundmass materials among these blades immediately react to diluted hydrochloric acid, which indicates it is late calcite (Fig. 46).

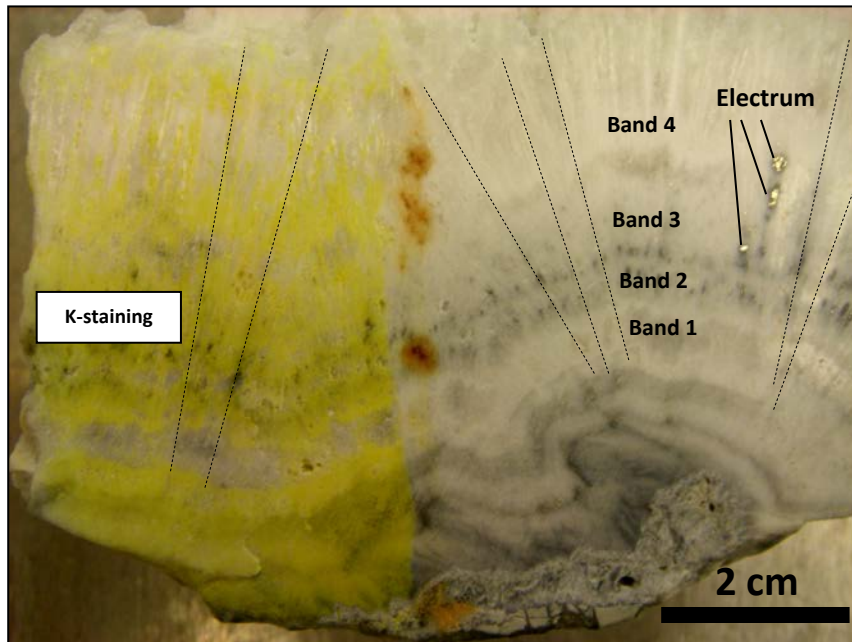


FIG 45. Photograph of fibrous-acicular texture in colloform bands found in the Fire Creek deposit. Colloform bands contain black tiny metallic minerals such as electrum and Ag-S-Se phases located along fibrous acicular structures (dashed lines).

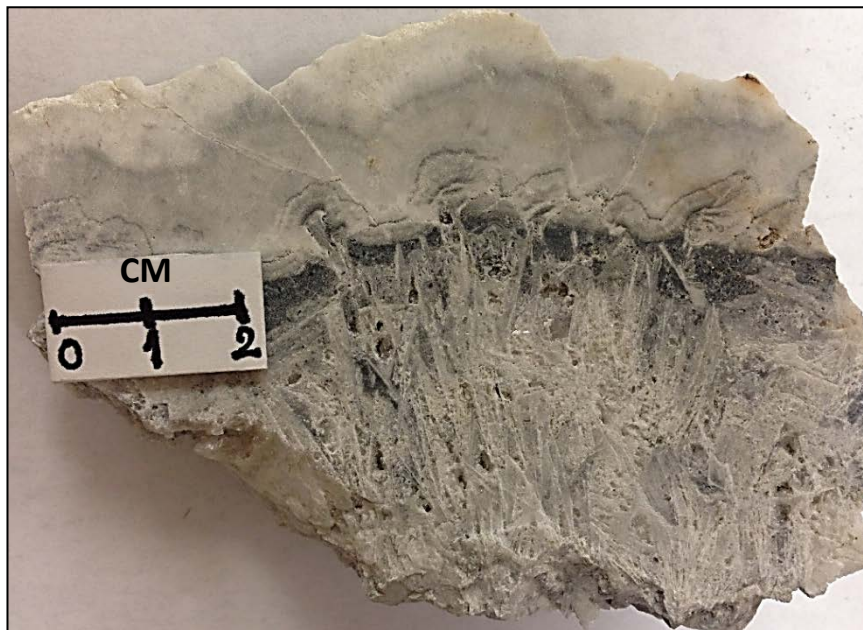


FIG 46. Photograph of lattice bladed texture occurring with colloform bands from the Fire Creek deposit. The bladed calcite cross-cut other blades, forming an “x-shaped” structures. Late stage calcite (not bladed) is also present along pseudomorphs.

Under the microscope, the major minerals found in the bonanza veins from the Fire Creek deposit commonly include quartz, adularia, and calcite. Vein textures were enhanced by using staining methods to highlight mineral compositions including the carbonate staining using Alizarin-red S (ARS) for calcite and the cobalt-nitrite staining for potassium feldspar (adularia).

Under plane-polarized light, red colors during Alizarin-red S method indicate calcite compositional zones that vary in structures such as blades, platy, and rhombohedra. Zones of no staining color strongly represent pseudomorphs of quartz and adularia after blades of unknown minerals. Under cross-polarized light, calcite exhibits two distinct features including platy calcite and replacement bladed calcite. Bladed calcite is partially replaced by quartz and adularia that formed parallel seams within that calcite, whereas platy calcite is not replaced by silica and probably lately formed after the silica replacement of calcite ended. These late calcite crystals mostly occur perpendicular to the orientation of former blades. They also exhibit the crystal growth-zoned structures (Fig. 47).

Adularia is a more common mineral in the Fire Creek veins than was found in the Buckskin National samples. Adularia, a monoclinic crystal, exhibits euhedral to subhedral pseudo-rhombic crystal structure and varies in size ranging from less than 0.05 mm to 0.5 mm. Under plane-polarized light, adularia grains can be identified by cobalt-nitrite staining and its crystal structure. It is indicated by yellow color during the staining, whereas quartz does not. Adularia typically occur as euhedral pseudo-rhombic crystals and aggregate along former bladed crystals (Fig. 48).

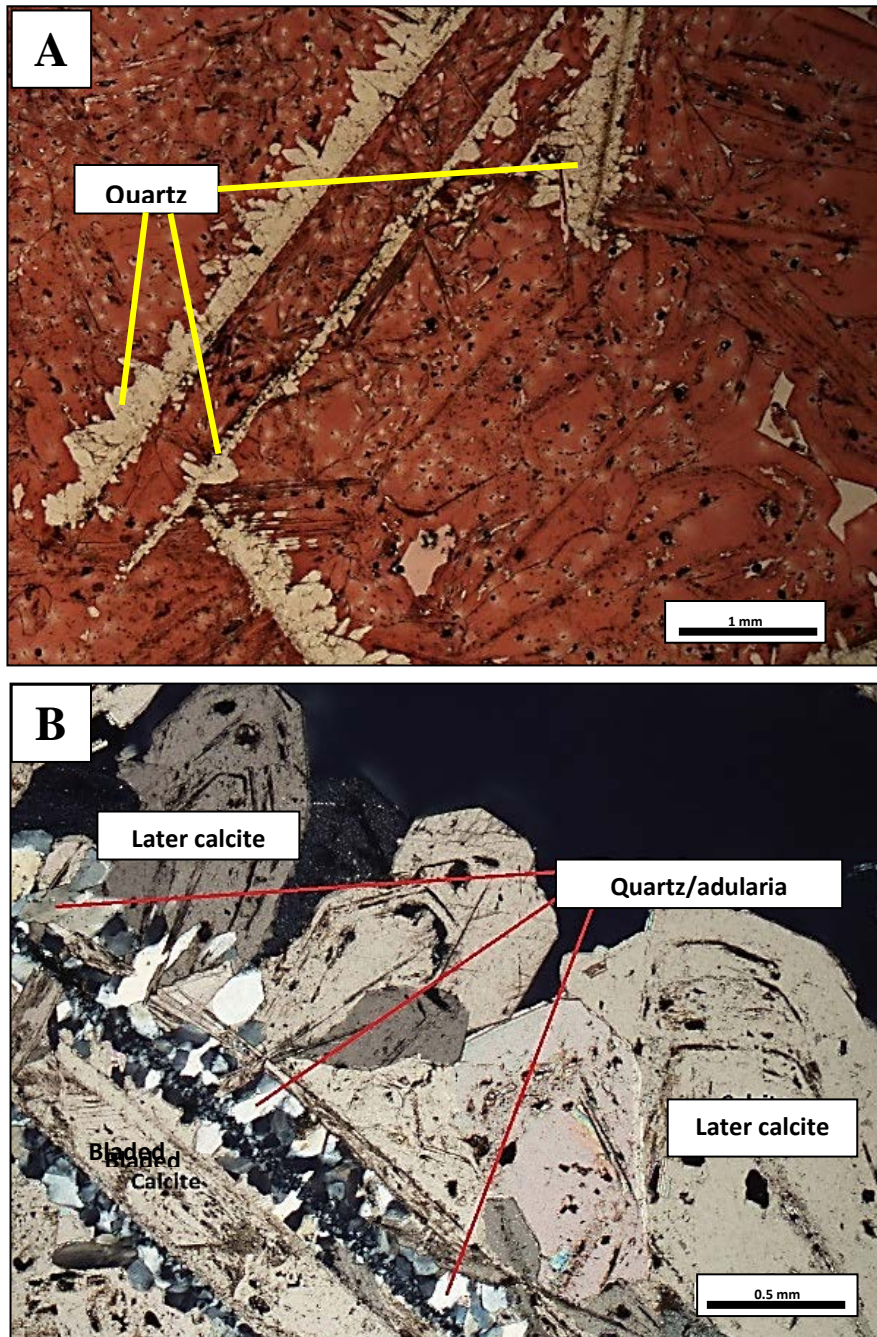


FIG 47. Photomicrographs of calcite found in the Fire Creek deposit. A: Calcite staining with Alizarin red S represents calcite that are indicated by red colors. This photomicrograph was taken under plane-polarized light. Colorless minerals including small grains of quartz and adularia replace carbonates. B: Photomicrograph taken under cross-polarized light showing blades and platy calcite partially replaced by silica. Later calcite likely occur perpendicular to these bladed structures exhibiting crystal growth-zoned patterns.

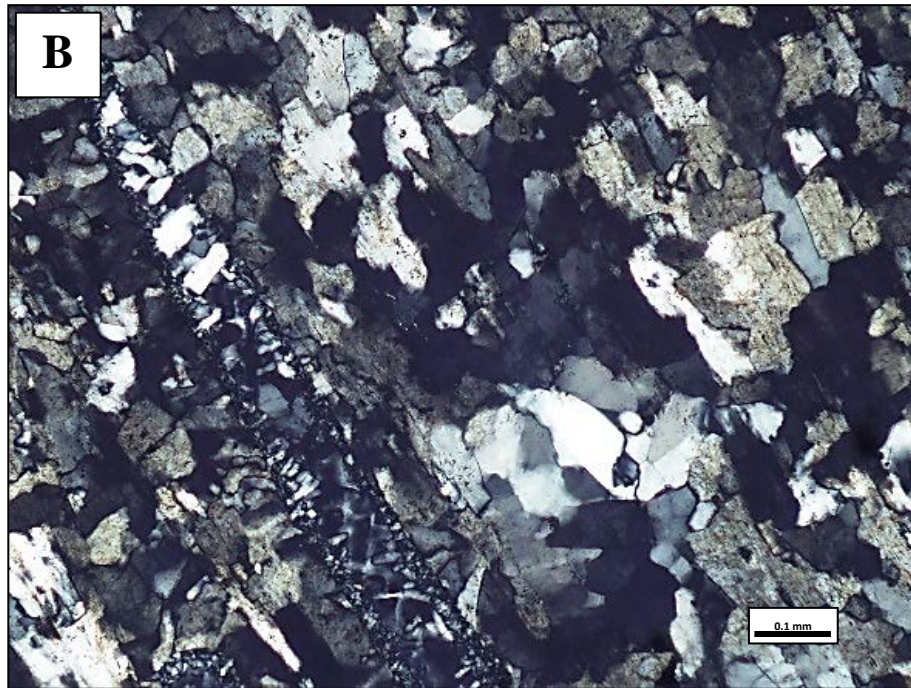
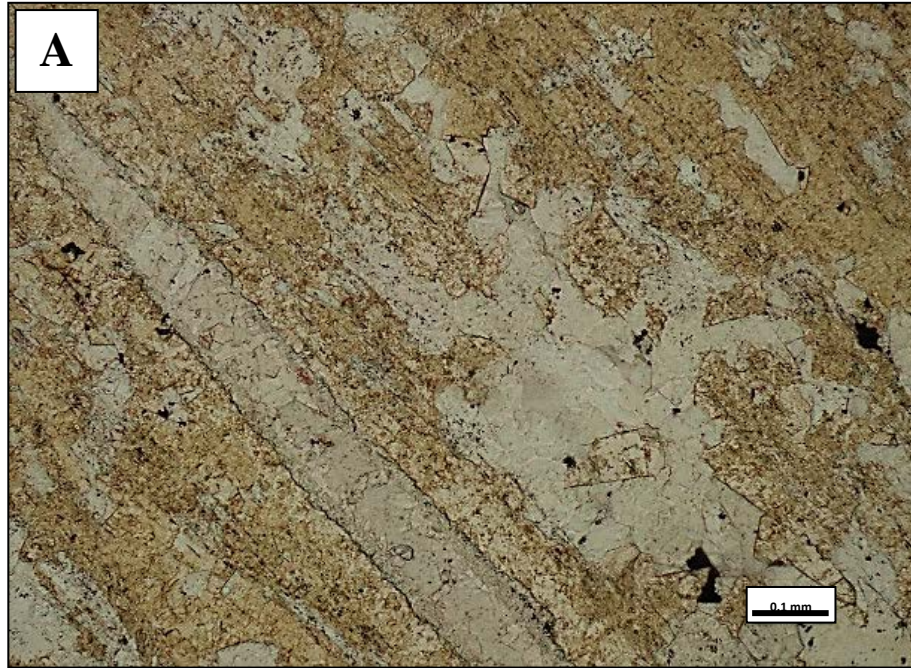


FIG 48. Photomicrographs showing adularia encrusting silica replacement texture from the Fire Creek deposit. A: Photomicrograph (plane-polarized light) exhibits adularia, which are indicated by yellow colors, during cobalt-nitrite staining. No color zone is exhibited on quartz grains. B: Photomicrograph (crossed polars) exhibits parallel bladed texture that consists of quartz and adularia that are replacing bladed minerals (e.g. calcite).

The most common texture at the Fire Creek deposit is jigsaw texture, which is similar to that at the Buckskin National. Jigsaw texture found in the Fire Creek deposit exhibits sharp and straight boundaries among crystal grains. Adularia is also present as euhedral to subhedral pseudo-rhombic forms that occur with subhedral to anhedral quartz grains (Fig. 49). Jigsaw features also commonly occur with other textures such as fibrous acicular structures in colloform bands. These jigsaw textures is composed of adularia or potassium-rich minerals more than quartz grains that are indicated by yellow colors of the staining. Adularia also varies in sizes ranging from less than 0.01 mm to 0.1 mm. Relic colloform features are also present (Fig. 50).

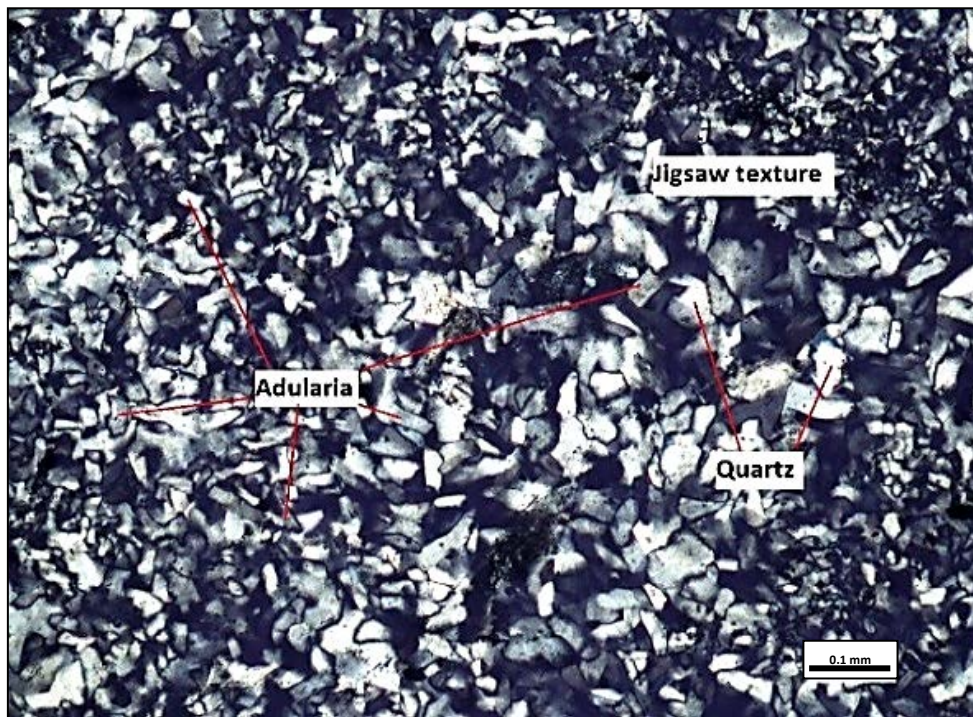


FIG 49. Photomicrograph of jigsaw texture that are found in the Fire Creek samples. This photomicrograph was taken under cross-polarized light. Pseudo-rhombic adularia and quartz grains are present. The crystal boundaries exhibit sharp and straight patterns more than irregular and interpenetrated boundaries.

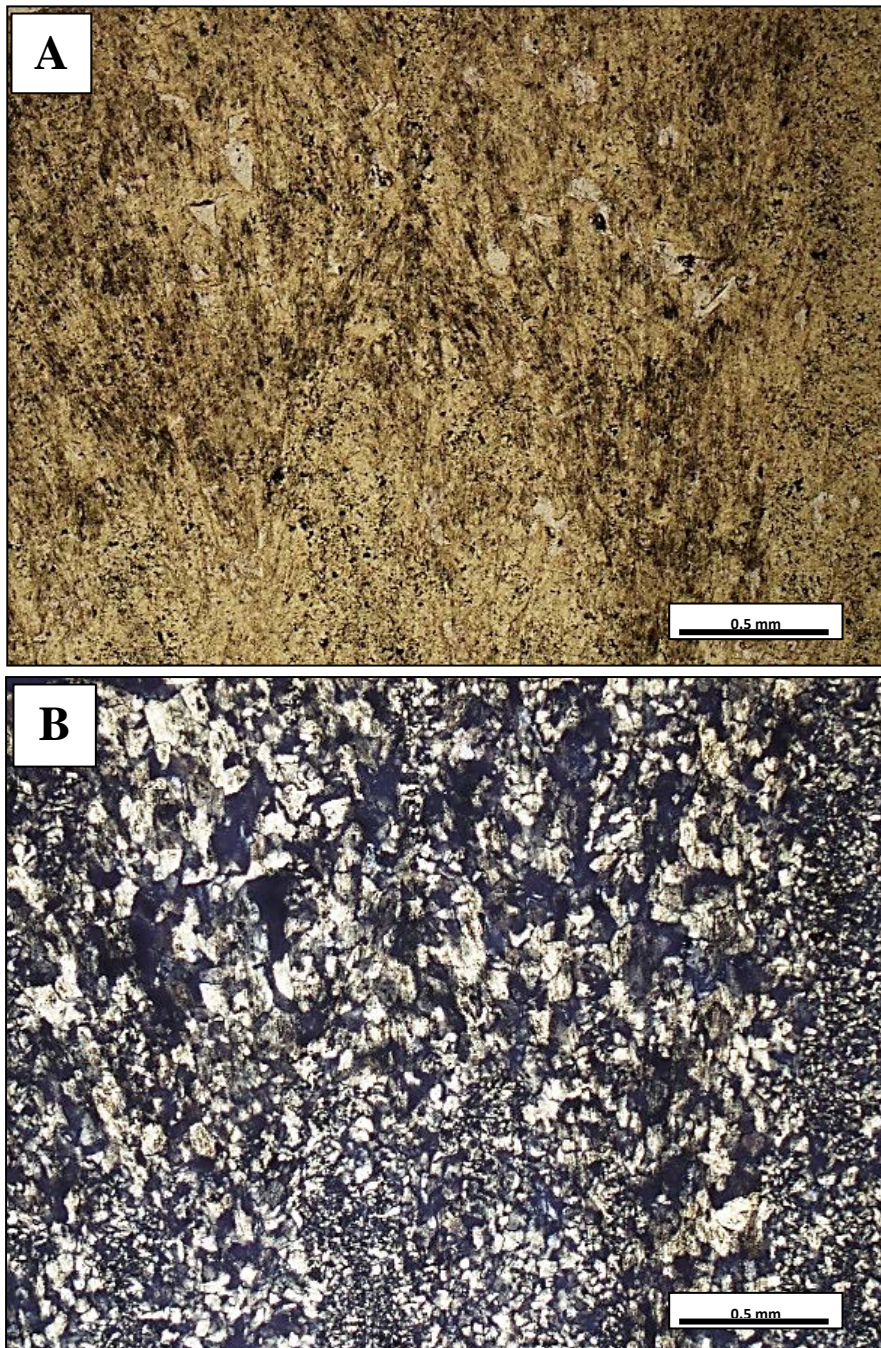


FIG 50. Photomicrographs of jigsaw texture that occurs with other textures in the Fire Creek deposit. Fibrous-acicular structures that likely formed in colloform layers occur with jigsaw textures. A: Photomicrograph (plane-polarized light) represents yellow staining colors of adularia, which is a major mineral in this texture. B: Photomicrograph (crossed polars) of A represents jigsaw features in colloform layers exhibiting various grain sizes.

In another sample exhibiting fibrous-acicular jigsaw texture, adularia is much more abundant and exhibits pseudo-rhombic crystal forms, and is associated with quartz. The adularia crystals vary in sizes ranging from less than 0.01 mm to 0.1 mm and occur as same-sized zones. In this sample, calcite blades rarely occur. Inclusions and impurities are found along the needle-like structures, which aid in defining this texture (Fig. 51).

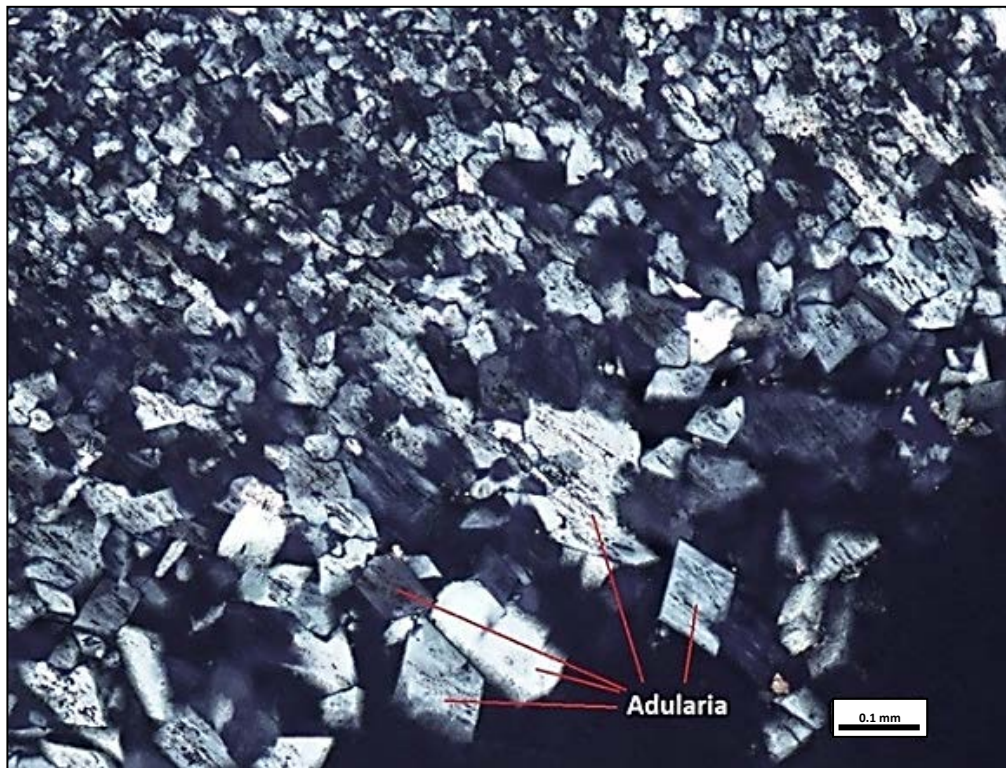


FIG 51. Photomicrograph (crossed polars) of fibrous-acicular structures and jigsaw texture from the Fire Creek deposit. Adularia is present as a pseudo-rhombic crystal associated with quartz grains. The crystals vary in sizes and shapes. Needle-like shapes containing aligned inclusions and impurities are found through the crystals.

The second-most common silica texture observed at the Fire Creek deposit is a replacement texture that occurs in 13 of 20 samples. Calcite blades are commonly partially or completely replaced by quartz and partially crystallized amorphous silica. The quartz grains exhibit euhedral to subhedral structures and recrystallized textures (such as plumose) encrusting on replaced calcite. Inclusions also occur with some of these euhedral quartz. Another phase, which likely is chalcedony, encrust the euhedral quartz and exhibit (re)crystallized textures that are probably the result of precursors of amorphous silica (Fig. 52).

Some replacement texture can be subdivided into three typed-zones using forms of bladed calcite and mineral composition including; 1) the blades cross-cut others forming an “x-shape” morphology; 2) euhedral to subhedral quartz crystals found in open spaces ranging from 0.1 to 0.5 mm; and 3) the remaining of calcite and/or later calcite. This texture indicates a lattice-bladed texture that occurs with jigsaw and zonal euhedral quartz crystals (Fig. 53).

The last common replacement texture is a parallel-bladed texture. This texture exhibits multiple parallel-bladed forms that are composed of different feature such as bladed calcite and quartz grains formed in the bladed boundaries. Fine-grained quartz with less than 0.1 mm of sizes are found along the rims of bladed calcite. Adularia is probably found to occur with quartz. This replacement texture also occurs with jigsaw, comb, and plumose textures (Fig. 54).

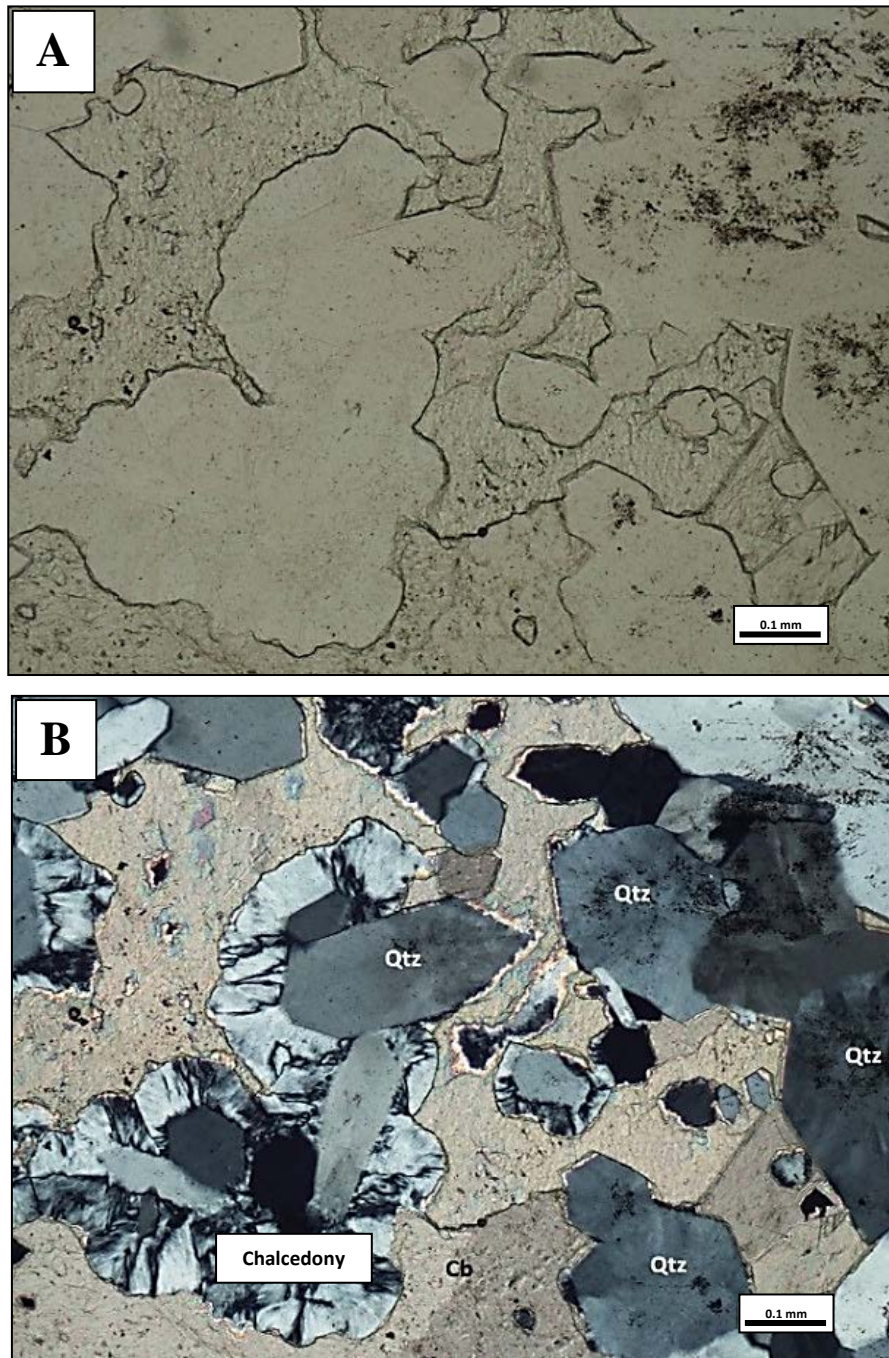


FIG 52. Photomicrographs of precursor amorphous silica and quartz replacement of calcite found in the Fire Creek deposit. A: Photomicrograph (plane-polarized light) exhibits calcite (high-relief) and quartz (low-relief). B: Photomicrograph (crossed polars) represents some perfectly euhedral crystals and elongated quartz surrounded by crystallized and recrystallized silica that are found in platy calcite. [Qtz = Quartz, Cb = Carbonates such as calcite]

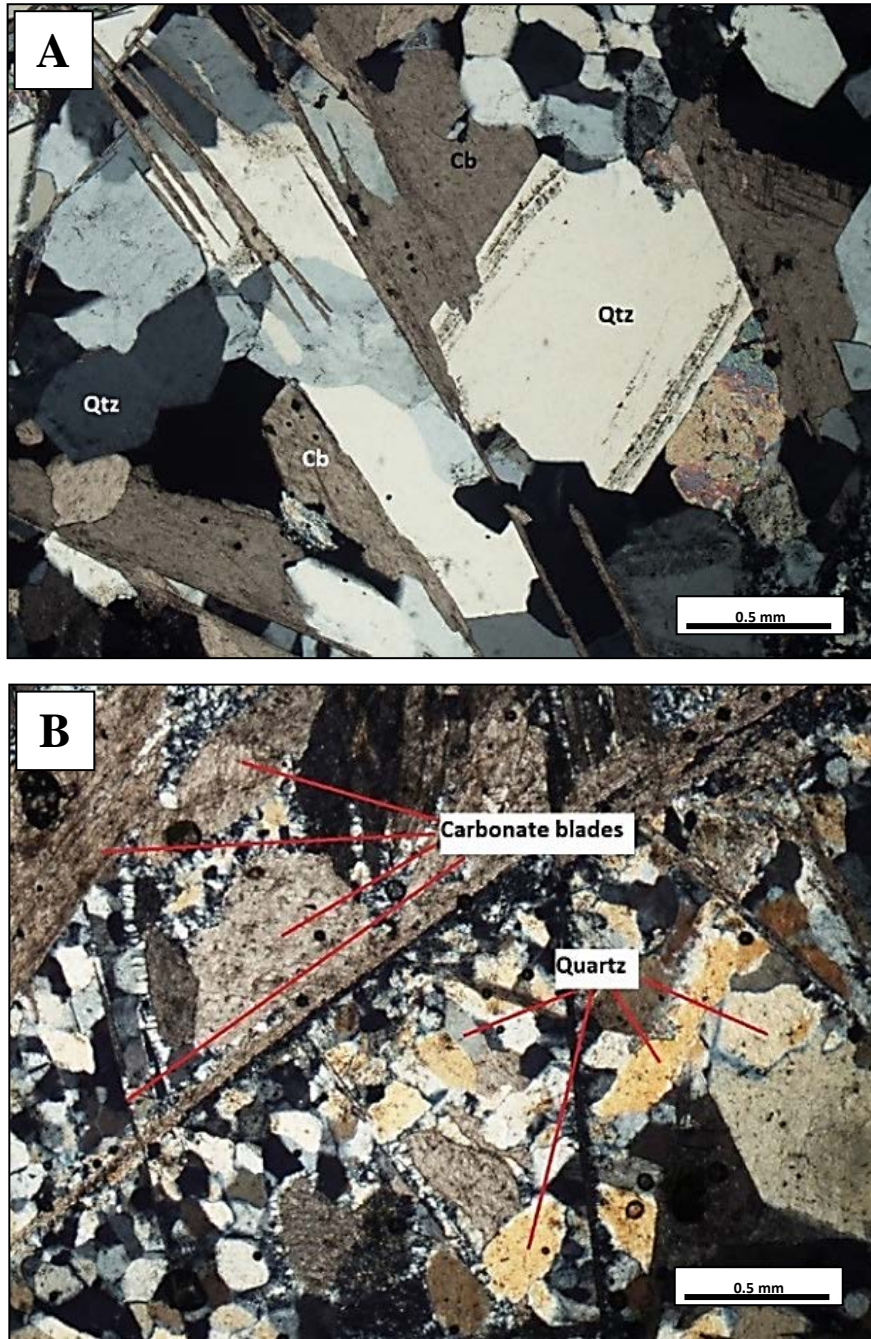


FIG 53. Photomicrographs (crossed polars) of lattice-bladed textures. A: Photomicrograph represents calcite plates that are partially replaced by euhedral quartz. Quartz crystals contain inclusions and impurities along growth zones. B: Photomicrograph exhibits intersected blades separated by quartz grains. Amorphous silica are also found in some platy calcite as replacement materials. [Cb = calcite blades, Qtz = Quartz]

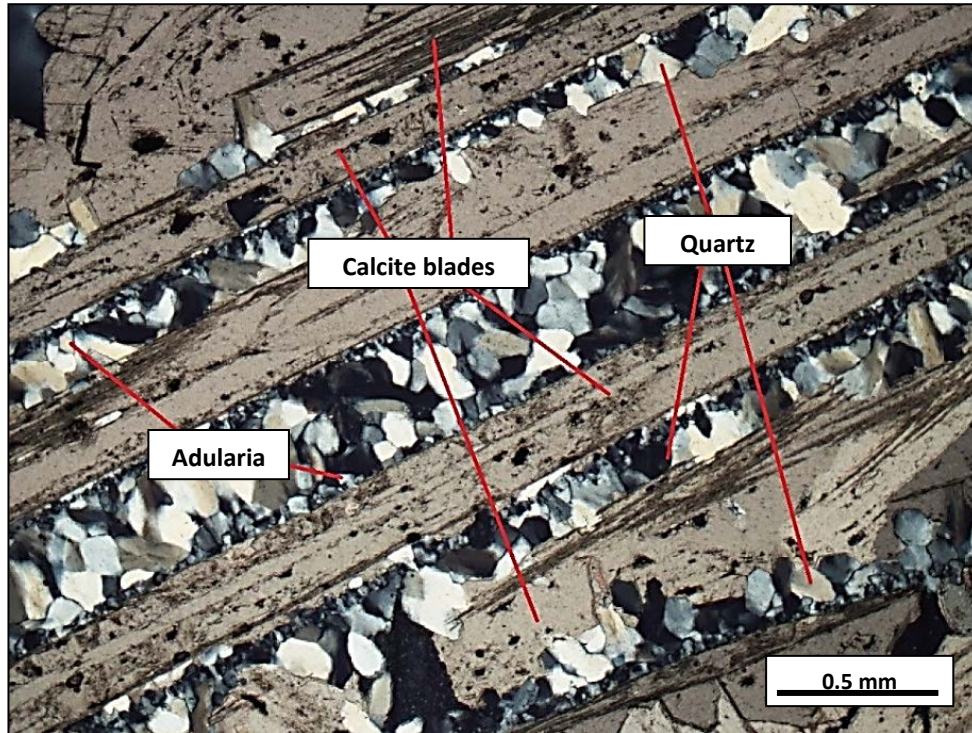


FIG 54. Photomicrograph (crossed polars) showing parallel-bladed texture found in the Fire Creek deposit. Quartz and adularia range from less than 0.1 to 0.2 mm that are found along grain boundaries of calcite. Quartz also form in multiple textures such as jigsaw and plumose.

A less-common texture observed at the Fire Creek deposit, which is found in 4 of 20 samples, exhibits multiple thin layers that define spherical colloform bands. Some of these bands encrusted large euhedral quartz crystals and also older colloform layers. The layers can be separated by black, brown, and yellow color zones. Radial fibrous structures are found in some spherical forms as well as concentric spheres. Some spheres have euhedral clear quartz crystals formed at the crust of spheres pointing out to open space (Fig. 55). These features are similar to “agate”, which is typically formed from layers of fibrous chalcedony (Hart, 1927).



FIG 55. Photomicrograph (plane-polarized light) of amorphous silica layers formed as spherical and colloform structures. The layers are separated by inclusions and subtextures exhibiting black, dark brown, or pale yellow color zones.

Some samples contain multiple crystallized and recrystallized layers of apparent former amorphous silica bands deposited along rims of flower-shaped aggregates of quartz and adularia crystals. Most of these layers include elongate and jigsaw quartz, and some of them exhibit fan-like extinction. Comb quartz crystals range from 0.3 to 0.5 mm in width and approximately 1 cm long that radially formed as flower-like shapes. Some comb quartz exhibit zone of inclusions indicated by very tiny dark spots along the crystal rims that are met with colloform bandings. These colloform layers were probably subsequently (re)crystallized and grown together with the comb crystal (Fig. 56).

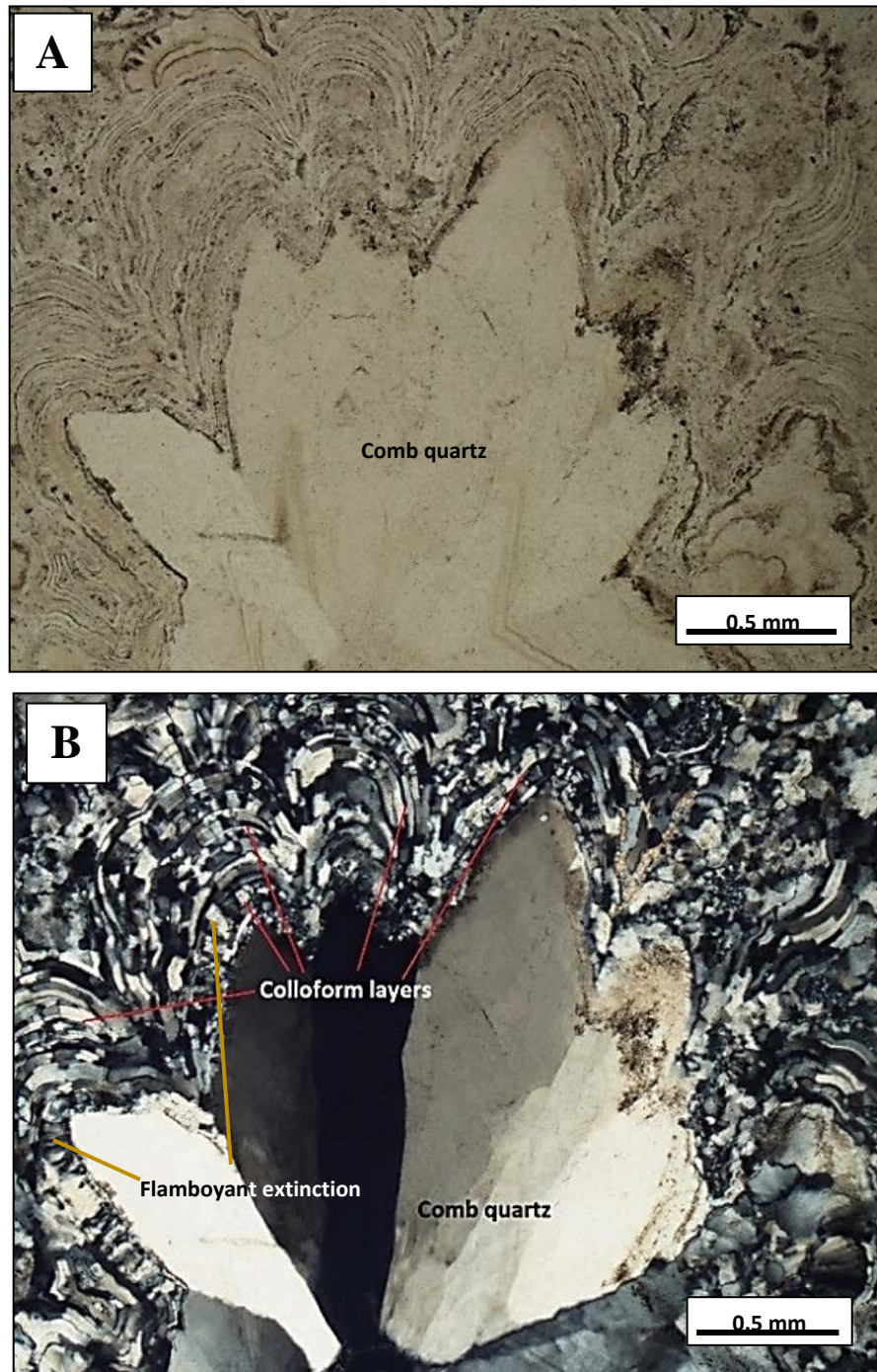


FIG 56. Photomicrographs showing flower-like structures and colloform-recrystallized bands from the Fire Creek deposit. A: Photomicrograph (plane-polarized light) shows radially euhedral quartz covered by very thin colloform layers. B: Photomicrograph (crossed polars) of A exhibits inclusion trapping zones between the rims of comb quartz and colloform layers. Flamboyant extinction and (re)crystallized textures are present along colloform structures.

Crystallized or recrystallized features in colloform bands found in the Fire Creek deposit can be subdivided into two features including 1) multiple concentric layers and 2) fibrous chalcedony. The concentric layers exhibit groups of colloform bands ranging from 0.01 to 0.02 mm of thickness that individually formed around a single grain of quartz and adularia, which is approximately 0.1 -0.2 mm of diameter. These colloform bands distinctly exhibit discrete (re)crystallized textures that are not related to other bands. This texture then mostly occurs as elongate jigsaw quartz in these colloform bands (Fig. 57).

Another feature consists of radial structures of fibrous chalcedony, which replaced colloform bands formed in the veins. The colloform bands that contained these fibrous structures are around 0.1 - 0.2 mm of layered thickness and they also encrust previous colloform layers and coarse-grained crystals. These fibrous features are indicated by flamboyant extinction that formed perpendicular to the walls of layers. Thus, this texture probably indicates that amorphous silica precursors likely crystallized to chalcedony (Fig. 58).

Additionally, some colloform bands exhibit a semispherical shape. This structure has radial-flamboyant extinction and it exhibits a feature that is similar to a handheld folding fan. Some flamboyant-colloform bands are subsequently recrystallized to microcrystalline quartz, yet their fan-shaped structures still remain. Zonal quartz, which ranges from 0.2 to 0.3 mm of diameter, is commonly encrusted by flamboyant-colloform features and occurs with jigsaw quartz (Fig. 59).

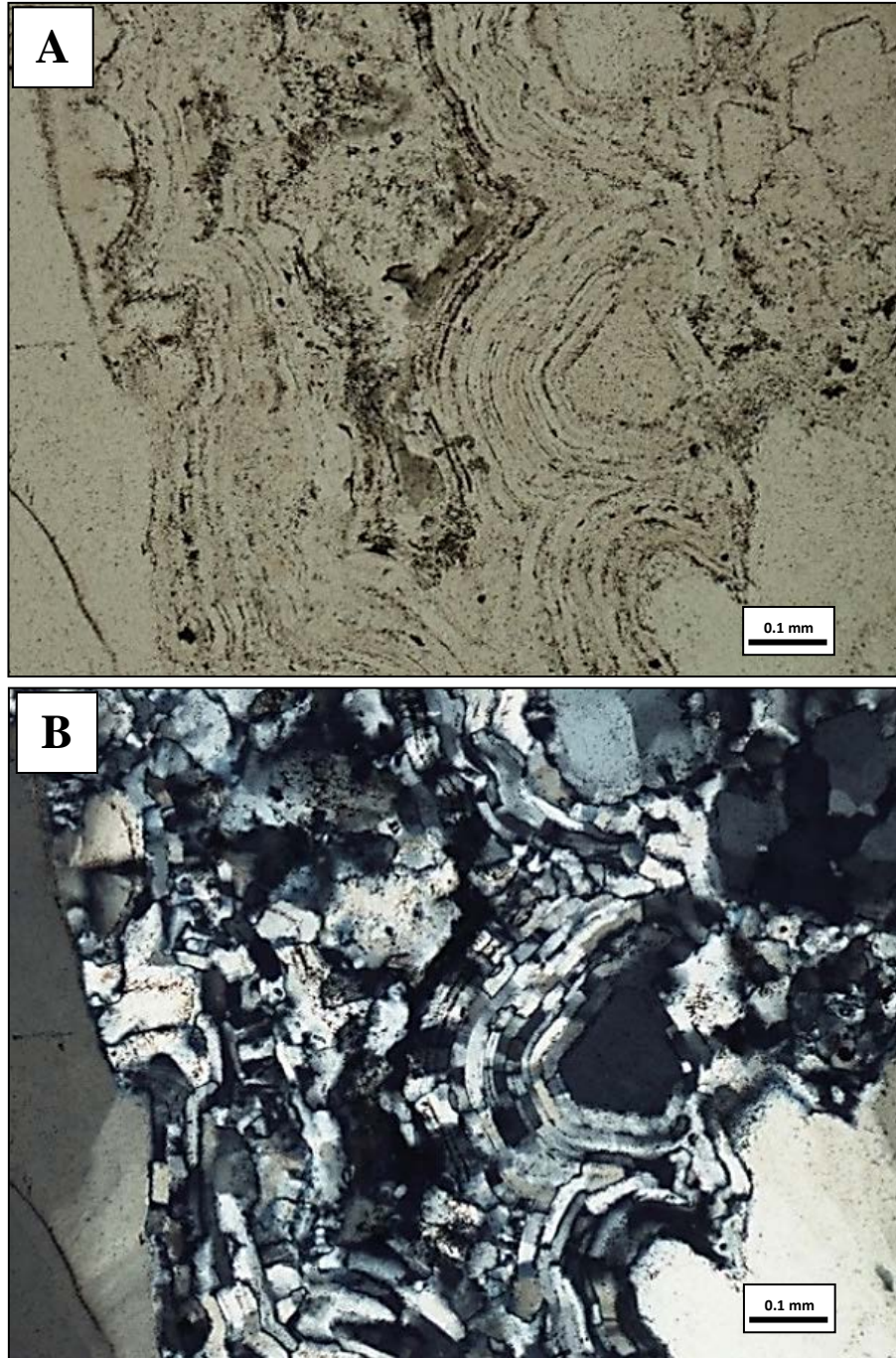


FIG 57. Photomicrographs of same area showing colloform textures found in the Fire Creek deposit. A: plane-polarized light; multiple concentric bands have encrusted larger crystals of mostly quartz and adularia along the vein walls. The open space is present at the middle between the vein walls. B: crossed polars; concentric layers individually exhibit (re)crystallized textures as elongate jigsaw quartz.

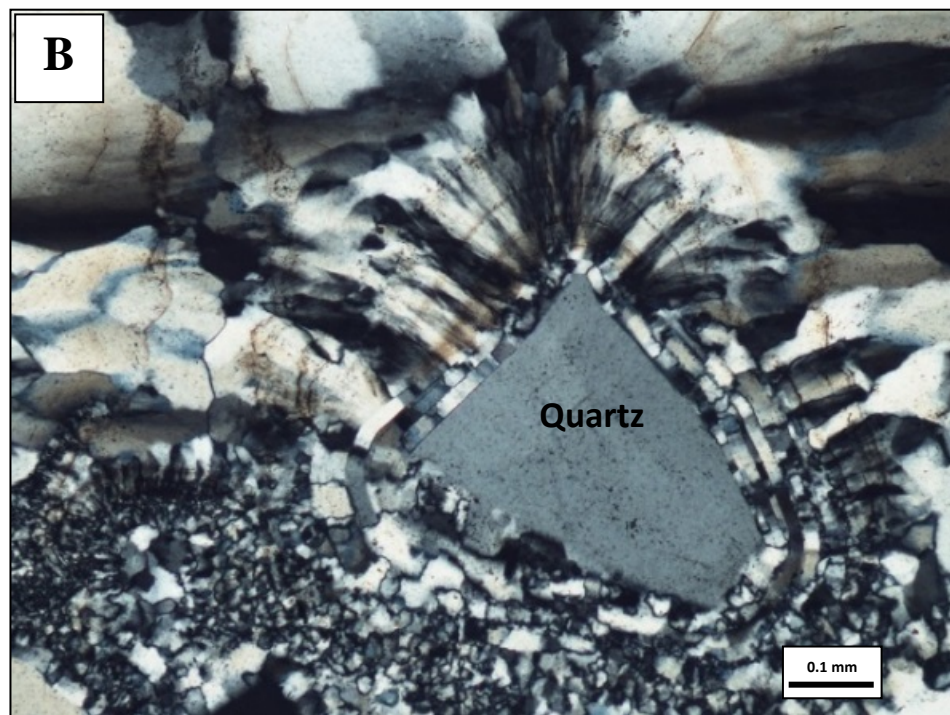
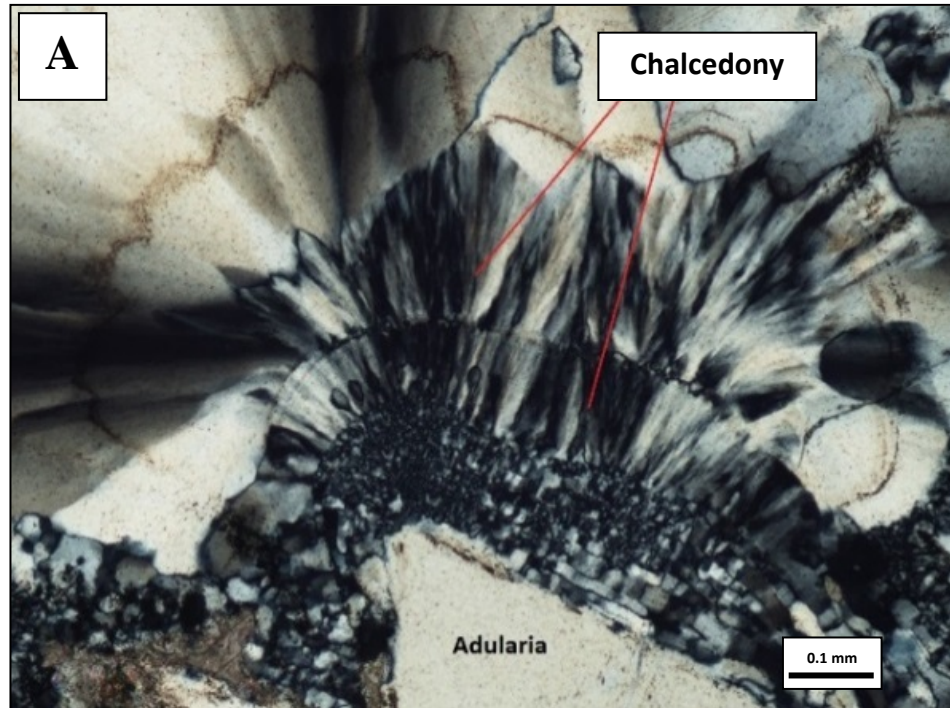


FIG 58. Photomicrographs (crossed polars) of fibrous chalcidony found in the Fire Creek deposit. A: Three colloform bands exhibit fibrous features that have encrusted other colloform layers and a crystal of adularia, which is approximately 0.5 mm of diameter. B: Fibrous chalcidony exhibiting flamboyant extinction occurs with a single quartz crystal and microcrystalline quartz.

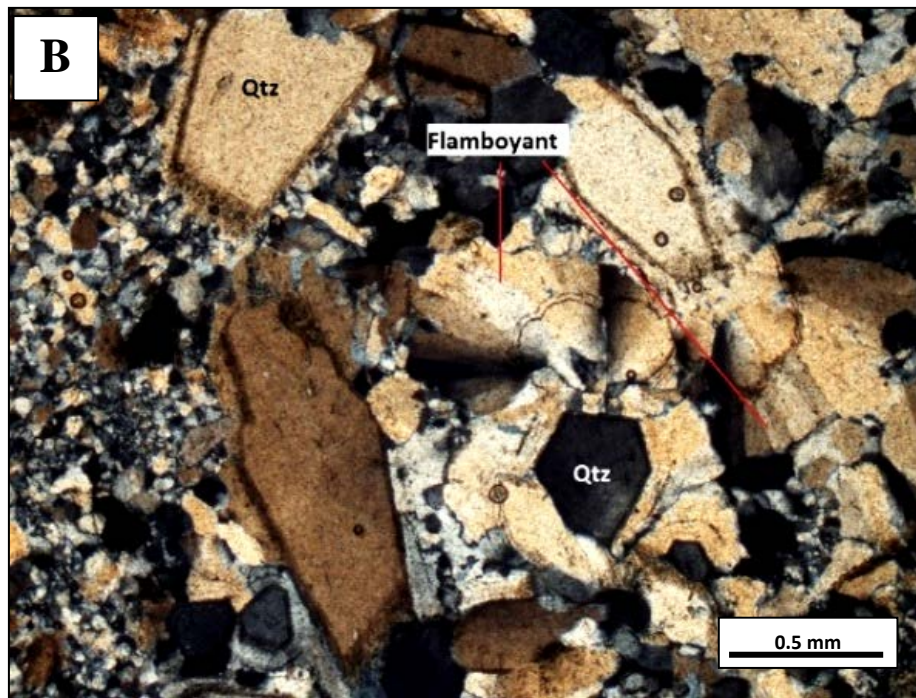
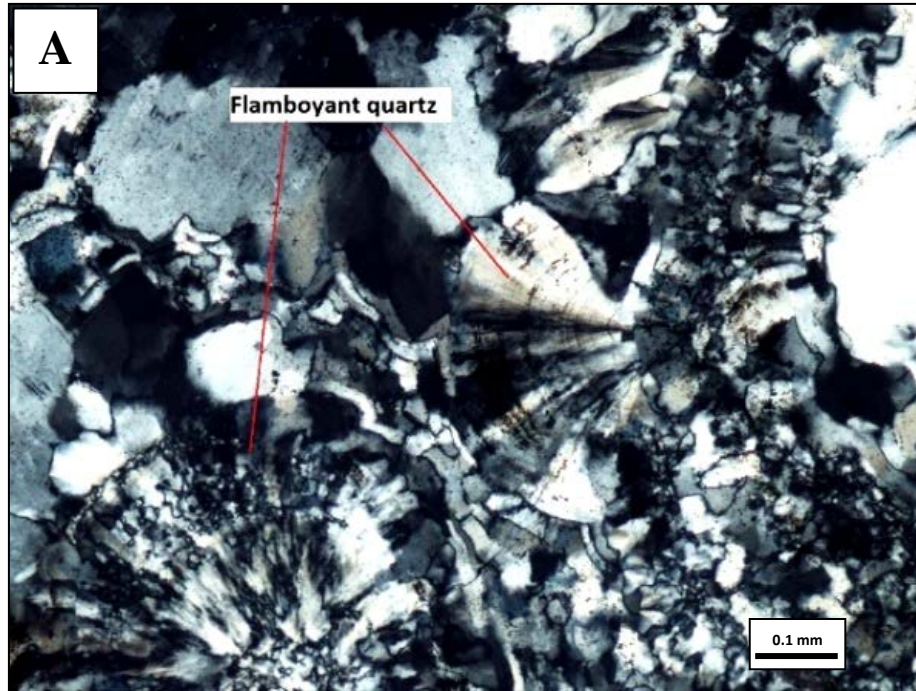


FIG 59. Photomicrographs (crossed polars) showing flamboyant textures in colloform bands. **A:** Fan-shaped structure perfectly exhibits flamboyant extinction, also visible is another fan-like shape that likely recrystallized to jigsaw quartz, yet still occurs with flamboyant extinction. **B:** Zonal euhedral quartz is encrusted by colloform textures showing flamboyant extinction. [Qtz = Quartz]

Moss quartz found in 3 of 20 samples are similar to that same at Buckskin National, and occurs as rounded quartz grains ranging from approximately 0.1 to 0.2 mm of diameter. These widespread rounded shapes and layers are possibly caused by the two-dimensions slicing through three-dimensions of colloform bands. These colloform layers have crystallized or recrystallized to form quartz. Inclusions and impurities are also found along banding boundaries. Spherical forms also exhibit radial and partly concentric patterns that are caused by different extinctions angles. Jigsaw quartz texture commonly occur as background (Fig. 60).

The final vein texture found in the Fire Creek deposit, is a plumose or feathery texture that consists of small elongated quartz crystals formed in a larger quartz crystals. This texture is rarely found in this deposit compared to other silica textures. It usually is a minor feature that associates with other textures such as comb, flamboyant, and zonal quartz. Quartz crystals that have plumose features are coarser grained than others, and range from 0.3 to 0.5 mm. They also can be found as micro-scaled plumose quartz that formed at the end of euhedral crystals showing small feathery features radiating out from a central crystal core (Fig. 61).

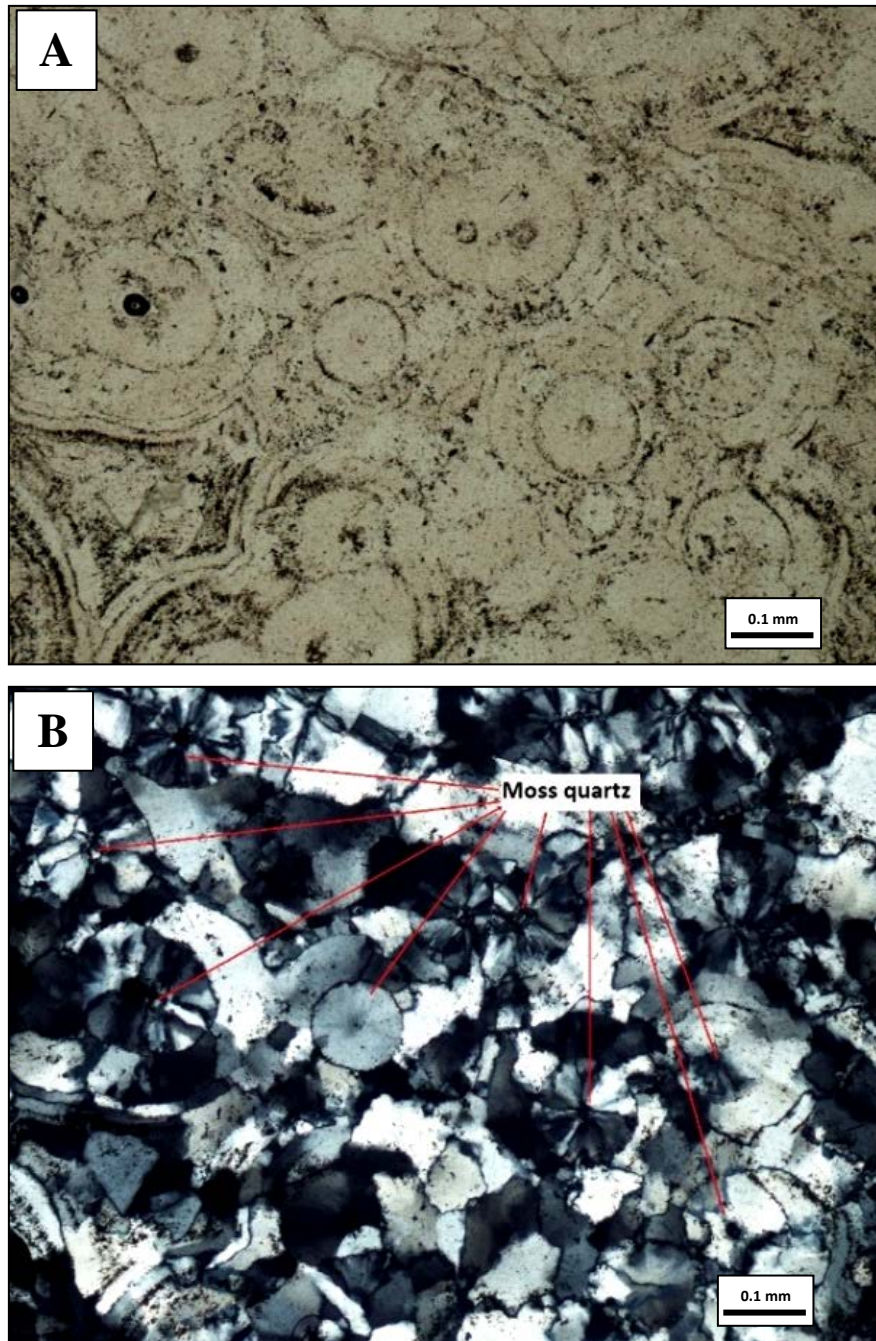


FIG 60. Photomicrographs of moss quartz or ghost-sphere texture found in the Fire Creek deposit. A: plane-polarized light; perfectly spherical forms in 2D slice with nucleuses that are accumulated by colloform bands. B: crossed polars; moss quartz in 0.1 – 0.2 mm of diameter. These moss quartz have radial structures typical of (re)crystallized textures, which occur with jigsaw quartz.

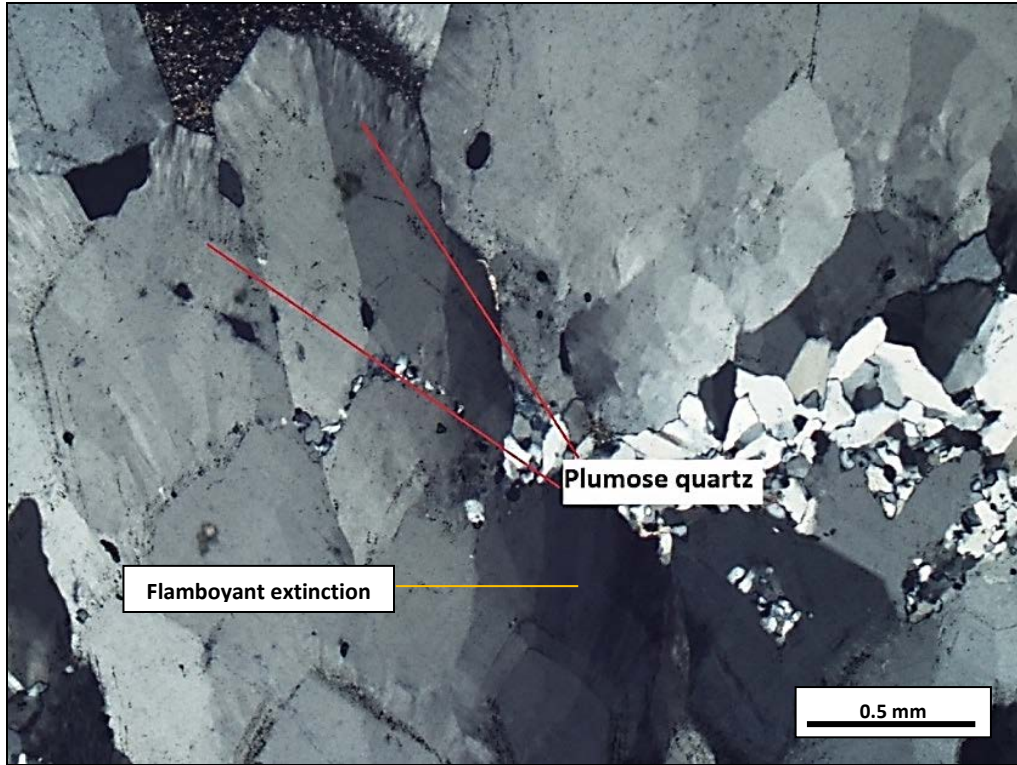


FIG 61. Photomicrograph (crossed polars) showing rare plumose textures in the Fire Creek deposit. Large crystals of euhedral clear quartz occur with group of smaller elongate quartz, which are subdivided by different extinction angles, has formed by encrusting the large euhedral crystals. Flamboyant and jigsaw quartz also occur.

4.3 Precious-Metal Minerals

Precious-metal minerals can be observed in both hand specimens and under the microscope at the Buckskin National and Fire Creek deposits. In hand sample, they exhibit metallic dark grey and black colors disseminated within silica veins. The identification of precious-metal minerals is beyond the scope of this study, although reconnaissance conclusions on the mineralogy are based on optical properties, and previous works of Vikre (1985 and 1987), Saunders (1990 and 1994), and Unger (2008). Common Au-Ag minerals in all of the middle Miocene epithermal ores include electrum, acanthite, naumannite, aguilarite, and silver sulfosalts. However, the ore minerals can be classified into three textural types in this study, including dendritic structure, needle-like texture, and disseminations.

Some vein samples collected from the dumps of the Buckskin National mine contain precious-metal minerals associated with gangue minerals such as quartz and adularia. They exhibit aggregation of black tiny spots and needle-like forms that have disseminated in silica layers. In the polished-sections, precious-metal minerals distinctly exhibit dendritic- or tree-shaped structures formed along the silica bands perpendicular to the vein walls. Dendritic features also occur with disseminated minerals that are found as black individual tiny grains. Moreover, some colloform layers contain numerous ore minerals and appear as metallic-colored layers (Fig. 62). Using a hand lens, these ore minerals exhibit bright silvery to bright pale yellow reflections. Some electrum grains reflect very strongly bright golden yellow. Disseminated ore minerals are found in

fibrous-acicular cavities of silica veins. The common silica textures exhibit glassy milky quartz to translucent quartz in colloform-crustiform bands.

Using the combinations of reflected and transmitted lights, we can clearly separate ores from gangue minerals. Under reflected light, the most reflective minerals are precious-metal minerals such as electrum, silver-selenides, and silver-sulfides. These precious-metal minerals are also found at Fire Creek but are more abundant than at Buckskin National.

The most common texture of precious-metal minerals is a dendritic structure that formed along colloform bands associated with (re)crystallized textures of gangue minerals. Quartz and adularia exhibit dull reflected light, whereas electrum has strongly bright silvery to bright yellow reflected colors. Other metal minerals, which are found in the veins, exhibit bright pale grey to silvery reflected colors. These minerals consist of Ag-S-Se phases that are typically silver-selenides, silver-sulfides, and silver-sulfosalts. The silica textures occurred with these ore minerals include microcrystalline quartz, which vary in grained-sizes, and colloform bands that are hosts to these metallic minerals (Fig. 63). Some precious-metal minerals are disseminated in cavities and pores of the veins and they range from 0.1 to 0.3 mm of diameter. These ore minerals exhibit zones of distinct and variable compositions that are indicated by different reflected colors. More bright yellow color exhibits higher gold ratio than less-bright pale-yellow color. Silvery and bright grey colors represent the Ag-S-Se phases with lower gold ratio. Euhedral and elongate quartz grains are commonly found with precious-metal minerals along the colloform bands. Jigsaw quartz in colloform bands are also present (Fig. 64).

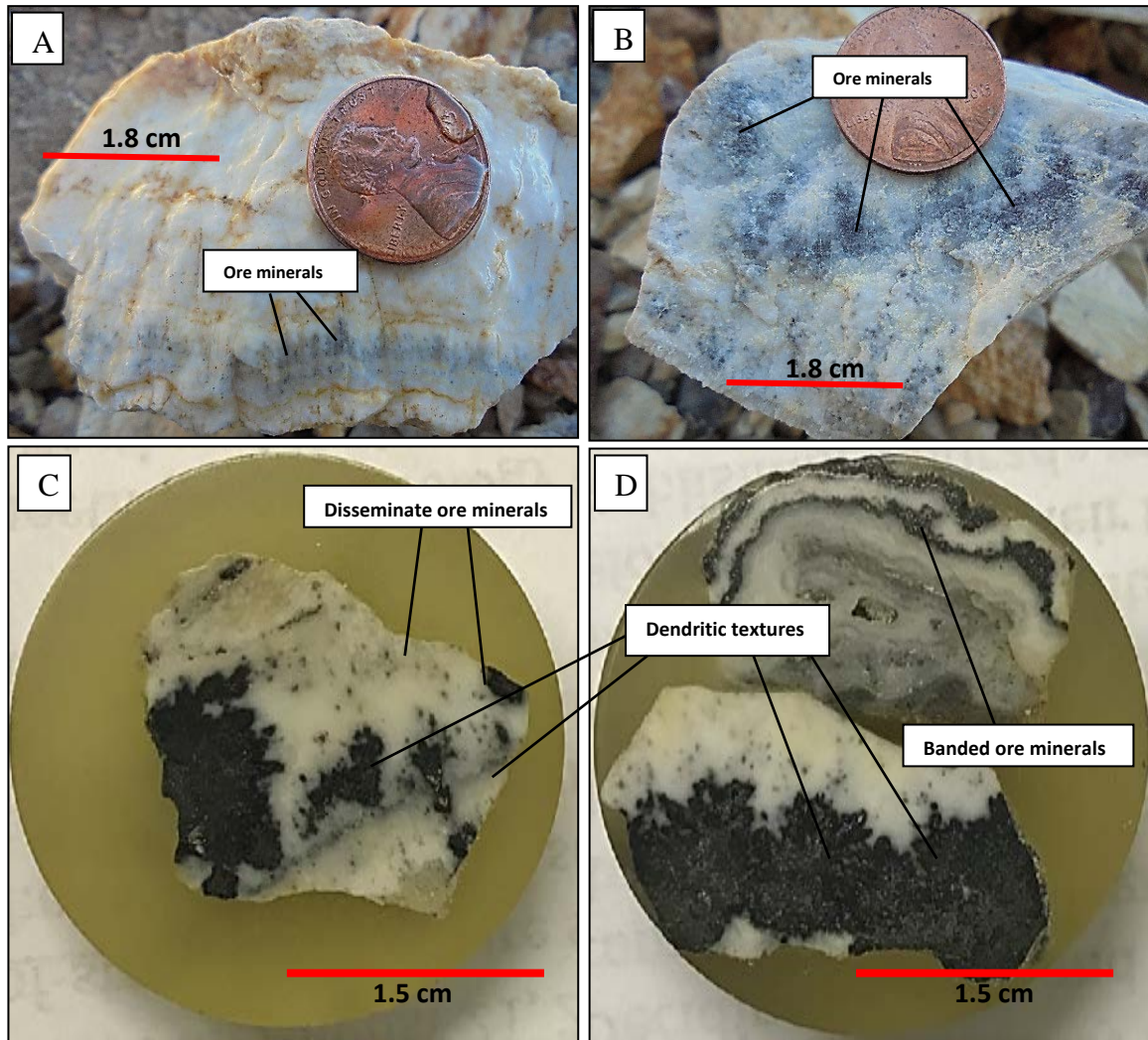


FIG 62. Photographs of precious-metal minerals found in Buckskin National samples. A: Ore minerals are indicated by dark fibrous-needle structure at the lower part of bands occurred with banded milky quartz. B: Ore minerals form along colloform bands. C: Polished-section of Buckskin National deposit shows dendritic and disseminated metal minerals. D: Polished-section exhibiting dendritic textures, disseminate minerals and banded ore minerals associated with colloform bands and milky glassy quartz.

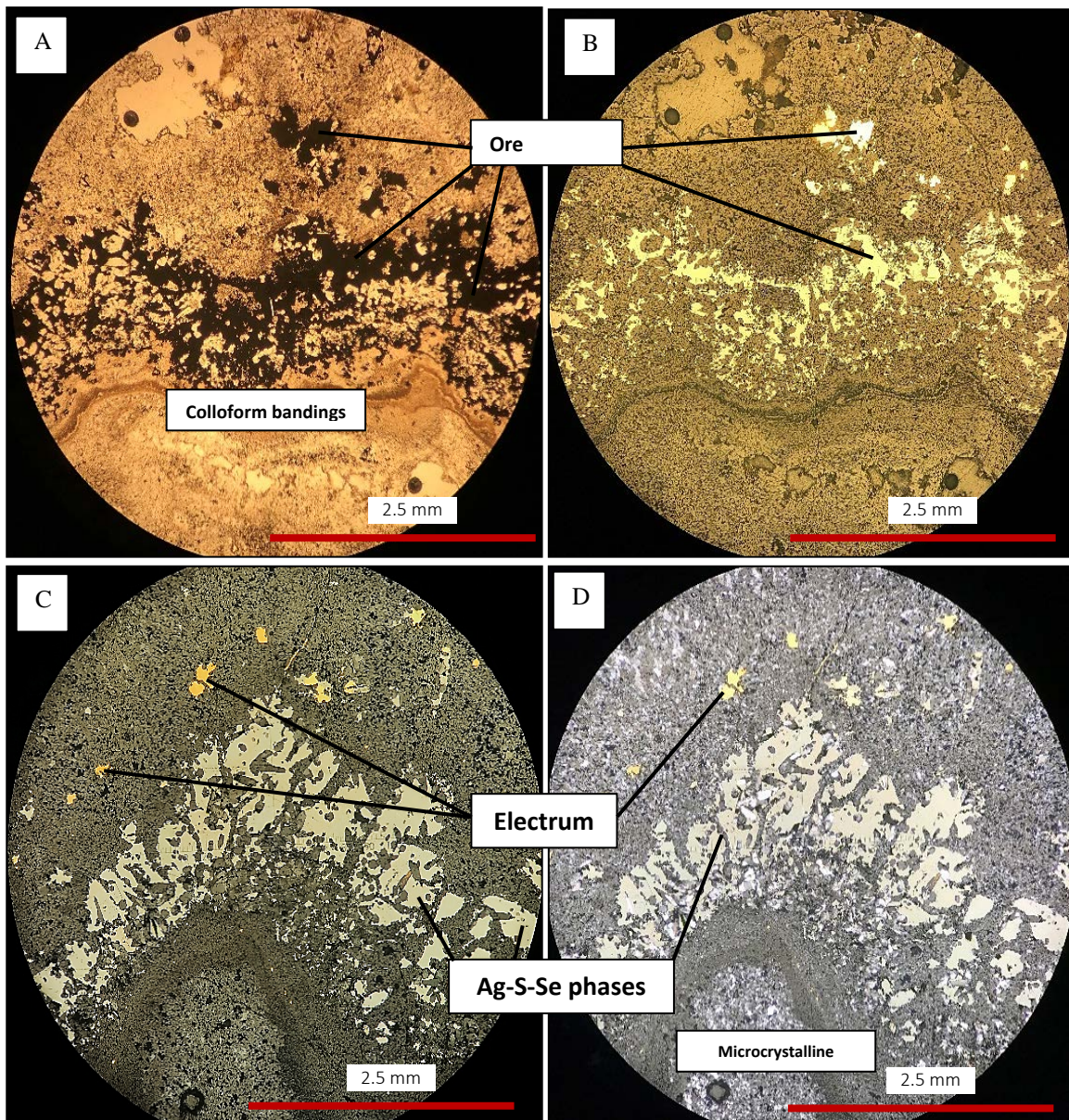


FIG 63. Photomicrographs of dendritic-banding structures of precious metals (electrum and silver-minerals) found at the Fire Creek deposit. A: Photomicrograph taken under plane-polarized (transmitted) light showing a dendritic band of silica and opaque ore minerals in colloform bands. B: Photomicrograph taken under reflected light of the same view as that of A. These opaque ore minerals exhibit bright yellow reflecting colors. C: Photomicrograph under reflected light exhibits bright yellow individual grains and bright pale grey minerals that indicate as electrum and Ag-S-Se phases. D: Photomicrograph under the combination of reflected and transmitted lights of the same view as that C showing colloform bands and microcrystalline textures occurred with these precious metal minerals.

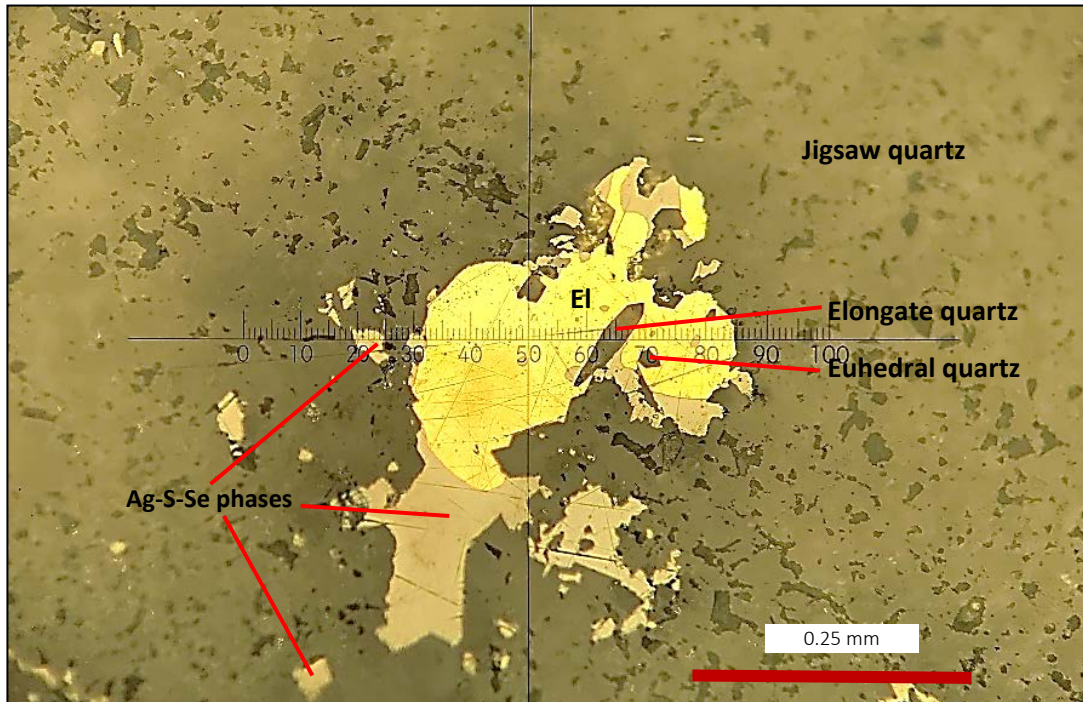


FIG 64. Photomicrograph (reflected light) of grains of silver-selenides (grey) electrum (yellow) associated with gangue minerals from the Fire Creek deposit.

In the Fire Creek deposit, some samples exhibit a relationship between precipitation of ore-minerals and gangue minerals, which occurred essentially of the same time as the Fire Creek deposit. Precious-metal minerals including electrum and Ag-S-Se phases commonly occur with euhedral and elongate quartz, which probably co-precipitated. On the other hand, these precious-metal minerals are also encrusted by calcite that exhibits a platy structure (Fig. 65).

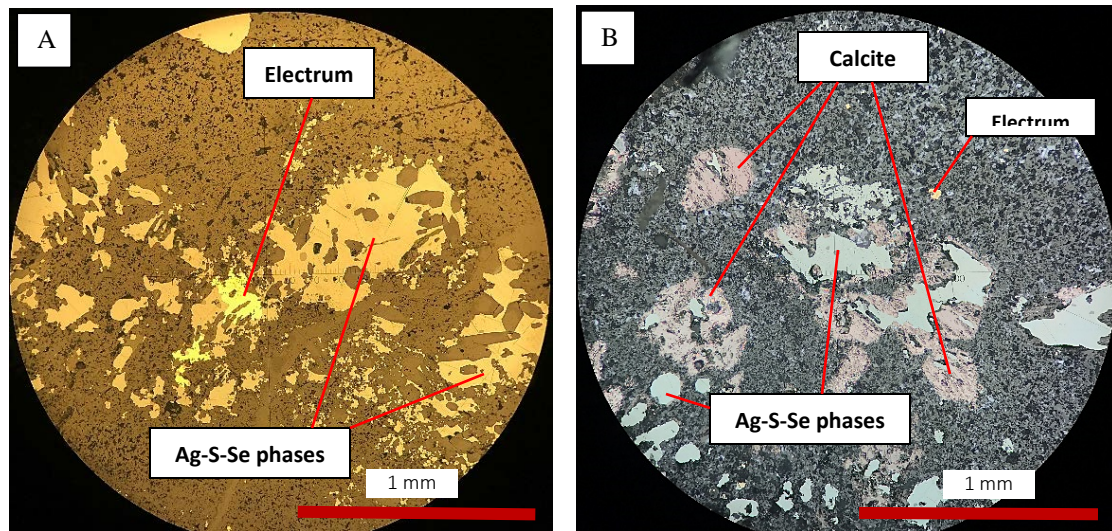


FIG 65. Images of ore minerals from the Fire Creek deposit and associated gangue minerals (silica and calcite). A: Photomicrograph (reflected light) showing precious metals form together with quartz and adularia that represent transformed textures. B: Photomicrograph (reflected light and crossed polars of transmitted light) showing precious metals are encrusted by calcite.

In addition, other precious-metal minerals including acanthite and pyragyrite (ruby silver) were observed in the Buckskin National deposit by Vikre (1987). Acanthite, which is a silver sulfide mineral, is present as elongated and pseudocubic structure with bright grey color (weakly anisotropic). It commonly occurs with other metal-sulfides minerals. Associated gangue minerals include colloform bands and milky glassy quartz (Fig. 66).

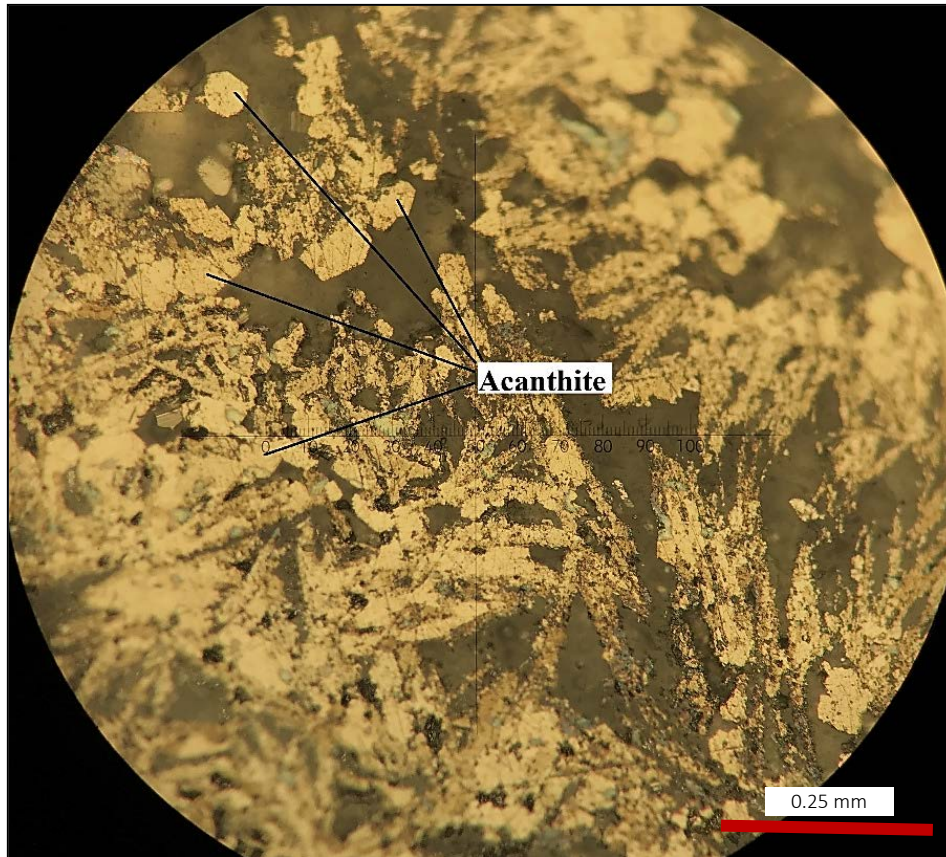


FIG 66. Photomicrograph (reflected light) of metal-sulfides found in the Buckskin National mine. Pseudocubic crystals indicate acanthite (Ag_2S) and associate with other sulfides in silica veins. Gangue minerals as quartz exhibit jigsaw-microcrystalline quartz in colloform banding.

Pyragyrite or ruby silver, a silver-bearing sulfosalt mineral, consist of silver, sulfur, and arsenic. It exhibits hexagonal structure with dark red to black colors and adamantine to sub-metallic lusters. It also occurs with other silver-bearing minerals as same as acanthite at the Buckskin National deposit. Pyragyrite grains are found along bands of ore minerals associated with colloform bands. Milky glassy quartz to translucent texture occurred as gangue minerals in the ore veins (Fig. 67).

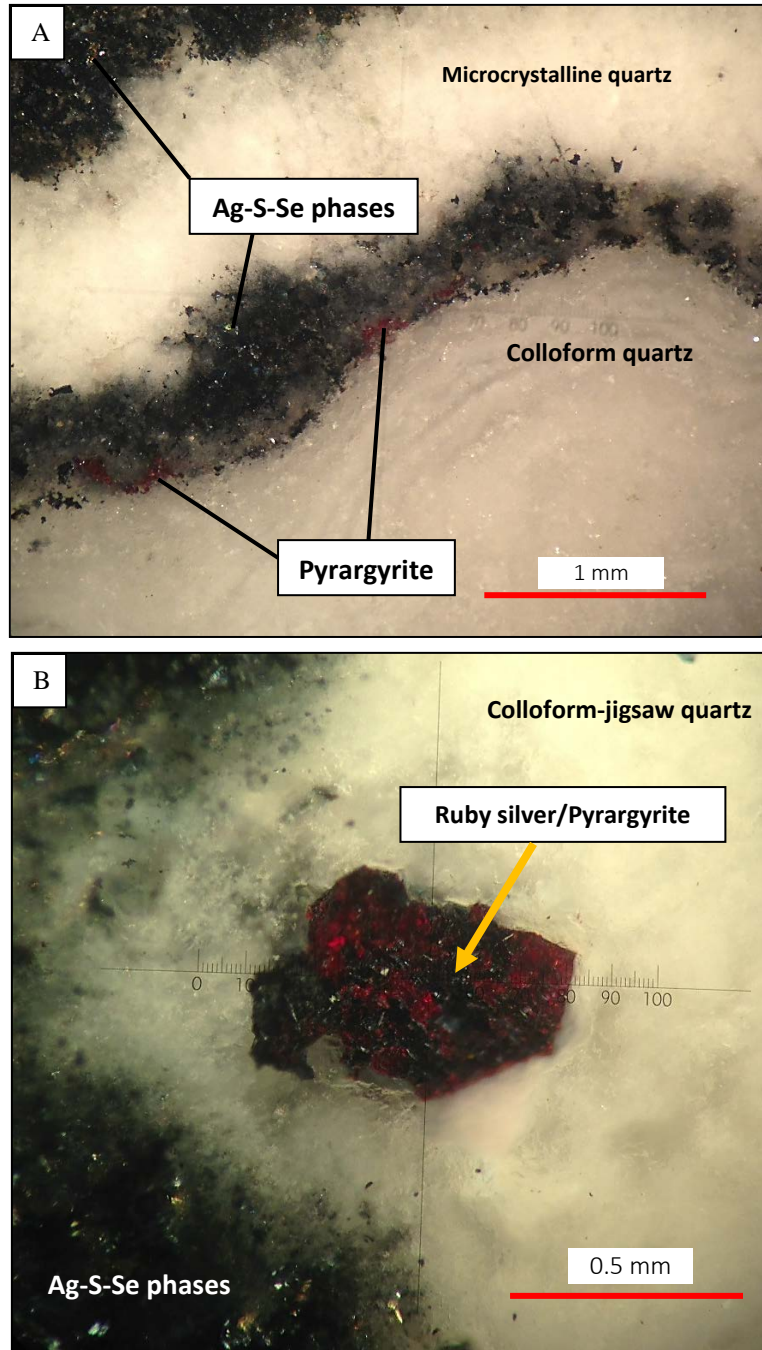


FIG 67. Photomicrographs (reflected light) showing pyrrargyrite or ruby silver minerals found in the Buckskin National deposit. A: Ore mineral band consisting of pyrrargyrite (red color) and Ag-S-Se phases (black and silvery reflected colors) occurs with colloform bands of gangue minerals such as milky quartz. B: Individual grains of pyrrargyrite exhibit sub-hexagonal structure and red to black colors with adamantine to submetallic lusters. These grains are surrounded by jigsaw quartz in colloform bands.

4.4 Cathodoluminescence (CL) images

Silica textures exhibit various colored patterns using the CL microscope. Quartz crystals have three characteristic luminescence manifestations, including yellow, orange and blue emitted colors. These colors can be continually captured by a video camera during a given time after the electron bombardment process started.

The CL colors observed in this study come from silica phases that consist of three CL characteristics. 1) A blue CL color indicates the shortest-lived emitted CL color, which commonly disappears approximately 7 to 10 seconds after the bombardment. 2) A long-lived yellow CL color are visible longer time than blue, but it continually decreases in brightness. 3) Another CL color is an orange or reddish brown CL color that is come as the last color after black CL colors. The three types of CL emitted colors can occur together to show variable silica phases in vein textures of Buckskin National and Fire Creek deposits (Fig. 68).

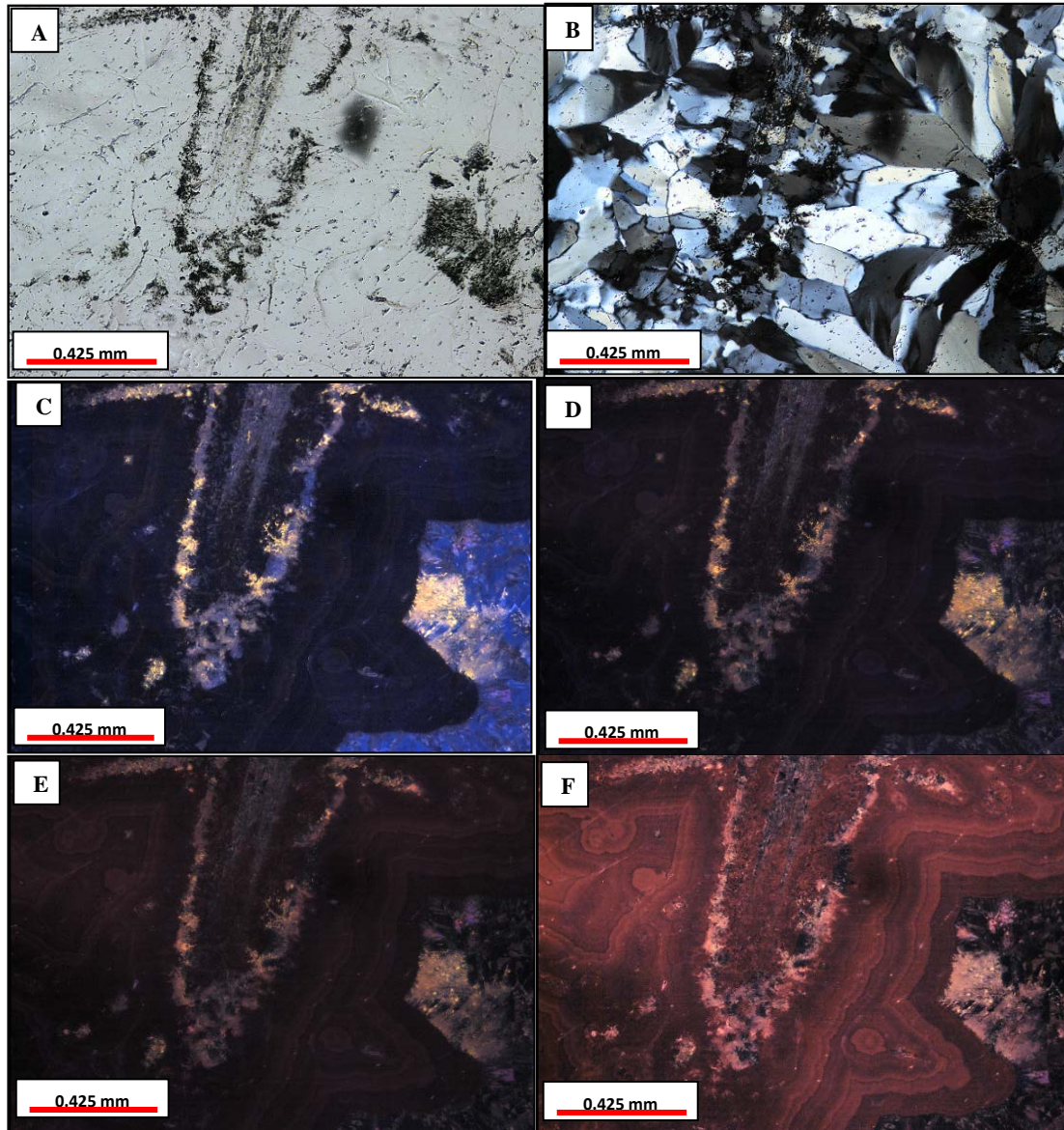


FIG 68. Photomicrographs of the CL emissions showing various colors that were emitted by silica phases in the same view. A: Photomicrograph (plane-polarized light) showing a replaced blade associated with clear quartz crystals and zones of inclusions that are the darker zones. B: Photomicrograph (crossed polars) of jigsaw and replacement quartz textures. C: CL photomicrograph taken at 11:58:14:734 (hr:min:sec:millisec), this is a beginning period after the electron bombardment started. There are blue, yellow and dark purple bands in this texture. D: CL photomicrograph taken for 9.469 seconds later showing the disappearance of blue band. (11:58:24:203) E: After the bombardment had been started for 18.922 seconds, the brightness of yellow band was decreased and dark band became brighter (11:58:33:656). F: Dark bands completely changed to be reddish brown for a minute later (11:59:20:953).

The CL system provides a different view of silica textures, which cannot be seen with the conventional microscope. Jigsaw texture contains various quartz sizes ranging from 0.01 to 0.1 mm in diameter associated with needle-like or fibrous-acicular structure. The jigsaw quartz grains emit two colors including long-lived yellow and short-lived blue CL emission. The quartz grains formed among and/or within needle-like structures still remains visible and exhibit long-lived yellow CL emission. Short-lived blue CL color likely represents a homogenous texture in all quartz sizes (Fig. 69). Approximately 8 seconds after the bombardment, blue emitted light mostly disappears and turns into reddish purple along with decreasing of yellow color. Later existence of bright blue color indicates epoxy filling in pores.

Clear quartz crystals distinctively emit short-lived blue color showing homogenous texture. Blue-colored CL emission is rapidly removed, after it was present for 9-10 seconds long. Carbonate minerals such as calcite are characterized by stable bright orange and red CL colors (Fig. 70).

Comb quartz sometimes contains impurities and inclusions that exhibit feather-like forms. These inclusion zones mostly release yellow CL color surrounded by blue CL emission. The non-inclusion zones in quartz only exhibit short-lived blue CL color. These euhedral comb quartz grains also represent various shades of blue CL color that were probably caused by irregular grained surfaces (Fig. 71).

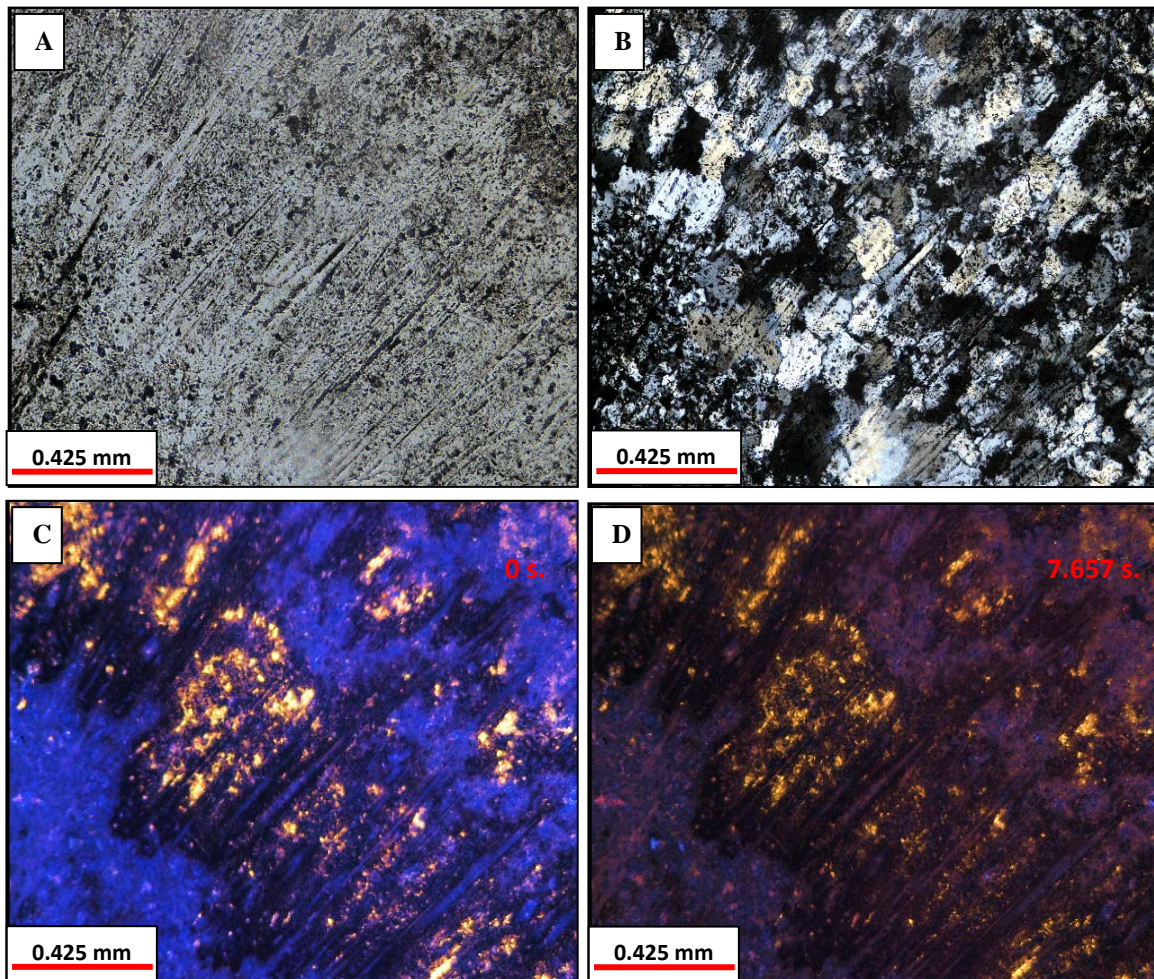


FIG 69. Images showing jigsaw-acicular texture from the Buckskin National deposit in same view. **A:** Photomicrograph (plane-polarized light) showing a needle-like structure. **B:** Photomicrograph (crossed polars) contains various sizes of microcrystalline-jigsaw quartz. **C:** Photomicrograph after the bombardment was started at 09:39:27:468, two CL colors were shown including blue and yellow. **D:** Photomicrograph taken on 7.657 seconds later, blue CL color is mostly disappeared and yellow band remains visible with lower brightness (at 09:39:35:125).

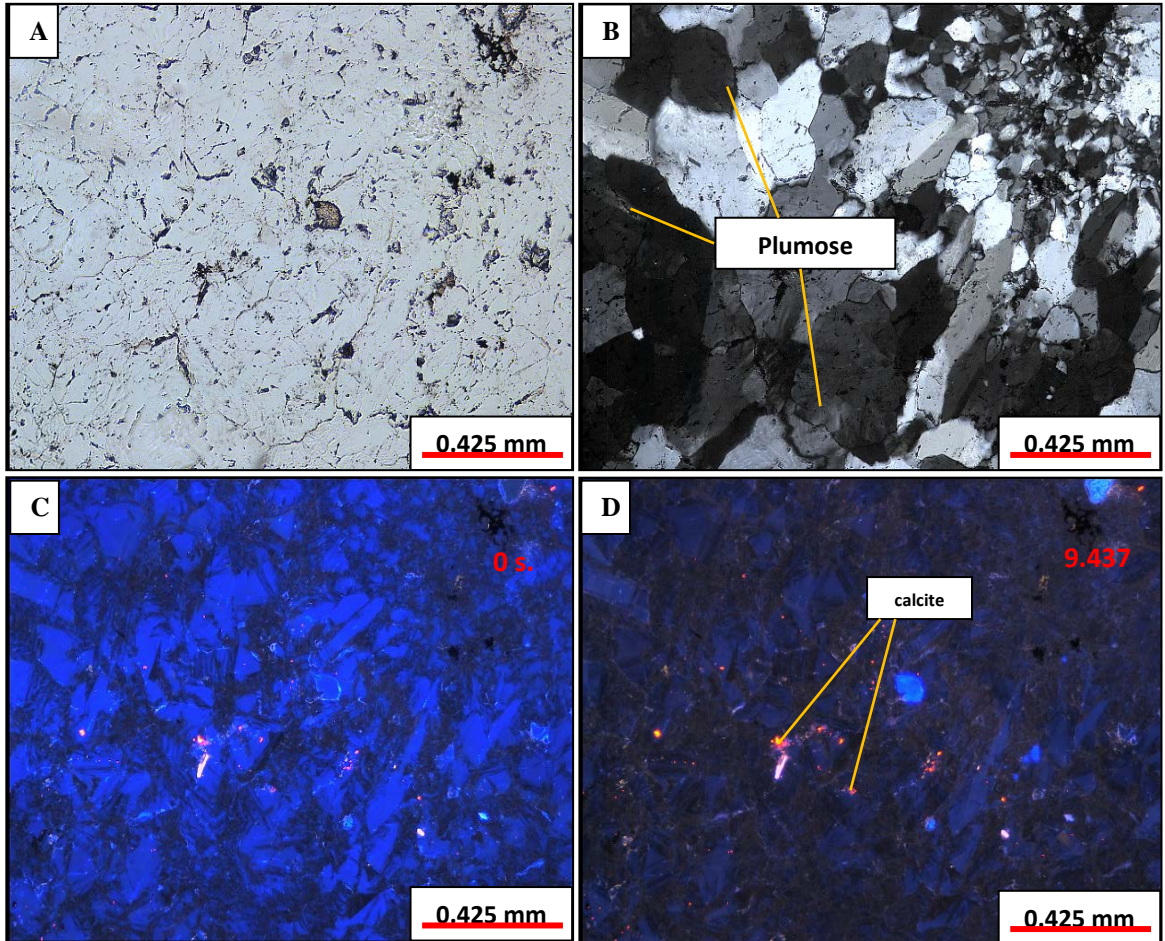


FIG 70. Images showing (re)crystallized texture including jigsaw and plumose quartz from the Buckskin National deposit in same view. **A:** Photomicrograph (plane-polarized light) showing clear quartz crystals and small particles of impurities. **B:** Photomicrograph (crossed polars) showing coarse- to fine-crystal sizes occurred with euhedral to subhedral crystal forms. **C:** Photomicrograph taken after the bombardment started (11:34:57:734), blue band is emitted showing a homogenous texture. **D:** Photomicrograph taken 9.437 seconds later (11:35:07:171), blue band is partly gone. Spots of bright reddish orange and blue colors represent calcite and pores, respectively.

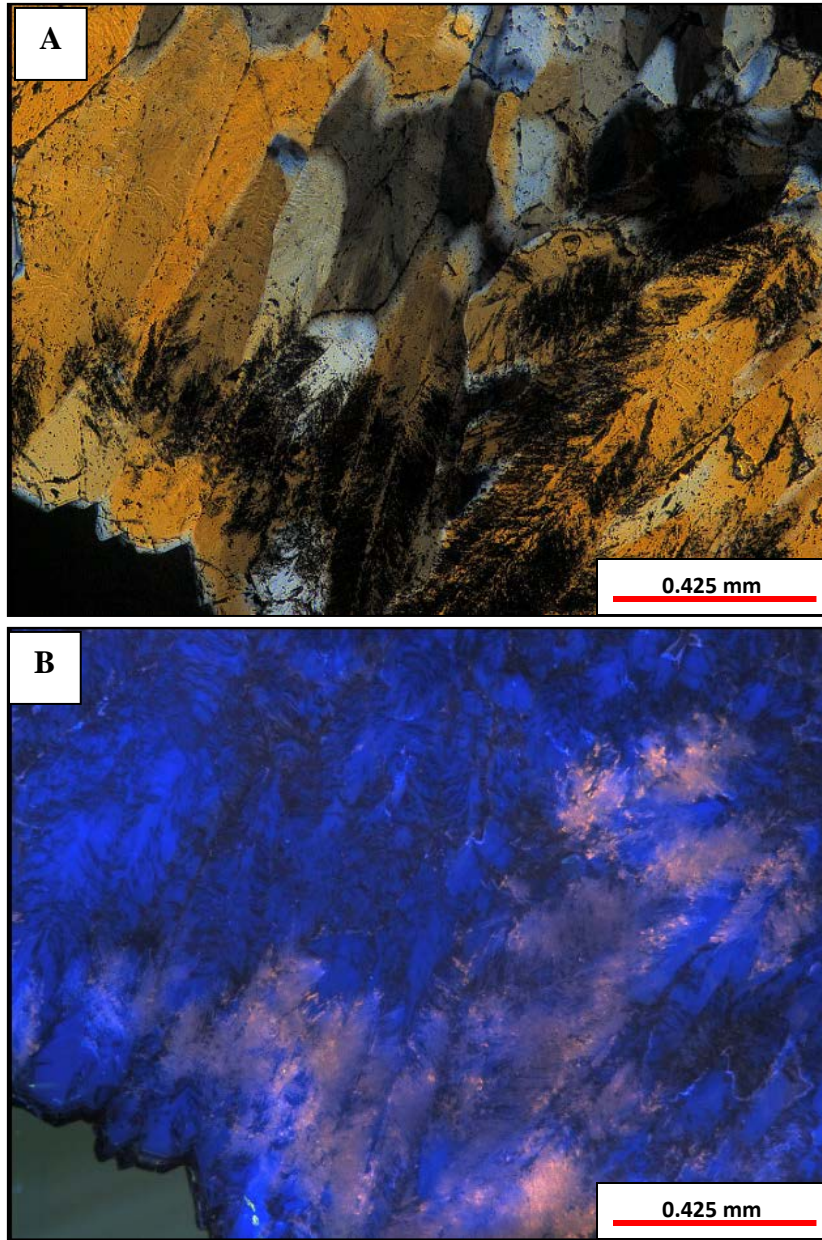


FIG 71. Images showing euohedral comb-plumose quartz crystals from the Buckskin National deposit. A: Photomicrograph (plane-polarized light) exhibits euohedral quartz containing inclusions and impurities. B: After electron bombardment started, short-lived blue CL emission occurs with long-lived yellow CL color, which is found in zones of inclusions and impurities.

Colloform textures observed under the petrographic microscope typically exhibit crystallized and recrystallized textures where amorphous silica and colloidal particles produced these colloform bands. Under the CL system, these colloform textures firstly exhibit dark purple or black CL colors, which indicate no CL emission. After the bombardment has progressed for a minute, each colloform band is indicated by distinct shade of reddish-brown CL colors. Short-lived blue and long-lived yellow CL emissions simultaneously occur, especially in the inclusion and impurities zones (Fig. 72).

Some colloform-recrystallized textures, which are only found under cross-polarized light, exhibit different details than from the CL system. For example, under cross-polarized light, quartz crystals clearly exhibit jigsaw and replacement textures. However, under the CL system, these quartz exhibits colloform layers and no jigsaw texture exists. Another luminescence behavior of colloform bands is a short-lived yellow CL emission. The short-lived yellow CL color feature mostly occurs with flamboyant quartz and fibrous chalcedony, whereas jigsaw quartz in colloform bands is indicated by dark CL color. After the bombardment has progressed for approximately 18 seconds, the yellow CL color was replaced by dark-cream CL color. The yellow colloform bands also encrust euhedral quartz crystals, which exhibit short-lived blue CL emission. Surrounded jigsaw textures exhibit dark CL color and consequently emit reddish-brown CL color. Different CL behaviors are likely caused by variations of textures that are described in the discussion (Fig. 73).

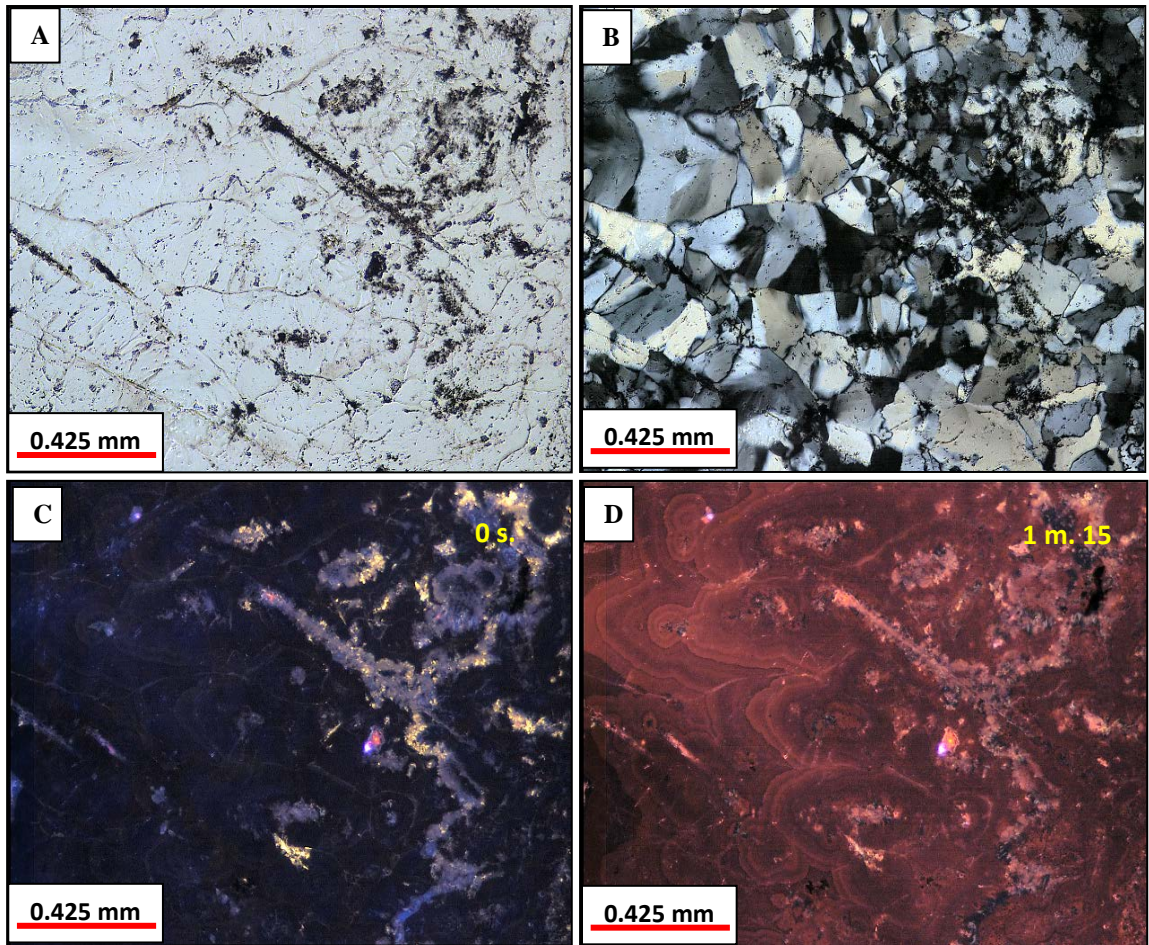


FIG 72. Images of colloform bands and jigsaw texture found in the Buckskin National deposit in same view. **A:** Photomicrograph (plane-polarized light) showing zones of inclusions and a needle structure cut across clear quartz crystals. **B:** Photomicrograph (crossed polars) of replacement and jigsaw textures. **C:** CL photomicrograph after the bombardment started (11:55:09:125), non-luminescence is occurred together with yellow and blue CL colors. **D:** CL Photomicrograph at 1 minute and 15 seconds after the process (11:56:24:750), multiple shades of reddish brown CL colors exhibit colloform bands.

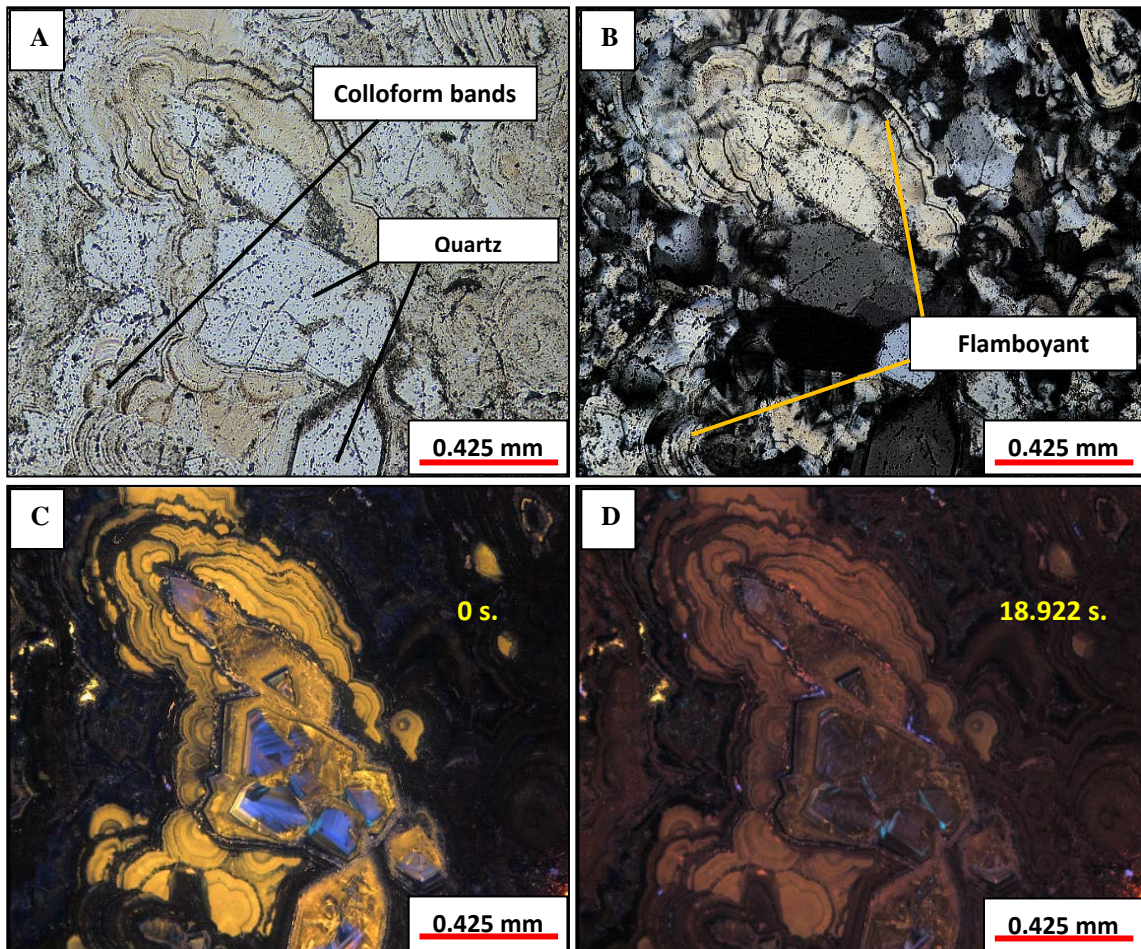


FIG 73. Images of colloform textures from the Fire Creek deposit in same view. **A:** Photomicrograph (plane-polarized light) showing numerous colloform layers that encrust euhedral quartz crystals. **B:** Photomicrograph (crossed polars) represents jigsaw, flamboyant, and zonal quartz. **C:** CL image taken at 14:09:46:296 exhibits yellow CL colors that mostly emit from colloform layers and these layers are separated by non-luminescence boundaries. Euhedral individual crystals contain blue CL color at the cores and yellow at rims. **D:** CL image taken at 18.922 seconds later (14:10:05:218), yellow CL colors decrease in brightness to cream as well as blue. Black zones become brown to

Individual crystals of euhedral quartz exhibit crystal growth-banding textures under CL. Short-lived blue emitted colors indicate crystal growth zones, whereas the crystal itself mostly does not release any CL colors. The quartz crystals are also encrusted by colloform layers, which have luminescence behaviors similar to that found in quartz crystals. (Fig. 74). The textures including colloform, zonal quartz, comb, and other recrystallized textures, as well as CL behaviors that are mentioned above can be found in both epithermal deposits, however, calcite are more common in the Fire Creek deposit than at the Buckskin National deposit.

Other interesting CL silica textures at Fire Creek deposit include crystal growth zones and colloform features. The crystal growth zonal textures are indicated by intergrowth zones of yellow, blue, and black CL colors. They also occur with colloform layers and two-dimensions of spherical forms that are produced by colloidal particles. The colloform features exhibit yellow CL colors and present as jigsaw quartz under cross-polarized light. The distinct features found under CL probably show the original vein textures before they have (re)crystallized (Fig. 75).

A final feature observed involves opaque minerals that are found associated with fibrous-acicular or needle-like structures. After the bombardment has progressed, these fibrous-acicular structures are indicated by scatters of short-lived blue CL colors surrounded by cream or pink CL colors. Opaque minerals are probably related to blue quartz precipitation. Rounded quartz and colloform features are indicated by cream CL colors (Fig. 76).

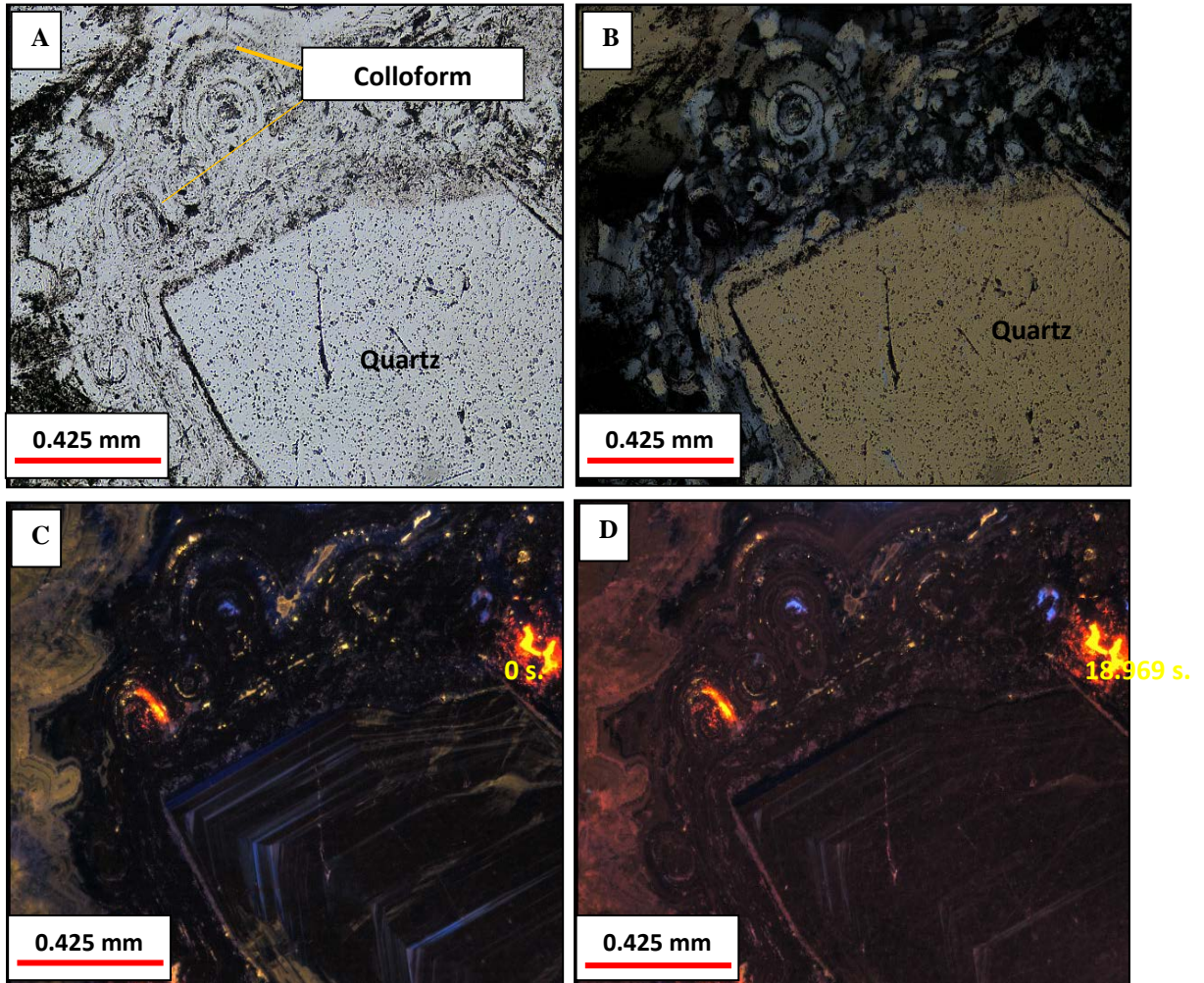


FIG 74. Images showing crystal growth zones in quartz and colloform textures in same view. A: Photomicrograph (plane-polarized light) exhibits a single quartz encrusted by colloform bands. Zones of inclusions and impurities are occurred. B: Photomicrograph (crossed polars) exhibits similar features found in A. Colloform bands (re)crystallized to jigsaw quartz. C: Photomicrograph (CL) at the beginning of bombardment (14:23:06:593), crystal growth zones are indicated by short-lived blue emitted colors. Note that: colloform bands do not emit any CL colors. D: Photomicrograph (CL) taken 18.969 seconds later (at 14:23:25:562), dark zones in colloform texture and in a single crystal show brown bands. Yellow and blue colors are completely disappeared.

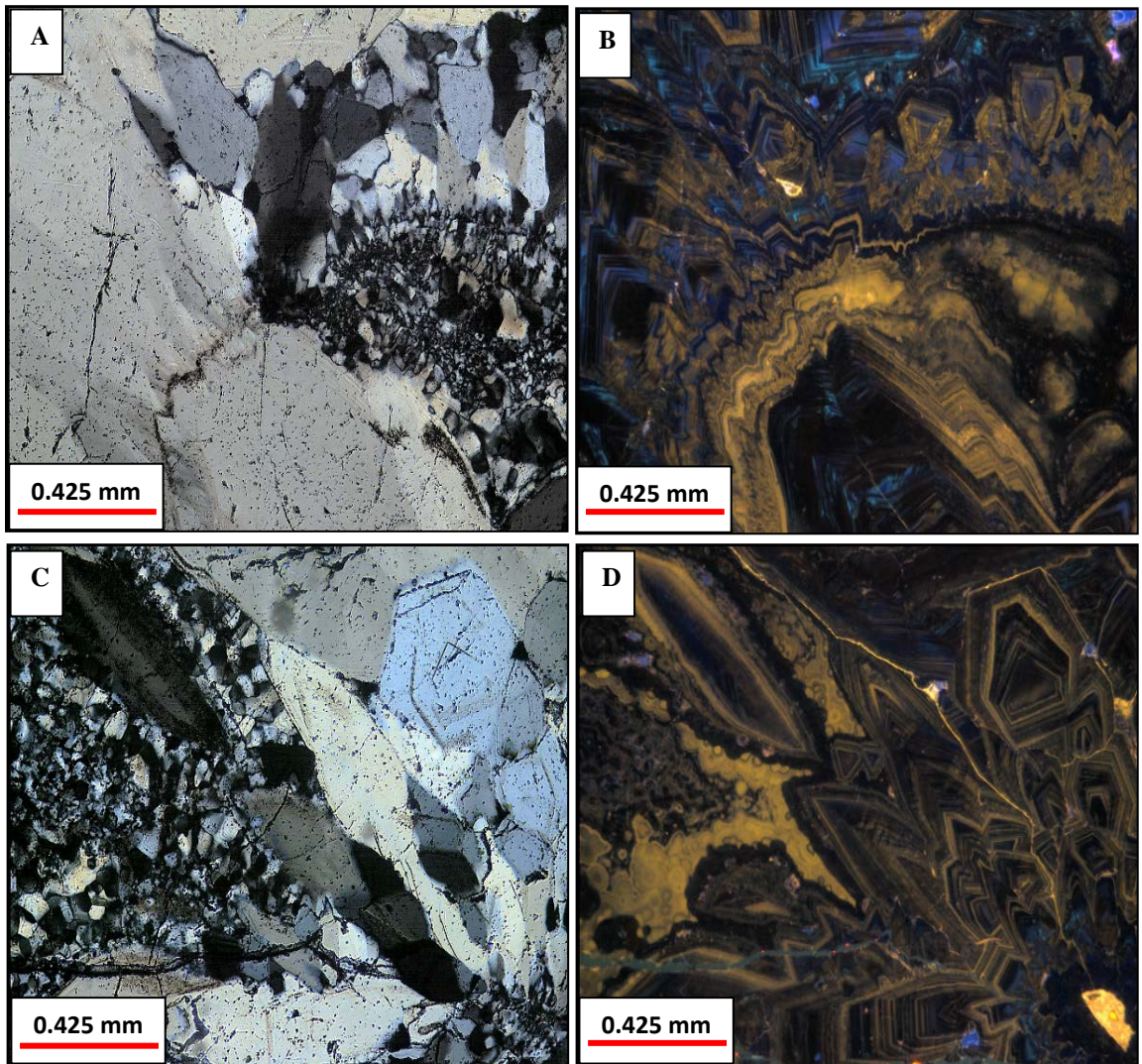


FIG 75. Images showing many crystal growth zonal textures from the Fire Creek deposit. A: Photomicrograph (crossed polars) contains likely large grains and various sizes of jigsaw quartz. B: Photomicrograph (CL) of same sample as A and CL brings out a new texture not observed under crossed polars. Yellow, blue, and dark CL colors are present. C: Photomicrograph (crossed polars) showing euhedral crystals associated with jigsaw quartz. D: Photomicrograph (CL) of C

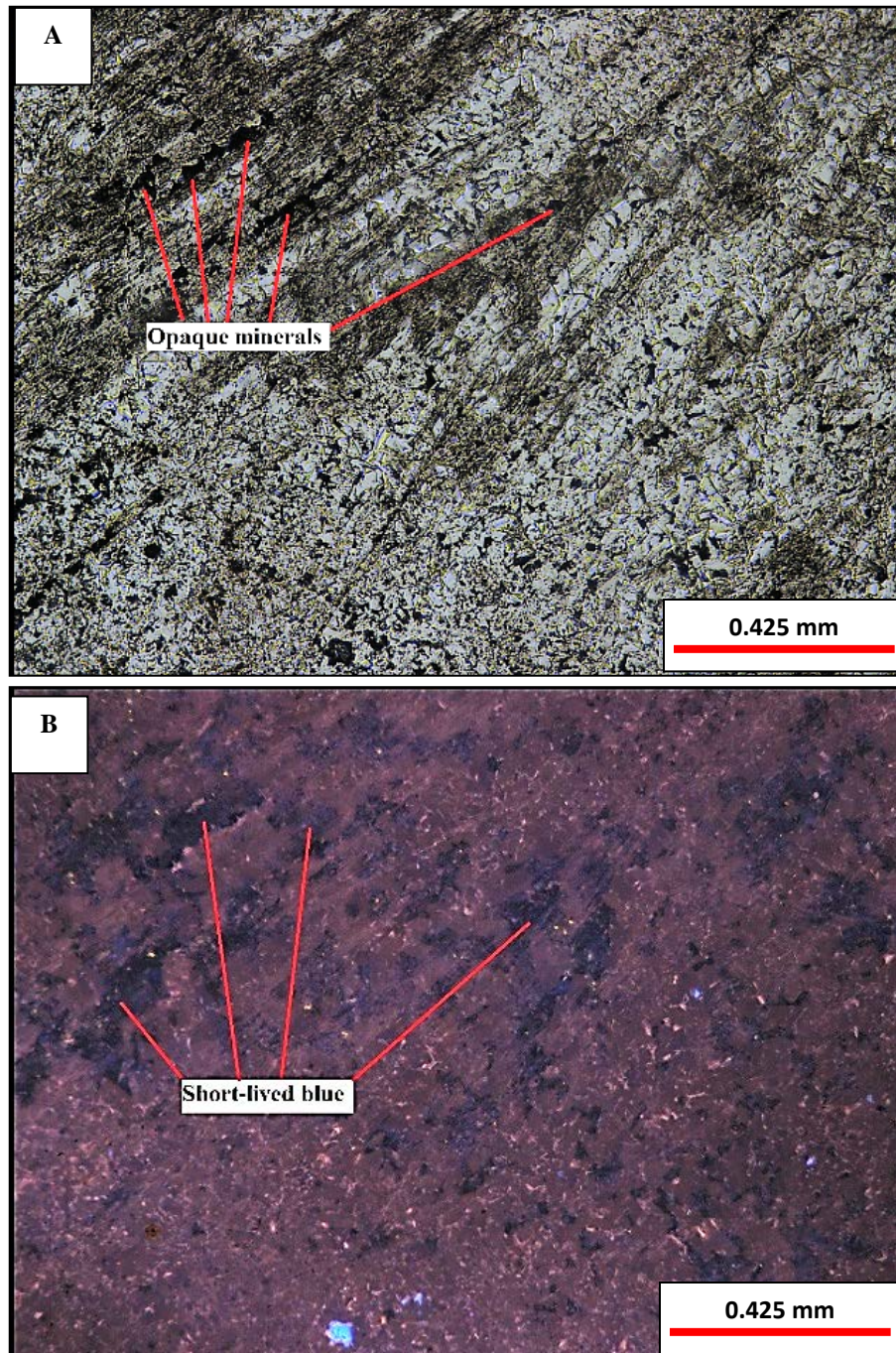


FIG 76. Images of fibrous-acicular textures from the Fire Creek deposit. A: Photomicrograph taken under plane-polarized light exhibiting acicular structures that contain opaque minerals, likely including precious-metal minerals. B: Photomicrograph (CL) of A represents reddish pink background associated with scatters of short-lived blue emitted colors that are caused by different quartz formations.

4.5 X-Ray Powder Diffraction Data

After microscopic studies were conducted, XRD was then applied to better characterize gangue-mineral composition in the veins. Five vein samples from The Buckskin National and three samples from the Fire Creek deposit were used. These selected samples exhibit various vein textures and their textural details as well as photographs of samples are attached in the appendix 2.

XRD data are interpreted using DIFFRAC.EVA and MS-Excel software to identify mineral components and produce the XRD graphs. The results showing in this study can be grouped into four types of X-ray diffraction patterns reflected their mineral compositions of the sample BN1, BN5, FC6, and a sample from Hishikari deposit, Japan (Fig. 77). Major minerals, which are clearly found in the vein samples, include quartz, kaolinite, and calcite. Adularia and sericite are found as minor minerals. The X-ray diffraction patterns are individually presented and described in the following paragraphs.

Results of this analysis indicate that the Buckskin National samples are primarily composed of low-quartz or alpha-quartz in undetermined quantities (Fig. 78). Selected samples exhibited recrystallized-jigsaw textures and chalcedony in black-colored colloform bands represent distinct quartz peaks. Another sample, which exhibits white to cream-colored layers that occur with fibrous-acicular structures, shows small peak of kaolinite at about 12.7 of $^{\circ}2\theta$. Sericite can be found by the matching process of the DIFFRAC.EVA software.

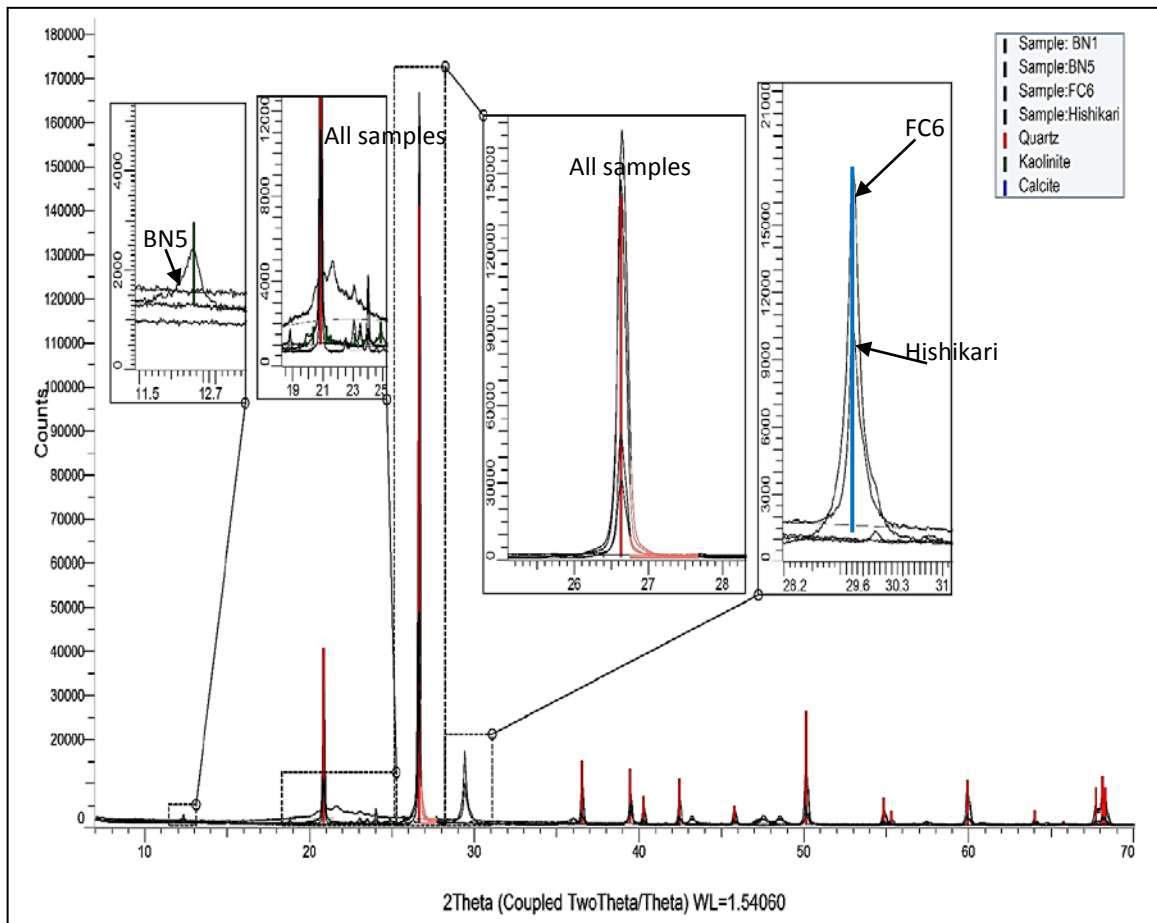


FIG 77. X-ray diffraction patterns of the epithermal veins at the Buckskin National, Fire Creek deposits, Nevada, and one sample from the Hishikari deposit in Japan. Quartz peaks occur in all samples indicated by red lines. Kaolinite peak (green color) exhibits small numbers than quartz and are found only in the Buckskin National samples. Calcite indicated by blue peaks only show in the Fire Creek and Hishikari samples.

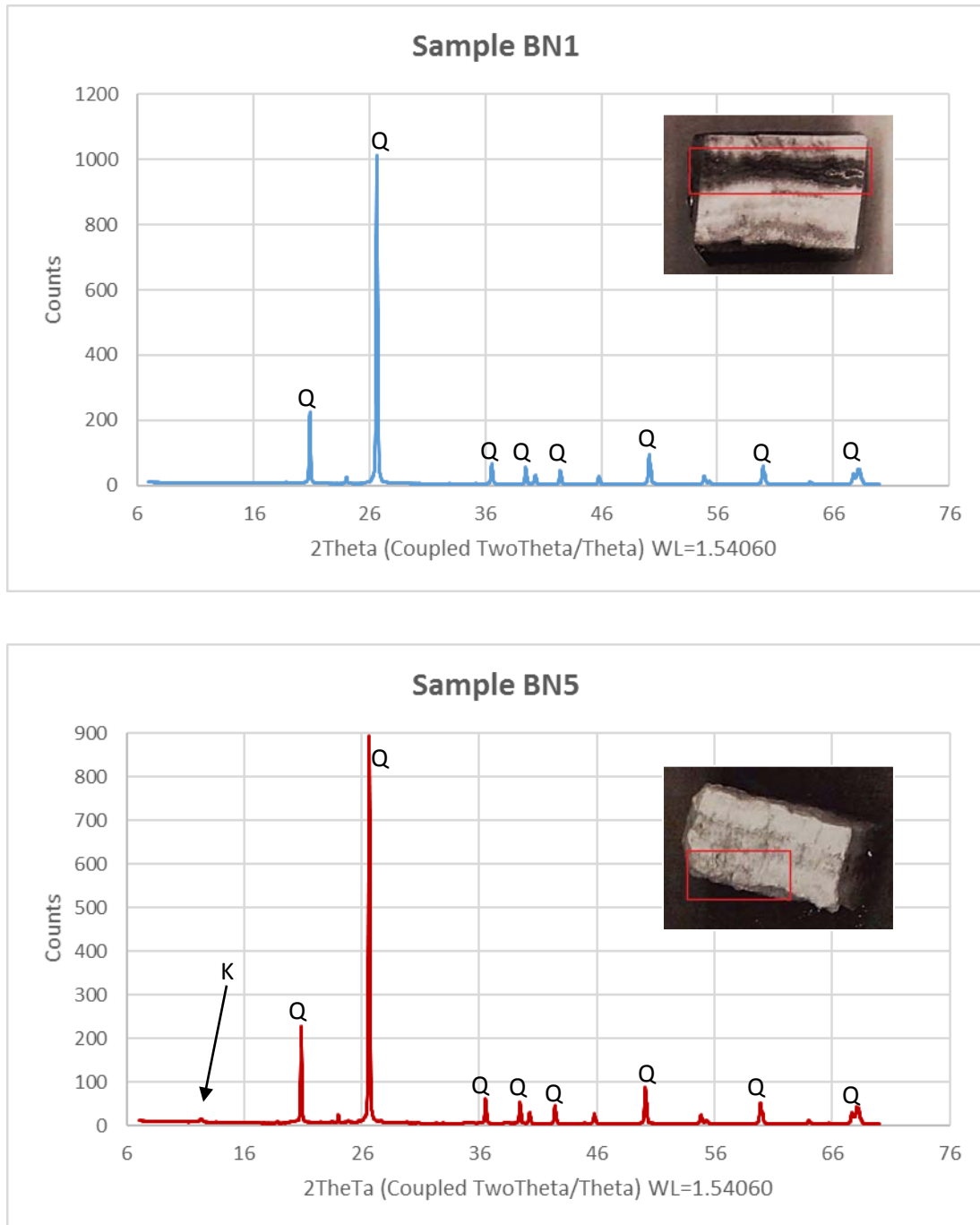


FIG 78. X-ray diffraction patterns of the Buckskin National samples showing almost similar patterns. (Top): XRD pattern of sample BN1 exhibits distinct quartz peaks (Q). The sample exhibits chalcedony and recrystallized-jigsaw textures in colloform layers observed by the microscope. (Bottom): XRD pattern of sample BN5 represents quartz peaks and very small kaolinite peak (K). This sample exhibits fibrous-acicular textures on hand specimen and under microscope.

According to petrographic analysis, the Fire Creek samples contain slightly different mineral components compared to Buckskin National. Results of this analysis indicate that the Fire Creek samples are primarily composed of quartz and calcite. This sample exhibits lattice-pseudobladed silica texture and late platy calcite.

A sample from the Hishikari epithermal deposit in Japan is also used for comparison to the Fire Creek sample. This sample contains white-colored bladed crystals, which are previously determined as truscottite (J.A. Saunders, pers. commun., 2016). Truscottite $((\text{Ca},\text{Mn})_{14}\text{Si}_{24}\text{O}_{58}(\text{OH})_8 \cdot 2\text{H}_2\text{O})$ is a phyllosilicate mineral and commonly found in low-sulfidation epithermal environment in Japan (Izawa et al., 1990; Watanabe, 2005). By the XRD technique used in this study, truscottite should be found at 28.39° , 31.47° , and 21.08° of 2θ with $I = 100, 80,$ and 70 , respectively. These results are depended on its inter-atomic spacing (“Truscottite Mineral Data”, 2017). As a result, the XRD pattern of the Hishikari sample exhibits peak of quartz and calcite, which are similar to the Fire Creek sample, and no truscottite peak is found. However, truscottite is probably not considered enough during sample-preparation processes. The XRD pattern of the Hishikari sample then represents distinct quartz and calcite peaks similar to the Fire Creek sample, and no truscottite peak occurs (Fig. 79). Thus, truscottite minerals found in the Hishikari deposit in Japan do not occur in the Fire Creek deposit in Nevada but their vein samples still exhibit identical XRD pattern and similar gangue-mineral bladed textures.

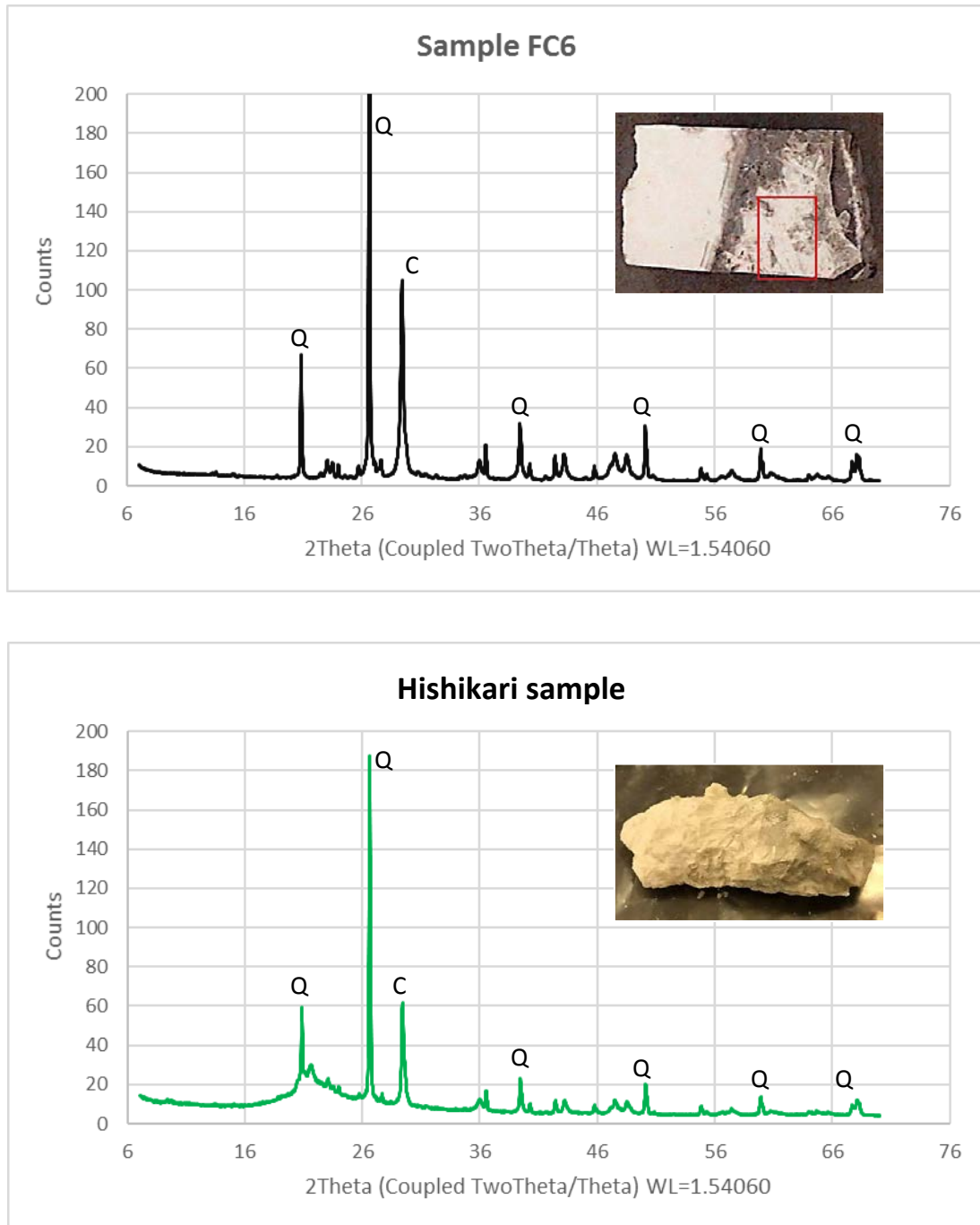


FIG 79. X-ray diffraction patterns of the samples from Fire Creek (top) and Hishikari (bottom) deposits. *Top:* XRD pattern exhibits quartz and calcite peaks found in the Fire Creek sample. The sample also exhibits lattice-pseudobladed silica texture occurred with late platy calcite. *Bottom:* XRD pattern showing peaks of quartz and calcite in a sample from the Hishikari deposit in Japan similar to Fire Creek. Probably, no truscottite peak distinctively occurs.

5. DISCUSSIONS

5.1 Gangue-Mineral Textures

Gangue-mineral textures formed as a consequence of ore-fluid geochemistry, presence or absence of boiling, and also the original nature of silica and other gangue deposited in earlier hydrothermal events. In particular, crystallization-recrystallization, and replacement processes are important in epithermal ores in general, and at the Buckskin National and Fire Creek deposits in particular. Principal silica textures exhibited at the Buckskin National and Fire Creek deposits include jigsaw quartz and colloform banding. As was mentioned in the introduction, jigsaw textures are microcrystalline and crystalline quartz assemblages that are separated by irregular boundaries. These features are induced by crystallization and/or recrystallization of silica solutions and colloidal silica particles that previously formed colloform bandings (Dong et al., 1995). Textures of silica in epithermal veins also vary in response to evolving hydrothermal fluid conditions. For examples, at the Koryu gold-silver deposit, microcrystalline and colloform quartz formed during intense boiling, which also causes precipitation of ore minerals. In contrast, comb quartz formed during non-boiling to gentle boiling, which induce transportation processes of ores and gangues to deposition areas (Shimizu, 2014). After deposition of amorphous silica, the temperature of ore

forming solutions apparently decreased, and perhaps had a different of chemical composition. As a result, silica bands in the veins are characterized by textures such as flamboyant, plumose, zonal, comb, and ghost-sphere as a function of the initial depositional history and subsequent (re)crystallization or replacement.

Different CL colors emitted by quartz crystals are evidence of different formation and structures (Ramseyer et al., 1988). Götze et al. (2001) reviewed previous interpretation of CL-color characteristics of quartz in different forms. They suggested that short-lived blue CL color indicates alpha quartz and amorphous silica that were precipitated by low-temperature hydrothermal fluids, whereas long-lived yellow, orange and red CL colors were detected in silica colloidal precursors, agates, and cryptocrystalline quartz found in hydrothermal veins. Additionally, dark CL color or weakly luminescent emissions indicate authigenic quartz that formed in its present morphology. In this study, most of microcrystalline crystals exhibited (re)crystallized features probably include either alpha-quartz or silica colloidal precursors. The short-lived blue CL emission in this study commonly occurs with jigsaw, plumose, comb, and zonal textures. On the other hand, the long-lived yellow CL emission exhibits multiple colloform bands, spherical shapes, and needle-like structures associated with flamboyant, moss, and colloform layers that are found under the microscope. Long-lived yellow CL color also occurs in zones of inclusions and impurities trapped along crystal growth zones. The dark- or weakly CL color firstly occurs in jigsaw textures with free-inclusions observed on the microscope. These dark CL colors eventually emit reddish brown color and exhibit colloform bands, which are totally dissimilar textures to that observed on the microscope. Demars et al. (1996) suggested that the short-lived or unstable CL behaviors

is likely related to the original hydrothermal solutions, rather than diagenetic process (as cited in Götze et al., 2001). Calcite is not useful for the CL system used in this study because it commonly emits strong bright color and it disrupts other luminescent colored bands of quartz textures that are the focus of this study. Bladed shapes of replaced minerals can emit by both blue and yellow CL colors. These features are probably caused by multiple cycles of hydrothermal solutions that induce replacement and recrystallization events.

Although silica textures of this study are mostly identified as recrystallized textures, the CL technique likely provides original silica textures in the veins. This method is very useful to observe on the origins of some significant recrystallized-replacement textures such as fibrous-acicular features in crustiform-colloform bands, which is commonly found in the Buckskin National and Fire Creek deposits. In these ores, silica colloids apparently aggregated to form spheroidal structures and colloform layers. These colloidal spheres consequently coalesced with other spheres, which produced botryoidal or mammillary layers. Surface tension, surface forces, and/or intermolecular forces, which are properties of colloids that have a high ratio of surface area to mass, affected the deposition of the amorphous precipitates (Aveyard and Haydon, 1973; Landmesser, 1984;). At least, some of the fibrous-acicular shapes appear to have filled up these tension cracks in colloform bands. Unknown minerals then probably formed along these fibrous-acicular features associated with other (re)crystallized silica. The unknown minerals were then removed and replaced by later silica precipitation (Fig. 80). These fibrous-acicular features formed in original colloform bands are distinctively observed by the CL system (Fig. 81). Next generations of

hydrothermal fluids then induce alteration of materials at porous zones that cause the elongated cavities and silica replacement. Precious-metal minerals are sometimes disseminated in these structures, based on original micro-scale features. Additionally, alpha-quartz and silica colloids appear to have precipitated together in the veins, and they can be separated by intergrowth zones of CL colors. Alpha-quartz that emits blue CL color exhibits trigonal euhedral crystals, whereas yellow-colored layers exhibit mammillary-colloidal forms. These features represent multiple varieties of silica formations that episodically precipitated in this vein (Fig. 82).

Bladed calcite, which is formed during boiling of the hydrothermal solutions (Simmons and Christensen, 1994), and pseudomorphic replacement by silica occurs in both deposits, especially the Fire Creek deposit. Amorphous silica likely replaced calcite blades along their cleavage planes. Thus, replacement textures including pseudo-parallel bladed, pseudo-acicular, and lattice-bladed are found in the calcite pseudomorphs. The amorphous silica in calcite blades then crystallize or recrystallize to microcrystalline quartz and chalcedony. Calcite blades are completely replaced by silica in the Buckskin National deposit, whereas calcite blades are generally not replaced at the Fire Creek deposit. The differences in calcite replacement processes are probably caused by the different host-rocks, hydrothermal fluid compositional pathways, and boiling history.

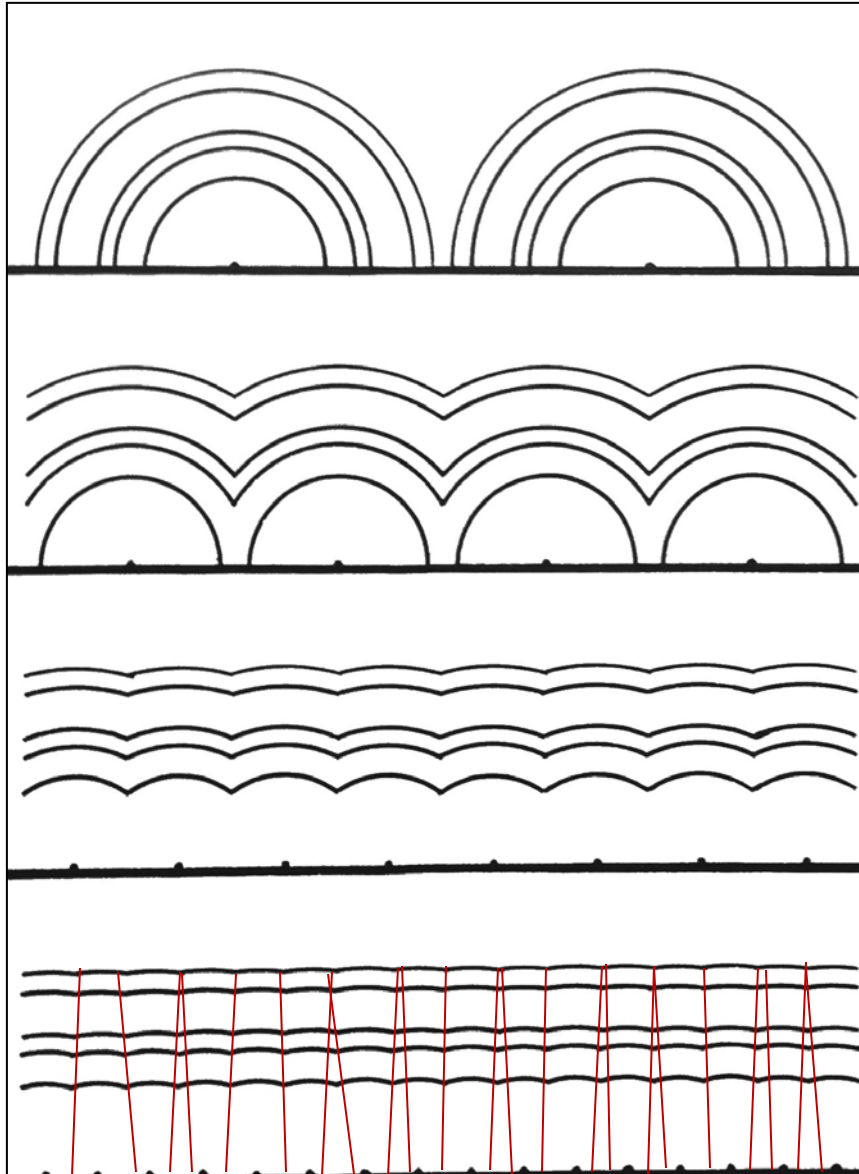


FIG 80. Diagrammatic sketches of interpreted agate-forming processes from top to bottom. Spherical layers are accumulated by surface tensional forces of colloidal particles. When these spheres are connected, the fibrous-acicular structures appear to have filled tension cracks (red lines) and cross-cut colloform bands (adapted from Landmesser, 1984).

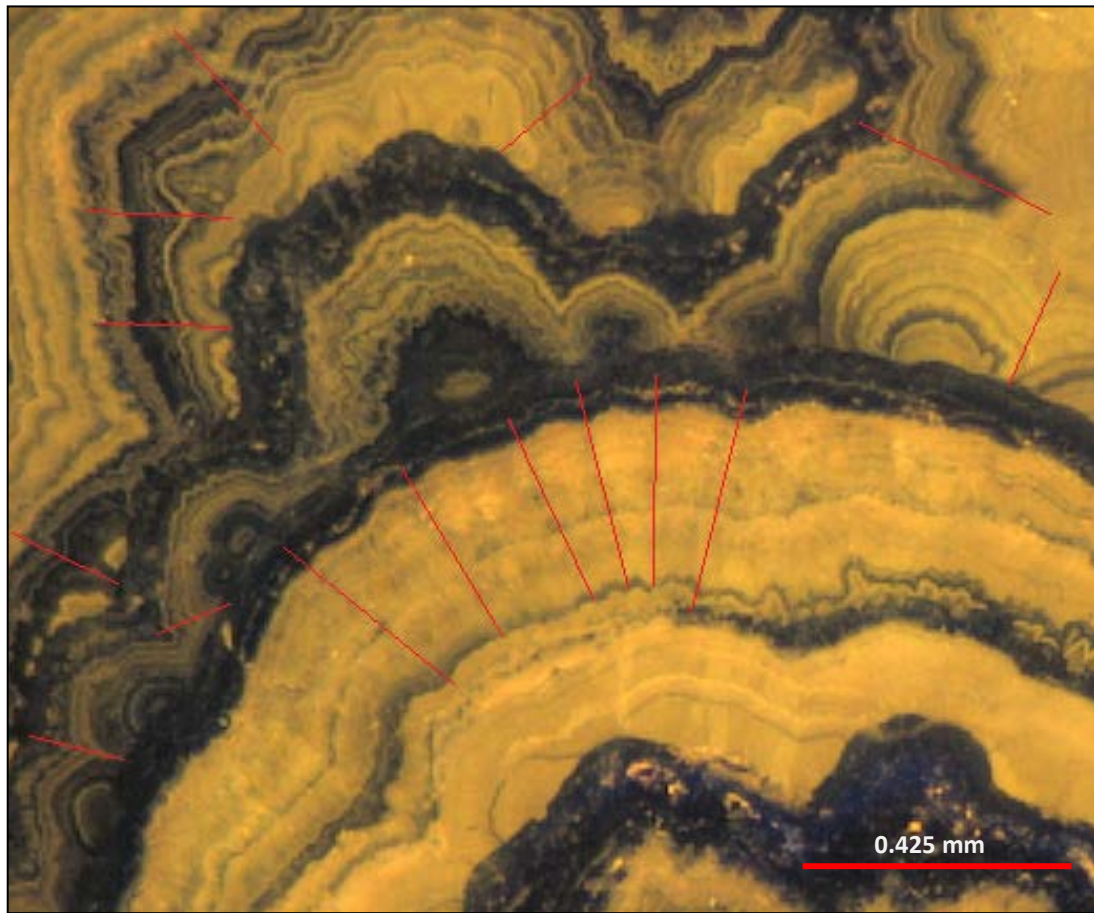


FIG 81. Photomicrograph (CL) of the Fire Creek sample showing hypothetical fibrous-acicular structures highlighted by red lines that are perpendicular to the colloform bandings. Colloform layers emit yellow CL color, whereas blue and dark CL colors exhibit alpha-quartz crystals.

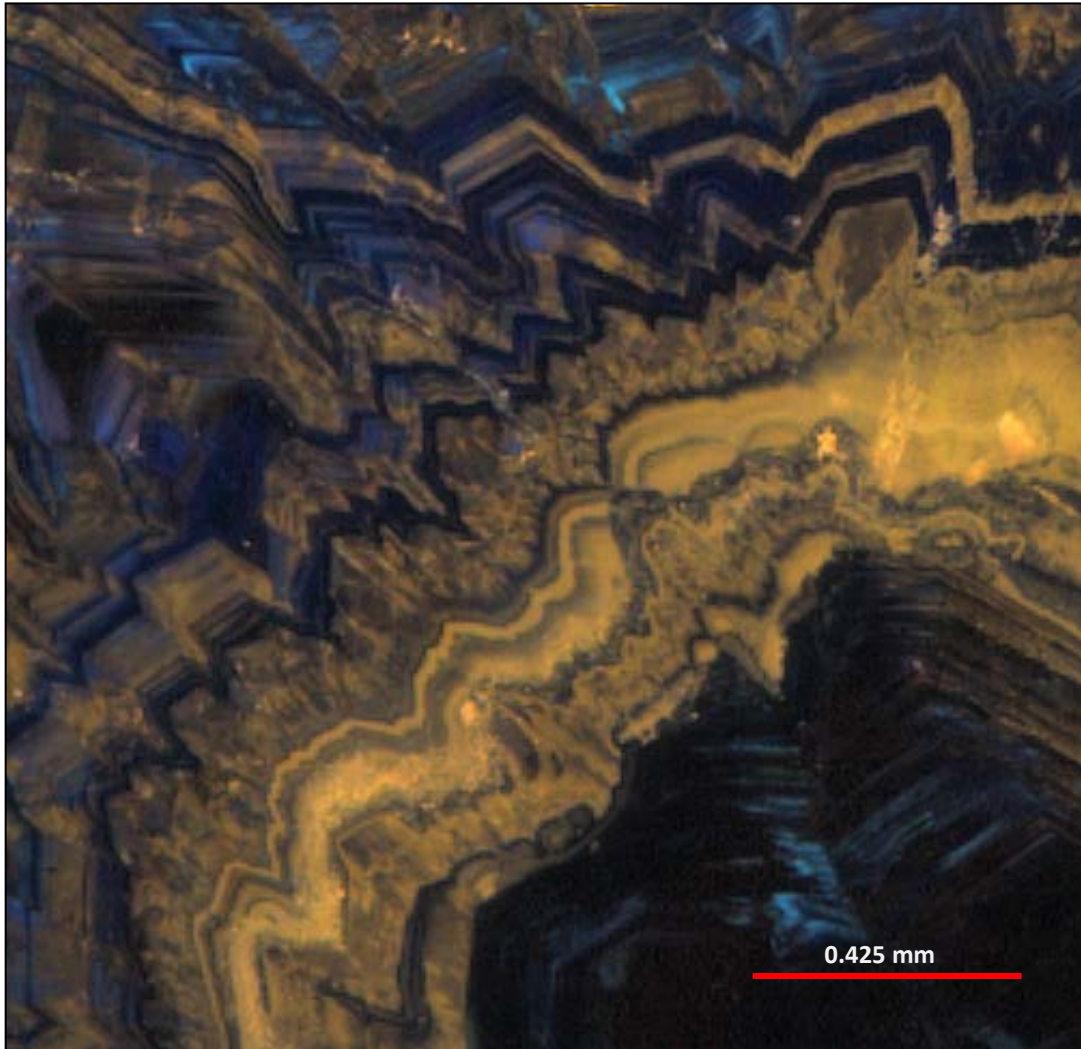


FIG 82. Photomicrograph (Fire Creek sample) of interlayers of alpha-quartz and recrystallized silica colloid showing progressive growth directions of vein-forming hydrothermal fluids. Alpha-quartz (blue colors) represent trigonal structures perpendicular to wall rocks and vein direction. Silica colloids (yellow colors) repeatedly precipitated to form colloform layers.

The Buckskin National veins (refers to the Bell veins) occur within Miocene igneous rocks that vary in composition from basalt to rhyolite and hosted by rhyolite ash-flow tuff in older age (Vanderburg, 1938; Willden, 1964; Vikre, 1985), whereas the Fire Creek veins are hosted by basalts (Klondex Mines Ltd., 2015). These distinct magmatic composition forming the veins are probably caused some different features in the vein textures from the Buckskin National and Fire Creek deposits in this study. Basalts, which have higher Ca than rhyolites, and it provides to the hydrothermal solutions that formed calcite in the veins at the Fire Creek and Buckskin National deposits. Calcite found in the veins can be subdivided into two features including pseudomorphs of silica after calcite and a later stage calcite. Samples from Buckskin National exhibit only silica replacement of bladed calcite, and no calcite is found. Moreover, the amount of the former calcite at Buckskin National is reflectively minor compared to Fire Creek, which perhaps is related to rhyolites being the principal wall rocks there. On the other hand, the Fire Creek deposit is hosted by basalts, and has two abundant stages of calcite deposition. Thus, the various epithermal vein textures and their mineral composition are likely influenced by the composition of host-rocks formed by specific magmatism. Moreover, the occurrence or absence of calcite, perhaps is also dependent on amount dissolved $\text{CO}_2(l)$, in the hydrothermal solutions. Loss of CO_2 due to boiling can increase the pH of hydrothermal solutions and consequently induce calcite precipitation and silica solubility, whereas low-pH solutions in low temperature allow calcite to dissolve and is replaced by silica (Shettel, 1974; Fournier, 1985). The processes caused by boiling and subsequent cooling appear to control the silica vein textures that are observed on the Buckskin National and

Fire Creek deposits, such as silica replacement textures including lattice-pseudobladed, parallel-pseudobladed, and pseudoacicular.

Additionally, according to the XRD interpretation, truscottite peaks are not found in the Fire Creek and Buckskin National samples. It also unclearly exhibits in the Hishikari sample, which is previously determined that it is composed of truscottite. These results are probably caused by lack of truscottite powder during sample preparation of Hishikari sample. However, the XRD patterns of Fire Creek and Hishikari samples identically exhibit peaks of quartz and calcite in different intensities. These are probably caused by variations in the chemistry of the low-sulfidation hydrothermal fluids, which are dependent on the magmatic or volcanic contributions to the meteoric-water dominated ore-forming solutions, and also their respective country-rock compositions as well as their country rocks. Otherwise, the mineral assemblages of these epithermal deposit in Nevada and Japan are quite the same including quartz, adularia, and calcite (Shimizu et al., 1998; Sanematsu et al., 2004; Watanabe, 2005; Shimizu, 2014).

5.2 Comparisons of Silica Textures to Sleeper, Midas, and Mule Canyon Deposits

The Sleeper deposit located 45 km northwest of Winnemucca, is similar in several ways to the Buckskin National and Fire Creek deposits. For example, all show evidence of the common deposition of amorphous silica to form microcrystalline textures. At the Sleeper deposit, deposition during vein formation, which bladed calcite has been completely replaced by silica, and thus no calcite remains. Moreover, dendritic, banded, interconnected, and disseminated textures of precious-metal mineral are observed at the

Sleeper deposit. From previous studies by Wood (1988), Sander and Black (1988), Saunders (1990), Nash et al. (1991), and Saunders (1994), hydrothermal veins in the Sleeper deposit are hosted by the upper sequence of bimodal magmatic assemblages, which consist of rhyolite porphyry dykes, flows, and domes (as cited in Romberger, 1991). Vein textures at the Sleeper deposit commonly contain many colloform bandings that contain bonanza ores rich in electrum. Recrystallization of opaline silica to quartz is widely observed. The co-deposition of opal and dendritic electrum and naumannite indicates all 3 phases were transported together in the hydrothermal solution as colloids (Saunders et al., 2010). Silica gels and opal layers then partly crystallized to very fine-grained jigsaw quartz. Other gangue textures also occur in the Sleeper deposit, such as elongated quartz, euhedral quartz crystals, and chalcedonic silica, as well as pseudo-rhombic adularia (Saunders, 1994). However, the Sleeper deposit also exhibits features not observed at the Buckskin National and Fire Creek deposits, such as opaline bands, and reticular quartz. As we discussed above, silica vein textures from the Sleeper deposit are generally more similar to the Buckskin National than Fire Creek deposit. This is probably due to the similar country-rock composition. On the other hand, the Fire Creek deposit contains a much higher (original) calcite content than Sleeper. The Fire Creek ore minerals include higher amount of electrum than Ag-S-Se phased minerals like at Sleeper, whereas at Buckskin National, silver-selenides, silver-sulfides, and silver-sulfosalts are much more common than electrum.

Hydrothermal veins from the Midas deposit are generally composed of calcite blades, adularia, and jigsaw quartz that form a banded texture. Precious-metal minerals including electrum, aguilarite, and naumannite occur in dark bands (Leavitt et al., 2004).

Leavitt and Arehart (2005) also found layers of quartz, calcite, and adularia associated with precious-metal minerals that formed in crustiform bands. Midas samples described by Unger (2008) are used to compare to Buckskin National and Fire Creek deposits at Midas. Silica replacement of calcite textures is commonly found as well as jigsaw quartz in colloform-crustiform bandings. Unreplaced bladed calcite commonly remains at Midas, and thus is similar to the Fire Creek deposit. Electrum and naumannite occur as disseminations and dendrites within jigsaw silica at the Midas deposit. These vein textures of the Midas deposit are similar to the Fire Creek deposit than the Buckskin National deposit.

The close proximity of Fire Creek to the Mule Canyon deposit, with their similar age and host-rock composition (basalts) invites a comparison of vein ores between the two deposits. However, there are some differences in the wall rocks between the Mule Canyon and Fire Creek deposits. In the Mule Canyon deposit, ore minerals including electrum, Ag-selenides, and sulfide minerals were found in weakly and intensely altered rocks with high As and Fe-oxides, but these oxidized features are not found in both Fire Creek and Midas (Wallace and John, 1998). Gangue minerals found in Fire Creek and Mule Canyon are similar that include adularia, quartz, chalcedony, calcite, and opal (John et al., 2003). Moreover, the rock sequence of Fire Creek exhibits numerous joints and faults (Kassos et al., 2015) (Fig. 12), whereas joints and faults are uncommon in the Mule Canyon deposit (John et al., 2003). These features in Fire Creek appear to be induced by absence or lack of extensive water-rock reactions within host-rocks, in contrast to Mule Canyon where such reactions are extensive. Although these two deposits were formed in the same tectonic setting, they were probably formed under different stress conditions of

basin extensions, and then separate these deposits into two distinct systems (note: Mule Canyon = wet condition, Fire Creek = dry condition) (A. Wallace, pers. commun., 2017).

Adularia can be found in bonanza ore veins associated with quartz and exhibit colloform-crustiform bands in all 5 deposits considered in this study, especially in Midas, Mule Canyon and Fire Creek deposit. Adularia occurs in the high-grade ores, colloform quartz, opal, and chalcedony found in the Sleeper deposit (Nash et al., 1989). Samples from the Buckskin National deposit observed in this study rarely contain adularia grains under the microscope, yet kaolinite, which can be an alteration product of adularia, is also found under the microscope and by the XRD method. John et al. (2003) also noted that adularia is rare at Mule Canyon but occurs with other silicate phases in open-space filling in the ore veins there. Adularia from the Midas deposit was also reported by Unger (2008) as shown in Fig. 83. At Fire Creek, adularia is easily observed by cobalt-nitrite staining, which was confirmed by the XRD, and under the microscope shows pseudo-rhombic crystals associated with more common quartz.

On a large scale, the host-rock geology seems to be important in explaining some differences in the low-sulfidation epithermal ores studied here. For example, Sleeper and Buckskin National deposits are hosted primarily by rhyolitic rocks, whereas Midas, Fire Creek, and Mule Canyon deposits occur in predominantly basaltic host-rocks. Chalcedony and amorphous silica replaced in bladed calcite are observed in both Fire Creek and Midas deposits, and parallel-pseudobladed textures are found in the Buckskin National and Sleeper deposits. On the other hand, Mule Canyon and Fire Creek deposits exhibit slightly different vein features perhaps as a result of variable amounts of meteoric

water (e.g. precipitation) available (A.R. Wallace, pers. commun., 2017). The middle Miocene was in general much wetter from higher amounts of precipitation than today, but topography could have affected its availability for the hydrothermal systems (Vikre, 1987). Thus, vein textures in the deposits appear to be affected by the host-rocks compositions, tectonic settings, and water-rock reactions.

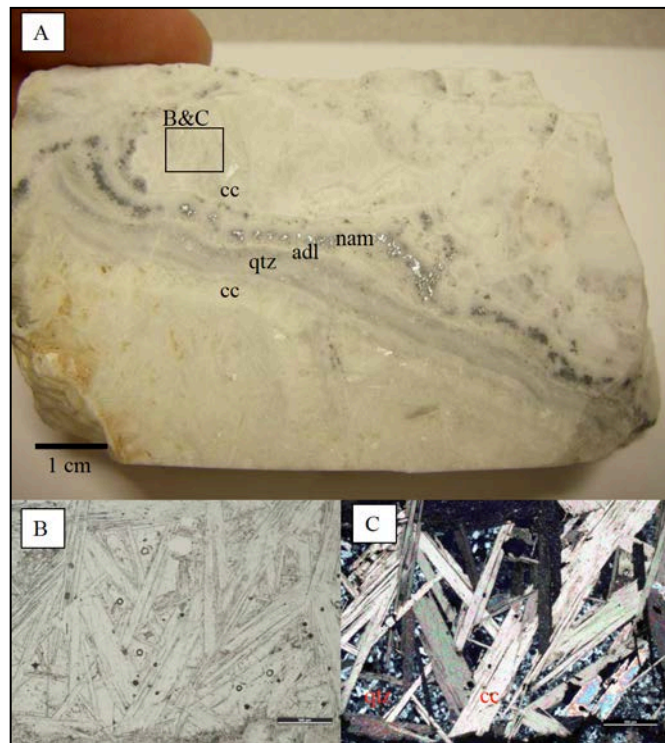


FIG 83. Photograph and photomicrographs of samples from the Midas deposit showing adularia (A), and bladed calcite (B and C) found in the hydrothermal veins (from Unger, 2008).

5.3 Relationships of Silica Textures and Precious-Metal Minerals

A variety of silica textures are common in the epithermal Buckskin National and Fire Creek deposits, but only a limited number of textures are associated with precious-metal minerals. Precious-metal minerals observed in this study include electrum, Ag-S-Se

phases (aguilarite and naumannite), and silver-sulfides (acanthite) identified using reflected light and its crystal habits (Fig. 84). At the Buckskin National deposit, sulfide-minerals are also found including pyrite, pyrrhotite, chalcopyrite, sphalerite, arsenopyrite, marcasite, stibnite and galena (Vikre, 1985). These ore minerals occur as coarse-grained (interconnected), disseminated, sub-dendritic, and banded patterns within crystallized colloform layers. Although colloform textures are formed by deposition of colloidal silica particles as gels and opal, these materials are probably (re)crystallized to microcrystalline quartz over time by episodic introduction of hydrothermal fluids. The precious-metal minerals are also found with euhedral and elongated quartz crystals (Fig. 85). These quartz crystals were probably (re)crystallized from amorphous silica formed by colloidal particles that were transported upward together with precious-metal minerals from deeper sources and deposited within the veins (Saunders et al., 2013; Shimizu and Saunders, 2013). Late calcite also encrusts the metallic minerals found in the Fire Creek deposit. Bladed calcite appearance probably relates to boiling event occurred after the precious-metal minerals formed (Fig. 86). Thus, precious-metal minerals clearly occur within amorphous precursor to form colloform bands that is now jigsaw texture (Fig. 87).

Previous works by Shimizu et al. (1998) from Japanese epithermal ores and Saunders (1994) from the Sleeper deposit, found that silica textures, which are closely related to co-deposited precious-metal minerals, include colloform bands as primary structures and (re)crystallized textures such as jigsaw, moss, and flamboyant. In contrast, other silica textures such as comb, plumose, zonal, and silica replacement of bladed calcite do not directly contain gold-silver minerals. However, these textures are still useful for understanding the conditions of hydrothermal events such as boiling and non-

boiling stages, composition of solutions, and relative periods of precious-metal minerals precipitation (Moncada et al., 2012). Moreover, the Buckskin National deposit provides many examples of silica colloidal precursors, which were co-deposited with precious-metal minerals in veins. Additionally, opaline-silica colloform bands are also observed together with bands of electrum and silver-minerals at the Fire Creek deposit (Fig. 88). This observation is consistent with a previous study by Saunders (1990), who proposed that silica and electrum colloids could both be transported by ore-forming hydrothermal solutions in epithermal systems.

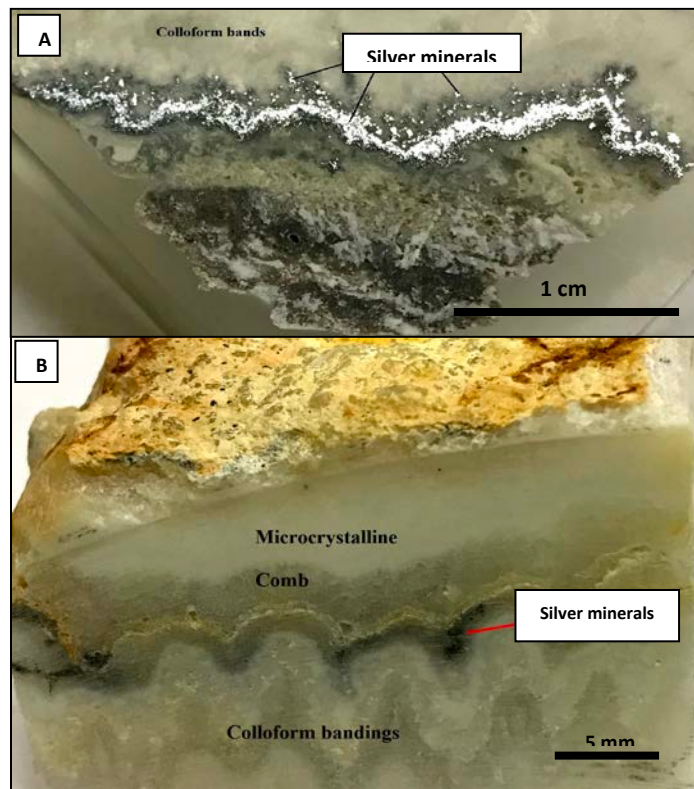


FIG 84. Photographs of precious-metal minerals are associated within spherical colloform bands A: Photograph showing silver-mineral band found in the Fire Creek deposit occurs with colloform bands. B: Photograph showing mammillary-colloform layers contain clearly comb euhedral quartz and milky quartz found in the Buckskin National deposit. Silver minerals also occur along colloform textures.

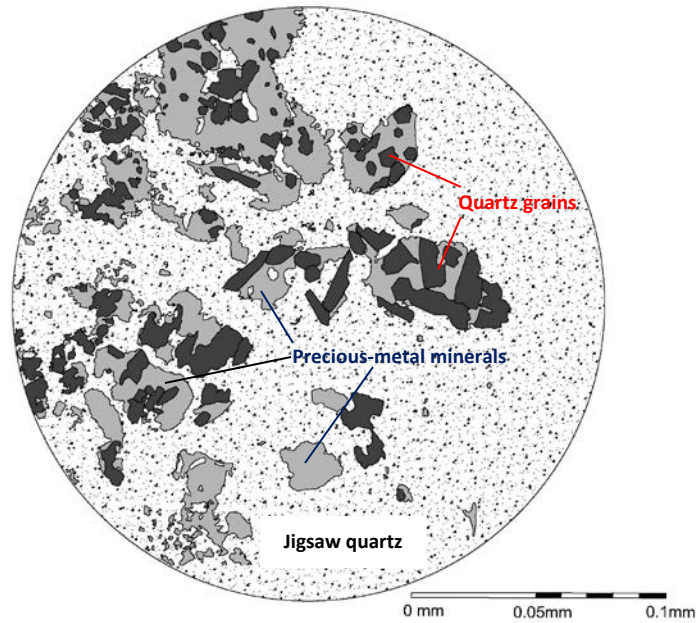


FIG 85. Sketch showing coarse-grained aggregates of precious-metal minerals (light grey) occur with quartz crystals (dark grey) found in the Fire Creek deposit. These features are surrounded by microcrystalline jigsaw quartz.

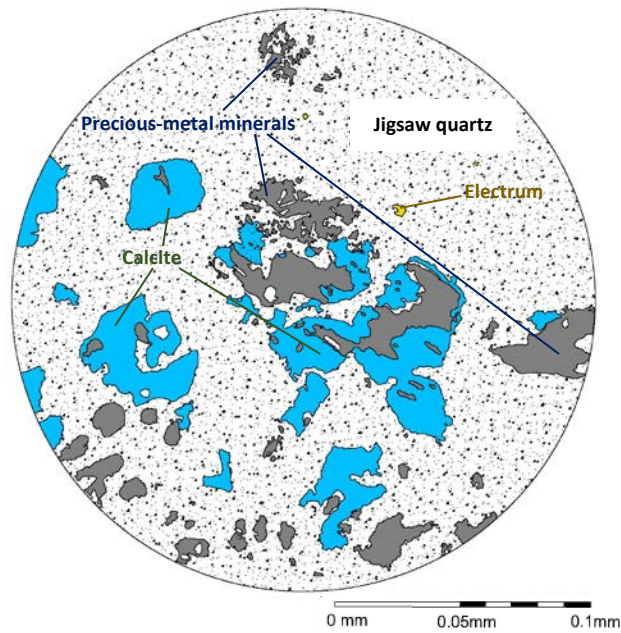


FIG 86. Sketch of precious-metal minerals (grey) in late platy calcite (indicated by blue color) from the Fire Creek deposit. Yellow particles indicate electrum. These features are surrounded by microcrystalline jigsaw quartz.

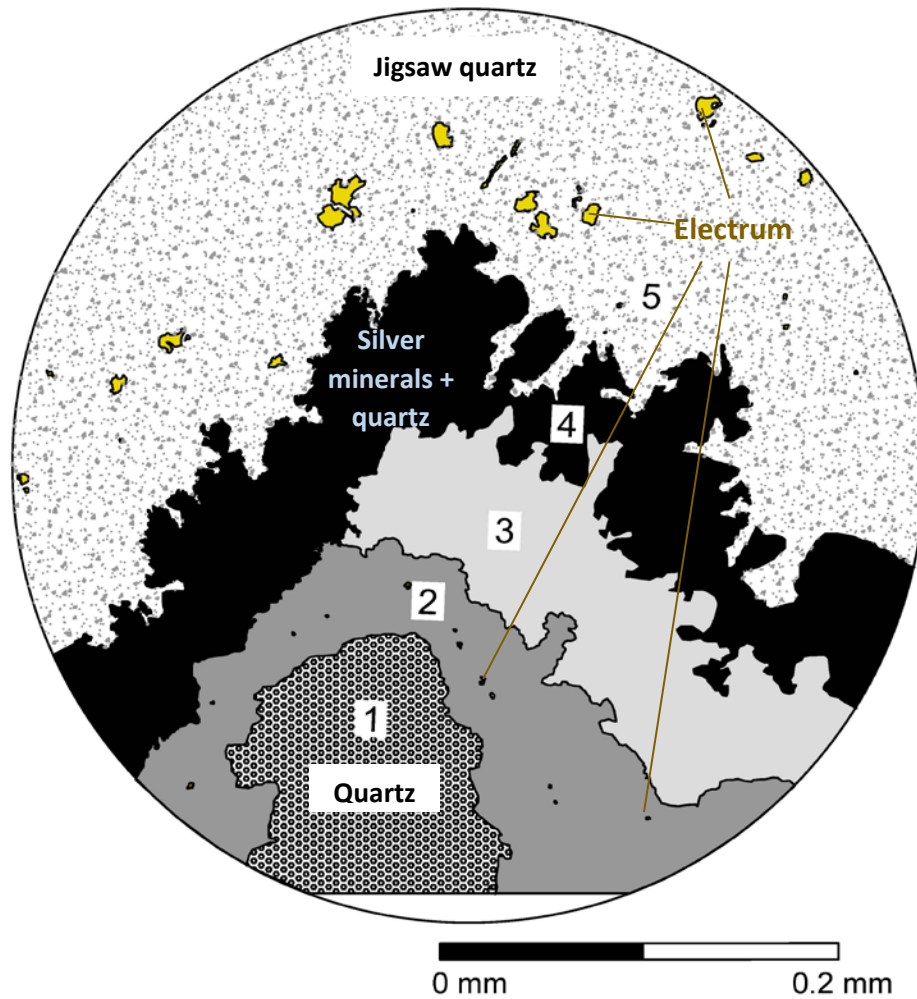


FIG 87. Sketch showing precious-metal minerals and multiple colloform bands in a high-grade sample from the Fire Creek deposit. Each number indicates specific feature including; 1 = Large quartz crystal, 2 = Cryptocrystalline quartz bands with disseminated electrum, 3 = Microcrystalline quartz band slightly contains coarse-grained silver minerals, 4 = Dendritic precious-metal minerals associated with euhedral and elongated crystals, and 5 = Jigsaw quartz disseminated by electrum (yellow particles).

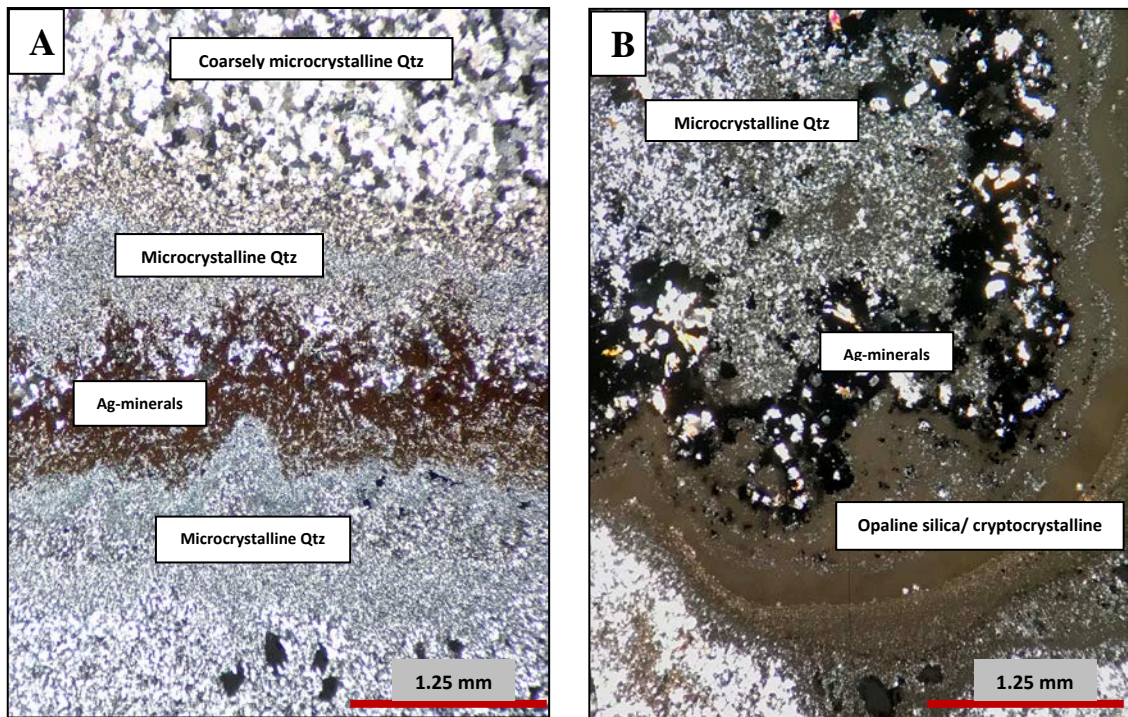


FIG 88. Photomicrographs (crossed polars) of (re)crystallized-colloform bands A: Photomicrograph of Buckskin National sample showing an ore-mineral-rich band is formed between microcrystalline bands. B: Photomicrograph of Fire Creek sample exhibits opal bands interlayered with cryptocrystalline and microcrystalline colloform layers that occur below ore-rich bands (black).

6. CONCLUSIONS

Banded epithermal veins at the Buckskin National and Fire Creek deposits exhibit a variety of silica textures such as colloform-crustiform-comb bands, (re)crystallized textures, and bladed calcite pseudomorphs replaced by silica phases. Jigsaw silica textures found in most bands are caused by (re)crystallization of colloidal precursors such as amorphous silica, gels, opal, and cryptocrystalline silica. Other features including comb, moss, ghost-sphere, zonal, plumose or feathery, flamboyant, and pseudobladed structures are observed within colloform-crustiform layers. Present-day silica textures evolved by (re)crystallization due to time, temperature effects, and subsequent introduction of new hydrothermal solutions after initial silica deposition. Precious-metal minerals in both deposits include electrum, Se-bearing silver minerals such as aguilarite, naumannite, Se-rich acanthite, acanthite, and pyrargyrite (ruby silver). The Au-Ag minerals typically occur in dendritic bands associated with euhedral and elongated quartz or colloform silica, the latter formed by deposition of colloidal silica particles. Precious-metal minerals also occur as disseminated grains in the Buckskin National and Fire Creek deposits.

Although similar in many respects, there are significant differences in the banded veins from the Buckskin National and Fire Creek deposits. Samples from the Buckskin National deposit typically consist of quartz, kaolinite, and sericite, which are more abundant than adularia and calcite. In contrast, Fire Creek samples are predominantly composed of calcite, quartz, and adularia. Vein mineralogy of the two

deposits probably reflect their respective host-rock compositions (Saunders et al., 2008). The Buckskin National deposit is hosted by rhyolitic ash-flow tuffs, but overall middle Miocene igneous rocks at Buckskin National deposit vary in composition from basalt to rhyolite. In contrast, the veins from Fire Creek deposit are hosted by basaltic to andesitic rocks including flows, tuffs, dikes, and sills.

Enigmatic fibrous-acicular textures are common in both deposits, and are mostly observed in the colloform bands, and they appear to have a complex genesis. In this study, samples exhibiting that texture were investigated using optical microscope, cathodoluminescence imaging, and XRD analysis. The fibrous-acicular structures can cross-cut several colloform bands. There are also surface tension cracks, which possibly is not related to fibrous crystal growth. These cracks are induced by weak intermolecular forces, which is a property of colloidal surfaces, and hold colloidal particles together within a colloidal system. These particles then formed initially by aggregation of silica colloids that (re)crystallized to microcrystalline quartz and chalcedony. Alpha quartz, kaolinite, and sericite are commonly found in these acicular cavities as probably replacing minerals, which suggests they may have locally replaced a precursor phase or filled shrinkage cracks. These fibrous-acicular textures do not occur in all colloform bands at the Buckskin National and Fire Creek, suggesting that they might be caused by specific chemical compositions of the hydrothermal fluids that formed them. Furthermore, fibrous-acicular textures can sometimes exhibit similar features to pseudo-acicular bladed, which is silica replacement of calcite texture, but the fibrous-acicular texture mineral appears to have silica replaced another (unknown) mineral, and they only occur within colloform bands.

CL imaging is a powerful method to observe the details of silica textures and augments standard petrography, as varying morphologies of silica phases emit different luminescent colors. Colloform-crustiform bands observed in this study consist of amorphous silica (yellow color emitted) interlayered with alpha-quartz (short-lived blue color emitted). Short-lived luminescent bands can be captured using only this hot cathode-CL technique, whereas the scanning electron microprobe-CL cannot detect these short-lived CL emissions. Textures observed under CL system can show original vein textures prior to (re)crystallization that cannot be seen using the petrographic microscope, and different CL colors emitted from colloform bands demonstrate the episodic nature of the vein-forming solutions, which formed both alpha-quartz and silica colloids in colloform bands. Moreover, fibrous-acicular structures and surrounded colloform textures observed under CL system were filled and formed by different silica phases.

Comparisons of the deposits studied here to the Sleeper, Midas, and Mule Canyon deposits indicate that vein gangue textures are generally similar, with Sleeper most similar to Buckskin National, and Midas most similar to Fire Creek. However, the ore mineralogy (great predominance of electrum) at Sleeper is much more similar to Fire Creek than Buckskin National. The general origins of all four of these deposits are probably very similar: deep basaltic magma chambers releasing Au, Ag, S, etc. to the shallow hydrothermal system (Kamenov, 2007, Saunders et al., 2008). Thus, differences in vein gangue textures are more likely the result of the variations in the chemical composition of the host rocks (note: Buckskin National = rhyolites, Fire Creek = basalts). The Mule Canyon deposit (15 km from Fire Creek deposit) is essentially the same age and is hosted by similar composition wall rocks, but significant differences in vein gangue and ore minerals are observed. For examples, 1)

high As, sulfides and Fe-oxides in wall rocks at Mule Canyon but they are not common in Fire Creek, 2) weak and highly altered host rocks in Mule Canyon, which are absent in Fire Creek, and 3) numerous amount of joints and faults in Fire Creek but less in Mule Canyon (John et al., 2003; Kassos et al., 2015). These discrete differences between two deposits, which are located in the same area, are probably caused by differing climatic conditions in the rock sequences during ore-forming processes related to volcanic activities in northern Nevada rift.

Electrum, silver-selenides, and silver-sulfides usually occur in spherical layers of colloform-jigsaw bands. Other textures such as comb, zonal, flamboyant, plumose, and silica replacement textures are commonly observed in these deposits, and other low-sulfidation epithermal deposits, but they are not useful predictors of the occurrence of precious-metal minerals. Although gangue minerals have no economic value, they can be used constrain the physicochemical conditions of the ore-forming solutions, both during and subsequent to Au-Ag mineral deposition. In general, the Buckskin National deposit and the Fire Creek deposit in northern Nevada contain silica textures similar to other epithermal deposits including the Sleeper, Midas, and Mule Canyon deposits in the US, Koryu and Hishikari deposits in Japan, and epithermal deposits in Queensland, Australia. Because of complexity of hydrothermal events and processes, these epithermal veins can exhibit variable characteristics. Results from this study still have implications for understanding ore-forming processes in other low-sulfidation epithermal deposits around the world.

More study of the gangue mineral textures in low-sulfidation epithermal ores appear to be warranted to better understand the origins of the observed textures associated with both ore-mineral deposition and also the “barren” bands that intervene. In particular, more research is required to determine the original precursor

and/or origin of the fibrous-acicular texture common in bonanza ores from the Buckskin National and Fire Creek deposits. Laboratory studies should be conducted to try to reproduce both original silica depositional features and subsequent (re)crystallization processes.

REFERENCES

- Adams, S.F., 1920, A microscopic study of vein quartz: *Economic Geology*, v. 15, p. 623-664.
- Anthony, J.W., Bideaux, R.A., Bladh, K.W., and Nichols, M.C., Eds., 1995, *Handbook of Mineralogy*, Mineralogical Society of America, Chantilly, Virginia 20151-1110, UAS (<http://www.handbookofmineralogy.org/>).
- Aveyard, R., and Haydon, A., 1973, *An introduction to the Principles of surface chemistry: Cambridge University Texts*, Cambridge, 232p.
- Bartlett, M.W., Enders, M.S., and Hruska, D.C., 1991, Geology of the Hollister gold deposit, Ivanhoe district, Elko County, Nevada, *in* Raines, G.L., Lisle, R.E., Schafer, R.W., and Wilkinson, W.H., eds., *Geology and ore deposits of the Great Basin*, Symposium Proceedings: Geological Society of Nevada, p. 957-978.
- Barton, P.B., Jr., and Skinner, B.J., 1979, Sulfide mineral stabilities, *in* Barnes, H.L., ed., *Geochemistry of Hydrothermal Ore Deposits* 2nd ed.: New York, Wiley Interscience, p. 278-403.
- Best, M.G., Christiansen, E.H., Deino, A.L., McKee, E.H., and Noble, D.C., 1989, Excursion 3A: Eocene through Miocene volcanism in the Great Basin of the western United States: New Mexico Bureau of Mines and Mineral Resources Memoir 47, p. 91-133.
- Blakely, R.J., and Jachens, R.C., 1991, Regional study of mineral resources in Nevada—insights from three-dimensional analysis of gravity and magnetic anomalies: *Geological Society of America Bulletin*, v. 103, p. 795-803.
- Buchanan, L.J., 1981, Precious metal deposits associated with volcanic environments in the southwest, *in* Dickson, W.R. and Payne, W.D., eds., *Relations of Tectonics to Ore Deposits in the Southern Cordillera: Arizona Geological Society Digest*, v. 14, p. 237-262.

- Chitwood, R.A., 2012, Geochemistry and Mineralogy of Eastern Ag-rich Epithermal Veins in the Midas District, Nevada, USA: Unpublished M.Sc. thesis, Auburn, Alabama, The Auburn University, 122 p.
- Christiansen, R.L., and Yeats, R.S., 1992, Post-Laramide geology of the U.S. Cordilleran region: Geological Society of America, *Geology of North America*, v. G-3, p. 261-406.
- Conrad, J.E., Mckee, E.H., Rytuba, J.J., Nash, J.T., and Utterback, W.C., 1993, Geochronology of the Sleeper deposit, Humboldt County, Nevada: epithermal gold-silver mineralization following emplacement of a silicic flow-dome complex: *Economic Geology*, v. 88, p. 317-327.
- Demars, C., Pagel, M., Deloule, E., and Blanc, P., 1996, Cathodoluminescence of quartz from sandstones: interpretation of the UV range by determination of trace element distributions and fluids-inclusion P-T-X properties in authigenic quartz: *American Mineralogist*, v. 81, p.891-901.
- Diggings™, 2017, Buckskin National Project: Gold Deposit In Nevada, The United States, (<https://thediggings.com/mines/usgs10310424>).
- Dong, G., Morrison, G. and Jaireth, S., 1995, Quartz textures in epithermal veins, Queensland--classification, origin, and implication: *Economic Geology*, v. 90, p. 1841-1856.
- Drummond, S.E., and Ohmoto, H., 1985, Chemical evolution and mineral deposition in boiling hydrothermal systems: *Economic Geology*, v. 80, p. 126-147.
- Foley, N.K., and Ayuso, R.A., 2012, Gold deposits of the Carolina Slate Belt, southeastern United States — Age and origin of the major gold producers: U.S. Geological Survey Open-File Report 2012-1179, 26 p.
- Fournier, R.O., 1985, Silica minerals as indicators of conditions during gold deposition, *in* Tooker, E.W., ed., *Geologic characteristics of sediment- and volcanic-hosted disseminated gold deposits – search for an occurrence model*: U.S. Geological Survey Bulletin 1646, p. 15-26.
- Giggenbach, W.F., 1992, Magma degassing and mineral deposition in hydrothermal systems along convergent plate boundaries: *Economic Geology*, v. 87, p. 1927-1944.
- Goldstrand, P.M., and Schmidt, K.W., 2000, Geology, mineralization, and ore controls at the Ken Snyder gold-silver mine, Elko County, Nevada: *Geological*

- Society of Nevada, Geology and Ore Deposits 2000: the Great Basin and Beyond Symposium, May 15-18, 2000, Reno-Sparks, Nevada, Proceedings, p. 265-287.
- Google, Google Map, 2017, Location of Buckskin National mine, Nevada, USA (<https://www.google.com/maps/place/Buckskin+National+Mine/@41.1733892,-118.1651332,9z/data=!4m5!3m4!1s0x54b4a350f38aabdf:0xc771f707bbfacc54!8m2!3d41.7923911!4d-117.5406907>).
- Google, Google Map, 2017, Location of Fire Creek mine, Nevada, USA (<https://www.google.com/maps/place/Fire+Creek+Mine/@40.4451139,-116.6619802,12z/data=!4m5!3m4!1s0x80a4251c1a6954cd:0xf62497227bfc2f0!8m2!3d40.4695716!4d-116.6582466!5m1!1e4>).
- Götze, J., Plötze, M., and Habermann, D., 2001, Origin, spectral characteristics and practical applications of the cathodoluminescence (CL) of quartz - a review: *Mineralogy and Petrology*, v. 71, p. 225-250.
- Hames, W., Unger, D., Saunders, J., and Kamenov, G., 2009, Early Yellowstone hotspot magmatism and gold metallogeny: *Journal of Volcanology and Geothermal Research*, v. 188, p. 214-224.
- Hart, G., 1927, The nomenclature of silica: *American Mineralogist*, v. 12, p. 383-395, (http://www.minsocam.org/MSA/collectors_corner/arc/silica_nom.htm; 03/13/17).
- Heald, P., Foley, N.K., and Hayba, D.O., 1987, Comparative anatomy of volcanic-hosted epithermal deposits: Acid sulfate and adularia-sericite types: *Economic Geology*, v. 82, p.1-26.
- Hedenquist, J.W., and Lowenstern, J.B., 1994, The role of magmas in the formation of hydrothermal ore deposits: *Nature*, v. 370, p. 519-527.
- Hedenquist, J.W., Aribbas, A., and Gonzales-Urien, E., 2000, Exploration for epithermal gold deposits: *Reviews in Economic Geology*, v. 13, p. 245-277.
- Hedenquist, J.W., Matsuhisa, Y., Izawa, E., White, N.C., Giggenbach, W.F., and Aoki, M., 1994, Geology, geochemistry, and origin of high sulfidation Cu-Au mineralization in the Nansatsu district, Japan: *Economic Geology*, v. 89, p. 1-30.
- Henley, R.W. and Ellis, A.J., 1983, Geothermal systems, ancient and modern: *Earth Science Reviews*, v. 19, p. 1-50.
- Holland, H.D., and Malinin, S.D., 1979, On the solubility and occurrence of non-ore minerals, *in* Barnes, H.L., ed., *Geochemistry of hydrothermal ore deposits* 2nd ed.: New York, John Wiley and Sons, p. 461-508.

- Izawa, E., Urashima, Y., Ibaraki, K., Suzuki, R., Yokoyama, T., Kawasaki, K., Koga, A., and Taguchi, S., 1990, The Hishikari gold deposit: high-grade epithermal veins in Quaternary volcanic of southern Kyushu, Japan: *Journal of Geochemical Exploration*, v. 36, p. 1-56.
- John, D.A., 2001, Miocene and early Pliocene epithermal gold-silver deposits in the northern Great Basin, western USA: Characteristics, distribution and relationship to magmatism: *Economic Geology*, v. 96, p. 1827-1853.
- John, D.A., Garside, L.J., and Wallace, A.R., 1999, Magmatic and tectonic setting of late Cenozoic epithermal gold-silver deposits in northern Nevada, with an emphasis on the Pah Rah and Virginia Ranges and the northern Nevada rift: *Geological Society of Nevada, 1999 Spring Field Trip Guidebook Special Publication 29*, p. 64-158.
- John, D.A., Hofstra, A.H., Fleck, R.J., Brummer, J.E., and Saderholm, E.C., 2003, Geologic setting and genesis of the Mule Canyon low-sulfidation epithermal gold silver deposit, north-central Nevada: *Economic Geology*, v. 98, p. 425-463.
- Kamenov, G.D., 2007, Mafic magmas as sources for gold in middle Miocene epithermal deposits of the Northern Great Basin, United States--Evidence from Pb Isotope compositions of native gold: *Economic Geology*, v.102, p. 1191-1195.
- Kassos, G., Marma, J., and Milliard, J., "The Fire Creek gold project: an update on Nevada's newest high-grade epithermal gold deposit": the Geological Society of Nevada 2015 Symposium, 2015: Presentation.
- Klondex Mines Ltd., The Midas and Fire Creek Au-Ag projects, Elko and Lander counties, Nevada, USA (<http://www.pdac.ca/docs/default-source/convention---2015/convention---exhibitors---core-shack-2015/klondex-mines-ltd.pdf?sfvrsn=4>).
- Landmesser, M., 1984, Das Problem der Achatgenese [The Problem of the Agate Genesis],-*Mitt. Pollichia*, 72:5-137, Bad Dürkheim/Pfalz (*in German*).
- Leavitt, E.D., and Arehart, G.B., 2005, Alteration, geochemistry, and paragenesis of the Midas epithermal gold-silver deposit, Elko County, Nevada, *in* Rhoden, H.N., Steininger, R.C., and Vikre, P.G., eds., *Geological Society of Nevada Symposium 2005: Window to the World*, Reno, Nevada, May 2005, p. 563-627.
- Leavitt, E.D., Spell, T.L., Goldstrand, P.M., and Arehart, G.B., 2004, Geochronology of the Midas low-sulfidation epithermal gold-silver deposit, Elko County, Nevada: *Economic Geology*, v. 99, p. 1665-1686.

- Lindgren, W., 1915, Geology and mineral deposits of the National Mining district, Nevada: United States Geological Survey bulletin 601, 66 p.
- Lindgren, W., 1933, Mineral deposits, 4th ed.: New York, McGraw-Hill, 930 p.
- Long, K.R., DeYoung, J.H., and Ludington, S.D., 1998, Database of significant deposits of gold, silver, copper, lead, and zinc in the United States: U.S. Geological Survey Open-File Report 98-0206-A, 33 p., 98-206B, one 3.5-inch diskette.
- Lovering, T.G., 1972, Jaspertoid in the United States – its characteristics, origin, and economic significance: U.S. Geological Survey Professional Paper 710, 164 p.
- Ludington, S., Cox, D.P., Moring, B.C., and Leonard, K.W., 1996, Cenozoic volcanic geology of Nevada: Nevada Bureau of Mines and Geology Open-File Report 96-2, p. 5-1 to 5-10.
- Marfunin, A.S., 1979, Spectroscopy, luminescence and radiation centers in minerals: Springer Verlag, Berlin, 325 p.
- Marinova, I., Ganev, V., and Titorenkova, R., 2014, Colloidal origin of colloform-banded textures in the Paleogene low-sulfidation Khan Krum gold deposit, SE Bulgaria: *Mineralium Deposita*, v. 49, p.49-74, DOI 10.1007/s00126-013-0473-4.
- Mason, M.S., Saunders, J.A., Brueseke, M.E., Aseto, C., and Hames, W.E., 2015, Epithermal Au-Ag ores of War Eagle and Florida Mountains, Silver City District, Owyhee County, Idaho: Geological Society of Nevada 2015 Symposium: New Concepts and Discoveries, v. 1, p. 1067-1078.
- McKee, E.H., and Moring, B.C., 1996, Cenozoic mineral deposits and related rocks: Nevada Bureau of Mines and Geology Open-File Report 96-2, p.6-1 to 6-8.
- Moncada, D., Mutchler, S., Nieto, A., Reynolds, T.J., Rimstidt, J.D., and Bodnar, R.J., 2012, Mineral textures and fluid inclusion petrography of the epithermal Ag-Au deposits at Guanajuato, Mexico: Application to exploration: *Journal of Geochemical Exploration* 114, p. 20-35.
- Morris, G.A., Larson, P.B., and Hooper, P.R., 2001, “Subduction style” magmatism in a non-subduction setting: the Colville Igneous Complex, NE Washington state, USA: *Journal of Petrology*, v. 41, p. 43-67.
- MyTopo, 2017, Google Maps and Topographic Map for Buckskin National mine, Nevada, USA (<http://www.mytopo.com/maps/>).

- Nash, J.T., Ulterback, W.C., and Saunders, J.A., 1991, Geology and geochemistry of the Sleeper gold-silver deposit, Humboldt County, Nevada – an interim report, *in* Raines, G.L., et al., eds., *Geology and Ore Deposits of the Great Basin: Geological Society of Nevada*, p. 1063-1064.
- Nash, J.T., Ulterback, W.C., and Saunders, J.A., 1989, Geology and geochemistry of the Sleeper deposit, Humboldt County, Nevada-An interim report: U.S. Geological Survey Open-File Report 89-476, 39 p.
- Noble, D.C., 1972, Some observations on the Cenozoic volcano-tectonic evolution of the Great Basin, western United States: *Earth and Planetary Science Letter*, v. 17, p. 142-150.
- Noble, D.C., McCormack, J.K., McKee, E.H., Silberman, M.L., and Wallace, A.B., 1988, Time of mineralization in the evolution of the McDermitt caldera complex, Nevada-Oregon, and the relation of middle Miocene mineralization in the northern Great Basin to coeval regional basaltic magmatic activity: *Economic Geology*, v. 83, p. 859-863.
- Ramsayer, K., Banmann, J., Matter, A., and Mullis, J., 1988, Cathodoluminescence colours of alpha-quartz: *Mineralogical Magazine*, v. 52, p. 669-677.
- Ransome, F.L., 1907, The association of alunite with gold in the Goldfield district, Nevada: *Economic Geology*, v. 2, p. 667-692.
- Rimstidt, J.D., 1997, Gangue mineral transport and deposition, *in* Barnes, H.L., ed., *Geochemistry of Hydrothermal Ore Deposits 3rd ed.*: New York, John Wiley & Sons, v. 1, ch. 10, p. 487-488.
- Rogers, A.F., 1917, A review of the amorphous minerals: *Journal of Geology*, v. 15, p. 515-541.
- Romarco Minerals Inc., October 17, 2006, Romarco completes drilling at its Buckskin-National and Roberts Mountains gold project, (<http://hailegoldmine.com/news/news-releases/Press-Release-Details/2006/RomarcoCompletesDrillingatitsBuckskin-NationalandRobertsMountainsGoldProjects/default.aspx>).
- Romberger, S.B., 1991, A Model for Bonanza Gold Deposits: *Geoscience Canada*, v. 19, n. 2, p. 63-72.
- Rye, R.O., 1993, The evolution of magmatic fluids in the epithermal environment: the stable isotope perspective: *Economic Geology*, v. 88, p. 733-752.

- Sander, M.V. and Black, J.E., 1988, Crystallization and recrystallization of growth-zoned vein quartz crystals from epithermal system--Implications for fluid inclusion studies: *Economic Geology*, v. 83, p. 1052-1060.
- Sanematsu K., Watanabe, K., Duncan, R., Izawa, E., 2004, The temporal change of mineralization in time deduced from $^{40}\text{Ar}/^{39}\text{Ar}$ dating at the Hishikari gold deposit (in Japanese), Abstract with Program: Society of Resource Geology, O-31.
- Saunders, J.A., 1990, Colloidal transport of gold and silica in epithermal precious-metal systems: Evidence from the Sleeper deposit, Nevada: *Geology*, v.18, p. 757-760.
- Saunders, J.A., 1994, Silica and gold textures in bonanza ores of the Sleeper deposit, Humboldt County, Nevada--Evidence for colloids and implications for epithermal ore-forming processes: *Economic Geology*, v. 89, p. 628-638.
- Saunders, J.A., and Schoenly, P.A., 1995, Boiling, colloid nucleation and aggregation, and the genesis of bonanza Au-Ag ores of the Sleeper deposit, Nevada: *Mineralium Deposita*, v. 30, p. 199-210.
- Saunders, J.A., Schoenly, P.A., and Cook, R.B., 1996, Electrum disequilibrium crystallization textures in volcanic-hosted bonanza epithermal gold deposits: *Proceedings of the International Symposium on the Geology and Ore Deposits of the America Cordillera: (Reno, NV)* p. 173-179.
- Saunders, J.A., Unger, D.L., Kamenov, G.D., Fayek, M., Hames, W.E. and Utterback, W.C., 2008, Genesis of Middle Miocene Yellowstone hosted-related bonanza epithermal Au-Ag deposits, Northern Great Basin, USA: *Mineralium Deposita*, DOI 10.1007/s00126-008-0201-7.
- Saunders, J.A., Beasley, L., Vikre, P. and Unger, D.L., 2010, Colloidal and physical transport textures exhibited by electrum and naumannite in bonanza epithermal veins from western USA, and their significance: *Great Basin Evolution and Metallogeny: Geological Society of Nevada, 2010 Symposium*, v. 1, p. 825-833.
- Saunders, J.A., Kamenov, G.D., Mathur, R., Shimizu, T., and Brueseke, M.E., 2013, Transport and deposition of metallic nanoparticles and the origin of bonanza epithermal ores: *SGA Proceedings Volume*, Uppsala, Sweden, July, 2013, p. 868-871.
- Shettel, D.L., 1974, The solubility of quartz in supercritical $\text{H}_2\text{O}-\text{CO}_2$ fluids: University Park, Pennsylvania State University, M.S. thesis, 52 p.

- Shimizu, T., 2014, Reinterpretation of quartz textures in terms of hydrothermal fluid evolution at the Koryu Au-Ag deposit, Japan: *Economic Geology*, v. 109, p. 2051-2065.
- Shimizu, T., and Saunders, J.A., 2013, Petrographic and copper isotopic study of epithermal bonanza ores in Japan: Evidence from Hishikari and Koryu deposits: Geological Society of America Annual meeting, Denver, CO, GSA Abstracts with Programs Vol. 45, No. 7, Abstract No: 228239.
- Shimizu, T., Matsueda, H., Ishiyama, D. and Matsubaya, O., 1998, Genesis of epithermal Au-Ag mineralization of the Koryu Mine, Hokkaido, Japan: *Economic Geology*, v. 93, p. 303-325.
- Simmons, S.F., and Christensen, B.W., 1994, Origins of calcite in a boiling geothermal system: *American Journal of Science*, v. 294, p. 361–400.
- Simmons, S.F., White, N.C., and John, D.A., 2005, Geological Characteristics of Epithermal Precious and Base Metal Deposits: *Economic Geology* 100th Anniversary Volume, p. 485-522.
- Spurr, J.E., 1926, Successive banding around rock fragments in veins: *Economic Geology*, v. 21, p. 519-537.
- Steven, T.A. and Ratte, J.C., 1960, Geology and ore deposits of the Summitville district, San Juan Mountains, Colorado: U.S. Geological Survey Professional Paper 343, 70 p.
- Stoffregen, R., 1987, Genesis of acid sulfate alteration and Au-Cu mineralization at Summitville, Colorado: *Economic Geology*, v. 82, p. 1575-1591.
- The Hudson Institute of Mineralogy, n.d., The mineral Pyrrargyrite (<http://www.minerals.net/mineral/pyrrargyrite.aspx>).
- Truscottite Mineral Data, 2017, Retrieved from: <http://www.webmineral.com/data/Truscottite.shtml#.WOK6g28rKig>.
- Unger, D.L., 2008, Geochronology and Geochemistry of mid-Miocene Bonanza Low-Sulfidation Epithermal Ores of the Northern Great Basin, USA: Unpublished M.Sc. thesis, Auburn, Alabama, The Auburn University, 151 p.
- Vanderburg, W.O., 1938, Reconnaissance study of mining districts in Humboldt County, Nevada: Information Circular 6995, the United States Bureau of Mines, Washington D.C.

- Vikre, P.G., 1985, Precious metal vein systems in the National District, Humboldt County, Nevada: *Economic Geology*, v. 80, p. 360-393.
- Vikre, P.G., 1987, Paleohydrology of Buckskin Mountain, National District, Humboldt County, Nevada: *Economic Geology*, v. 82, p. 934-950.
- Vikre, P.G., 2007, Sinter-vein correlations at Buckskin Mountain, National District, Humboldt County, Nevada: *Economic Geology*, v. 102, p. 193-224.
- Wallace, A.R., and John, D.A., 1998, New studies of Tertiary volcanic rocks and mineral deposits, northern Nevada: Contributions to the gold Metallogeny of northern Nevada Open-File Report 98-338, p. 264-278.
- Wallace, A.R., 2003, Geology of the Ivanhoe Hg-Au district, northern Nevada: influence of Miocene volcanism, lakes, and active faulting on epithermal mineralization: *Economic Geology*, v. 98, no. 2, p. 409-424, DOI 10.2113/gsecongeo.98.2.409.
- Watanabe, Y., 2005, Late Cenozoic evolution of epithermal gold metallogenic provinces in Kyushu, Japan: *Mineralium Deposita*, v. 40, p. 307-323, DOI 10.1007/s00126-005-0025-7.
- Wherry, E.T., 1914, Variations in the compositions of minerals: *Journal of the Washington Academy of Science*, v. 4, p. 111-114.
- White, N.C. and Hedenquist, J.W., 1994, Epithermal environments and styles of mineralization; variations and their causes, and guidelines for exploration, In: *Epithermal gold mineralization of the Circum-Pacific; geology, geochemistry, origin and exploration*; II. Siddeley, G., eds., *Journal of Geochemical Exploration*, 36; 1-3, p. 445-474.
- White, N.C. and Hedenquist, J.W., 1995, Epithermal gold deposits: styles, characteristics and exploration: *SEG Newsletter*, v. 23, p. 1, 9-13.
- White, N.C., Leake, M.J., McCaughey, S.N. and Parris, B.W., 1995, Epithermal deposits of the southwest Pacific: *Journal of Geochemical Exploration*, v. 54, p. 87-136.
- White, N.C., Wood, D.G. and Lee, M.C., 1989, Epithermal sinters of Paleozoic age in North Queensland, Australia: *Geology*, v. 17, p. 718-722.
- Willden, R., 1964, Geology and mineral deposits of Humboldt County, Nevada: *Nevada Bureau of Mines and Geology Bulletin* 59.

- Williams, L.A., Parks, G.A., and Crerar, D.A., 1985, Silica diagenesis, I: Solubility controls: *Journal of Sedimentary Petrology*, v. 55, p. 301-311.
- Wood, J.D., 1988, Geology of the Sleeper gold deposit, Humboldt County, Nevada, *in* Schafer, R.W., Cooper, J.J. and Vikre, P.G., eds., *Bulk Mineable Precious Metal Deposits of the Western United States: Geological Society of Nevada*, p. 293-302.
- WordNet 3.0, 2006, Colloids, Princeton University (<https://www.wordnik.com/words/colloid>).
- Zoback, M.L. and Thompson, G.A., 1978, Basin and range rifting in northern Nevada--clues from a mid-Miocene rift and its subsequent offsets: *Geology*, v. 6, p. 111-116.
- Zoback, M.L., Anderson, R.E., and Thompson, G.A., 1981, Cenozoic evolution of the state of stress and style of tectonism of the Basin and Range province: *Philosophical Transactions of the Royal Society of London*, v. A300, p. 407-434.
- Zoback, M.L., McKee, E.H., Blakely, R.J., and Thompson, G.A., 1994, The northern Nevada rift: Regional tectonomagmatic relations and middle Miocene stress direction: *Geological Society of America Bulletin*, v. 106, p. 371-382.


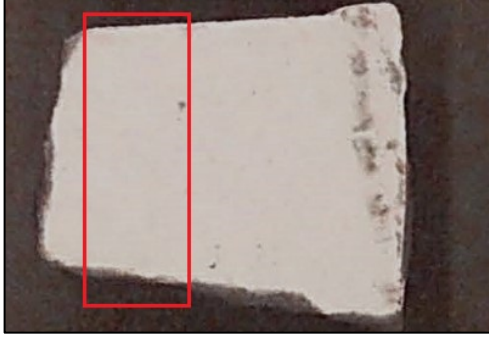


**Appendix 1: Silica Textural Counts of the Buckskin National (BN)
and Fire Creek (FC) Samples.**


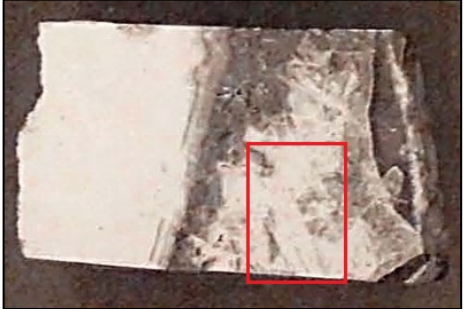



Sample No.	Comb	Colloform	Moss	Zonal	Mosaic	Plumos	Flamboyant	Lattice-bladed	Pseudo-parallel	Crustiform	Fibrous-acicular
BN-01	✓	✓	✓		✓	✓	✓			✓	✓
BN-02	✓	✓	✓	✓	✓	✓	✓			✓	✓
BN-03	✓	✓			✓					✓	
BN-04	✓	✓	✓		✓	✓	✓		✓	✓	✓
BN-05	✓	✓		✓	✓		✓			✓	
BN-06		✓			✓			✓		✓	✓
BN-07		✓			✓					✓	
BN-08	✓	✓			✓					✓	
BN-09		✓			✓	✓	✓	✓			
BN-10			✓		✓	✓					
BN-11			✓		✓						
BN-12		✓	✓		✓						✓
BN-13		✓	✓		✓						✓
BN-14	✓	✓			✓					✓	✓
BN-15	✓	✓			✓					✓	✓
BN-16					✓						✓
BN-17			✓		✓					✓	✓
BN-18			✓		✓			✓			
BN-19	✓				✓	✓					
BN-20	✓	✓	✓		✓	✓		✓			
BN-21					✓						✓
BN-22	✓		✓		✓	✓		✓	✓		
BN-23					✓						✓
BN-24					✓						
BN-25					✓						
BN-26	✓				✓	✓		✓		✓	
BN-27					✓	✓	✓	✓			✓
BN-28	✓	✓			✓	✓		✓			
BN-29					✓	✓		✓		✓	✓
BN-30	✓	✓	✓		✓	✓				✓	
BN-31	✓	✓	✓		✓		✓				
BN-32	✓	✓		✓	✓	✓	✓				

Sample No.	Comb	Colloform	Moss	Zonal	Mosaic	Plumose	Flamboyant	Lattice-bladed	Pseudo-parallel	Crustiform	Fibrous-acicular
BN-33	✓		✓		✓	✓	✓				
BN-34	✓				✓						
BN-35	✓	✓	✓		✓	✓		✓		✓	✓
BN-36	✓	✓	✓		✓		✓				✓
BN-37	✓	✓	✓	✓	✓	✓	✓				
BN-38	✓	✓	✓		✓	✓					
BN-39	✓	✓			✓						
Total	23	23	18	4	39	17	11	10	2	14	16

Sample No.	Comb	Colloform	Moss	Zonal	Mosaic	Plumose	Flamboyant	Lattice-bladed	Crustiform	Fibrous-acicular
FC01	✓				✓	✓		✓		
FC02	✓			✓	✓	✓		✓		
FC03	✓				✓			✓		
FC04					✓		✓			✓
FC05	✓	✓	✓	✓	✓	✓	✓			✓
FC06					✓					✓
FC07					✓				✓	✓
FC08		✓			✓			✓		
FC09	✓	✓			✓			✓	✓	✓
FC10		✓			✓				✓	✓
FC11	✓				✓					
FC12	✓			✓	✓			✓		
FC13	✓			✓	✓			✓		
FC14					✓		✓			
FC15	✓				✓			✓	✓	✓
FC16					✓			✓		
FC17					✓			✓		
FC18			✓	✓	✓		✓	✓		
FC19			✓	✓	✓			✓		
FC20	✓				✓			✓		
Total	10	4	3	6	20	3	4	13	4	7

Appendix 2: The XRD Samples from the Buckskin National and Fire Creek Deposit in Nevada, and additionally Hishikari Deposit in Japan.

Sample No.	Photograph	Note
BN-1		<p>Dark grey transparent colloform layers like smoky quartz, Petrographical details: recrystallized and fibrous chalcedonic textures.</p>
BN-2		<p>White milky colloform layers showing jigsaw and spherical textures.</p>
BN-3		<p>Fibrous-acicular spherical colloform bandings, some layers include black metals.</p>
BN-4		<p>Yellowish cream colloform layer, soft and loosed materials. Kaolinite are mostly found intergranular among quartz under an optical microscope.</p>

Sample No.	Photograph	Note
BN-5		<p>Fibrous-acicular recrystallized band including white soft and loosed materials.</p>
FC-6		<p>White platy calcite with lattice-bladed texture.</p>
FC-7		<p>Greenish white granular texture of carbonates and quartz.</p>
FC-8		<p>White to yellowish brown bladed calcite formed lattice-bladed texture. Glassy lusters can be observed by these blades.</p>
Hishikari		<p>Truscottite in the sample are indicated by white bladed minerals like calcite. Radial forms are common.</p>